RIGID BODY COLLISIONS: SOME GENERAL CONSIDERATIONS, NEW COLLISION LAWS, AND SOME EXPERIMENTAL DATA

Anindya Chatterjee

January 6, 1997

Abstract

This thesis attempts to present a unified view of the subject of rigid body collisions. This includes discussion of basic assumptions, fundamental and reasonable constraints on collision laws, a survey of commonly used laws, some new collision laws, a brief discussion of non-rigid body collisions in the context of rigid-body collisions, and some new experimental data, interpreted in the context of the previous theoretical considerations.

Contents

List of Tables

List of Figures

Chapter 1

Introduction

The objective of this thesis is to present a unified view of the subject of rigid body collisions. This includes discussion of basic assumptions, fundamental and reasonable constraints on collision laws, a survey of commonly used laws, some new collision laws, a brief discussion of non-rigid body collisions in the context of rigid-body collisions, and some new experimental data.

When two objects collide, understanding and modeling the resulting mechanical interaction is far from a purely academic exercise. In the physical world, at human length scales, one of the primary modes of interaction between bodies is through contact, including collisional contact.

In dynamic models of mechanical systems, an extremely popular and useful idealization of a solid object is as a *rigid body*. The world of ideal rigid bodies has clear and well defined rules for how objects move under the action of forces and moments, as well as how constraints like rolling, sliding or pivoting affect the motions of systems of objects. Yet, in a world of ideal rigid bodies where objects are allowed to collide, it is neither widely known nor completely understood how general, sensible rules for collisional interaction between ideal rigid objects might be constructed; how good the underlying assumptions are behind the rules that *are* available; and how meaningful, physically, the predictions of these or any other rules really are in a world of not-truly-rigid bodies. In the classical treatises on rigid body dynamics, the treatment of collisions is practically always restricted to one of two basic approaches: an *incremental* approach (see Routh [52]) and an *algebraic* approach (see Whittaker [71]). One or the other of these two approaches is frequently adopted as the rational basis for describing collisions, with little discussion of either the accuracy of these, or the possible validity of other approaches. More recent, specialized texts also present treatments of the subject that are restricted in that neither the weaknesses of the procedures they present nor the strengths of other possible, general approaches are discussed at any depth. The subject of rigid body dynamics is incomplete at present, due to the lack of breadth in available rigid body collision models. There is a need for a variety of collision models within the structure of rigid body mechanics, for use in important modern applications like robotics, dynamics of machines or other mechanical systems with intermittent impacts, and multibody dynamics in general.

Collisions between stiff solid objects are characterized by complicated nonlinear deformations occuring in the colliding bodies, at least in the vicinity of the contact region; and by complicated surface interactions between the bodies in the contact region. Consequently, simplistic (and possibly inaccurate) approaches are often used in collision modeling. The problems in modeling collisions are further discussed in Section 1.1 below.

A brief review of existing approaches to collision modeling is presented in Section 1.2. These approaches are discussed again in greater detail at various appropriate places in this thesis.

The contribution of this thesis is outlined briefly in Section 1.3.

An outline of the remainder of this thesis is then presented in Section 1.4.

1.1 Why Collisions are Hard to Model, and Simplistic Models are Popular

There is a hierarchy in the models available for describing various phenomena in mechanics. The laws of linear and angular momentum balance are strictly and precisely true, for essentially all engineering purposes. The accuracy of these balance laws is greater than that of most measuring devices. In predictions of translational and rotational motions of stiff, solid objects under the action of known forces and moments, rigid body mechanics can be very accurate in many cases, and may be ranked second. Models of how bodies deform in response to forces, while they can be very good, are not quite so accurate and therefore rank lower. For example, a model of a real material as linearly elastic or linearly viscous can have accuracies down to a fraction of a percent. Thus, such models are very good, yet not as accurate as rigid body mechanics can sometimes be. Many nonlinear material behaviors can only be modeled to accuracies of several percent, and should be ranked even lower. In this category are models for friction between solid bodies, models for fracture and models for nonlinear material response such as elastoplasticity. Of the constitutive laws needed for modeling material motion, the laws for collisions are amongst the least accurate.

Collisions are difficult to understand and model because they involve many interacting phenomena, each one difficult to model accurately even by itself. The collisional behavior of a given body is not determined by that body alone. When a body collides with something else, the outcome is not determined solely by the properties of the interior of the body (say its shape, mass distribution, material properties ...) and/or the properties of its surface (say frictional properties or local surface shape). The properties of both colliding bodies affect the outcome of the collision. If one colliding body happens to be touching a third body at the time of the collision, that other interaction is important, too. The real outcome of a collision could, in principle, be computed if all the relevant mechanical interactions could be captured by the mathematical model. However, the final accuracy of the predicted outcome would probably be about the same as that of the least accurate component of the model (material or contact behavior), or even less.

In order to accurately model the mechanical interactions in a collision, we need to know what nonlinear constitutive law to use for the material, and also to know detailed small scale geometrical characteristics of the contacting surfaces. This information is not usually available to any great precision. In modeling collisions, even if we are prepared to spend the time and effort required for a careful numerical solution of a complicated nonlinear problem (say, a finite element solution), we might still expect low accuracy due to incomplete information about constitutive laws as well as boundary conditions. In other words, the difficulty in trying to model collisions accurately arises at several levels:

1. Constitutive laws for essential phenomena like friction, fracture, and nonlinear deformation are not known accurately.

2. If they are known accurately, they still require detailed geometric information, information about ambient conditions that affect the contact behavior of the bodies, and various initial conditions that are not known accurately due to lack of sufficient data.

3. Even if sufficient data exists, and geometric information and initial conditions are available to great accuracy, the required calculations for an accurate prediction are difficult from the point of view of computer power as well as numerical techniques.

4. Even if such a calculation can be and is carried out, the results apply to only one *specific* pair of bodies, *at the time* when measurements of geometric properties and ambient conditions were made, since ambient conditions and hence contact behavior change with time.

While it is probably true that much of the detailed information referred to above may, in the end, average out and become somewhat irrelevant for some collisions of some bodies, it is extremely difficult to construct very accurate, yet general, collision laws for fully general bodies in general configurations.

For these reasons, simpler approaches with compromises on possible accuracy are often used for practical applications. For example, a simulation of granular flow (see Drake and Walton [16]) might involve too many collisions for a detailed approach (say, a finite element solution for each collision) to be feasible, and a simpler model is used. For such applications the correct mean behavior, as averaged over many collisions, might still be reasonably predicted although predictions for individual collisions are inaccurate. Other examples of simplified collision modeling may be found in robotics, where a simulation of a collision is part of a larger simulation, and some error is often accepted. For example, Raibert's hopping robots [50] were successfully designed on the basis of simplified analyses in which springs and dashpots were used to model contact in the intermittent collisions. A third application of simple collision models is in general-purpose rigid body dynamics simulation programs. Such programs usually *cannot* include realistic collision models, since relevant information about the bodies is not available. Moreover, computational complexity issues usually limit the sophistication of collision models in such applications (for a discussion of some of the issues involved, even with a crude collision model, see e.g., Baraff[1] [1]). In simulations using such programs, if and when bodies collide, the outcome of the collision is predicted using a simple model, and the simulation continues.

As indicated above, there are many applications where simple collision models are required. Let us briefly consider how such simpler models might be constructed. A collision between two solid bodies involves two interacting processes. First, there is a contact region where the bodies interact according to some contact law. Second, the contact forces cause deformations and affect the overall motions of the bodies. A simplified collision model comes from simplifications at one or both of these levels. Of these two levels, simplifying assumptions about how the bodies deform and move as a whole can drastically reduce the complexity of the problem. One common approach is to treat the colliding bodies as rigid bodies *for purposes of calculating their response to impulses at the contact region.* The assumption made is not that deformations are absent, but that they are small in a sense described in Section 2.2. Under this assumption, if forces are integrated over the collision time interval, impulse-momentum relations for a rigid body may be used. Such bodies, for which the net collisional interaction is accurately described by rigid body impulse-momentum relations, are referred to as *impulse-response rigid* in this thesis. Models based on this "rigid body" simplification may be called *rigid body collision models.* Simplifying assumptions about the contact often involve treating the contact region as small (or even as a point). In this thesis we concentrate on rigid body collision models with the small contact region assumption. Usually, Coulomb friction is assumed to act in the contact region. Some simplistic rigid body collision modeling approaches try to describe the net impulse transmitted during the collision through some algebraic equations which are assumed to describe the net interaction.

[1]Baraff's model is based on the assumption that the tangential component of relative velocity at the contact point does not change direction *or* reverse in a collision. It can, at most, go to zero. Baraff's model is more restrictive than Kane and Levinson's model (see Chapter 5 of this thesis), and can predict physically unrealistic outcomes of collisions, like increases in system kinetic energy (see Section 2.2 of this thesis).

Some approaches treat the collision as an interaction between two truly rigid bodies interacting in the contact region through a pseudostatic micromechanism, perhaps constructed from springs, dashpots and frictional contacts. Such approaches assume rigidity in the bodies *through the collision*, and lead to ordinary differential equations which can be integrated numerically. Such bodies, for which the net collisional interaction is accurately described by rigid body force-acceleration equations at all instants during the collision, are referred to as *force-response rigid* in this thesis.

It is clear that the assumption of force-response rigidity is stronger than the assumption of impulse-response rigidity. All force-response rigid bodies are impulse-response rigid; the converse is not true.

1.2 Brief Review of Existing Approaches

This section briefly mentions the popular modeling approaches that are currently available in rigid body collision modeling. Most of the approaches mentioned here are described in greater detail later in this thesis.

In the 19th century, Routh [52] presented a method of predicting the outcomes of three dimensional impacts of rigid bodies with friction. An analysis of Routh's collision model in a general 3D setting was presented early in the 20th century by Mayer [41]. Routh's model may be described as an incremental rigid body collision model based on a special point-contact with the assumption of no tangential compliance. Routh's model, the assumptions implicit in it, and its place in a more general framework of several possible models are discussed in some detail later in this thesis.

In the last decade, perhaps partially driven by interest in robotics and the greater possibilities of computer simulation in general, there have been several investigations of collision models for rigid bodies, or for manipulators made of rigid parts.

Some recent papers rediscover or analyze Routh's model. For a few examples, see Plyavniyeks (analysis of special solutions) [48], Keller (rediscovery, nice formal statement, some analysis) [33], Wang and Mason (2D analysis) [70], Bhatt and Koechling (3-D analysis) [6, 7, 5, 9], Ivanov (elegant proof of nonnegative energy dissipation in 3D collisions) [24], Mac Sithigh (partial 3-D analysis) [37], Stronge (very similar to Routh's model; same contact model except the collision may terminate at a different instant) [64] and Batlle (analysis of special collisions in 3D, called *balanced* collisions, in which there is no inertial coupling between normal and tangential directions) [4]. Routh's approach is commonly used (e.g., Mirtich and Canny [45]).

There are other modeling approaches available, based on alternative contact assumptions. Maw, Barber and Fawcett [40] present an approach based on the behavior of spheres under oblique contact forces as analyzed by Mindlin and Deresiewicz [44]. In their model, the small contact region is circular and stick/slip occurs on concentric annular regions. Stronge [63] presents a simpler point contact model using springs. A survey of several such contact models in the context of granular flows may be found in Walton [69]. In all the articles mentioned so far in this section the collision is modeled as occurring between two essentially rigid bodies with negligible internal deformations and with a specified contact law describing their interaction, i.e., between force-response rigid bodies (for an extended discussion of force-response rigidity see Section 2.2). This general *incremental* approach in modeling rigid body collisions is discussed in some detail in this thesis, in Chapters 5 and 8.

Some simpler rigid body collision models avoid the complications of incremental contact laws and seek to predict the outcome through algebraic formulas. Brach [10, 11] presents models with linear equations containing various dimensionless parameters that characterize the collision. Smith [55] presents a model with nonlinear equations that depends on just two dimensionless parameters.

These models are discussed in some detail in Chapter 5. The general aim of such approaches is to extend the ideas related to the coefficient of restitution to three dimensional collisions of arbitrarily shaped bodies with friction. In fact, there have been several papers which discuss what a proper generalization of the coefficient of restitution from one to two or three dimensions might be. Stronge's papers [59, 61, 60] and his discussion [62] present a definition of restitution based on energy dissipation. Stronge's definition is based on an idea of stored strain energy, and involves a calculation of the work done by the normal component of the interaction force during collision. It turns that Stronge's "energetic" restitution depends on the time history of contact forces (or path in impulse space)[2]. Ivanov [24] introduces an alternative definition of restitution, also based on energy considerations; this definition is described briefly in Section 3.3, and in some detail in Section 10.5 of this thesis[3]. Batlle [3] and Smith and Liu [57] compare different generalizations of the coefficient of restitution.

A simplistic analysis of impacts where the bulk of the bodies is not treated as rigid has been presented by Cohen and Mac Sithigh [14], where the deformation in the colliding bodies is assumed to be "homogeneous", i.e., the displacement field is assumed to be linear. This "pseudo-rigid" body approach has not been pursued much further in the literature. In this thesis we do not study this approach to simplifying collision models, not only because it falls outside rigid body mechanics anyway, but also because the assumption of homogeneous deformations is violated in many collisions, including two simple cases for which experimental data exists: light impacts of spheres, which are characterized by strongly *localized* deformations (see Goldsmith [20]), and impacts of slender rods, which have significant *bending* vibrations and multiple "micro-collisions" during the overall collisional interaction (see Stoianovici and Hurmuzlu [58]). Readers interested in the pseudo-rigid approach may also find the paper by Baraff [2] useful, in which the deformation in the bodies is assumed to be given by low order polynomials.

1.3 Contribution of this Thesis

Many of the approaches to modeling collisions mentioned above are reasonable, though all have shortcomings like the inability to capture certain types of behavior. For example, slip reversal for spheres ("superball-like" behavior [18]) or energy conserving frictional collisions between arbitrary bodies (see Crawford [15]) cannot be captured by Routh's model, while *non*-superball like behavior cannot be captured by Smith's model [55].

Almost all of the models mentioned above make an effort to satisfy various reasonable constraints. Most papers on collision models mention basic assumptions behind those specific models. However, there appears to be no self-contained source which clearly presents the general subject of rigid body collision models as a whole. For example, Goldsmith's text [20], an excellent reference on impacts in general, contains only one chapter on "stereomechanical" impact (this chapter contains a description of Routh's method).

[2]Stronge's restitution is, therefore, (a) dependent on the incremental contact model used in a collision law, and (b) *not* completely determined even if, say, the net outcome of a collision is known in an experiment. The issues involved are presented in greater detail in the related discussion of Routh's model in 3D, in subsection 5.2.4

[3]Ivanov's restitution depends on a knowledge of the direction of the net impulse transmitted in a collision, and is therefore completely determined if the net outcome of a collision is known from an experiment, since in this case the impulse direction is known. In collision *modeling*, however, specific hypotheses have to be made about the impulse direction.

This thesis attempts to make two principal contributions in the area of rigid body collision modeling:

- It presents a self-contained discussion of the general subject of rigid body collision models as a whole, including discussion of the necessity, utility and validity of various assumptions commonly made in collision modeling, as well as discussion of general properties automatically possessed by all collision laws based on these assumptions.

- It presents some new collision laws which are easy to use, are based on a small number of collision parameters, and have desirable behavior at least for the simplest collision configurations (frictionless and/or one dimensional collisions, and frictional collisions of spheres and disks).

In addition, this thesis

- Presents some new experimental results for two dimensional collisions of flat pucks on an air table (the experiments were conducted by undergraduate students John Calsamiglia and Scott Kennedy, under my supervision). The experimental results nicely illustrate some of the ideas developed in this thesis about rigid body collisions, particularly frictional collisions.

1.4 Outline of Remainder of this Thesis

This section presents a brief outline of the remainder of this thesis.

Chapter 2 presents some preliminary ideas. In Section 2.1, the idea of a collision in rigid body dynamics is made precise, collision laws are defined, and a list is given of desirable properties in a collision law. The usual assumptions of rigid body collision modeling are discussed in Section 2.2. The assumption of rigidity is discussed at some length. Two qualitatively distinct types of rigidity are described; the explicit distinction between these two types of rigidity, in a general setting, may be one of the strengths of the treatment presented in this thesis. The impulse-momentum relations used in rigid body collision dynamics are discussed in Section 2.3. These equations, for general collisions, reduce to a linear relation between the equal and opposite collisional impulses and the change in the relative velocity at the contact point in the collision. A matrix called the *local mass matrix* is described, and some of its properties are discussed. Nonnegative dissipation of kinetic energy in a collision is discussed.

Chapter 3 contains a general discussion of rigid body collision laws, and of various properties of collision laws that are based on the assumptions discussed in Chapter 2. The chapter includes discussion of a normality principle (apparently not noticed before), a geometric construction in impulse space showing the region accessible to general collision laws (built out of known ideas, but not presented before in complete form), collision laws based on local interaction models, collision laws that are homogeneous in the velocity and/or mass (laws based on dimensionless parameters have this property which, though almost self-evident, has apparently not been explicitly mentioned in a general setting before), and a brief section on the number of input and output variables for a simple, general rigid body collision law.

Chapter 4 contains a discussion of some simple collision configurations, and their place in the general framework of three dimensional collisions. Collisions between ellipsoids are then discussed as a departure from collisions between spheres, along with some modeling issues that arise. The ideas in this chapter are not new, but a general discussion of these ideas has apparently not been published before.

Chapter 5 presents a survey of some currently known collision models. While the assumptions of Section 2.2 and the local interaction assumption of Section 3.5 might seem restrictive, a large variety of collision models may be, and have been, constructed based on even these strong assumptions, as Chapter 5 shows. Of the collision models discussed, it is not clear which one, if any, is superior (in fact, it is not quite clear what "superior" means in this context – see footnote on page 50).

Chapter 6 presents three new algebraic laws for rigid body collisions. The three new laws each depend on three nondimensional collision parameters with clearly defined and simple bounds. These laws apply to general bodies – they are not restricted to two dimensions or to fortuitously aligned bodies. In the case of general three dimensional frictionless collisions, these laws reduce to Newtonian restitution, which is perhaps the most commonly known and used collision model for the *frictionless* case. Moreover, in the case of frictional collisions of spheres in three dimensions, or of disks in two dimensions, these laws reduce to a well known bilinear law.

Chapter 7 is devoted to an examination of the 2D restrictions of three well-known 3D algebraic collision laws, along with the three new laws of Chapter 6. The laws are studied by comparing the regions in *impulse space* that are accessible to each law for particular collisions, which are themselves described only by specifying the local mass matrix and the pre-collision velocity direction. The rationale for adopting this approach is that **(a)** by the impulse momentum relations, for a given mass matrix and pre-collision velocity, knowing the transmitted impulse is equivalent to knowing the outcome of the collision, **(b)** given any pair of colliding bodies in any configuration, there is a unique local mass matrix, and given any mass matrix, there is always a pair of colliding objects that have that mass matrix (therefore, looking at "interesting" pairs of bodies is equivalent to looking at "interesting" mass matrices), and **(c)** the collision laws studied *all* depend on purely nondimensional collision parameters, and so the magnitude of the pre-collision velocity may be scaled to unity (see Section 3.6); only the direction of the pre-collision velocity is required. The particular collisions studied in Chapter 7 are a generic collision, a collision with a diagonal mass matrix (as in spheres and disks), a tangential or grazing collision, a collision with infinite friction, and a collision of a pendulum with a wall (where one eigenvalue of M is infinite).

Chapter 8 continues the discussion of incremental collision laws started in Chapter 5, and contains discussions of some specific, simple, incremental models for rigid body collision laws. These laws are discussed separately from Chapter 5, because some of the ideas and interpretations presented are new (while Chapter 5 is purely review). The incremental models studied include a split-mass model (apparently new), a model with a special type of nonlinear damping used by some authors, the linear spring/dashpot model (much studied by many), a pair of bilinear spring models (one old, one new), and contact models with spring/dashpot elements aligned with the eigenvectors of the local mass matrix (a detailed look at a particular case of general linear spring/dashpot models studied by other authors, and including a demonstration of possible nonuniqueness of solutions in the presence of friction). In the discussion in Chapter 8, attention is paid to whether the incremental laws considered do or do not possess the properties of homogeneity in velocity and/or mass, which are features of many simple collision models, as discussed earlier.

Chapter 9 attempts to put the discussion of rigid body collisions into perspective by considering a fairly simple kind of *non-rigid* body collision, where the internal dynamics of the colliding bodies is linear. By considering this example, it is possible to see the place and the validity of various aspects of rigid body collision modeling. The discussion helps to clarify the difference in the contact interaction between collisions of force-response rigid and of impulse-response rigid objects. Issues of homogeneity in velocity and/or mass are discussed.

Chapter 10 contains several miscellaneous topics that, though relevant to rigid body collisions, do not fit naturally into the development of the other chapters. Included are a discussion of the ill-posedness of simultaneous multiple impacts, some general theoretical conclusions about the

collisional behavior of nearly spherical objects, a proof of existence of solutions for Smith's law (discussed in Chapter 5), a proof that arbitrary local mass matrices are in fact physically realizable using unconstrained bodies of finite mass (in Chapter 3 it is only demonstrated that arbitrary mass matrices were realizable using *mechanisms*, which may be thought of as unconstrained objects with infinite inertia in some directions), a discussion of a somewhat little-known, alternative definition of the coefficient of restitution due to Ivanov [24], and finally a brief discussion of some of the issues involved in constructing an algebraic collision law that can access the entire region in impulse space that is reasonably available in a general collision (i.e., a law that, for suitably chosen values of collision parameters, can capture *any* observed outcome, and that can predict impossible behaviors for *no* permissible values of collision parameters).

Chapter 11 presents the results of experiments conducted under my supervision by undergraduate students Calsamiglia and Kennedy. Calsamiglia's experiments were with axisymmetric flat pucks colliding with a heavy steel plate on an air table, and Kennedy's experiments were with a nonaxisymmetric (semicircular) puck colliding with a heavy steel plate. The principal conclusions reached from the experiments are that *for the collisions investigated* **(a)** the coefficient of normal restitution is approximately constant, with only a slight dependence on the direction of the pre-collision velocity and on the location of the contact point on the puck (even for the asymmetric puck case), and **(b)** the tangential component of impulse is *not* equal to μ times the normal impulse even for collisions where the tangential component of contact point relative velocity *does not* change direction in the collision. Conclusion (b) above is particularly interesting because it is in direct contradiction to the predictions of practically all rigid body collision models. A discussion is presented of the anomalous frictional behavior observed in these collisions, in the context of lack of force-response rigidity in the disks.

Chapter 2

Preliminaries

2.1 Collision Laws for Rigid Bodies and Ideal Mechanisms

In this section we define what we mean by collision laws for rigid bodies, and for mechanisms that are modeled as made of rigid parts and ideal joints. We present a list of properties that collision laws might be hoped to have.

2.1.1 Collisions

The word *collision* describes a brief interaction between solid bodies that involves large accelerations, finite changes in velocities, and small changes in position and orientation. The bodies collide when their motion causes them to come into contact with velocities which, if unaltered, would cause interpenetration of the bodies (interpenetrating velocities). After a brief interaction with finite net impulse transmitted, they have non-interpenetrating velocities and relatively smaller or zero interaction force. At this point, the collision is over.

We are specifically interested in collisions between bodies that may be treated as rigid, in that the integrated Newton-Euler equations, or the impulse-momentum relations for rigid bodies, may be used to describe the net responses of the bodies to the collisional contact forces. Note that no restrictions have been placed on what the contact forces or impulses themselves might be. Different hypotheses made about the relationship between the contact impulse and various system parameters correspond to different rigid body collision models. If the rigid body simplification is valid, and if the correct impulse is predicted by the assumed collision model, then the correct outcome will be predicted for the collision.

Collisions of mechanisms may also be studied under the framework developed in this thesis, although mechanisms are not rigid bodies. The key assumption about colliding mechanisms is that they may be treated as objects made up of rigid bodies connected by ideal joints such as frictionless hinges. Here again, the term "rigid bodies" is used to describe bodies whose response to collision impulses is close to that of rigid bodies. We refer to such mechanisms as *ideal mechanisms.* The net responses of colliding ideal mechanisms to large forces acting briefly on the contact region may be calculated using impulse-momentum relations (see Section 2.3).

2.1.2 Definition of a Collision Law

We now define a collision law for rigid bodies. We assume that the configuration of the bodies at the start of collision, their respective masses, moment of inertia matrices, and the point or region of contact are known. Given the velocities of centers of mass and the angular velocities of the bodies

at the instant before collision, a *collision law* is a rule which predicts the corresponding velocities after the collision. A collision law may require relevant physical details in the form of various other input parameters, such as material properties, geometric characteristics of the bodies, local radii of curvature, friction properties in the region of contact, etc.

Collision laws for ideal mechanisms may be defined in an analogous manner. We assume that the configurations of the mechanisms, all mass properties of all component rigid parts of each mechanism, and the point or region of contact are known. We assume that linear and angular velocities of all the component rigid parts at the instant prior to collision are known, and that these velocities are consistent with the constraints of the various joints in each mechanism (the velocities are kinematically admissible). Given these kinematically admissible velocities, a collision law is a rule which predicts the corresponding kinematically admissible velocities after the collision. As above, a collision law may require various relevant physical details.

Most of the ideas about rigid body collisions discussed in this thesis apply with little or no modification to collisions between ideal mechanisms. In what follows we discuss ideal mechanisms separately from rigid bodies only when significant differences exist between the two cases.

2.1.3 Desirable Properties in a Collision Law

What should we expect from rigid body collision laws? Since the mechanics of interaction between the colliding bodies is commonly modeled through gross approximations or even ignored, such models are generally not expected to make accurate predictions over a wide range of collisions. Roughly ordered from reasonable to optimistic to probably impossible, given below is a list of properties any general rigid body collision law might be expected to have.

1. *Fundamental constraints:* A collision law should never violate fundamental laws of mechanics which we believe to be true, like conservation of energy, frame invariance or linear or angular momentum balance.

2. *Generality:* It should apply to colliding bodies with arbitrary shapes, mass distributions, orientations, velocities, and material and surface properties.

   Most of the complications that arise in writing down collision laws do so when arbitrary bodies are allowed. In this thesis we consider collision laws for arbitrary bodies, and as particular cases examine what they predict for special bodies like spheres.

   However, for specific applications, it is reasonable to look for good collision laws that only apply to certain special bodies (say, glass spheres), so allowing arbitrary bodies is not a fundamental requirement for collision models.

3. *Consistency with "lesser" laws:* It should be consistent with our understanding of other phenomena which we can model with some success using less accurate laws, such as laws of friction.

4. *Matching data for simple objects:* It should, for appropriately chosen values of input parameters, be able to match observed behavior for the simplest collision configurations, like those between spheres or disks.

   For example, a collision model should be able, for properly chosen parameter values, to predict reversal of tangential relative velocity ("superball-like" behavior [18]) for the case of a sphere hitting a wall. Since some balls are not superballs, a model should be able to predict non-reversal of tangential relative velocity for other choices of parameter values.

5. *Capturing varied behaviors for general cases:* For more complicated collision configurations, it should be able to capture a wide variety of observed behavior, for appropriately chosen values of input parameters.

   In other words, the collision law should be able to predict the outcome or the results of a collision experiment, for suitably chosen values of the input parameters. These values may be chosen after the fact, if necessary. In the above, we might replace "observed behavior" with "physically permissible behavior" to include theoretically possible behavior not yet observed in experiments.

6. *Few parameters and overall simplicity:* A collision law should depend on a reasonably small number of input parameters, and involve a reasonably simple calculation.

   What "reasonable" means here is clearly debatable. Roughly speaking, any simplifying assumptions in the model leading to loss of accuracy should be accompanied by an acceptable reduction of computational effort.

7. *Physical interpretations for parameters:* The input parameters to the collision law should have simple physical interpretations.

   An example of such a parameter is the coefficient of restitution for head-on collisions, defined as a ratio of normal components of relative velocities (see Section 3.4).

8. *Independently measurable parameters:* The input parameters should be measurable in separate experiments, under conditions and configurations not identical to the particular collision being modeled.

9. *General predictive capability:* Measured input parameters, used in calculations for arbitrary collision configurations, should predict outcomes that match subsequent experiments.

2.2 The Usual Assumptions of Rigid Body Collision Modeling

This section contains a list of the basic assumptions that are usually made about rigid body collisions. The implications, validity and utility of these assumptions are discussed. Many, or most, of these assumptions are discussed to various degrees of depth in various papers on collisions. However, a comprehensive and careful discussion seems to be unavailable.

In particular, I have not seen the explicit emphasis on the distinction between two types of rigidity elsewhere in the literature.

1. *Rigidity – (a) Impulse-response rigidity, and sometimes (b) force-response rigidity:* The colliding bodies may be treated as rigid (colliding mechanisms may be treated as made up of component links that are rigid, connected by frictionless joints).

   As mentioned in the introduction, we do not mean that there are no deformations at all.

   We assume that before and after the collision the bodies move almost like rigid bodies, with deformations that may be neglected in calculations of linear and angular momentum. Any non-rigid behavior occurring during the collision is limited to small deformations over much of the bodies with perhaps large deformations localized to small portions of the bodies near the contact regions (for mechanisms, large deformations might also occur in small regions close to the joints). Such assumptions about the deformations can be made at two levels.

   At one level, we assume that far from the contact region the deformations are negligible and that *during* the collision the bodies may be treated as rigid bodies moving under the

influence of forces acting at the contact region (see Fig 2.1). Analogously for ideal mechanisms,

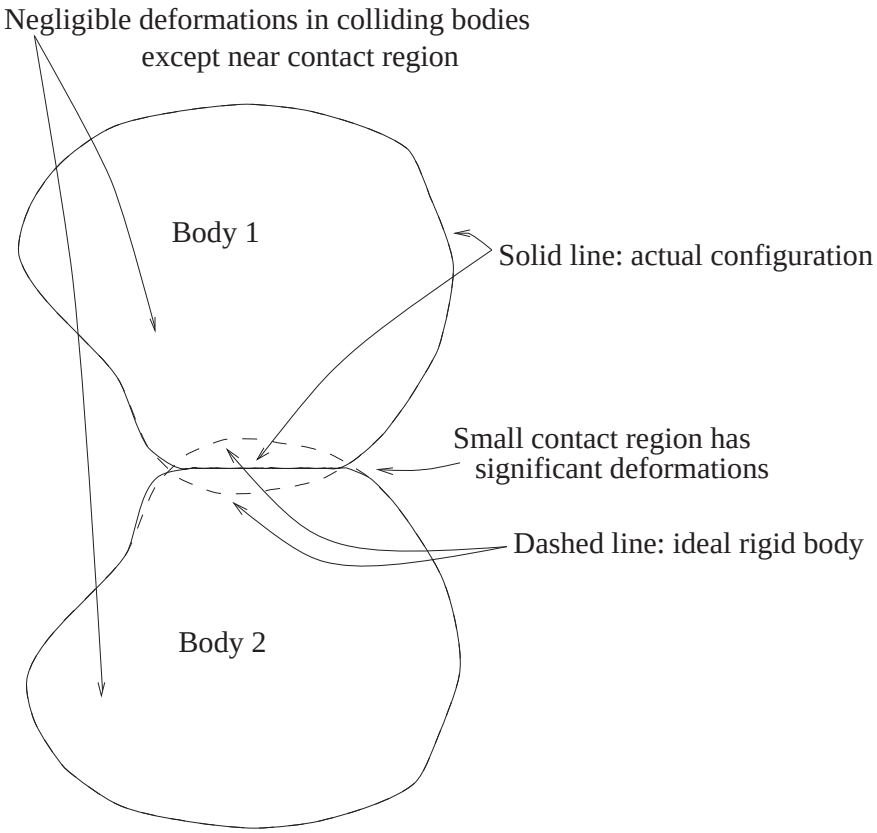

Figure 2.1: Collision of force-response rigid objects

we assume that the component bodies may be treated as rigid bodies moving under the influence of forces acting at the contact region (if applicable) and joints. Thus, for such bodies, momentum balance equations in the differential (or $F = ma$) form are assumed to be valid *during* the collision. This assumption can be accurate for light impacts of bulky bodies where the transient stress waves die out quickly compared to the (relatively slower) time scale of the collision itself. Bodies for which this assumption of rigid body response *throughout* the collision is valid will be referred to as *force-response rigid*. Johnson [31], in his introduction to the Hertz contact solution for head-on collisions of spheres (see Chapter 5), motivates that pseudo-static approach by an analogy which applies very well to the force-response rigidity idea:

> The impact may be visualized, therefore, as the collision of two rigid railway trucks equipped with light spring buffers; the deformation is taken to be concentrated in the springs, whose inertia is neglected, and the trucks move as rigid bodies.

In collision models based on force-response rigidity, the spring buffers are replaced by more general pseudostatic contact force models, and the railroad trucks or colliding bodies move like rigid bodies in 3D. The assumption of force-response rigidity may not be valid for transverse impacts of thin rods or plates with slow bending modes of vibration (see e.g., the experimental results of Stoianovici and Hurmuzlu [58]).

If the colliding bodies are not force-response rigid, they may have small but significant transient deformations which persist through the collision duration. Yet these deformations might either die out well before the bodies attain any appreciable overall displacements/rotations or suitably average to zero on such time scales (for a discussion of colliding bodies with significant internal vibrations, see Chapter 9). Under these conditions, the response of the bodies to contact forces *during* the collision is not well represented by the corresponding rigid body motions. However, integrated over the collision interval, the response to the net impulse will be close to that of the corresponding rigid body, and therefore the impulse-momentum relations for a rigid body may still be used. Thus, although momentum balance equations are not valid in the differential (or $F = ma$) form, they are valid in the integrated (or $P = m\Delta v$) form. Bodies of this kind will be referred to as *impulse-response rigid* (see Fig. 2.2). Many

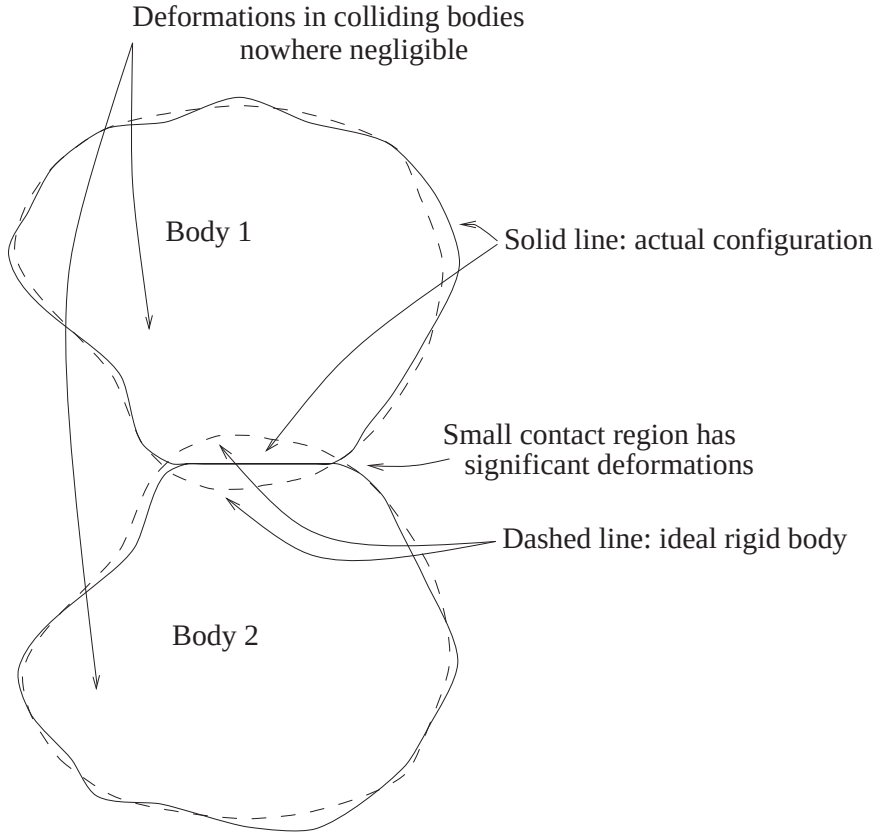

Figure 2.2: Collision of impulse-response rigid objects

contact force laws used to model collisions assume that the bodies are force-response rigid. If such contact laws are used to model collisions between bodies that are reasonably idealized only as impulse-response rigid, then the predicted time history of the contact force may be inaccurate, leading to possibly wrong predictions of the final velocities.

Under the rigid body assumption, in one of the two senses discussed above, impulse-momentum or force-acceleration equations for rigid bodies may be used to describe the collision. If the transients die out, the final motion after the collision will be well approximated by rigid body motion and will be close to the motion predicted by the impulse-momentum relations for rigid bodies. If the transients persist but suitably average to zero, the mean motion of the body will be close to the same rigid body motion.

On the other hand, if large transient deformations are present, then several complications arise. The contact point may have large motions in space, in which case the point of application of the transmitted impulse will not be known. Even if an effective point of application is known, if large transient motions are allowed, the final motion of the colliding bodies may not match that of corresponding rigid bodies (recall the commonly discussed example of a cat turning itself around while in free fall, illustrating that knowledge of net angular momentum does not determine change in configuration).

2. *Short time:* The collision occurs over a very brief time interval. Accelerations are very large, velocities change by finite amounts, and displacements and rotations are negligible.

   This assumption leads to the simplification that displacements and rotations through the collision may be neglected in that the moment of inertia tensor $\mathbf{I}$ in the rigid body equations of motion does not change through the collision (in a Newtonian frame).

3. *Neglect of finite forces:* Impulses from sources other than the large contact forces may be neglected.

   The contact forces are assumed to be very large (consistent with large accelerations assumed above). Other forces acting on the bodies, such as finite applied forces or body forces, are assumed to make negligible contributions to the impulse-momentum equations over the brief collision interval.

   For collisions between ideal mechanisms, both contact forces as well as constraint forces are assumed to be large and are retained. Body forces and other finite applied forces are neglected.

4. *Neglect of centrifugal terms:* Over the duration of the collision, ω^2 terms in the angular momentum balance equations are assumed to be negligible compared to other terms such as the $\dot{\omega}$ terms. In the equations of motion for a rigid body, $\vec{\omega} \times \mathbf{I} \cdot \vec{\omega}$ terms are neglected while $\mathbf{I} \cdot \dot{\vec{\omega}}$ terms are retained.

   Some of the ideas behind the three previous assumptions can be clarified with the help of an example. Consider a body acted on by a large force at a point (we assume that the body is force-response rigid). The equations for momentum balance are of the form

$$\mathbf{r} \times \mathbf{F} = \mathbf{I} \cdot \boldsymbol{\alpha} + \boldsymbol{\omega} \times \mathbf{I} \cdot \boldsymbol{\omega}, \tag{2.1}$$

   and

$$\mathbf{F} = m\mathbf{a}_{cm},$$

   where $\mathbf{F}$ is the force, $\mathbf{r}$ is the position vector from the center of mass to the contact point, $\mathbf{I}$ is the moment of inertia tensor, $\boldsymbol{\alpha}$ is the angular acceleration vector, $\boldsymbol{\omega}$ is the angular velocity vector, m is the mass, and $\mathbf{a}_{cm}$ is the acceleration of the center of mass.

   The relative acceleration at the contact point is the difference of the accelerations of the contact points on the two colliding bodies (here we really mean the accelerations of the corresponding points of truly rigid bodies with the same shapes and mass distributions as the bodies under consideration, acted upon by equal and opposite contact forces). The acceleration of the contact point on each body is given by an expression of the form

$$\mathbf{a}_{cp} = \frac{\mathbf{F}}{m} + \boldsymbol{\alpha} \times \mathbf{r} + \boldsymbol{\omega} \times \boldsymbol{\omega} \times \mathbf{r}, \tag{2.2}$$

   where $\mathbf{a}_{cp}$ is the acceleration of the contact point. Note that when ω^2 terms are neglected, $\boldsymbol{\alpha}$ is linearly related to $\mathbf{F}$ by Eq. (2.1), and thus the acceleration of each contact point is linearly related to $\mathbf{F}$ by Eq. (2.2).

For bodies that are impulse-response rigid, impulse-momentum equations for a rigid body may still be used though Eq. (2.2) might not be meaningful, as discussed earlier. For such bodies, therefore, the impulse transmitted during the collision at the contact point is linearly related to the change in the velocity of the contact point (again, when finite external forces, ω^2 terms and changes in configuration are neglected).

We present a simplistic order of magnitude analysis of the various terms in these equations (a more formal presentation of essentially the same ideas may be found in Keller [33]). Assume that units of mass, length and time may be chosen such that the magnitudes of $\mathbf{r}, m, \mathbf{I}, \boldsymbol{\omega}$ and $\mathbf{v}_{cm}$ (velocity of center of mass) are all $O(1)$. Let $\epsilon \ll 1$ represent the order of magnitude of the time duration of the collision and the displacements and rotations that occur during the collision. Then changes in the moment of inertia matrix as well as the amount of interference between the colliding bodies are both $O(\epsilon)$. Further assume that the contact force is $O(\epsilon^{-1})$. This implies that the magnitudes of $\mathbf{a}_{cm}$ and $\mathbf{a}_{cp}$ are $O(\epsilon^{-1})$, causing $O(1)$ velocity changes and $O(\epsilon)$ displacements in $O(\epsilon)$ time. In the angular momentum balance equation, the $\mathbf{r} \times \mathbf{F}$ and $\mathbf{I}\cdot\boldsymbol{\alpha}$ terms are expected to be $O(\epsilon^{-1})$ and are retained, while the $\boldsymbol{\omega} \times \mathbf{I}\cdot\boldsymbol{\omega}$ term is $O(1)$ and is neglected. In the integrated or impulse-momentum equations, the $O(\epsilon^{-1})$ terms make $O(1)$ contributions while the $O(1)$ terms make $O(\epsilon)$ contributions (neglected). Comparing magnitudes in this way, we loosely say that $\dot{\omega}$ terms are much bigger than ω^2 terms. Over the duration of the collision, the $O(\epsilon)$ changes in $\mathbf{I}$ are also neglected. Thus, displacements are used to calculate the interference between the colliding "rigid" bodies in order to predict contact forces, but neglected in that $\mathbf{I}$ is treated as a constant through the collision.

Though the displacements and collision duration might scale in more complicated ways for general collisions, the basic ideas are still valid for all but the lightest impacts. (For example, the orders of magnitude assumed above may not be valid for light impacts of spherical bodies where the contact forces are well described by the Hertz contact theory. Collision models based on Hertz contact are discussed briefly in Chapter 5.)

Very light impacts of rapidly spinning bulky bodies with frictionless contact provide an example where the assumptions made here may be violated. The $\mathbf{r} \times \mathbf{F}$ can be exactly zero for certain geometrical configurations; in such cases $\dot{\omega}$ terms are comparable to the ω^2 terms. Moreover, if we assume that the contact behavior is described by the Hertz contact theory, then the collision time duration does not stay small for extremely light impacts, and significant displacements may occur. In such cases changes in $\mathbf{I}$ should not be neglected.

5. *Finite bodies:* The mass, moments of inertia and dimensions of both bodies are nonzero, and those of at least one body are finite.

   We will use impulse-momentum relations in discussing the collision. These equations are meaningless for zero inertia. For example, a massless rod with a point mass at one end is not allowed in our treatment, since its moments of inertia about its center of mass are zero. In many cases, massless bodies may be allowed as appropriate limiting cases of well defined bodies with small mass. For example, if a uniform sphere collides with a wall, the mass of the sphere may be treated as negligible compared to the wall so long as it is clear that we are considering a uniform sphere.

   In this thesis, we consider the impact of solid bodies with nonzero dimensions and with both translational and rotational motions. We study collision models with the objective of predicting the outcome of a given collision. It is possible to take a different view of the matter and to study collisions of particles, i.e., collisions where rotational motions are ignored and only the motions of the centers of mass are monitored. Surface erosion and wear due to many

colliding particles may be studied from such a viewpoint (see Brach [11] for a brief introduction and further references). For a collision between two particles, some general statements may be made about the possible outcomes, but an accurate prediction of the outcome requires further information about shapes, moments of inertia, and rotations, at least. The section on particle collisions in Brach [11] has special assumptions about the behavior of the colliding bodies. This matter is touched upon to some extent by Brach [12] in his discussion of Smith's paper [55] and by Smith [56] in his reply. For the purposes of this thesis, the colliding bodies are assumed to have nonzero dimensions and are not treated as particles.

It will be seen later that the assumption of finite mass can be relaxed a little. Much of the discussion in this thesis involves an inertia matrix we call the "local mass matrix", and we usually assume that this matrix is invertible and finite. Such finite matrices can in fact arise in collisions where both bodies have infinite mass. A less restrictive assumption might be that the mass matrix has finite, strictly positive eigenvalues.

In an even less restrictive situation, such as the collision between a spherical pendulum and an immobile surface (as in Stronge [64]), the mass matrix may have an infinite eigenvalue. In such cases, the impact is assumed to occur in such a way that through the entire duration of the collision, the relative acceleration at the contact point has no component along the eigenvector corresponding to this infinite eigenvalue. This provides a kinematic constraint, and the problem is essentially tackled as a two dimensional one.

Note that the special cases mentioned above can be approximated closely by using large but finite masses. Therefore, these cases can be handled by the theory described in this thesis, along with suitable limiting processes. For ease of presentation, these special cases are avoided, except briefly in Chapter 7.

6. *Point contact:* The bodies interact at one point.

   Rigid body collision models are usually based on an assumption of "point contact", although no real bodies can sustain nonzero forces at one point, and contact occurs over a region. The assumption really is that the contact region has dimensions much smaller than the characteristic length of the smaller colliding body. For example, if a sphere hits a wall, the diameter of the contact region is assumed to be much smaller than that of the sphere. A flat plate falling on to a flat surface, making contact over a large area, falls outside the scope of this thesis.

   We also assume that there is only one such contact region. For example, a chair landing simultaneously on two legs is outside our treatment. In ideal rigid body modeling simultaneous impacts are low probability events, though such impacts obviously occur frequently in idealized models with special geometries. Collisions of robotic manipulators should be viewed as multiple impact problems, if one wishes to accurately model the interactions at the joints. These problems are even more ill-posed than single contact problems and require additional hypotheses before a solution can be found (for a discussion of some of the issues involved, see Section 10.1, or the excellent paper by Ivanov [25]). For examples of deterministic models for simultaneous multiple impacts, based on special additional hypotheses, see Glocker and Pfeiffer [19], Pfeiffer and Glocker [47] (see discussion in Subsection 5.1.5), or Marghitu and Hurmuzlu[1] [38]. In this thesis, we concentrate on impacts with single contact; for linkages

[1]Marghitu and Hurmuzlu consider single impacts at one end of a manipulator which already has one or more other ends in contact with rigid surfaces. Their solution is based on a special hypothesis about the kinematic constraints at the non-impact contact locations, and an analysis

with frictionless hinges, we concentrate on collisions with one frictional, collisional contact.

A further assumption implicit here is that the location of the (small) contact region has negligible motions in space. This assumption may be violated in some cases. Consider a slightly curved rod falling on to a flat surface. At different instants of time through the collision, different points along the rod may be making contact with the surface if the rod rolls or deforms slightly during the collision.

To summarize, we assume that the distributed contact forces on the colliding bodies, acting on small contact regions, may be replaced by an effective force at one point. This point should be well defined and fixed both on the colliding bodies as well as in space. Under these assumptions, the net effect of the contact interaction may be well approximated as a net impulse transmitted instantaneously to each body at a known point.

7. *Action and reaction:* Equal and opposite impulses act on the bodies at the point of contact.

   This follows from the law of action and reaction, or linear momentum balance.

8. *No contact torques:* There are no impulsive moments transmitted about the contact point.

   If the contact area is small, and if there are no distributed moments acting in this area, then the magnitude of the moment about the nominal contact point of the contact forces will be small and often insignificant.

   This small moment may be qualitatively significant in some cases. An example is the frictional moment about the vertical axis that is generated when a ball spinning about that axis falls vertically on to a horizontal floor (see Brach [11] for a discussion and other references). However, this effect is often unimportant, and most rigid body collision models ignore the finite size of the contact region. In this thesis, we assume that the location of the collision impulse is at a point about which no impulsive moments are transmitted.

   The no-moment assumption may easily be inaccurate in cases where the contact area is not small. However, we exclude such cases under the previous assumptions.

9. *Non-negative energy dissipation:* Kinetic energy is not created in a collision.

   For most collisions studied in practice, the net kinetic energy of rigid body motion in the bodies after the collision will be less than or equal to the initial kinetic energy. In this thesis, we assume that collisions cause non-negative dissipation of kinetic energy into heat or other forms. For brevity, we loosely refer to non-negative dissipation of kinetic energy as "conservation of energy".

   This assumption may be violated if, for example, the collision causes an explosion, releasing energy. Similarly, if the colliding bodies *before* collision have significant amounts of energy in the form of internal vibrations, then that energy might be converted into kinetic energy of rigid body motion during the collision. Since kinetic energy of internal vibrations is not part of the usual rigid body motion quantities, it would appear as if kinetic energy had been "created" in the collision.

10. *Well defined tangent:* There is a well defined tangent plane at the point of contact.

in the spirit of Routh's method for single contact impacts (see Chapter 5). In the special case when the non-impact contacts are frictionless and contact is maintained at all locations through the collision, their system becomes an ideal mechanism in the sense of this thesis.

In order to deal with friction, we need clearly defined normal and tangential directions. These are assumed to exist whenever required.

Typically, collisions occur through contact between two surfaces or between one surface and one vertex. In these cases, the tangent plane is well defined.

In rigid body dynamics, it is possible though exceptional to have contact between two corners or vertices. In order to accommodate such cases into a collision law with friction, we would need to define a normal direction.

11. *No finite interpenetration:* The bodies do not pass through each other (interpenetrate).

    For most collisions of practical interest, especially in two or three dimensions, there is no interpenetration, and we assume that this holds. In any case, interpenetration violates the point contact assumption.

    Interpenetration may be allowed in some special cases. The undergraduate dynamics textbook problem of a bullet passing through a block of wood provides a one dimensional example.

2.3 Impulse-Momentum Relations; the Local Mass Matrix

Based on assumptions (1) through (8) we may write the impulse-momentum relations for the collision in a convenient form. Consider two rigid bodies interacting at a point as shown in Fig. 2.3.

The contact points on the two bodies are shown with a relative displacement of $\boldsymbol{\delta}$ (exaggerated). In a collision between real bodies, the bodies will be in contact; $\boldsymbol{\delta}$ is a small variable that shows the relative displacement between the contact points on the two bodies that would occur were the bodies perfectly rigid, and interpenetration was allowed. As mentioned in Section 2.2, $\boldsymbol{\delta}$ is ignored for purposes of writing impulse-momentum relations for the rigid bodies. However, it may be used for calculating the contact force that acts between the bodies. The first derivative $\dot{\boldsymbol{\delta}}$ is assumed to be bounded, while the second derivative $\ddot{\boldsymbol{\delta}}$ is assumed to be very large.

Let us briefly examine what $\boldsymbol{\delta}$ signifies in terms of force-response or impulse-response rigid bodies. Figure 2.4 shows the interference $\boldsymbol{\delta}$ between idealized rigid bodies at some instant of time during a collision. If the actual colliding bodies are force-response rigid, then the idealized rigid body interference of Fig. 2.4 can give an accurate estimate of the true contact region at some instant, as shown in Fig. 2.1. On the other hand, if the true colliding bodies are *not* force-response rigid but only impulse-response rigid, then the instantaneous rigid-body interference does *not* correspond to the true contact region, as indicated in Fig. 2.5 showing the collision of a slender rod with a rigid wall.

Equal and opposite forces act on the two bodies at the contact point. This automatically ensures conservation of linear momentum and of angular momentum about the contact point. If the effects of finite external forces are ignored over the duration of the collision, momentum conservation principles provide no further information. Using rigid body mechanics, it is possible to find a relation (see e.g. Keller [33], Smith [55], Mac Sithigh [37], Ivanov [26] or Bhatt and Koechling [8]) between the force $\mathbf{F}$ and $\ddot{\boldsymbol{\delta}}$, the relative acceleration at the contact point. $\mathbf{F}$ and $\ddot{\boldsymbol{\delta}}$ are linearly related via an anisotropic local inertia tensor (the basic argument is given for the special case of unconstrained rigid bodies in the discussion following Eq. (2.2); the result also holds for ideal mechanisms). As indicated in Fig. 2.3, the sign convention is that $\boldsymbol{\delta}$ is measured from the body on which the force is $-\mathbf{F}$ to the body on which the force is $\mathbf{F}$.

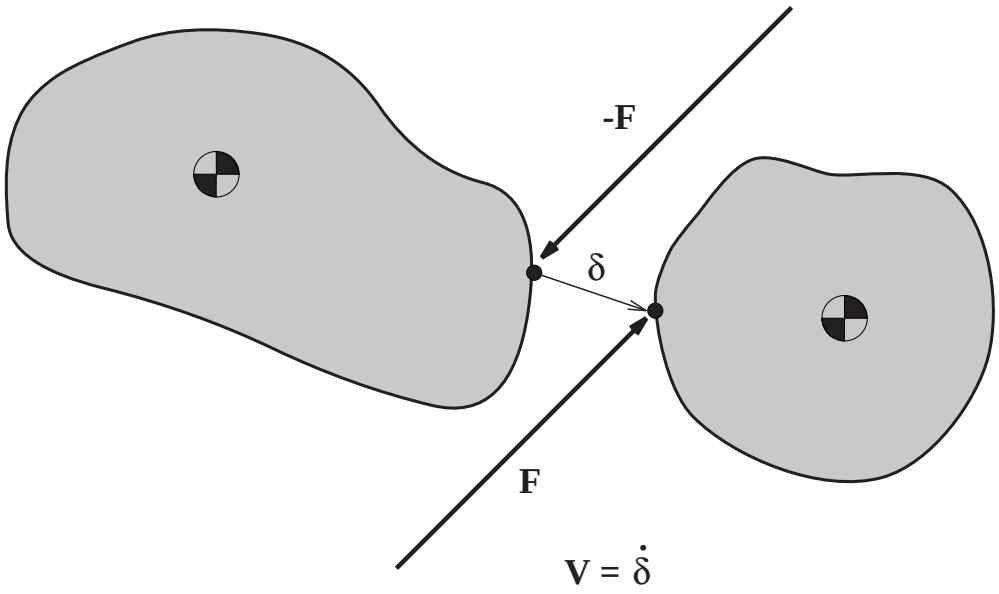

Figure 2.3: Two colliding bodies

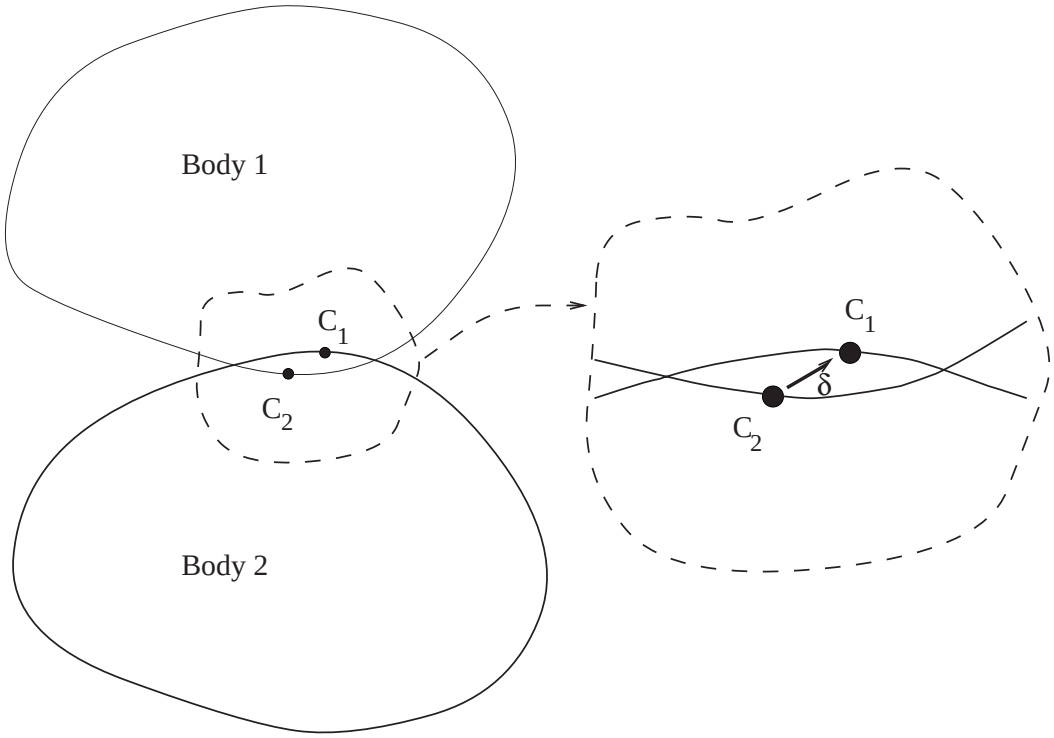

Figure 2.4: The interference for ideal rigid bodies

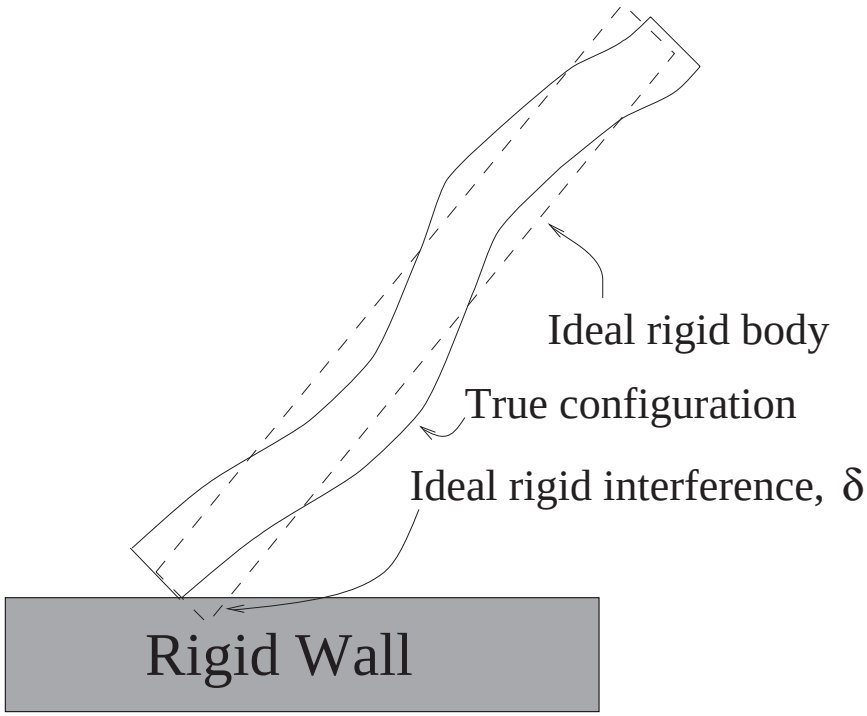

Figure 2.5: Collision of slender rod; true contact region cannot be predicted from rigid body response

If we pick a coordinate system, the equations may be written in matrix form,

$$M\ddot{\delta} = F. \tag{2.3}$$

Here, δ and F are the column-matrix representations of $\boldsymbol{\delta}$ and $\mathbf{F}$, respectively, in the chosen coordinate system. M, the local *mass matrix,* is symmetric positive definite. It relates the relative acceleration at the contact point, for ideal rigid bodies, to the equal and opposite forces acting on the two bodies at this point. Let V represent the relative velocity at the contact point, and P the accumulated impulse. Then we may write

$$\ddot{\delta} = \dot{V},\ \dot{P} = F, \text{ and } M\dot{V} = \dot{P}.$$

Note that we neglect changes in the configuration and hence changes in the matrix M through the collision. We may integrate over the collision time interval to obtain

$$M(V_f - V_i) = P, \tag{2.4}$$

where V_i and V_f are the relative velocities before and after the collision. Here M and V_i are assumed known, while V_f and P are to be determined. Note that M is usually not a scalar multiple of the identity, and so P and $\Delta V := V_f - V_i$ are usually not parallel. For the remainder of this thesis, f and i subscripts refer to post-collision and pre-collision quantities respectively.

We emphasize that though the derivation of Eq. 2.4 above is based on integrated force-acceleration equations and therefore on an assumption of force-response rigidity, in the integrated form the equation is valid for general impulse-response rigid bodies also. This is because, by definition, the mean or overall rigid body motion of impulse-response objects before and after the collision

matches the motion of force-response rigid objects; the motions differ only during a small period of time comparable to that of the collision. In other words, Eq. 2.4 is valid for all bodies that satisfy assumption (1) of rigidity, whether they are impulse-response rigid (1a) or force-response rigid (1b).

Some studies contain detailed derivations of the various terms in the mass matrix above for special collision configurations (see e.g., Stronge [59], Brach [10]). We omit those details and just consider a general symmetric positive definite matrix.

It is shown later in this chapter that every such matrix has a realization in terms of rigid bodies (possibly with kinematic constraints and/or peculiar mass distributions). This new result shows that any rigid body collision law meant for general collisions of arbitrary solid bodies must at least pass various tests for reasonableness for arbitrary symmetric positive definite mass matrices. In other words, while discussing the relative merits of two collision laws, one might just as easily compare what the laws predict for an arbitrarily chosen mass matrix along with similarly arbitrarily chosen values of relevant collision parameters, as compare what they predict for a specific pair of bodies.

Equation (2.4) above, based only on impulse-momentum relations, is valid whenever assumptions (1a) and (2) through (8) are valid, and has nothing to do with the details of the collision law. It need not be derived repeatedly for different collisions. Given this equation, knowing the transmitted impulse is equivalent to knowing the relative velocity at the contact point after the collision. Once the transmitted impulse is known, impulse-momentum relations for each rigid body may be used to calculate its velocity and angular velocity after the collision.

A collision law might predict either the transmitted impulse or the final relative velocity. In this thesis, we use one form or the other, as convenient.

2.3.1 The Local Mass Matrix for Some Special Cases

Many of the difficulties that arise in collision modeling do so when the eigenvectors of the local mass matrix are not lined up suitably with the normal and tangential directions (defined by the contact surfaces), and inertial coupling makes frictional collisions complicated, at least for 3-D collisions. In modeling frictional collisions, a natural choice of coordinates has one axis lined up with the normal, and two others lying in the tangent plane. Of these, one might perhaps be chosen to lie along the projection on the tangent plane of the pre-collision relative velocity at the contact point. We discuss frictional collisions later in the thesis; we mention for now that there usually is some convenient coordinate system, and that in this system the mass matrix need not be diagonal. Difficulties in collision modeling often arise when the mass matrix has large off-diagonal elements (a situation which arises, say, when slender objects collide in crooked configurations).

The mass matrix M is symmetric positive definite, so it has real, positive eigenvalues and orthogonal eigenvectors. Sometimes the eigenvalues and eigenvectors can be found by inspection. We now look at the mass matrix for a few special cases.

1. **One body infinitely massive.**

   Consider collisions between one body of finite mass and another that is infinitely massive (see Fig. 2.6). In such cases any changes in relative velocity at the contact point are due to the acceleration of the finite body. Since a force at the contact point directed towards the center of mass of the finite body will produce a relative acceleration in the same direction, that is the direction of one eigenvector. The corresponding eigenvalue is the mass of the finite body,

   $$\lambda_1 = m.$$

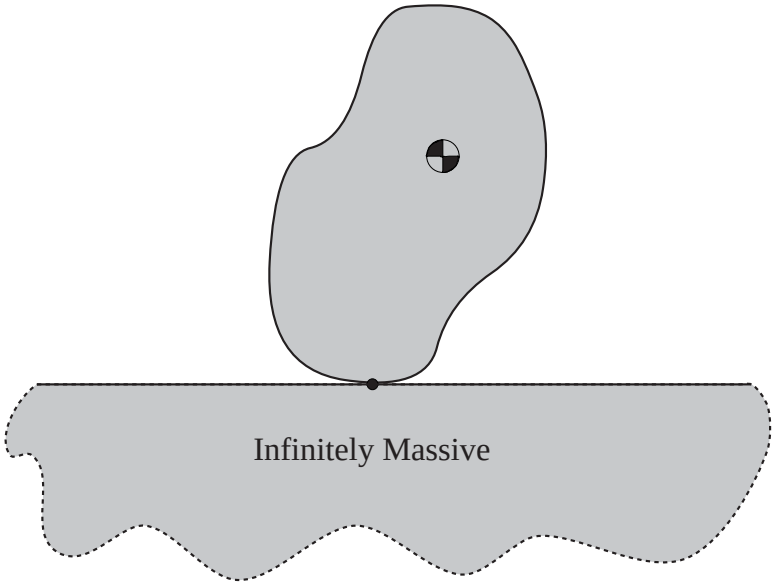

Figure 2.6: Collision with one infinitely massive body

In three dimensional collisions, the remaining two eigenvectors may be seen in special cases of some symmetrical bodies.

2D collisions: In two dimensions the second eigenvector is also known, since it is orthogonal to the first. In terms of the mass m, the distance to the center of mass r, and the moment of inertia about the center of mass I, the second eigenvalue is

$$\lambda_2 = \frac{I}{I + mr^2}\,\lambda_1.$$

2D collision of thin uniform rod and infinitely massive body: Consider the case of a thin uniform rod hitting an infinitely massive body. In this case the ratio of the eigenvalues is

$$\frac{\lambda_2}{\lambda_1} = \frac{I}{I + mr^2} = \frac{1}{4}.$$

2D collision of thin non-uniform rod and infinitely massive body: If there is a heavy point mass at the far end of the rod, then the ratio λ_2/λ_1 may be made as small as we like. Similarly, if there is a heavy point mass very close to the contact point, then the ratio of eigenvalues can be very close to one. In both this case and the case of uniform mass distribution, the direction of one eigenvector is along the rod, which may make any desired angle with the normal.

The preceding examples show that the directions of the eigenvectors are arbitrary and need not be aligned with the normal and tangential directions.

2. **A special 2D collision with $\lambda_2 = \lambda_1$.**

   For collisions of a finite body with an infinite mass, the second eigenvalue is always less than the first one. The ratio of eigenvalues can approach but cannot equal unity. However, the eigenvalues may well be exactly equal for collisions where *both* bodies have finite mass, as

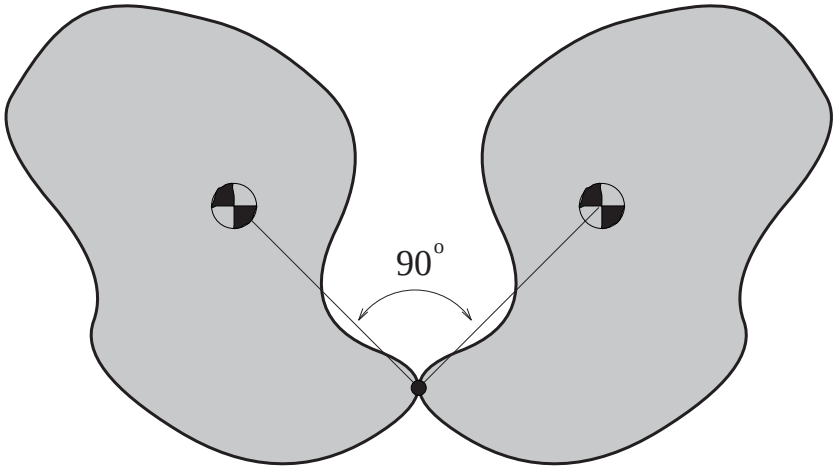

Figure 2.7: Collision between two finite bodies

shown next. Figure 2.7 shows a special two dimensional configuration where the two bodies are mirror images of each other. The lines joining the contact point and the centers of mass are perpendicular to each other. For this configuration, the mass matrix is a scalar multiple of the identity matrix. Thus, for this special pair of objects, the impulse P is parallel to the velocity jump ΔV.

This example, together with the previous ones, proves that in two dimensional collisions all eigenvalue ratios and all eigenvector directions (thus, all symmetric positive definite mass matrices) have realizations in terms of rigid bodies.

3. **Contact point and centers of mass collinear; spheres.**

   In collisions between two finite bodies, the contact point and the two centers of mass will generally not be collinear (e.g., as in Fig. 2.7). When the centers of mass and the contact point *are* collinear, the direction of this line will give an eigenvector of M.

   Now consider a collision between two uniform spheres (the masses and/or radii may be unequal). The two centers of mass and the contact point are collinear. Moreover, the line joining these points is normal to the tangent plane. One eigenvector is along this line. The other two eigenvectors lie in the tangent plane; by symmetry, the two corresponding eigenvalues are equal. The three eigenvalues are in fact in the ratio 7:2:2, as may be shown using the facts that for a sphere, $I = \frac{2}{5}mr^2$, and that the mass matrix for the collision of two identical spheres is one half the mass matrix for a collision of one sphere with an infinitely massive object. Collisions between spheres are discussed further in Chapter 4.

2.3.2 The Mass Matrix for Collisions Between Linkages

Collisions between linkages, or between a linkage and a solid body, involve complicated impulsive interactions at the bearings, and are multiple-contact problems. Connections which are effectively frictionless and nondissipative during smooth motions are generally capable of significant energy dissipation in impacts. However, one might reasonably model such collisions using the rigid body approaches described in this thesis, retaining the frictionless behavior of the bearings (see e.g., Bhatt

and Koechling [8], Seabra Pereira and Nikravesh [54], or the example of the spherical pendulum discussed by Stronge [64]).

In such models, it is assumed that the change in the relative velocity at the contact point can be expressed in terms of the transmitted impulse and a local mass matrix, i.e., an equation of the form Eq. 2.4. Thus, impulse-response rigidity is assumed. Under these assumptions, collisions of manipulators may be modeled, for example, using simple algebraic collision laws, as in Seabra Pereira and Nikravesh [54].

Under a stronger rigidity assumption, viz., force-response rigidity, and on dropping ω^2 terms and finite forces, the equations of motion for the constrained linkage reduce to a linear relationship between the applied force and the relative acceleration at the collision contact point. Therefore, *if* the collisional contact behavior of a linkage can be well approximated as a force-response rigid interaction, i.e., the relative acceleration at the contact point *during the collision* is accurately given by the corresponding ideal rigid body force-acceleration equations, then collision models based on force-response rigidity may justifiably be used (as in the treatments of Bhatt and Koechling [8] and Stronge [64]). However, as discussed below, the the collisional contact behavior of a linkage can typically *not* be well approximated as a force-response rigid interaction; in such circumstances, the use of incremental models based on force-response rigidity is just as *ad hoc* as any algebraic model.

Since collisions of linkages are also included in our treatment, we might replace Fig. 2.3 by Fig. 2.8.

The accuracy of collision models for mechanisms: The impulse-momentum relation (Eq. 2.4) may be used to predict the outcome of collisions between mechanisms, using the appropriate mass matrix for the given pair of contacting points. However, rigid body collision models often assume that the interference δ may be calculated from the rigid body motions of the colliding bodies (i.e., the motions the bodies would have if they were truly rigid). This assumption is based on the idea that for the colliding bodies (assumed to be force-response rigid), there are significant deformations only in one small region around the contact point. For mechanisms made of force-response rigid parts, however, there will typically be significant deformations both near the contact point as well as near the joints. Therefore, the interference at the contact point cannot be calculated based on rigid body motions alone. If the contact force model used in the calculation depends on accurate knowledge of this interference, then predictions of the contact forces may be inaccurate. So the assumptions behind force-response models, such as Routh's model, are probably not well met for most mechanisms.

Physical realization of arbitrary mass matrices: If collisions between linkages are included, then it is easy to show that all symmetric positive definite mass matrices have realizations in terms of rigid bodies or mechanisms made from such bodies. Figure 2.9 shows two single-link mechanisms in a collision configuration. Mechanism 1 consists of three identical rigid, light rods welded together, and supported by a ball and socket joint at O. There are masses attached to the ends of the rods, as shown in the figure. Mechanism 2 is a planar pendulum hinged at C. The rods are lined up with coordinate axes 2 or 3, as shown. The mass M_b can only move in the 2-direction, while the mass M_a can move in the 1 and 3-directions. We may assume that $M_a \leq M_b \leq M_a + 2m$. The three coordinate axes are then eigenvectors of the mass matrix, and the eigenvalues are M_a, M_b and $M_a + 2m$ respectively. The normal and tangential directions can be oriented as we please by small changes in the positions of the pivots at C and O, or by suitably selecting the shapes of the masses M_a and/or M_b. This example demonstrates that all symmetric positive definite matrices are realizable mass matrices. In fact, all symmetric positive definite matrices are in fact realizable using only two unconstrained rigid bodies of *finite mass*, as shown in Chapter 10.

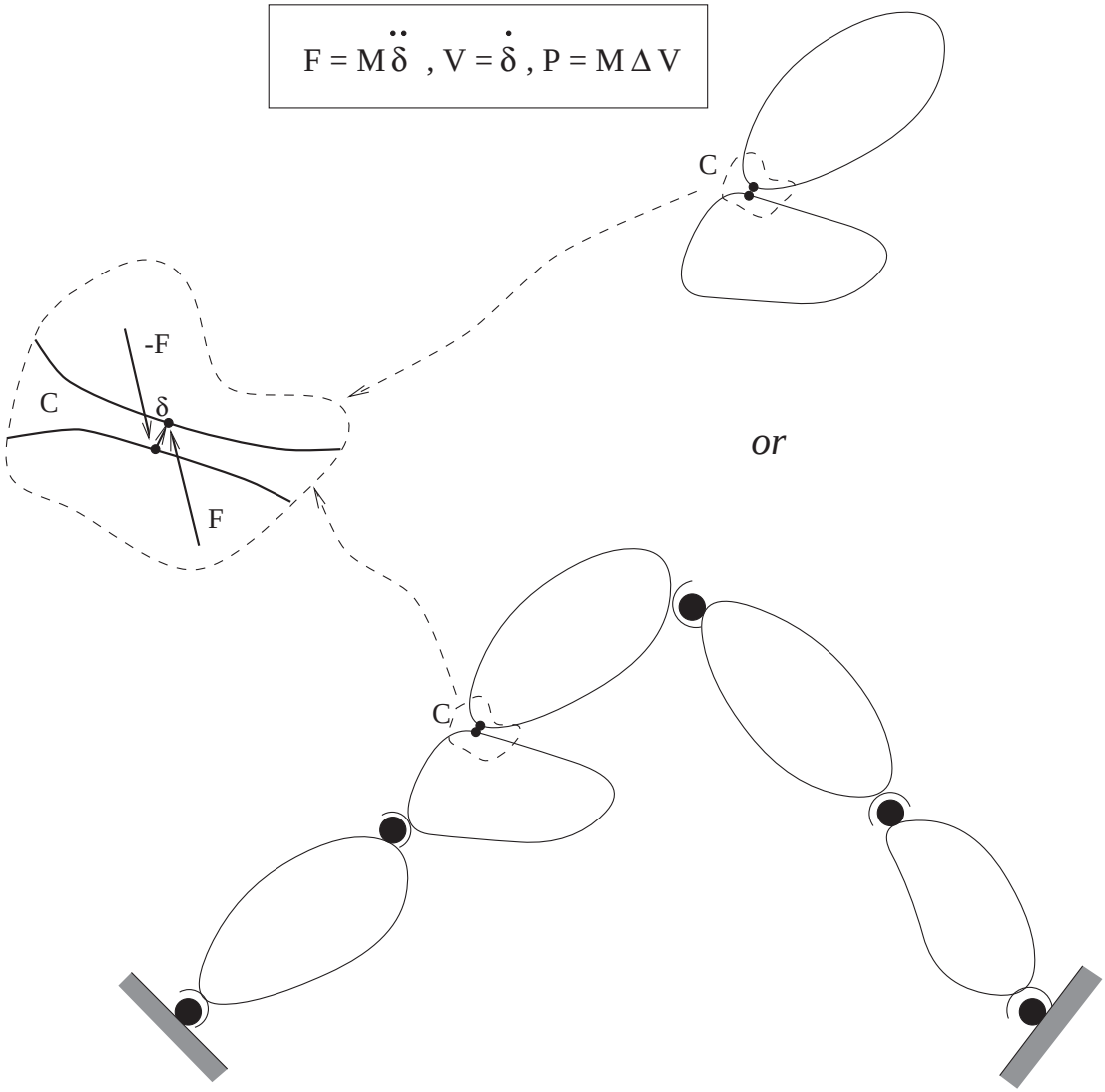

Figure 2.8: Two colliding bodies or mechanisms

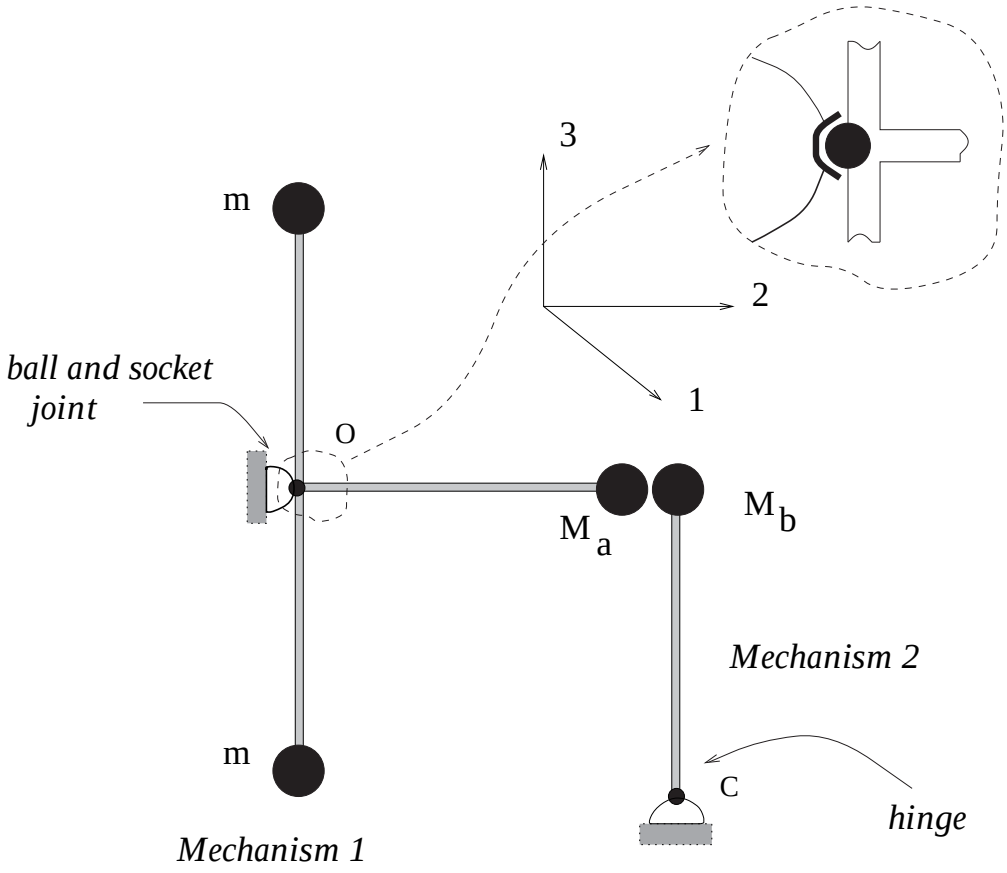

Figure 2.9: Collision configuration for general mass matrix

2.3.3 Energy Considerations

Expressions for energy lost in a general collision have been derived, for example, by Smith [55]; of those, a form that we find convenient is given below with some comments.

Recall that during the collision $M\dot{V} = \dot{P} = F$. Now, Power $= V^T F = V^T M\dot{V} = \dfrac{d}{dt}\left(\dfrac{1}{2}V^T MV\right)$, therefore Work Done $= \Delta\left(\dfrac{1}{2}V^T MV\right)$, the change in a term we call the "local" kinetic energy. Here and in the rest of this thesis, the superscript T denotes matrix transpose. The local kinetic energy is obviously not the actual kinetic energy of the system. However, in a collision, changes in one are equal to changes in the other. The initial local energy is also the maximum energy that can be dissipated in a collision; this happens when $V_f = 0$. Note that the "actual" kinetic energy of the bodies will be different in different reference frames. But the local energy, based on relative velocity, will be the same in all.

The derivation above is based on the assumption that the colliding bodies are force-response rigid. The reasoning used is not valid for impulse-response rigid bodies (because $M\dot{V} = \dot{P} = F$ is not valid for such bodies). However, bodies that are impulse-response rigid will have the same motions before and after the collision as bodies that are force-response rigid, provided the same impulse is transmitted. Given the same motions, the energies before and after must also be the same. It follows that the expression for energy dissipated must hold for both force-response bodies *as well as* impulse-response bodies.

Energy Ellipsoid: Recall the non-negative energy dissipation assumption (9) ("conservation" of energy). This yields the inequality,

$$V_f^T MV_f \leq V_i^T MV_i.$$

The right hand side is known, and constrains the final relative velocity to lie within an ellipsoid for three dimensional collisions and an ellipse for two dimensional collisions.

Using Eq. (2.4), this may be expressed as an equivalent constraint on the transmitted impulse,

$$(P + MV_i)^T M^{-1}(P + MV_i) \leq V_i^T MV_i. \tag{2.5}$$

Setting $P = 0$ yields equality; no energy is dissipated if no collision occurs.

Chapter 3

On General Rigid Body Collision Laws

This chapter presents a general discussion of rigid body collision laws, and of various properties of collision laws that are based on the assumptions discussed in Chapter 2. We introduce the idea of studying general rigid body collisions in impulse space, mention some basic geometric consequences of the nonnegative energy dissipation assumption, discuss a normality principle (apparently not noticed before), a geometric construction in impulse space showing the region accessible to general collision laws (built out of known ideas, but not presented before in complete form), collision laws based on local interaction models (such laws, which are extremely common, have a feature not pointed out before in a general setting), collision laws that are homogeneous in the velocity and/or mass (laws based on dimensionless parameters have this property which, though almost self-evident, has apparently not been explicitly mentioned in a general setting before), and finally, the number of input and output variables for a simple, general rigid body collision law.

3.1 The Impulse Space

As discussed in Chapter 2, under the usual assumptions of rigid body collision modeling with single contacts, the collisional interaction is described by impulse-momentum relations of the form of Eq. 2.4, reproduced below:

$$P = M(V_f - V_i).$$

Equation 2.4 is general (i.e., it applies to all collisions considered in this thesis). It uniquely determines the post-collision relative velocity V_f if the impulse P is known, and vice versa. For any pair of bodies colliding in a given configuration, the mass matrix M is uniquely determined and is 3×3, symmetric and positive definite. For any 3×3, symmetric and positive definite matrix M, it is possible (as shown in Chapter 2) to find a pair of colliding objects that are characterized by the same M.

Given M, V_i, and various collision parameters (incorporating physical information about the colliding objects), a collision law computes either V_f or P (the two are equivalent, by Eq. 2.4).

The actual impulse transmitted in a collision corresponds to a point in three dimensional impulse space. Also, for any M and V_i, the set of all possible values of P that a given collision law can predict, for all possible choices of its collision parameters, correspond to some region in impulse space. This region in impulse space may be called the region accessible to the collision law under consideration. Finally, the set of all *physically permissible* outcomes (by our assumptions, non-interpenetrating V_f, non-negative energy dissipation, and an impulse that does not violate the

Coulomb friction inequality) correspond to some region in impulse space. Note that while the actual impulse transmitted in any real collision depends on various physical properties of the colliding bodies that cannot be known from just M and V_i, the point in impulse space corresponding to that real collision *must* lie inside the region corresponding to all physically permissible outcomes for a given M and V_i.

In much of this thesis, collisions and collision laws are viewed geometrically in impulse space. In all discussions in this thesis of general issues in collision modeling, the mass matrix M is assumed to be a general 3×3, symmetric and positive definite matrix.

3.2 Energy Considerations

By the non-negative energy dissipation assumption, as discussed in Chapter 2, we have the inequality,

$$V_f^T M V_f \leq V_i^T M V_i,$$

which constrains the final relative velocity to lie within an ellipsoid for three dimensional collisions and an ellipse for two dimensional collisions. The equivalent constraint on the transmitted impulse is Eq. 2.5,

$$(P + MV_i)^T M^{-1} (P + MV_i) \leq V_i^T M V_i.$$

The ellipse (or ellipsoid, in 3D) defined by the above relation is referred to as the *energy ellipse (or ellipsoid, in 3D)* in impulse space (the energy ellipsoid is well known). As noted earlier, setting $P = 0$ yields equality – the origin, in impulse space, lies on the surface of the energy ellipsoid.

Some properties of the energy ellipse (ellipsoid, when applicable) are given below. Let the coordinate system chosen be such that the initial relative velocity has both components negative, i.e., it comes in to the origin from the first quadrant of the 1-2 plane (see Fig. 3.1). We conclude that:

1. The possible impulses corresponding to fixed amounts of energy dissipation lie on the surfaces of concentric ellipses (or ellipsoids), whose common center is at $P = -MV_i$ (giving $V_f = 0$).

2. Since V_i comes in from the first quadrant, and $V_i^T M V_i > 0$ (because M is symmetric positive definite), the point $-MV_i$ must lie in quadrants 1, 2 or 4 for 2D collisions.

3. The ellipse of zero energy dissipation passes through the origin with negative slope.

3.3 A Normality Principle

In this section we point out a general normality principle for rigid body collision laws.

Consider Eqs. (2.4) and (2.5). Consider all possible outcomes with identical energy dissipation, such that

$$(P + MV_i)^T M^{-1} (P + MV_i) = \alpha V_i^T M V_i, \tag{3.1}$$

for some $0 < \alpha \leq 1$. Let P correspond to a collision with this amount of energy dissipation, and let the resulting final relative velocity be V_f. It may be seen that the gradient w.r.t. P of the left hand side of Eq. (3.1) is exactly $2V_f$. Thus for any point P in impulse space, the corresponding V_f is normal to the ellipsoid of constant energy dissipation passing through that point. If $P + \Delta P$ is a "neighboring" collision with the same energy dissipation, then up to first order in small terms,

$$(\Delta P)^T V_f = 0. \tag{3.2}$$

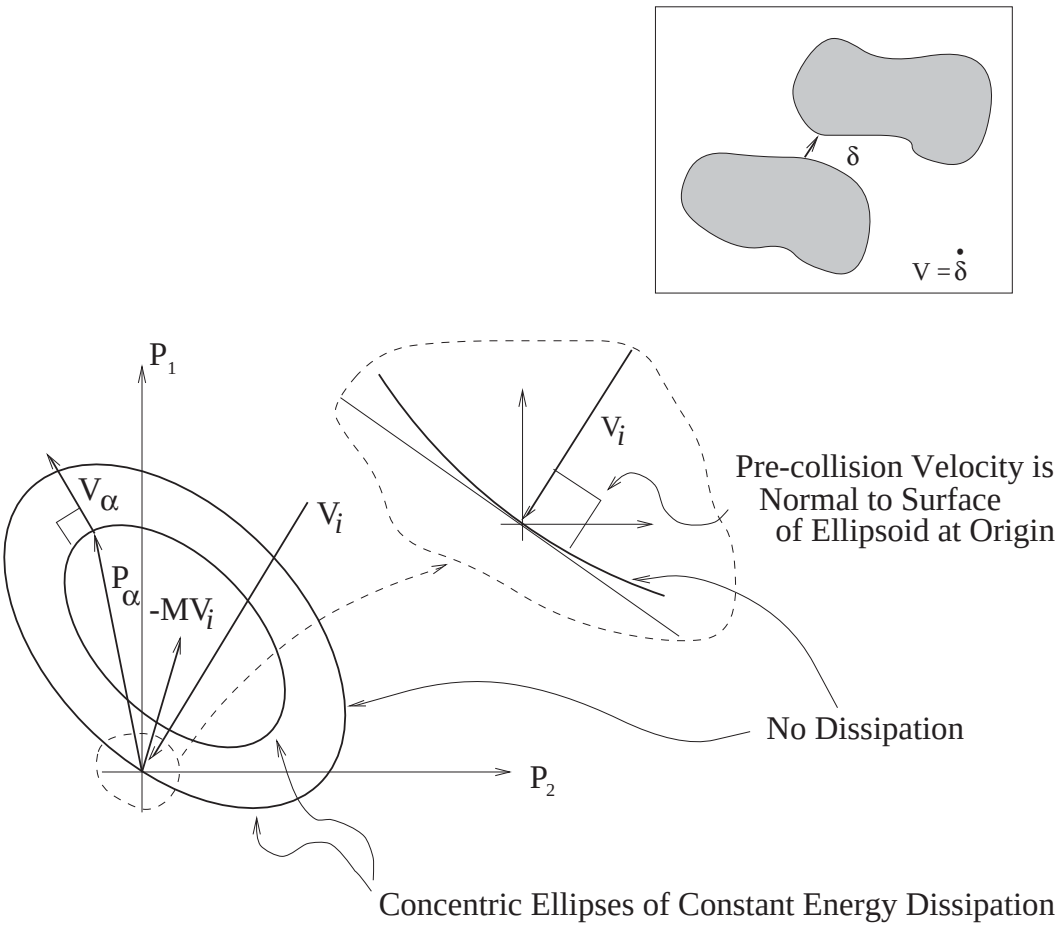

Figure 3.1: The energy ellipse

This general normality principle is illustrated in Fig. 3.1, where an impulse P_α, the corresponding ellipse of constant energy dissipation, and the resulting V_f, labeled as V_α, are shown.

The normality principle expressed by Eq. (3.2) provides some geometrical insight into some constraints on collision laws.

Since $P = 0$ implies $V_f = V_i$ and no energy dissipation, it follows that the ellipsoid of no dissipation is oriented such that the pre-collision relative velocity vector is normal to it at the origin (shown in Fig. 3.1). It follows that if the transmitted impulse is to lie inside the energy ellipsoid, then we have the necessary (*not* sufficient) condition

$$P^T V_i < 0. \tag{3.3}$$

Note that inequality 3.3 is independent of M.

It is clear that a line drawn in the impulse space of Fig. 3.1, along the direction of any P that satisfies inequality (3.3) above, will intersect the ellipsoid of no energy dissipation at two points. As shown schematically for 2D in Fig. 3.2, outer ellipsoids (with low kinetic energy dissipation)

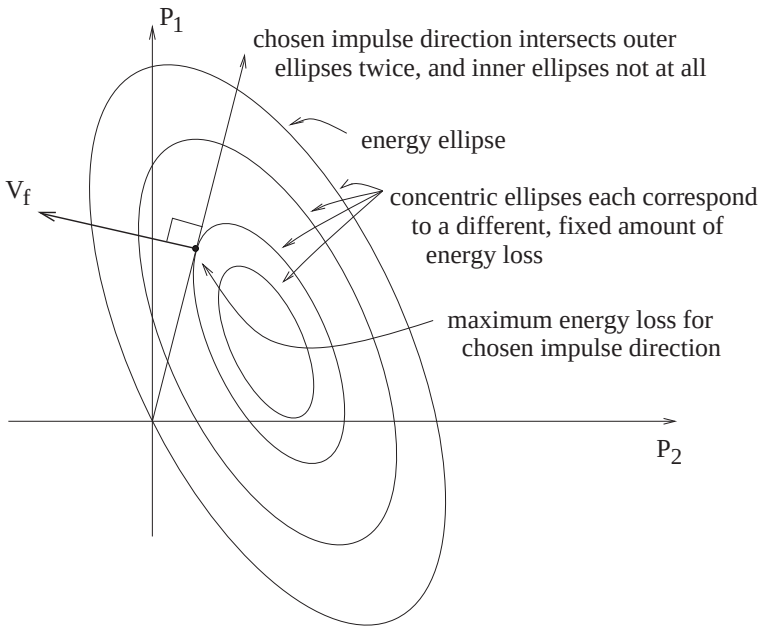

Figure 3.2: Geometrical proof of Ivanov's theorem

will generally be intersected twice, while inner ellipsoids (with high energy dissipation) may not be intersected at all. There will be a unique ellipsoid which the line will touch tangentially at one point. That point corresponds to the maximum possible energy dissipation for the chosen impulse direction. At that point, the resulting V_f will be normal to the impulse (this is in fact a geometrical proof of Theorem 3 in Ivanov [24]).

Ivanov's Definition of the Coefficient of Restitution: Using these ideas, we can briefly discuss a definition of coefficient of restitution η defined by Ivanov [24]. Let $\hat{P}$, a unit vector in impulse space, be given such that inequality (3.3) is satisfied. Assuming that the impulse transmitted in the collision is along the direction of $\hat{P}$, let E_{min} be the minimum value of the final local kinetic energy possible for an impulse in this direction (as described in the previous paragraph). Let E_i represent the initial local kinetic energy, and E_f the actual final local kinetic

energy. Then the coefficient of restitution η is defined by Ivanov to be:

$$\eta^2 := \frac{E_f - E_{min}}{E_i - E_{min}}.$$

It is shown in Section 10.5 of this thesis that this definition of a coefficient of restitution reduces to the usual definition of e for frictionless collisions (e is defined later in this chapter).

3.4 The Contact Tangent Plane and Friction

With assumptions (10) and (11) we can talk about normal and tangential components of velocities, and friction. We now discuss and geometrically interpret several basic constraints on collision laws.

We choose an orthonormal basis. The normal to the contact surface is chosen as one coordinate axis. The second coordinate axis, lying in the tangent plane, is chosen so that the pre-collision relative velocity lies in the plane of this axis and the normal. The third axis is chosen to be orthogonal to the first two. For a general three dimensional collision, with this choice of coordinates, the pre-collision relative velocity vector always lies in the 1-2 plane and can be specified using a magnitude and one angle for direction. This reduces the number of explicit input variables for the collision model to a minimum. Other choices of coordinate systems could be used to reduce the number of explicit input variables. For example, Bhatt and Koechling (e.g., [6, 5]) pick the axes in the tangent plane so as to kill certain off-diagonal terms in the mass matrix.

Friction Now we consider friction in collisions. Our ability to model rigid body collisions is so poor that we assume Coulomb's law of friction is good enough for our purposes. We do not distinguish between static and kinetic friction, and assume that the friction law is isotropic for three dimensional collisions. So we assume a single friction coefficient, μ. As Brach [11] notes, Coulomb friction may not be the dominant mechanism for tangential forces if, for example, significant indentation is present. In such cases, so long as the small contact region assumption is not violated, much of what follows is still applicable. The discussion of friction lines and friction cones is based on Coulomb friction and is not applicable.

3.4.1 Maximum Compression, Sticking, and Friction

We now define the plane of maximum compression and line of sticking. Figure 3.1 is still applicable for two dimensional collisions, if the vertical axis is along the normal and the horizontal axis is along the tangent. We may assume that the pre-collision relative velocity comes in from the first quadrant. Thus we assume that the initial 1- and 2-components of the velocity are nonpositive. We also assume for now that the initial relative velocity has a strictly negative normal component. While it is possible under certain configurations to have collisions with the normal component of the initial relative velocity exactly zero, these nongeneric "tangential" collisions require special treatment. See Wang and Mason [70] for a discussion and further references, and Chapter 7 of this thesis for an example. Much, but not all, of the treatment of grazing collisions fits in a straightforward way into the development of this thesis. For now, we note that grazing collisions must be handled as special cases.

Figure 3.3 shows the energy conservation ellipse for a typical two dimensional collision.

The *line of maximum compression* is the line joining all impulses which bring the normal component of the pre-collision relative velocity to zero. All points on the line of maximum compression lead to V_f's that lie in the tangent plane. In two dimensions, this line joins the two points on the ellipse where the tangent is vertical. In three dimensions, the line becomes a plane. The term

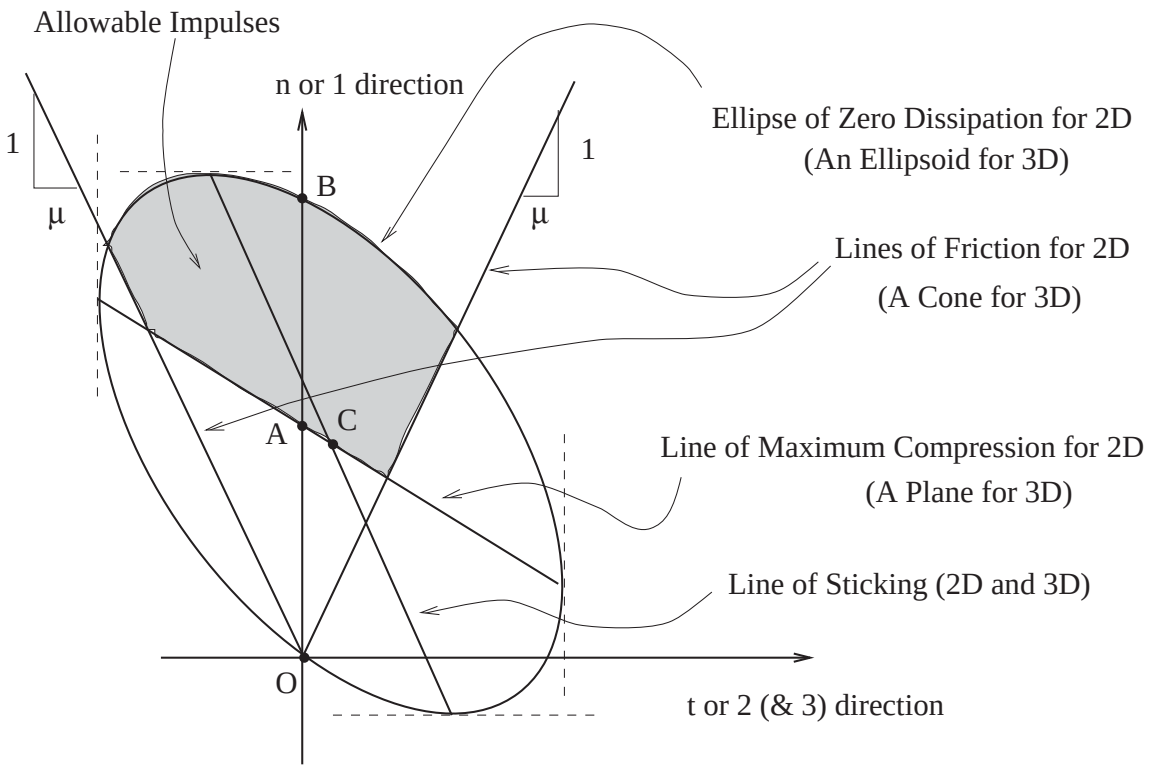

Figure 3.3: Impulse space; allowable impulses as restricted by non-interpenetration, positive dissipation and the friction inequality

"maximum compression" is based on the assumption that the normal component of the interference δ increases to a well-defined maximum as the collision proceeds in time, and then decreases to zero. The instant when the maximum is reached is referred to as the "point" of maximum compression. Clearly, the idea of a monotonic increase followed by a monotonic decrease in the normal component of δ may not be valid for bodies that are impulse-response rigid but not force-response rigid. The definition of the line of maximum compression remains valid for such bodies, because the impulse-momentum relations remain valid, although the point of maximum compression is no longer well-defined.

The *line of sticking* is the line joining all impulses for which the V_f's have no tangential component (the bodies stick). This is a line in both two and three dimensions, and joins the two points on the ellipse or ellipsoid where the tangent is horizontal.

The lines of maximum compression and sticking intersect at the center of the ellipse, C (both velocity components are zero, or $V_f = 0$). The intersection of the ellipse and the vertical axis, point B, marks an energy preserving frictionless collision. It may be shown that the intersection of the line of maximum compression and the vertical axis, point A, is midway between B and the origin O (the argument uses the linearity of Eq. 2.4 along with the fact, shown in subsection 3.4.3, that $e = 1$ corresponds to an energy preserving collision in the frictionless case).

If the bodies are not to interpenetrate, the collision must terminate in the upper half of the ellipsoid or ellipse, on or above the line of maximum compression.

If we assume that through the duration of the collision, the magnitude of the tangential component of the contact force is bounded by μ times the normal component (Coulomb friction), then the tangential and normal components of the transmitted impulse satisfy the same inequality. If F_T and F_N are the tangential and normal forces acting during the collision and P_T and P_N are the tangential and normal components of the impulse transmitted, then (integrating over the collision duration)

$$|P_T| = \left| \int_0^\tau F_T dt \right| \leq \int_0^\tau |F_T| \, dt \leq \mu \int_0^\tau F_N dt = \mu P_N, \text{ or } |P_T| \leq \mu P_N,$$

where the normal force is assumed always positive. In two dimensions, this gives us two limiting lines called friction lines, while in three dimensions it gives us a friction cone. Thus a two dimensional collision must terminate somewhere in the region of intersection of the upper half of the ellipse with the region inside the friction lines. Three dimensional collisions terminate in the intersection of the upper half of the ellipsoid with the interior of the friction cone. Points on the boundaries are allowed.

3.4.2 The Accessible Region in Impulse Space

Figure 3.3 shows the accessible region in impulse space for a typical rigid body collision with friction. Note that for high coefficients of friction, one or both of the friction lines may fail to intersect the upper half of the ellipse. The constraint of $P_N \geq 0$ is automatically satisfied for any impulse within the friction cone.

Therefore, in both two and three dimensional collisions, the transmitted impulse is restricted to lie in some well defined (closed, bounded, convex) region. It seems that all points in these regions should be accessible to a general collision law.

A collision law, given input parameter values, should pick a point in the accessible region. The various possibilities of intersection or nonintersection seen above indicate why naive algebraic collision laws frequently predict increases in kinetic energy. This violation of conservation of energy is discussed further in the next section.

3.4.3 Energy Conservation, Friction, and the Coefficient of Restitution

In one dimensional collisions, or in two or three dimensional collisions without friction, a popular parameter found in many collision models is the coefficient of restitution, e. While it has doubtful fundamental significance, it is popular because of its simplicity. It is a "constant", sometimes stated to be a material property, and usually at least assumed to be known in advance. It is generally assumed to take values between zero and one.

It is known that for many collision problems e may not be treated as a material property – for example, Goldsmith [20] presents experimental data for head on collisions between spheres, where e varies with impact velocity. More recently, Stoianovici and Hurmuzlu [58] have presented data for collisions of slender steel rods with a massive anvil, where e depends strongly on collision configuration but not much on velocity magnitude.

As mentioned in the introduction, attempts have been made to generalize the concept of a coefficient of restitution to three dimensional collisions with friction (see e.g., Stronge [59, 61, 60], Ivanov [24] Batlle [3] and Smith and Liu [57]). However, for the cases of frictionless or one dimensional collisions, the various proposed generalizations are equivalent to each other.

The coefficient of restitution, for one dimensional collisions, is defined to be the ratio of the velocity of separation to the velocity of approach, and is discussed in most undergraduate dynamics texts. For frictionless collisions in two or three dimensions, it is defined as the ratio of the normal components of these velocities. In terms of the notation used so far, the coefficient of restitution e is defined via

$$V_f^T n = -e V_i^T n,$$

where n is the column matrix $\{1, 0, 0\}^T$ representing the unit normal vector at the surface tangent.

From Eq. (2.4), we obtain

$$V_f^T M V_f - V_f^T M V_i = V_f^T P, \text{ and } V_i^T M V_f - V_i^T M V_i = V_i^T P.$$

Adding, we have

$$V_f^T M V_f - V_i^T M V_i = V_f^T P + V_i^T P.$$

From energy considerations, the left hand side is non-positive. Therefore, $V_f^T P + V_i^T P \leq 0$. For a frictionless collision, let $P = \alpha n$ for some $\alpha > 0$. This yields $V_f^T n + V_i^T n \leq 0$ (the α drops out). By our choice of coordinate system, $V_i^T n < 0$ (here we leave out the nongeneric situation of tangential collisions, discussed by Wang and Mason [70] and others), while by our assumption of no interpenetration, $V_f^T n \geq 0$. Therefore we have,

$$0 \leq V_f^T n \leq -V_i^T n.$$

If we set

$$V_f^T n = -e V_i^T n, \tag{3.4}$$

it follows that e must lie between zero and one for any energy conserving *frictionless* collision.

The coefficient of restitution has advantages as a parameter for a collision law with a simple physical interpretation and clearly defined constraints (say, $0 \leq e \leq 1$). For any frictionless collision, even if e is not known in advance, it can be measured and will be between zero and one. However, for collisions with friction, if we take Eq. 3.4 to be the definition of e, then the bound of $e \leq 1$ does not have simple interpretations in terms of energy dissipation. In terms of Eq. (2.4), for 2D collisions a given value of e constrains the impulse P to lie on a straight line in the impulse space of Fig. 3.3. While the intersection of this line with the normal or n axis (the frictionless case)

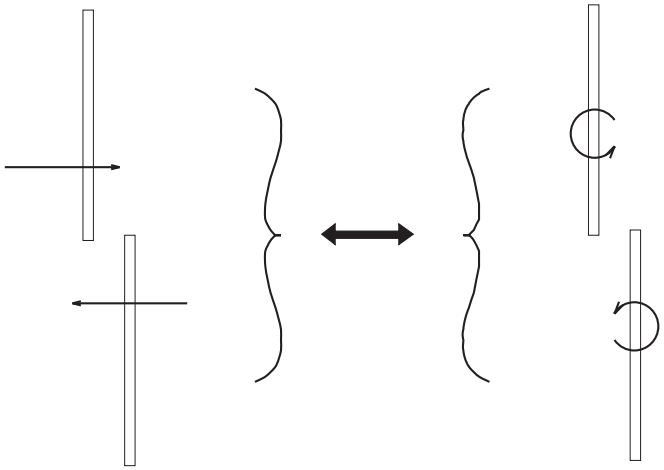

Figure 3.4: Two equivalent collisions (with same contact point velocities)

is guaranteed to be within the ellipse, the line will extend into forbidden regions if the frictional component of the impulse is allowed to be high enough (for example, point D in Fig. 3.3 lies outside the energy ellipse although it lies within the friction lines, and on a line for which $e < 1$). Similar problems occur in three dimensions.

In order to extend the use of e to two or three dimensional frictional collisions, it is necessary to either make hypotheses about the frictional effects or to redefine e in a suitable way. Some such approaches are problematic and are discussed further in Chapter 5.

3.5 Local Interaction Models

A local interaction model is one where the impulse transmitted is assumed to be determined by the velocities of only the contact points before collision. Such models ignore the particular combination of center of mass velocity and angular velocity that produces a given velocity at the contact point. Under assumptions (1) through (4) of Chapter 2, this is a reasonable approximation. Figure 3.4 shows two possible collisions between the same pair of objects. Different combinations of linear and angular velocities produce the same relative velocity at the contact point. The predicted impulse for the collision will be the same for these two cases if the model is a local one.

There is an important consequence of the local interaction assumption. Consider a collision law based on a local interaction model. The collision law predicts P, the impulse transmitted in the collision, given various model parameters and u_1 and u_2, the absolute velocities of the contact points on the two bodies before the collision.

Let the collision law be expressed as

$$P = f(u_1, u_2, \text{ mass matrix, parameters }).$$

Here, the mass matrix is the one from Eq. (2.4), and "parameters" refers to any general inputs to the collision model, like material properties, direction of local normal, local radii of curvature, coefficients of friction and restitution, etc. For a local model, we assume that "parameters" does not include any further information about the instantaneous velocities of the bodies. Given this, we rewrite the equation above as

$$P = g(u_1 - u_2, u_2, \text{ mass matrix, parameters }).$$

Note that all arguments of the function g other than the second one have the same values in all reference frames. By frame invariance, g cannot depend on its second argument, u_2. This shows that local interaction models take as inputs only the relative velocity at the contact point; absolute velocities are irrelevant. For such models, the form of Eq. (2.4) becomes especially convenient.

3.6 Collision Laws Homogeneous in Velocity and/or Mass

Consider a general collision law, stated in terms of relative velocities in the form

$$V_f = g(V_i, M, \text{ parameters }). \tag{3.5}$$

We call the collision law homogeneous of degree α in the input velocity V_i if, for any positive number k,

$$g(kV_i, M, \text{ parameters }) = k^\alpha g(V_i, M, \text{ parameters }),$$

for every choice of V_i, M, or "parameters". Linear laws are special cases of laws that are homogeneous of degree one. Collision laws homogeneous of degree α in the mass matrix are defined in an analogous way.

Example from Granular Flow: Consider some evidence from the field of granular flow. Jenkins [29] says:

> When a granular material is sheared at a sufficiently high rate, the shear stress and the normal stress required to maintain its motion are observed to vary with the square of the shear rate ....

Thus, a twofold increase in the mean speed of the flow leads to a four fold increase in the mean shear stress. While this may be the consequence of many possible things, one simple hypothesis that leads to this result is that the collision law is homogeneous of degree one in the input velocity. This may be seen as follows. Consider a given granular flow simulation, calculated on the basis of such a collision law. Neglect the effects of gravity (valid for sufficiently high shear rates). Then, speeding each particle up by a factor of two gives another valid solution to the system equations if the collision law is homogeneous of degree one. The net momentum flux across any real or imagined surface is then twice-doubled, once for the momentum of the grains and once for the frequency of surface crossings. Hence the stress is quadrupled.

In reality models that are homogeneous of degree one in velocity might only be approximately valid over some range of velocities. For example, the coefficient of restitution for even one dimensional collisions is known to depend on the approach velocity (see Goldsmith [20]). Thus, "real" collision laws are not homogeneous of degree one in velocity.

While the assumption of homogeneity of degree one in the input velocity may seem to be a strong one, essentially all popular collision models fall in this category. This is because (see Eq. (3.5)) if all the parameters in the collision model are dimensionless then, in order to be dimensionally consistent the collision law automatically has to be homogeneous of degree one in the input velocity *and* homogeneous of degree zero in the mass matrix. In particular, models based solely on dimensionless parameters like coefficients of restitution and friction have this property.

Clearly, it is possible to have collision models that do not have this property. For example, the speed of sound in a material may be one of the parameters in a collision model. The corresponding collision law need not be homogeneous in the input velocity.

3.7 The Number of Input Parameters

Let us consider collision models for which all the input parameters are dimensionless. As discussed above, such models are somewhat unrealistic, but they are popular because of their simplicity.

The coefficient of restitution is a widely used dimensionless parameter for collision models. Its fundamental validity is doubtful. But it has a clear interpretation in terms of energy dissipation, at least in frictionless collisions, and therefore is a somewhat meaningful parameter. For example if someone (say, Isaac Newton[1]) says, "The coefficient of restitution for collisions between glass spheres is 15/16," the statement conveys simple and clear information, again, at least for frictionless collisions. It seems desirable that all the parameters in a collision model should have similarly simple interpretations. This places practical limitations on the number of parameters a model may have.

It is worthwhile to think about the practical use of collision models. We foresee two possible uses.

Sometimes the simulation of a collision is part of a larger dynamic simulation, and is only a small part of the whole matter under investigation. The same collision model may be used for bodies of widely different shapes, masses, and material properties. Perhaps the problem might involve collisions of linkages (see e.g., Bhatt and Koechling [8] or Marghitu and Hurmuzlu [38]). The chance is slight that a collision model will make consistently accurate predictions under such circumstances, and it may be practical to use a simple model that will hopefully not make wildly erroneous predictions. For such applications, the number of parameters should be low, perhaps two or three.

Another situation might be as in granular flow, where the modeler is interested in a large number of collisions between very specific kinds of bodies (see Drake and Walton [16] and Thornton and Randall [66]). For example, the modeler may be interested in all possible collisions between pairs of soybeans, or glass ellipsoids of a given aspect ratio. In such situations, it may be worthwhile to use models using several parameters, chosen to fit available experimental data. However, even for such problems, researchers might prefer simple models (see e.g., Foerster et al. [17], Jenkins [30]).

It appears from experimental data that the (2D) collisional behavior of spheres and of disks can be fairly well characterized by models with two parameters in addition to a friction coefficient (as in Foerster et al. [17]). As Brach mentions in his book [11], good experimental data for truly 3D collisions is not readily available. It might be worthwhile to consider 3D models also with only two parameters in addition to a friction coefficient. Recall, however, that the accessible region in impulse space for such collisions is also 3D, for any given nonzero coefficient of friction. In order to properly parameterize this region, one would therefore need at least three parameters in addition to a friction coefficient.

Let us assume for now that a reasonable rigid body collision model might take two or three dimensionless parameters over and above the mass matrix, the pre-collision velocity and the friction coefficient. The output from the collision model will be the post-collision relative velocity or the transmitted impulse. Although the restrictions on the model are strong, the form of the collision law itself is not specified. Several rigid body collision models are designed within these restrictions.

All inputs and outputs are listed in Table 3.1 below. In Chapter 4, we discuss various simple configurations where one or more of the input or output parameters are known from symmetry considerations. In particular, we indicate why collisions between spheres or disks are easy to study and model.

[1] See Stronge [59]

Table 3.1: Counting variables for simple rigid body collision laws

Variables	**2D**	**3D**	**Comments**
Mass	2	5	number of mass matrix components minus one
Velocity	1	1	angle from normal (coordinate axes lined up with pre-collision velocity, which is scaled to unit magnitude)
Friction coefficient	1	1	friction is assumed given *a priori*
Other parameters	2	2 or 3	perhaps one for normal and others for tangential restitution
Outputs	2	3	post-collision velocity or net impulse

Chapter 4

Some Simple Collision Configurations

We now consider some simple collision configurations, and their place in the general framework of three dimensional collisions. We then consider collisions between ellipsoids as a departure from collisions between spheres, and discuss some modeling issues that arise. The ideas in this chapter are not new, but a general discussion of these ideas has apparently not been published before.

4.1 One Dimensional Collisions Between Three Dimensional Bodies

One dimensional collisions have been studied in great detail from both theoretical and experimental viewpoints (see Goldsmith [20]).

Consider a collision where one eigenvector of the mass matrix is along the normal to the tangent plane, and the pre-collision relative velocity is also along this normal. For collisions between two ellipsoids, three possible configurations are shown in Fig. 4.1. If we assume isotropic behavior, then the rebound velocity must also be along the normal due to symmetry. Such a collision is one dimensional.

For one dimensional collisions, the impulse must also be along the normal, and the coefficient of restitution is a meaningful parameter. There are no frictional effects.

4.2 Two Dimensional Collisions Between Three Dimensional Bodies

Now consider a collision where the pre-collision relative velocity and the normal direction lie exactly in the plane of two of the eigenvectors of the mass matrix. If the transmitted impulse lies in the same plane, then the change in relative velocity and the final relative velocity also lie in the same plane. There is no action along the direction of the third eigenvector. We refer to such collisions as two dimensional. As a specific example, consider an arbitrary collision between two spheres. Here, the eigenvectors may be chosen appropriately to make the problem two dimensional.

In this thesis, for the most part, we consider models where collisions that start off as one or two dimensional remain one or two dimensional, respectively. This assumption is common in the literature and follows from isotropic constitutive behavior.

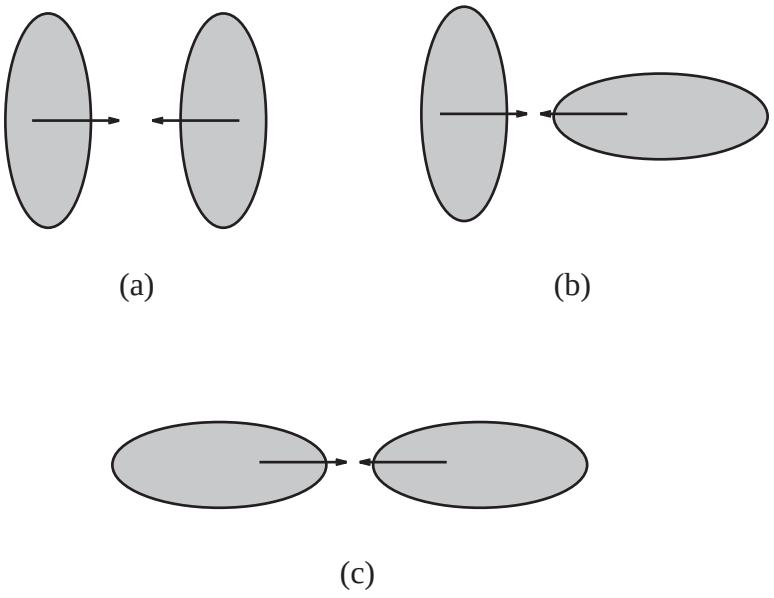

Figure 4.1: One dimensional collisions between ellipsoids

4.3 Collisions Between Spheres and Between Disks

Let two uniform spheres be made of given materials, and have given, possibly different, radii. Assume that all collision and mass properties of these spheres are isotropic and homogeneous. All points on the surface of any sphere are then identical. Let us consider all possible collisions between these spheres.

The problem has a lot of symmetry. The mass matrix for any collision between the two spheres is always the same. The friction coefficient and all other parameters are fixed, too. We assume dimensionless collision parameters. Therefore the collision law is homogeneous of degree one in the pre-collision velocity, which we may scale to unit magnitude. There is only one input to the collision model that changes from collision to collision, and that is the angle that specifies the direction of the pre-collision relative velocity (see Table 3.1).

The same arguments apply for collisions between uniform disks in a plane.

Collisions between spheres and between disks are two dimensional. There are only two output quantities – say, the two components of the post-collision relative velocity. Both these quantities should therefore be expressible as functions of one variable, the input angle. The experimental data of Foerster et al. [17] and Maw et al. [40] for colliding spheres and disks, respectively, show that these quantities are indeed well approximated as functions of one variable.

For collision laws restricted to the case of spheres or disks, note that it is not necessary to know the general form of the collision law, nor is it necessary to define what the dimensionless parameters are. Under the assumption of homogeneity in velocities, experimental data can be plotted as two scalar functions of a single scalar variable. An arbitrary (say, bilinear [17]) curve fit to the data then provides a valid collision model. The parameters used in the curve fit need not have any physical interpretations that apply to general collisions.

Collisions between aspherical bodies are much more complicated than those between spheres, because it is necessary in these cases to address detailed questions that are irrelevant for spheres.

4.4 Collisions Between Ellipsoids

For slightly more complicated bodies than spheres, it might seem tempting to consider collisions between ellipsoids. However, even with ellipsoids the problem attains almost full complexity. This is discussed next.

What is the intended scope of our collision model? Is it intended for all ellipsoidal bodies, for pairs of ellipsoids of given materials, or only for collisions at specific locations on these ellipsoids? Let us assume that we are looking for a collision model for all possible collisions between two given, identical ellipsoids.

First consider the mass matrix. Unlike the case of spheres, the particular contact point on each ellipsoid needs to be known. Thus the mass matrix may be specified, in principle, by two coordinates for each contact point on the two ellipsoids, the relative rotation of the ellipsoids about the normal at the contact point, as well as the direction of the tangential component of the pre-collision relative velocity. That is a total of six parameters. If we use only dimensionless parameters, as discussed earlier, then the mass matrix may be scaled by a constant. That reduces the dimension by one. So in terms of number of inputs, the mass matrix is already five dimensional, the maximum for three dimensional collisions.

Recall that the inputs to the collision model include the coefficient of friction and two other dimensionless parameters. Do the values of these three inputs vary with the location of the contact points on the colliding bodies? That makes each of them arbitrary functions of four variables (two for the location of the contact point on each body). Alternatively, the input parameters to the model may be assumed constant for a given pair of ellipsoids.

What is a good choice for these parameters? Perhaps one parameter might be the observed coefficient of restitution in head on (one dimensional) collisions, where friction plays no role. This seems like a reasonable choice if only because in the one dimensional case the model reduces to Newtonian restitution. However, will the observed coefficient of restitution be constant for a range of impact speeds? Will it be constant for the three possible head on configurations shown in Fig. 4.1? Probably not. The amount of variation observed in experiments will give an indication of the least amount of error we should expect in the predictions of a collision model based on this parameter[1]. We still have to decide how the model should use this parameter to predict the results of general three dimensional collisions with friction.

A choice for the second parameter might be based on the tangential restitution, or the relationship between the tangential components of the pre-collision and post-collision relative velocities for nearly head-on collisions. There are some suggestions in this regard (see Brach [11] or Jenkins [30]), but it is not known how best to think about tangential restitution for collisions between aspherical bodies. Several models do not include tangential restitution effects explicitly as parameters. Such models include Smith's model [55], Routh's model [52], or models based on the contact behavior of elastic spheres [44], such as those of Maw et al. [40] and Jaeger [27]. These and other models are discussed next.

[1]The data of Stoianovici and Hurmuzlu [58] suggests that the variation might be small for ellipsoids that are not too elongated.

Chapter 5

Some Currently Known Collision Models

Assumptions (1) through (11) of Section 2.2 and the local interaction assumption of Section 3.5 might seem at first to be very restrictive. However, a large variety of collision models may be constructed based on even these strong assumptions. In this chapter we briefly examine some such models proposed in the literature. All of the models considered satisfy assumptions (1) through (11) about rigid body collisions. It is not clear which one, if any, is superior[1].

In general, collision models may be divided into two groups[2]. We loosely refer to the first group as *algebraic*. These models assume that the inputs and outputs satisfy various simultaneous algebraic or transcendental equations. The parameters in the collision model appear in these equations. There might be checks for various physical constraints, and division into cases and sub-cases. Algebraic models only depend on impulse-response rigidity in the colliding bodies. The second group of collision models may be called *incremental*. Models of this group are based on differential or evolution equations. Each model has a set of simultaneous differential equations, usually ODE's, which are solved using initial conditions calculated from the inputs. Incremental rigid body collision models are based on an assumption of force-response rigidity.

5.1 Algebraic Models

5.1.1 All-Linear Equations; Brach's Approach

The simplest models, in implementation, are those in which the algebraic equations are all linear. Brach [11] has looked into collision models of this type. The parameters used in the collision law are dimensionless ratios of various physical quantities. Newtonian or kinematic restitution is used in the normal direction. An impulse ratio (or two ratios, in three dimensions) gives the tangential impulse in terms of the normal impulse. In this way, the details of the frictional interaction are not

[1] It is really not even clear what "superior" means in the context of this chapter. The suitability or unsuitability of a collision model depends on the specific application, which is not assumed to be known in this general discussion. Moreover, there is very little experimental data available in the literature about the three dimensional collisional behavior of general bodies with significant frictional interaction.

[2] This same division of collision models into two categories is found in Mac Sithigh [37], though his treatment of evolution methods concentrates only on Routh's method and is thus less broad (though more detailed in its analysis of Routh's method) than the survey presented here.

predicted but assumed known. Various other such ratios - all nondimensional - are assumed known as needed. When these ratios are known and used as input parameters to the collision model, the final velocities may be calculated by solving systems of simultaneous linear algebraic equations.

The bounds on these nondimensional ratios – say, in order to not violate energy conservation (assumption (9), Section 2.2) – depend on the specific collision configuration and are only known through implicit nonlinear inequality constraints. For general collision modeling, there is no specific collision configuration that is known *a priori*; consequently the bounds on the collision parameters are themselves unknown in a general setting.

The values of the parameters used in Brach's models, for a given pair of bodies, are understood to be not constants but rather quantities measured through experiments. However, it is not clear that these "parameters" *can* be measured in experiments that do not involve re-creating the collision being modeled. As an example, consider the ratio of tangential to normal impulses in the collision of an object with a massive wall (the *impulse ratio*). In reality, this ratio varies with the angle made with the normal direction by the initial relative velocity vector (incidence angle), as well as the configuration of the body itself. If the particular impulse ratio for a given incidence angle and collision configuration is assumed to be measured experimentally, then it is an unsatisfactory collision parameter in the sense of item (8) of Section 2.1, since it cannot be measured in an independent experiment.

In principle, the impulse ratio can be measured in a series of experiments for collisions of a given pair of bodies, in a variety of collision configurations, with different incidence angles. However, it is not clear that storing the impulse ratio as a function will be simpler or easier than storing, say, the post-collision relative velocities themselves.

In conclusion, Brach's approach allows a modeler to pick a point in impulse space, based on the values of certain collision parameters. Whether or not the point picked is inside the region that is physically permissible, i.e., allowed by fundamental constraints, has to be determined in a separate calculation. At the same time, there is no point inside the accessible region that *cannot* be predicted by the collision law, since all points are accessible for some choices of the collision parameters[3]. There is no basis for specifying the values of the collision parameters, except either in the simplest cases such as collisions of spheres, or after already modeling or experimentally studying the same collision. Consequently, the essence of the approach is to choose some values of the collision parameters that result in an impulse being predicted that is inside the accessible region. This is an indirect way of picking a point inside the accessible region based either on intuition, guesswork, or extra information. In this sense Brach's approach is equivalent to a change of variables.

5.1.2 Kane and Levinson's, or Whittaker's, Model

A commonly used collision model, described briefly in Whittaker's text [71], and described in Kane and Levinson's text [32] with explicit attention to the direction of the tangential component of the contact impulse, uses kinematic restitution and a frictional impulse based on the post-collision relative velocity direction. The collision law is expressed by the equation

$$V_{fN} = -e\, V_{iN},$$

and the condition that either **(a)** $V_{fT} = 0$ and $\|P_T\| \leq \mu P_N$, or **(b)** $P_T = -\mu P_N \dfrac{V_{fT}}{\|V_{fT}\|}$. These conditions, in addition to Eq. 2.4, are sufficient to determine the outcome of the collision. This

[3]If one allows $e > 1$ (there is no reason not to).

collision law can predict large *increases* in system kinetic energy, as noted by Kane and Levinson ([32], pg. 438), and as also demonstrated by a numerical example in Section 7.5 of this thesis. For a graphical view of increase in energy predicted by this collision model, for the case of a sticking collision in 2D, see Fig. 7.5.

5.1.3 Smith's Model

Some overly simple models, such as Kane and Levinson's model, violate conservation of energy for apparently reasonable values of various input parameters. This feature of collision models has attracted some attention of late, and several relatively recent papers on the topic check for energy conservation.

An algebraic model proposed by Smith [55] uses the kinematic definition of the coefficient of normal restitution, and a frictional impulse that is defined using an intuitively appealing weighted average of the pre-collision and post-collision tangential components of the relative velocities. Smith shows that this model is guaranteed not to create kinetic energy in a collision, i.e., it satisfies assumption (9).

In terms of the notation used in this thesis, let P_N be the normal component of the transmitted impulse, P_T the 2-vector denoting the tangential component of the impulse, V_{iN} and V_{fN} the normal components of the pre-collision and post-collision relative velocities, and V_{iT} and V_{fT} the 2-vectors denoting the tangential components of the pre-collision and post-collision relative velocities respectively. Then for Smith's model,

$$P_T := -\mu P_N \frac{\|V_{iT}\|\, V_{iT} + \|V_{fT}\|\, V_{fT}}{\|V_{iT}\|^2 + \|V_{fT}\|^2}.$$

The kinematic ("Newtonian") definition of the coefficient of restitution e is used, i.e.,

$$V_{fN} = -e\, V_{iN},$$

where e is assumed to lie between zero and one. The impulse P and the relative velocities V_i and V_f still must satisfy Eq. (2.4). This provides three simultaneous equations which must be solved for P_N and V_{fT} (two equations in 2D):

$$P_N \left\{ \begin{array}{c} 1 \\ -\mu \frac{\|V_{iT}\|\, V_{iT} + \|V_{fT}\|\, V_{fT}}{\|V_{iT}\|^2 + \|V_{fT}\|^2} \end{array} \right\} = M \left\{ \begin{array}{c} -(1+e)\, V_{iN} \\ V_{fT} - V_{iT} \end{array} \right\}. \tag{5.1}$$

Smith's model has the following attractive features. The intuitive meaning of the coefficient of restitution is clear. Energy dissipation is assured. The frictional impulse incorporates direction and magnitude information about the tangential components of both pre-collision and post-collision velocities, and satisfies the friction inequality.

As Smith himself indicates in his paper, the model ignores actual details of the frictional interaction between the bodies. It is quite likely that the predictions of the model will be inaccurate in many cases.

Unfortunately, equation (5.1) is strongly nonlinear. In terms of actual implementation of this model, the equation will most generally be solved by iterative numerical methods. For nonzero μ, the equation might possibly have multiple solutions; of these, any solutions with negative P_N are physically inadmissible and are automatically discarded. In numerical experiments with this model, it is sometimes troublesome to find a good initial guess that converges to a physically admissible solution ($P_N > 0$). Mac Sithigh [37] discusses Smith's model, and mentions that the equations might have zero or multiple physically admissible solutions. However, he does not provide

any examples. I have not been able to prove that this system always has exactly one physically admissible solution; neither have I been able to find a counterexample. Existence of solutions for Smith's law can be proved (see Section 10.3).

Note that for $\mu = 0$ the equation always has a unique solution. (Uniqueness may be proved using (a) the fact that for $\mu = 0$ the equation is linear, and (b) that positive definiteness of M implies that its (1,1) element is nonzero and its trailing 2×2 block is invertible.) That this solution is physically admissible ($P_N \geq 0$) is also easy to show. Let $P = \alpha n$, where n is the unit normal in the positive direction. Then

$$\alpha n = M\Delta V, \text{ therefore } \alpha(\Delta V)^T n = (\Delta V)^T M \Delta V,$$

but $(\Delta V)^T n$ is positive due to the specified restitution, while $(\Delta V)^T M \Delta V$ is positive due to positive definiteness of M. It follows that $\alpha > 0$.

In numerical examples, for finite μ, the solution can be found using continuation methods starting from the $\mu = 0$ solution (see Section 10.3). In practice, though, this method is roughly equivalent to solving a differential equation, which reduces the appeal of this algebraic approach to some extent.

A weakness in the predictive capability of Smith's model is its lack of control over tangential restitution. For many simple cases (say, as in Jenkins [30]) the idea of tangential restitution as an independent parameter might be attractive. For Smith's model,

1. in the limit of small incidence angles for fixed, nonzero μ, the coefficient of tangential restitution becomes unity for spheres (or any pair of objects for which the mass matrix is diagonal);

2. in the limiting case of μ arbitrarily large, for fixed pre-collision relative velocities and fairly general mass matrices, the tangential restitution is again unity.

Thus, this model can predict superball-like behavior (see Garwin [18]) but cannot, for example, predict less elastic tangential restitution for nearly head-on impacts of spheres. The degree of restitution in the tangential direction is not an independent parameter in Smith's law; it depends on the friction coefficient. This differs from the normal direction where his restitution is directly specified by the input parameter e.

5.1.4 Routh's Model in 2D

Routh's method is incremental in three dimensions, and we will discuss it again in that context. However, in two dimensions the differential equations can be integrated in closed form. Routh's model in two dimensions reduces to an algebraic model which has been investigated thoroughly by Wang and Mason [70]. In this model, the coefficient of normal restitution is defined as a ratio of impulses, specifically the normal component of the accumulated impulse from the point of maximum compression to termination divided by that from the start of collision to the point of maximum compression. This definition of the coefficient of normal restitution is credited to Poisson [49] by Routh [52], and is sometimes called kinetic restitution. The frictional impulse is assumed to accumulate according to Coulomb's law of friction whenever there is nonzero tangential relative velocity. This approach, too, is guaranteed to conserve energy in 2D collisions, as shown through various formulas by Wang and Mason.

One of the key features of Routh's model is that it assumes zero tangential compliance in the contact region. It cannot incorporate tangential restitution, and therefore cannot predict superball-like behavior (reversal of tangential relative velocity for impacts of spheres) for any choice of input parameters. This is a consequence of the infinite tangential stiffness assumed in Routh's law. Since

the surfaces of most real bodies have comparable compliances in normal and tangential directions, Routh's method makes inaccurate predictions in many cases. Occasionally one encounters a belief that Routh's model is "true". For example, Mac Sithigh [37] compares the prediction of Routh's model in a 3D problem with that of Smith's model, and refers to Routh's model as "more precise". In fact, both models are capable of making inaccurate predictions. Smith's model is not based on any model of material behavior ascribed to the colliding bodies, and consequently has small claim to realism. On the other hand, Routh's model is based on an unrealistic assumption, and can equally well lead to erroneous predictions.

5.1.5 Pfeiffer and Glocker's 2D Model, for Single Impacts

Pfeiffer and Glocker [47] (see also Glocker and Pfeiffer [19]) present a unified treatment of the dynamics of mechanical systems with unilateral contacts. Their treatment of simultaneous impacts (see the discussion in Section 10.1) is based on the hypothesis that maximum compression (see Section 3.4) occurs simultaneously at all impact locations where nonzero impulse is transmitted in the compression phase. Their development is only extended to 2D collisions. Their proof of energy conservation (see Section 3.4) in their paper [19] rests on the assumption that for a symmetric positive matrix A, a diagonal matrix D with nonnegative elements all between 0 and 1, and any column matrix u, the inequality $0 \leq u^T DADu \leq u^T Au$ holds. Since this is not always true, the proof is incorrect. It is not known whether the result (energy conservation) is correct or not. It does appear to be correct for single impacts, for in that case the matrix D reduces to a scalar. In the more recently published text [47], the oversight has been corrected, and at present energy conservation remains unproven for their model, for the case of simultaneous frictional impacts with different coefficients of restitution at different impact locations.

The restriction of Glocker and Pfeiffer's collision law to single frictional impacts in 2D is presented below. The collision law is based on a kinetic or impulse-based definition of the coefficient of restitution, somewhat similar to Routh's approach described above. It is necessary, as in all collision laws with kinetic restitution, to identify a "point of maximum compression", which depends on the path followed in impulse space and consequently on the incremental model used (for incremental laws). In algebraic collision laws, the point of maximum compression must be defined by additional algebraic relations.

We retain the subscripts i and f for pre- and post-collision quantities, and introduce the extra subscript C for quantities at the point of maximum compression. As before, subscripts T and N refer to tangential and normal components, respectively. The impulse transmitted in the collision is viewed as composed of two parts, P_C from start of collision to point of maximum compression, and P_E from point of maximum compression to termination (this latter period is usually called the "phase of expansion"). Thus, we have $P = P_C + P_E$, and the schematic

$$V_i \quad \overset{P_C}{\rightarrow} \quad V_C \quad \overset{P_E}{\rightarrow} \quad V_f.$$

The compression phase, somewhat similarly to Kane and Levinson's treatment, is given by the equations $M(V_C - V_i) = P_C$, $V_{CN} = 0$, and the condition that either **(a)** $V_{CT} = 0$ and $|P_{CT}| \leq \mu P_{CN}$, or **(b)** $P_{CT} = -\mu P_{CN} \dfrac{V_{CT}}{|V_{CT}|}$.

The normal component of impulse transmitted in the expansion phase is defined simply by $P_{EN} = e\ P_{CN}$, where e is the coefficient of normal restitution. The tangential component of impulse is defined in a slightly complex manner. Consider intermediate variables α, μ^*, and P_T^* defined as follows: $0 \leq \alpha \leq 1$ is an arbitrary scalar, $\mu^* := (1 - \alpha)\mu$, and $P_T^* := \alpha\mu P_{EN}$. Now,

the tangential interaction in the expansion phase is given by the condition that either **(a)** $|P_{ET} - P_T^* \text{ sign}(P_{CT})| \leq \mu^* P_{EN}$ and $V_{fT} = 0$, or **(b)** $P_{ET} = P_T^* \text{ sign}(P_{CT}) - \mu^* P_{EN} \dfrac{V_{fT}}{|V_{fT}|}$. Here, the quantity P_T^* represents "stored impulse" and may be used to model tangential restitution, such as in superball-like effects (see [18]). The quantity α is defined indirectly in terms of two new collision parameters, $0 \leq \nu, e_t \leq 1$, as follows:

$$P_T^* \text{ sign}(P_{CT}) = \frac{1}{2} \left(\mu\nu P_{EN} \text{ sign}(P_{CT}) + e e_t P_{CT} \right).$$

That this implies $0 \leq \alpha \leq 1$ may be seen by noting that

$$P_T^* = \frac{1}{2} \left(\mu\nu P_{EN} + e e_t |P_{CT}| \right),$$

which implies in turn that

$$\begin{aligned} \alpha \equiv \frac{P_T^*}{\mu P_{EN}} &= \frac{1}{2} \left(\nu + \frac{e e_t |P_{CT}|}{\mu P_{EN}} \right), \\ &\leq \frac{1}{2} \left(\nu + \frac{e e_t \mu P_{CN}}{\mu P_{EN}} \right), \\ &= \frac{1}{2} \left(\nu + \frac{e_t \mu P_{EN}}{\mu P_{EN}} \right), \\ &= \frac{\nu + e_t}{2} \leq 1. \end{aligned}$$

Glocker and Pfeiffer's model, if extended to 3D, would require further assumptions about the directions of the frictional impulses. Such a 3D extension is not available at this time.

5.2 Incremental Models

In this section we consider several incremental rigid body collision models. When we model the impact process through differential equations, we usually expect to obtain better accuracy in return for the extra effort.

For the purposes of modeling a very specific type of problem, say the impact of a rigid mass falling vertically onto the center of a simply supported beam, it may be possible to construct realistic models that incorporate many of the important dynamic effects involved in the problem. It is likely that the predictions of such models will provide deeper understanding of the whole process. Goldsmith's book [20] contains several analyses of this kind. Note that such models are not rigid body collision models, since the deformations of the entire bodies are monitored in the analysis. As discussed in the introduction, solving collision problems for general bodies, with accurate modeling of deformations in the entire bodies as well as of the contact interaction, will usually involve complicated numerical methods (like FEM, or the somewhat simpler approach discussed in Chapter 9). Such approaches are time consuming, and may be inaccurate anyway due to lack of sufficient information about material and contact behavior.

A class of models that lies in between the algebraic models and the finite element models is based on the assumption that the colliding bodies are force-response rigid. The contact interaction is assumed to be governed by some given law, usually one that only depends on the relative motions in the contact region (local interaction). The contact region itself is assumed small, and the contact interaction is pseudo-static. Under these approximations, the collision is governed by ordinary

differential equations which are integrated (usually numerically) until some specified termination condition is reached.

Incremental collision models will make accurate predictions if the correct contact law is used to model collisions of force-response rigid bodies. Even for bodies that are impulse-response rigid but not force-response rigid, if (by some coincidence) the correct net impulse is predicted by the collision calculation, then the correct net outcome will be predicted for the collision even though the predicted time history of contact forces is inaccurate. Finally, incremental collision models using physically based contact mechanisms (such as spring-dashpot type interactions) will automatically satisfy fundamental restrictions such as non-negative energy dissipation; to this extent, they offer a viable modeling approach for collisions of general bodies.

We discuss some incremental models in this section (a discussion of such models in the context of granular flows may be found in Walton [69]).

5.2.1 The Hertz Contact Model

We first mention the Hertz contact model for head on collisions of homogeneous, isotropic, linearly elastic spheres. A discussion of this model may be found in Goldsmith [20]. The spheres are assumed to accelerate as rigid bodies under the action of contact forces. The interference between the spheres is calculated by integrating the velocities of the spheres. The contact force is calculated using the interference, according to the Hertz contact solution (it is of the form $F = k\ \delta_n^{3/2}$, where F is the normal force, δ_n the normal component of the interference, and k a constant).

Villagio [67] presents some approximate correction terms to the Hertz contact solution, calculated from an approximate solution to an integral equation describing the static, elastic contact of a heavy sphere against a rigid surface. It is found that the finite size of the contact region introduces a correction to the Hertz contact solution; the correction is small as long as the radius of the contact region is small compared to that of the sphere. Villagio's proposed solution provides finer estimates than the simpler Hertz contact solution, of collision times and contact forces for ideal elastic spheres.

The high initial compliance of Hertz contact gives the collision a relatively slow time scale compared to the wave transit time in the spheres, and the local model is a good one for light impacts. One of the big advantages of such a model is that it provides estimates of actual force histories and interaction times. One disadvantage is that this approach cannot incorporate inelastic collisions – restitution is always perfect. While this can be "fixed" (see Goldsmith [20], Stronge [65] or Lankarani and Nikravesh [35], for example), the fixes usually involve *ad hoc* assumptions about dissipative material models, which would probably be inaccurate for any other than a few special bodies.

5.2.2 The Mindlin-Deresiewicz Contact Model

Extensions of the Hertz contact collision model to frictional collisions in 2D and 3D have been proposed. These models assume that the contacting bodies have locally spherical surfaces, where the contact behavior follows the approximate solution given by Mindlin and Deresiewicz [44], or approximations to it. For such analyses and applications, see Maw et al. [39, 40], Jaeger [27, 28] or Thornton and Randall [66].

In the Mindlin-Deresiewicz contact solution the normal components of tractions are given by the Hertz contact solution. The tangential tractions and displacements, or the state of the circular contact region, is given by a function of the radius. Incremental changes to the state depend on both the current state as well as the increments in the net relative normal and tangential

displacements. If the current distribution of tangential tractions and displacements (a function of radius) is considered to be a set of "state variables", then this history dependent contact model is infinite dimensional.

The Mindlin-Deresiewicz solution to the contact problem appears attractive because it might be realistic for perfectly elastic frictional spheres with smooth surfaces undergoing light impacts. It provides, as in head on collisions, estimates of actual forces and times. On the other hand, it has a few disadvantages. As with Hertz contact, restriction to a normal restitution of unity is still a problem. Moreover, in numerical implementation, it is complicated and time consuming because of its strong history dependence/high dimensionality. Maw *et al.* [39] present a finite dimensional approximation (they divide the potential contact region into a series of equi-spaced annuli) to the original procedure prescribed by Mindlin and Deresiewicz, but even the simplified approach involves checks for stick/slip on different annular regions at each time step. Their analysis, moreover, is for 2D collisions, where the direction of slip never changes beyond changes in sign. Extensions of the Mindlin-Deresiewicz solution to 3D collisions would require solving the contact problem for a varying normal force and a tangential force that changes both magnitude and direction.

Even in the area of 2D collisions of spheres, the approach based on Mindlin-Deresiewicz has other problems. Consider applications in granular flow. Drake and Walton [16] report that static force-deflection measurements indicate that the large forces in the collisions of interest are outside the region of validity of the Hertz contact model. In such situations the model does not apply. Again, while the particles in the experimental setups are nominally spheres, they are in reality slightly aspherical, and have imperfect surfaces. The "spheres" examined by Foerster *et al.* [17] are a few millimeters in diameter. The validity of the Hertz contact-based model depends on there existing an intermediate length scale much smaller than the particle radius, yet much larger than the typical surface irregularities. Such a length scale may not exist in practice. In such situations, it might be possible to achieve a similar level of inaccuracy with a simpler contact law. Foerster et al. [17] compare the results of their experiments with the predictions of the Mindlin-Deresiewicz model. In collisions which have sticking or partial slip, there is some mismatch between their data and the theory. Their data is about equally well matched by a simple algebraic bilinear model with two restitution parameters and a friction coefficient.

For 3D collisions of arbitrary bodies that are not force-response rigid, it is likely that any local contact model that assumes force-response rigid behavior will be inaccurate except by coincidence. In such collisions, if they are to be modeled as rigid body collisions, it is probably practical to use contact laws that are less complicated than the Mindlin-Deresiewicz approach.

If one is prepared to compromise on the accuracy (real or imagined) offered by the Mindlin-Deresiewicz approach, many simpler contact models become available.

5.2.3 Potential Functions and Dissipation Functions

A possible approach to modeling the contact forces in a collision might be through linear or nonlinear springs and dashpots. If the complications of stick-slip are ignored, then the springs and dashpots may be specified by potential functions and dissipation functions.

Ivanov [26] presents such an approach where the contact forces are assumed to arise from potential and dissipation functions. Different choices for potential functions are discussed for different contact assumptions. For collisions with friction, Coulomb friction is not assumed. Tangential forces are incorporated through a roughness coefficient in a proposed potential function. The predicted ratios of tangential to normal impulses calculated from this approach are presented, and shown to be similar to predictions based on Coulomb friction for some cases.

One potential function assumed for frictional collisions in Ivanov's model is

$$\varphi(\delta) = c_1 \left(h^2 + 2\mu h \|\delta\| \right), \tag{5.2}$$

where c_1 is an arbitrary constant, μ is a roughness coefficient, and h is the normal component of the interference δ. The corresponding contact force is

$$F = -\text{ grad } \varphi = -2c_1 \left(n(h + \mu\|\delta\|) + \mu h \frac{\delta}{\|\delta\|} \right),$$

where n is the unit normal vector. For this contact law, there is a net contact force in the normal direction when there is a net relative displacement in the tangential direction, even with zero interference in the normal direction. This is an unrealistic contact model. However, other potential functions than that in Eq. (5.2) might yield more realistic contact forces.

5.2.4 General Frictional Point-Contact Models

One general approach may be summed up as follows. First, the mass matrix corresponding to the collision is imagined to represent a single "anisotropic" non-rotating point mass. This point mass interacts with a rigid, flat, immovable surface. A mechanical device, usually consisting of springs, joins the point mass with the *contact point*. The contact point touches the flat surface, where Coulomb friction may be assumed. Next, a termination condition is chosen (often, the termination condition is zero normal force). Equations of motion of the anisotropic point mass are written[4] down and integrated, using initial values equal to the pre-collision relative velocity for the collision. When the termination condition is reached, the collision is over, and the velocity of the point mass at that instant are taken to be the post-collision relative velocity for the collision. The system is shown schematically in Fig. 5.1 (for a two dimensional collision).

Note that there is no contact "region" as in the Hertz or Mindlin-Deresiewicz contact solutions. If the contact point is massless, then its velocity may be found by static force balance, in terms of its position and the position and velocity of the anisotropic point mass. If the contact point does have mass, then its velocity is also one of the state variables, and the frictional force is known when the states of the point mass and of the contact point are known. Stronge, for example, uses a massless contact point [63]. The springs used may be linear or nonlinear, and typically there is some form of dissipation.

In Stronge [63] the tangential spring has no dissipation, while the normal spring has different linear loading and unloading curves. The energy dissipation in the normal spring becomes consistent with the definition of an "energetic" coefficient of restitution. The collision terminates when the force in the normal spring falls to zero.

Other possibilities in this general direction include dissipation through dashpots. One feature of linear dashpots is that they predict an instantaneous jump in the contact force at the beginning of impact, if they are assumed to be in parallel with springs. The instantaneous jump can be avoided by putting dashpots and springs in series, introducing an extra state variable. If the springs and dashpots are taken to be nonlinear, then the outcomes will generally not be specified by nondimensional parameters. This is because, in the case of linear springs and dashpots, the

[4]The time in these equations is an artificially "stretched" variable. Finite changes in this fast time correspond to small changes in real time. During the collision calculation, changes in the local mass matrix are ignored and the anisotropic mass is held constant. The compression in the springs is also a scaled variable and is typically assumed small enough so that changes in the orientations of the springs are negligible.

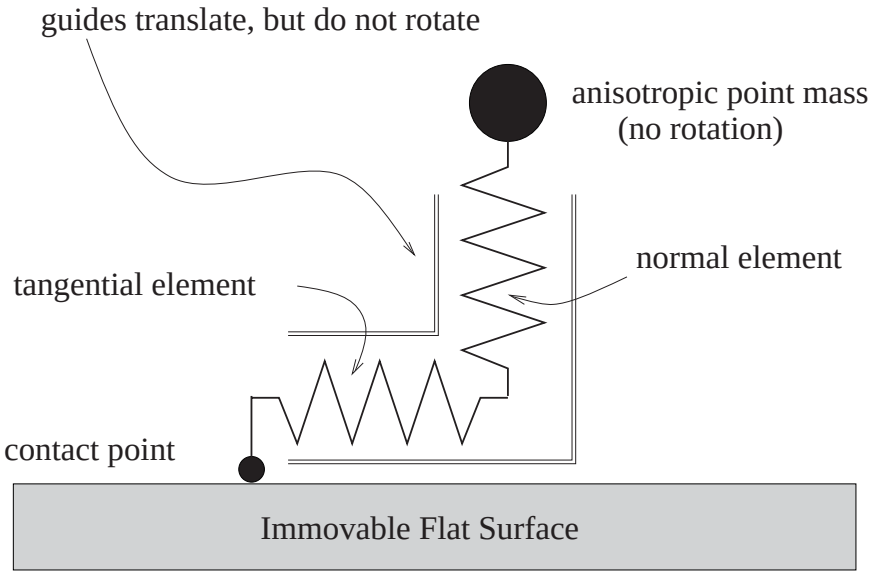

Figure 5.1: Schematic diagram for contact model

relative displacements (or the compressions in the springs) in the collision calculations can be scaled arbitrarily without affecting the equations of motion, making the actual magnitude of velocity irrelevant and thus making the collision law homogeneous of degree one in velocity. When the springs and/or dashpots are nonlinear, then the absolute displacement usually cannot be scaled arbitrarily (see e.g., Section 8.2), and thus the solution depends on dimensional (not dimensionless) terms. These terms play the role of dimensional parameters in the collision law. However, as shown by the example in Section 8.4, it is possible to have nonlinear, dissipative interaction mechanisms where the resulting collision law still is described by dimensionless parameters.

The connection between tangential restitution and the stiffness ratio of the normal and tangential springs may be illustrated qualitatively for the example of collisions between spheres. Assume that in the mass matrix the eigenvalue corresponding to the normal direction is known, and fixed. Since there is no inertial coupling in the two directions, the time of collision is determined by the normal spring-dashpot (and possibly the pre-collision velocity, for a nonlinear spring/dashpot). If there is a sufficiently high coefficient of friction and the pre-collision velocity has a small tangential component, then the contact point sticks for almost the entire duration of the collision. The inertia in the tangential direction and the tangential spring together lead to oscillations (simple harmonic motion, in the case of a linear spring with no damping). The phase at which this oscillation happens to be when the collision is terminated will depend largely on the ratios of inertias and of spring stiffnesses in the two directions. Adjusting the stiffness ratio can lead to tangential restitution as used approximately by Jenkins [30] and Brach [11], or to the negative tangential restitution for nearly head on collisions predicted in Maw et al. [40].

Routh's Model in 3D: the Special Case of Zero Tangential Compliance

Once the differential equations of motion and the termination condition are written down, they may be scaled or nondimensionalized to reduce the number of independent parameters to a minimum. One special case of such contact models, where the tangential compliance is zero, leads to a dramatic

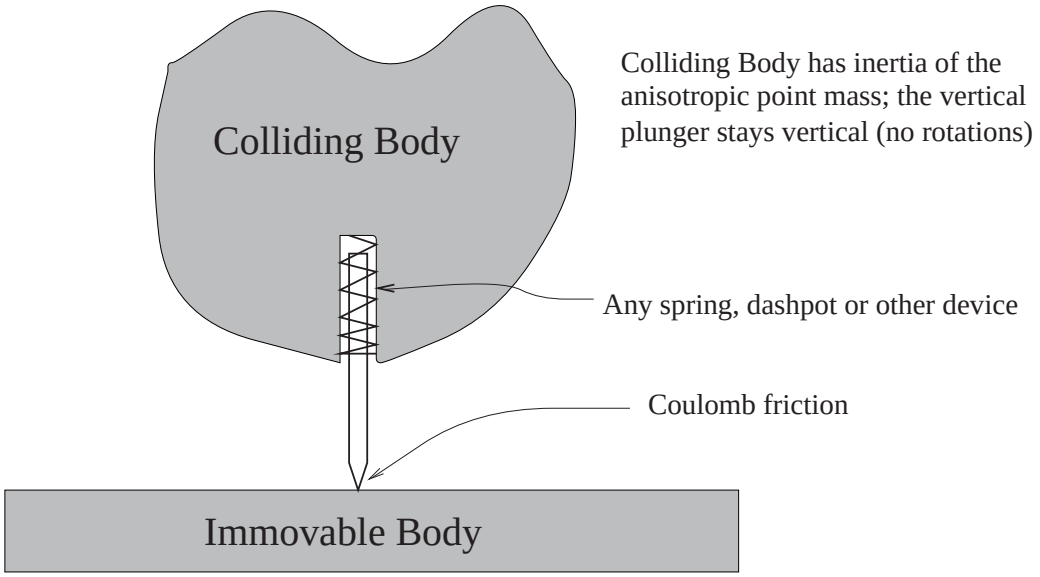

Figure 5.2: Zero tangential compliance

simplification (see Fig. 5.2). For this case, the independent variable may be changed from time to accumulated normal impulse. Accumulated normal impulse may be used as a time-like variable so long as it is increasing monotonically with time. For a given spring-dashpot combination, there comes a point when the normal force drops to zero. The change of independent variable is valid up to this point in time. If this change of variable is made, then the details of the normal spring-dashpot behavior disappear from the equations of motion. These details generally still remain important in the calculation, because they do determine when the system reaches the termination condition, i.e., when the collision ends. Note that the generally ill-defined concept of a point of maximum compression[5] is well defined for the special contact model used in Routh's collision law, because the lack of tangential compliance in this case makes the point of maximum compression independent of the details of the contact interaction in the normal direction also.

As mentioned above, in the special case of zero tangential compliance, on changing the independent variable from time to accumulated normal impulse, the details of the normal spring-dashpot behavior disappear from the equations of motion, but generally still remain relevant in that they determine when the collision terminates. In the further special case of Poisson restitution, the termination condition is given in the form of a ratio of impulses. It is tacitly assumed that there exists

[5]The definition of the point of maximum compression, as the unique point of time during the collision when the normal component of relative velocity is zero, assumes that the normal component of relative velocity increases monotonically in the collision. This may clearly not be the case [58]. In reality, for impulse-response rigid objects, there may be several micro-impacts within one impact, with at least as many "points of maximum compression". Even for force-response rigid objects, the details of the contact interaction mechanism generally decide when the normal component of relative velocity becomes zero. Thus, even in the general case of force-response rigid bodies, the point of maximum compression depends on the mass matrix M, the pre-collision velocity V_i *as well as* the details of the incremental collision law being used. A consequence of this is that if the net outcome of a collision is known from experiment, the point of maximum compression cannot be identified because the contact law is not known.

some physical passive local interaction mechanism which will reach this termination point *before* the normal force becomes zero. Under this assumption, even the point of termination becomes independent of the details of the spring-dashpot combination, and the model reduces to Routh's model. Thus, Routh's model is a special case of many possible incremental collision models based on local contact laws, with a special termination condition.

It is known that a local contact model with zero tangential compliance and a termination condition based on Newtonian restitution does occasionally violate conservation of energy; therefore we may conclude that for some collision configurations the Newtonian termination condition will *not* be reached by any passive device with zero tangential compliance, before the normal force becomes zero. Note that we do not know of any mechanism made of passive, dissipative devices like springs and dashpots which leads to Poisson restitution, either. It is not intuitively clear that Poisson restitution should satisfy energy conservation for general three dimensional collisions. However, Ivanov has proved that it does indeed always conserve energy [24].

Chapter 6

New Algebraic Collision Laws for Rigid Bodies

6.1 Motivation for the Construction of New Collision Laws

In order to evaluate various candidate collision laws, it is useful to make a list of properties that we might like collision laws to have. Some of the criteria discussed earlier (see Section 2.1) are satisfaction of fundamental constraints, generality, consistency with "lesser" laws, matching data for simple cases (including both reversal and non-reversal of slip for collisions of spheres, for proper choices of collision parameters), few parameters and overall simplicity, and physical interpretations for parameters.

There are no reported algebraic collision laws that satisfy these requirements besides the ones we present here[1].

In addition to the properties mentioned above one might like collision laws, with suitable choices of parameters, to be able to capture a large subset of the fundamentally allowable collisional impulses for any given collision, i.e., any given pair of objects colliding with given velocities at a given configuration. Such additional criteria may be used to evaluate or compare the new laws presented here with other available laws.

Three new algebraic collision laws for three dimensional, frictional impacts of rigid bodies and ideal mechanisms are presented in this chapter. To implement these laws, neither nonlinear algebraic nor differential equations need be solved. The three new laws each depend on three nondimensional collision parameters with clearly defined and simple bounds. The parameters are (1) a normal restitution parameter r_n, (2) a tangential restitution parameter r_t, and (3) a friction parameter μ. These laws apply to general bodies – they are not restricted to two dimensions or to

[1] One might think that the type of models proposed by Brach [11] satisfy the requirements mentioned above. However, as discussed in Chapter 5, Brach's models depend on a knowledge of "parameters" whose ranges are expressed through implicit nonlinear inequalities expressing nonnegative energy dissipation. The impulse ratio 'parameter' is really an arbitrary function of configuration, mass distribution, velocity and friction. Little is known about the nature of this function, including bounds on its values. From an experimental point of view, this means that the outcome of a particular collision can be predicted by the model only after it is already known from experiment. From the point of view of general multibody dynamics simulations, it is difficult to specify some impulse ratio function for fear of violating fundamental constraints for some configurations, since these configurations are not known *a priori*. In terms of practical utility, Brach's approach is equivalent to a change of variables.

fortuitously aligned bodies. In general three dimensional collisions, the possible predicted impulses from these laws lie in the three dimensional region that is allowed by fundamental constraints, as shown in Fig. 3.3. In the case of frictional collisions of spheres in three dimensions, or of disks in two dimensions, these laws reduce to a well known bilinear law. In the case of general three dimensional frictionless collisions, these laws reduce to Newtonian restitution.

The view taken in constructing these new laws is as follows. Most simple rigid body collision laws reduce to Newtonian restitution for general frictionless collisions as well as for frictional collisions with diagonal mass matrices. Of these, the bilinear law used for the case of diagonal mass matrices by Brach [11], Jenkins [30], Foerster *et al.* [17], etc., seems to match data fairly well for collisions of spheres and of disks. Hence, it might be worthwhile to construct general 3D collision laws that reduce both to the usual restitution model for the frictionless case *and* the bilinear model for the diagonal mass matrix case.

6.2 Some Commonly Used Collision Parameters

Algebraic collision laws are essentially attempts to extend ideas related to the coefficient of restitution, a collision parameter discussed in elementary dynamics texts, to frictional two or three dimensional collisions. In three dimensions, more parameters are needed; some candidates are discussed below.

The Coefficient of Coulomb Friction μ : Coulomb friction is usually assumed to act in the contact region during a collision. For algebraic collision laws, intermediate details of the contact interaction are not available; the tangential impulse cannot be directly calculated by integrating the tangential force. It must be chosen, either implicitly in the statement of the collision law, or explicitly. A reasonable constraint is that the interaction impulse obey the friction inequality,

$$\|\mathbf{P}_T\| \leq \mu P_N, \tag{6.1}$$

where $\mathbf{P}_T$ is the tangential component of the impulse, P_N the (positive) normal component, and μ the coefficient of friction. No distinction is made here between static and kinetic friction for collision calculations. We take inequality 6.1 to be a fundamental restriction on our collision models.

The Coefficient of Normal Restitution e_n : There are three commonly used definitions of the coefficient of normal restitution. All three are equivalent for frictionless collisions. Energy considerations show that $0 \leq e_n \leq 1$ for *frictionless* collisions.

The *kinematic* coefficient of restitution e_n is defined to be the ratio of the magnitudes of the normal components of the post- and pre-collision relative velocities at the contact point. Alternative definitions are the *kinetic* coefficient (see Routh [52] or the more recent treatment in Keller [33]) and the *energetic* coefficient (see e.g., Stronge [59]). Both these definitions of e_n depend on incremental interaction models with one point of "maximum compression". However, in 2 and 3 dimensions, the location of the "point of maximum compression" depends on the time history of the contact force, or the path in impulse space, and therefore the point of maximum compression is only defined in the context of both force-response rigid bodies *and* a particular incremental collision law. Thus the kinetic and energetic coefficients cannot be used in algebraic laws without specific extra assumptions about the point of maximum compression, as in the 2D model proposed by Pfeiffer and Glocker [47].

The Coefficient of Tangential Restitution e_t : The coefficient of tangential restitution e_t is often used to describe collisions where the mass matrix is diagonal (see e.g., Brach [11], Jenkins [30] or Foerster *et al.* [17]). For such collisions, the tangential component of post-collision relative velocity is approximated as a fixed fraction e_t of its pre-collision magnitude, provided the friction

inequality is not violated. That is,

$$V_{fT} = -e_t V_{iT} \text{ if } \|P_T\| < \mu P_N, \text{ else } \|P_T\| = \mu P_N,$$

where $-1 \leq e_t \leq 1$, and the subscript T denotes tangential component.

For general collisions with complicated geometries, where there is inertial coupling between the normal and tangential directions (i.e., M is not diagonal), there is no simple physical interpretation of tangential restitution. Nor are there any bounds on its values for general collisions.

6.3 The Impulse Direction

If $\|P\|$ is the magnitude and $\hat{P}$ a unit column vector in the direction of the impulse then from Eq. 2.4

$$\|P\|\hat{P} = M(V_f - V_i).$$

For given kinematic restitution $e_n := -(n^T V_f)/(n^T V_i)$, where $n^T := \{1, 0, 0\}$, we obtain

$$\|P\| = -\frac{(1+e_n)n^T V_i}{n^T M^{-1}\hat{P}}. \tag{6.2}$$

If the direction of the impulse is known explicitly (as assumed in Brach's laws), then the 3D collision calculation effectively reduces to a 1D calculation, since the impulse magnitude is the only remaining unknown.

For some collision laws the direction of the impulse is stated implicitly in terms of the post-collision velocity, i.e., $\hat{P} = \hat{P}(V_f)$. In such cases, Eq. 6.2 still involves V_f, and simultaneous equations (generally nonlinear) in $\|P\|$ and V_f need to be solved. As an example, consider the collision law discussed in Kane and Levinson's text [32], which states that $V_{fT} = 0$ if and only if an impulse satisfying the friction inequality (6.1) can make it so. Otherwise, the tangential impulse is given by

$$P_T = -\mu P_N \frac{V_{fT}}{\|V_{fT}\|}.$$

As is well known [32], and as demonstrated in Section 7.5, this collision law can predict very large *increases* in system kinetic energy for suitably chosen M and V_i.

As another example, consider the collision law proposed by Smith [55], where the tangential component of the impulse is assumed to be given by

$$P_T = -\mu P_N \frac{\|V_{iT}\|V_{iT} + \|V_{fT}\|V_{fT}}{\|V_{iT}\|^2 + \|V_{fT}\|^2}. \tag{6.3}$$

This collision law does not predict increases in kinetic energy. However, the strongly nonlinear equations make solving for P_N and V_{fT} difficult in a general 3D setting.

Algebraic collision laws are based on special hypotheses about the direction of the net impulse transmitted, just as incremental laws are based on hypotheses about the interaction forces. As demonstrated above, assuming that the impulse direction in a collision is given as a function of the (as yet undetermined) post-collision velocity leads to (generally nonlinear) equations that are harder to solve (at least, harder than solving linear equations). The new collision laws presented in this chapter all hypothesize impulse directions that are based on *pre-collision quantities*. Consequently, the calculations involved for these laws are simple.

6.4 A Bilinear Collision Law for Diagonal Mass Matrices

We now present a simple algebraic *bilinear* collision law for the special case when the mass matrix is diagonal in the chosen coordinate system (recall that the 1-axis is along the normal, the 2-axis is chosen so that the 1-2 plane includes the pre-collision relative velocity, and the 3-axis is chosen orthogonal to the first two axes). This bilinear law has been used for collisions of spheres and of disks by other researchers (e.g., Brach [11], Jenkins [30]), and matches experimental data reasonably well (see, e.g., Foerster *et al.* [17], or the data in Chapter 11). Let the diagonal elements of the mass matrix be $\lambda_1, \lambda_2, \lambda_3$. Note that collisions between spheres in 3D or disks in 2D have diagonal mass matrices. We may assume that the pre-collision relative velocity has negative 1- and 2-components, i.e.,

$$V_i = \{-v_{iN}, -v_{iT}, 0\}^T, \text{ for some scalars } v_{iN}, v_{iT} > 0. \tag{6.4}$$

The post-collision velocity is then stated to be

$$V_f := \left\{ e_n v_{iN}, -v_{iT} + \min\left((1+e_t)v_{iT},\ \mu(1+e_n)\frac{\lambda_1}{\lambda_2} v_{iN} \right), 0 \right\}^T$$

where $0 \le e_n \le 1$, $-1 \le e_t \le 1$ (though generally one expects $0 \le e_t \le 1$), e_n is the coefficient of normal restitution, e_t is the coefficient of tangential restitution, and μ is the coefficient of friction. In this law for diagonal mass matrices, there is no impulse component in the 3-direction. The normal component of the post-collision relative velocity is determined by the coefficient of restitution alone. The tangential component is determined by the coefficient of tangential restitution, provided the friction inequality is not violated. Otherwise, the tangential impulse is determined by the normal impulse and the friction coefficient.

The impulse transmitted in the collision is given by

$$P = \{\ \lambda_1(1+e_n)v_{iN},\ \min(\ (1+e_t)\lambda_2 v_{iT},\ \mu(1+e_n)\lambda_1 v_{iN}\ ), 0\}^T. \tag{6.5}$$

6.5 Three Algebraic Collision Laws

In the three collision laws presented in this section, we assume that the mass matrix M, the pre-collision relative velocity V_i, and three dimensionless parameters are given: r_n for normal restitution, r_t for tangential restitution, and μ, a friction parameter. The collision law predicts V_f, the post-collision relative velocity.

The following apply to all three collision laws:

1. *Coordinate system:* As mentioned earlier, the coordinate system has its 1-direction along the common normal at the contact point, its 2-direction chosen such that the 1-2 plane contains the pre-collision relative velocity V_i, and its 3-direction orthogonal to the 1- and 2-directions.

2. *Friction:* μ is interpreted as the coefficient of Coulomb friction (static = kinetic). However, the net frictional impulse is not calculated from integrals of instantaneous frictional forces as in some incremental models. Inequality 6.1 is satisfied for all collisions.

3. *Frictional impulse direction:* In three dimensional collisions, some currently known collision laws predict a tangential impulse direction that opposes some weighted average of the pre- and post-collision tangential relative velocities when both are nonzero, i.e.,

$$P_T = -(aV_{iT} + bV_{fT}), \text{ for some } a \ge 0, b \ge 0. \tag{6.6}$$

If this condition is met, we say that the tangential impulse is in the *negative span* of the pre- and post-collision tangential relative velocities. For brevity, we refer to this condition as the *span condition*. The span condition is obviously satisfied by Smith's law [55] (see Eq. 6.3). It is often (possibly always) satisfied by Routh's model (see e.g., Routh [52] or Keller [33]), which is an incremental model with *zero* tangential compliance. There is no fundamental reason why the span condition should be met for general collision laws (e.g., incremental models with arbitrary, finite, tangential compliances). The condition is intuitively appealing, however, and one might like collision laws to satisfy it often if not always. In the collision laws we present, this condition seems not to be satisfied in all cases.

4. *Tangential restitution:* We use r_t as an independent restitution parameter that corresponds, for simple collisions with diagonal mass matrices, to simple energy recovery and to velocity reversal in tangential directions; for all cases, $-1 \leq r_t \leq 1$. The precise use of this coefficient is different for each collision law, but reduces to the same thing for frictionless collisions and/or diagonal mass matrices. For some simple cases, r_t is the same as e_t (see Sections 6.2 and 6.4).

5. *Normal restitution:* As is fairly well known, and as also recently demonstrated in experiments by Stoianovici and Hurmuzlu [58], *no* definition of the coefficient of restitution, as a known constant that characterizes a material or a body in all possible collision configurations, has any fundamental validity. For a given individual collision between hard solid bodies, a kinematic coefficient of restitution does exist and can, in principle, be measured. In this spirit, we take the coefficient of restitution e_n to mean the true, physically observed ratio of magnitudes of normal components of post- and pre-collision relative velocities. We do not claim that the value of e_n should be the same for all collisions, only that some e_n exists and is well defined for any *given* collision. In terms of implementation in our collision laws, we assume that a normal restitution parameter r_n (not necessarily equal to e_n) is specified, and that $0 \leq r_n \leq 1$. Based on various calculations that differ for the three different laws, we predict an impulse P. Using this P, the resulting e_n for the collision can be computed. Often, but not always, this value of e_n equals the specified r_n.

6.5.1 Collision Law I (P Based on V_i)

Motivation: One way to go about constructing collision laws that reduce to the bilinear law of Section 6.4 whenever the mass matrix is diagonal might be to first consider collisions where the mass matrix M is *nearly* diagonal, i.e., its off diagonal terms are small. We then need to make a hypothesis about how the impulse direction changes if some small off-diagonal elements are present in the mass matrix. One simple possibility is that the impulse direction *does not* change. Thus, given an arbitrary mass matrix, we might *ignore* the off-diagonal elements (pretend they are all zero). We can then use the diagonal elements of the mass matrix to construct a diagonal matrix, and use the bilinear law to compute an impulse direction. In many cases, we can then suitably choose an impulse magnitude so as to match the specified restitution condition exactly or approximately. However, in some cases with large off-diagonal elements, the chosen impulse direction may have to be modified in order to keep from violating fundamental constraints. The modification suggested here is unrealistic, but it respects fundamental constraints and will often be unnecessary.

Details: In this collision law, we assume that the tangential component of the collision impulse opposes the pre-collision relative velocity. The direction of P in the 1-2 plane is chosen to agree with the bilinear model of Section 6.4, whenever the mass matrix is diagonal. The procedure is outlined below (see appendix for a detailed calculation algorithm).

1. Tentatively pick an impulse direction using the bilinear model, as follows.

   Let the diagonal elements of the mass matrix M be $\lambda_1, \lambda_2, \lambda_3$. We assume an impulse in the direction of that given by Eq. 6.5, using $e_n = r_n$ and $e_t = r_t$. Let the unit vector in this impulse direction be given by $\hat{P}_D$. Note that $\hat{P}_D$ points inside the friction cone, since the impulse of Eq. 6.5 satisfies the friction inequality. An impulse P points into the energy ellipsoid if $P^T V_i < 0$ (Inequality 3.3); thus, $\hat{P}_D$ also points into the energy ellipsoid since $\hat{P}_D^T V_i < 0$ (as may be verified from Eqs. 6.4 and 6.5).

2. Locate intersection of $\hat{P}_D$ direction with the energy ellipsoid, as follows.

   Since an energy preserving collisional impulse satisfies Eq. 2.5, substituting $P = \alpha \hat{P}_D$ into this equation yields a quadratic equation in α, with one root equal to zero and another strictly positive. Take the positive root.

3. For this value of $P = \alpha \hat{P}_D$, calculate a temporary V_{fN}, the normal or 1-component of V_f given by Eq. 2.4. We now have three possible cases, which we discuss below.

   (a) If $V_{fN} \geq -r_n V_{iN}$, we assign $e_n = r_n, V_{fN} = -e_n V_{iN}$, and find $P = \|P\| \hat{P}_D$ using Eq. 6.2.

   (b) If $0 \leq V_{fN} < -r_n V_{iN}$, then $P = \alpha \hat{P}_D$ is on or above the plane of maximum compression, but setting $e_n = r_n$ will create kinetic energy. In this case we use $P = \alpha \hat{P}_D$. Note that for this case, the prediction is that $0 \leq e_n < r_n$.

   (c) If $V_{fN} \leq 0$, i.e., $P = \alpha \hat{P}_D$ is below the plane of maximum compression, then we cannot use this impulse direction. We project the point $P = \alpha \hat{P}_D$ vertically upward (along n or the 1-direction) until it again intersects the energy ellipsoid. By this projection, we are assured that we stay inside the friction cone, that we reach a point above the plane of maximum compression (and thus some $V_{fN} > 0$, or $e_n > 0$), and that kinetic energy is not created. We take this new point to be the impulse transmitted in the collision.

A weakness of this collision law is that it predicts zero tangential impulse whenever the pre-collision relative velocity has no tangential component. This is unrealistic for general 3D frictional collisions. Moreover, for general 3D collisions where the center of the energy ellipsoid is not on the plane containing the normal n and the pre-collision velocity V_i, a perfectly plastic, sticking collision *cannot* be predicted by this collision law for any choices of collision parameters. However, the law is simple, works well for zero friction and/or diagonal mass matrices, and never violates fundamental constraints. Moreover, it has another use, as discussed in Section 6.6.

For this law the span condition of Eq. 6.6 is satisfied with $b = 0$.

6.5.2 Collision Law II (P Based on MV_i)

Motivation: The direction of the impulse transmitted in a collision, along with the normal direction, defines a "vertical" plane in impulse space. One way to construct a collision law might be to pick a suitable vertical plane first, and to pick an impulse in the plane afterwards. We note that for collisions with *diagonal* mass matrices, the vertical plane that includes the normal direction n and the pre-collision velocity V_i is the same as the vertical plane that includes the normal n and the pre-collision *momentum* MV_i. Suppose we restrict the impulse to be in the plane of n and MV_i for general collisions. Note that the intersection of this plane with the energy ellipsoid contains a portion of the normal axis n, allowing frictionless collisions. It also contains the center of the energy ellipsoid, $-MV_i$, and so a perfectly plastic, sticking collision might be captured by the law,

unlike law I above. It remains to suitably parameterize a reasonable portion of the plane. The portion chosen here is shown schematically for a generic 3D collision in Fig. 6.1, and described in detail below.

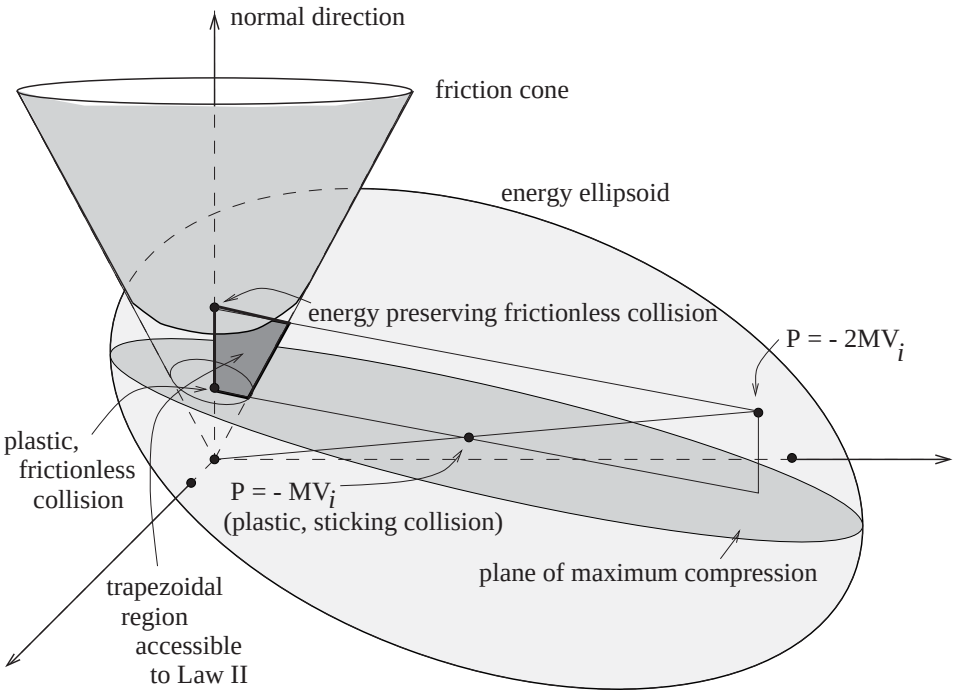

Figure 6.1: Construction of Law II

Details: In this collision law, we take the tangential impulse to oppose the tangential component of the pre-collision local momentum MV_i. In Fig. 3.3, observe that point B represents a collision with $e_n = 1$. If line OC is extended, it meets the ellipsoid at $P = -2MV_i$, which also yields $e_n = 1$. Similarly, point A represents a collision with $e_n = 0$; let the impulse corresponding to A be P_1. Point C corresponds to an impulse of $-MV_i$ and $e_n = 0$; let this impulse $-MV_i$ be P_2. Now for any $0 \leq e_n \leq 1$, impulses $(1 + e_n)P_1$ and $(1 + e_n)P_2$ both yield the given value of e_n. All points on the line through $(1 + e_n)P_1$ and $(1 + e_n)P_2$ yield the same e_n. From geometrical considerations, it may be seen that for $0 \leq \alpha \leq 2$ and $0 \leq \beta \leq 2$, impulses given by $\alpha P_1 + \beta(P_2 - P_1)$ lie inside a parallelogram which is totally contained inside the energy ellipsoid. In particular, for $0 \leq e_n \leq 1$ and $-1 \leq e_t \leq 1$, the impulse

$$P := (1 + e_n)P_1 + (1 + e_t)(P_2 - P_1) \tag{6.7}$$

lies inside the energy ellipsoid; this impulse will also yield the same normal restitution e_n.

For this collision law we set $e_n = r_n$, and $e_t = r_t$. If the point P given by Eq. 6.7 lies inside the friction cone, we assume that it is indeed the transmitted impulse and use Eq. 2.4 to calculate the outcome of the collision. If P lies outside the friction cone, we project it onto the surface of the friction cone along the line joining P and $(1 + e_n)P_1$, along which e_n stays constant.

For details of the calculations involved, see the appendix.

6.5.3 Collision Law III (V_f Based on V_i)

Motivation: It is known that arbitrarily specifying kinematic coefficients of restitution in normal and tangential (or other combinations of) directions can lead to violation of energy conservation as

well as the friction inequality. However, kinematic restitution coefficients are based on simple physical interpretations, and we might want to construct a model based on such restitution coefficients. We would have to check for energy conservation separately, and lower the restitution coefficients if necessary. It may be seen that – friction allowing – perfectly plastic, sticking collisions correspond simply to zero kinematic restitution in such a model. The reduction to the bilinear law in the case of diagonal matrices can also be foreseen, since that law is itself based on independent kinematic restitution coefficients in the normal and tangential directions.

Details: In this law we start with assumptions about the post-collision relative velocity V_f instead of direct assumptions about the impulse P. The procedure is outlined below (for details, see appendix).

Let the pre-collision relative velocity V_i be given by Eq. 6.4. First pick a tentative V_f, given by

$$V_f = \{r_n v_{iN}, r_t v_{iT}, 0\}^T.$$

Next, check for energy dissipation (this step is superfluous if the mass matrix M is diagonal) by computing

$$\gamma := \sqrt{(V_f^T M V_f)/(V_i^T M V_i)}.$$

If $\gamma \leq 1$, do nothing. If $\gamma > 1$, then divide the tentative V_f by γ. The new V_f satisfies both the kinetic energy and the non-interpenetration criteria. Next, check for satisfaction of the friction inequality. For the tentative V_f, compute the impulse required using Eq. 2.4; call this impulse P_2. For a *frictionless* collision with $e_n = r_n$, compute the impulse P_1 using Eq. 6.2. If P_2 is inside the friction cone, we take it to be the collision impulse. If P_2 lies outside the friction cone, we project it on to the friction cone along line P_1P_2. The numerical procedure for this projection is similar to that in subsection 5.2, but the projection is along a line on which e_n need not be constant.

6.6 A Combined Collision Law

The collision laws described in the previous three sections are all simple, three-parameter algebraic laws that satisfy all fundamental restrictions on rigid body collision laws. While they might possess varying degrees of aesthetic appeal, there is no real justification for preferring one over the others. Our reasons for presenting all these laws here are twofold.

First, there have been several similarly *ad hoc* algebraic collision laws proposed in the literature, which have problems such as nonlinearity and unresolved questions of existence/uniqueness (Smith [55]), parameters whose bounds are not known *a priori* (Brach [11]), or even the possibility of violating fundamental constraints such as non-negative dissipation of kinetic energy (Whittaker [71], Kane and Levinson [32]). The laws we present demonstrate that using geometrical ideas, it is possible to construct many collision laws which do not have such problems.

Second, all three laws we propose have the nice properties of reducing to the same kinematic restitution model for frictionless collisions and the same bilinear model for diagonal mass matrices. They reduce to different 2D models for general 2D collisions, and to different 3D models for 3D collisions. This feature lets us trivially construct a combined *five* parameter collision law that possesses all the advantages of these three laws, and has the added flexibility of two extra free parameters for possibly fitting experimental data in practical applications.

Given the collision parameters r_n, r_t and μ, we may use collision law I above to predict an impulse, say P_I, collision law II to predict an impulse P_{II}, and law III to predict an impulse P_{III}. Given two new dimensionless *interpolation parameters* s_1 and s_2 satisfying $0 \leq s_1 \leq 1$ and $0 \leq s_2 \leq 1 - s_1$, we may take the collision impulse P to be given by

$$P = s_1 P_I + s_2 P_{II} + (1 - s_1 - s_2) P_{III}.$$

Since the impulses P_I, P_{II} and P_{III} are all inside the accessible region of Fig. 3.3, and since the accessible region is convex, it follows that the impulse P will also lie inside the accessible region. P may be interpolated between any two of the three laws by setting $s_1 = 0$, $s_2 = 0$, or $s_1 = 1 - s_2$.

6.7 Details of Various Calculations

6.7.1 Calculating the Local Mass Matrix

We now present a simple recipe for calculating the matrix M. We assume that some algorithm is already available for calculating the accelerations of the individual contact points under the action of known forces at these points, and outline a procedure that uses this existing algorithm. For brevity we use the same label C for the contact points on the two colliding objects.

1. Label one mechanism as m_1 and the other as m_2, such that the normal direction from m_2 to m_1 is the positive 1-direction. Ignoring the collision, calculate the absolute acceleration of the contact point C on m_1 when no force acts at C; call this acceleration a_{10}. Also calculate the the absolute acceleration of the contact point C on m_2 when no force acts at C, and call it a_{20}. Now $a_0 := a_{10} - a_{20}$ is the relative acceleration at the contact point *in the absence of* any contact force (more precisely, it is the 3×1 column matrix representation of the relative acceleration vector in the chosen coordinate system). Note that if all angular velocities and finite external forces are artificially set to zero for the collision calculation, then $a_{10} = a_{20} = a_0 = 0$.

2. Define unit forces as follows: F_1 is in the 1-direction, i.e., $F_1 := \{1, 0, 0\}^T$. Similarly define $F_2 := \{0, 1, 0\}^T$ and $F_3 := \{0, 0, 1\}^T$.

3. For $i = 1, 2, 3$ find the acceleration of point C on m_1 due to a force F_i at C, and call this acceleration a_{1i}. Similarly, find the acceleration of point C on m_2 due to a force $-F_i$ at C, and call it a_{2i}. Now the relative acceleration due to contact force F_i is $a_i := a_{1i} - a_{2i}$. The part of the relative acceleration that is linear in the contact force is given by $A_i := a_i - a_0$.

4. Construct the 3×3 matrix, $[A_1, A_2, A_3]$. Invert this matrix, to obtain M.

6.7.2 Pseudo-code for Collision Law I (P Based on V_i)

Given: M, $V_i = \{-v_n, -v_t, 0\}^T$, r_n, r_t, and μ
$\lambda_1 := M(1,1)$; $\lambda_2 := M(2,2)$; $\lambda_3 := M(3,3)$;
$n := \{1, 0, 0\}^T$;
$P := \{\ \lambda_1(1 + r_n)v_n,$
$\quad \min(\ (1 + r_t)\lambda_2 v_t, \mu(1 + r_n)\lambda_1 v_n\ ),\ 0\}^T$;
$\hat{P} := P/\|P\|$; $\alpha := -2\hat{P}^T V_i/(\hat{P}^T M^{-1}\hat{P})$; $P := \alpha\hat{P}$;
Comment: the preceding line (3 steps) is equivalent
$\quad$ to $P := -2(P^T V_i)P/(P^T M^{-1} P)$;
$V_f := M^{-1}P + V_i$; $v_{fn} := V_f(1)$;
if $v_{fn} > r_n v_n$,
$\quad P := -(1 + r_n)(n^T V_i)\hat{P}/(n^T M^{-1}\hat{P})$;
$\quad$ *Comment:* the preceding step is equivalent to
$\quad\quad P := (1 + r_n)v_n P/(v_{fn} + v_n)$;
elseif $v_{fn} < 0$,

$\beta := -2(P^T M^{-1} n + n^T V_i)/(n^T M^{-1} n)$;
$P := P + \beta n$;
endif

$V_f := M^{-1} P + V_i$;

6.7.3 Pseudo-code for Collision Law II (P Based on MV_i)

Given: M, $V_i = \{-v_n, -v_t, 0\}^T$, r_n, r_t, and μ
$n := \{1, 0, 0\}^T$;
$P_1 := -(n^T V_i) n/(n^T M^{-1} n)$; $P_2 : -MV_i$;
$P := (1 + r_n)P_1 + (1 + r_t)(P_2 - P_1)$;
$b := P(1)$; $c := P(2)$; $d := P(3)$;
if $\sqrt{c^2 + d^2} > \mu b$,
$a := (1 + r_n)P_1(1)$;
$\alpha := \mu a/(\mu a - \mu b + \sqrt{c^2 + d^2})$;
$P := (1 - \alpha)(1 + r_n)P_1 + \alpha P$;
endif

$V_f := M^{-1} P + V_i$;

6.7.4 Pseudo-code for Collision Law III (V_f Based on V_i)

Given: M, $V_i = \{-v_n, -v_t, 0\}^T$, r_n, r_t, and μ
$n := \{1, 0, 0\}^T$; $V_f := \{r_n v_n, r_t v_t, 0\}^T$;
$\gamma := \max\left(1, \sqrt{(V_f^T M V_f)/(V_i^T M V_i)}\right)$;
$V_f := V_f/\gamma$; $P := M(V_f - V_i)$;
$b := P(1)$; $c := P(2)$; $d := P(3)$;
if $\sqrt{c^2 + d^2} > \mu b$,
$P_1 := -(1 + r_n)(n^T V_i) n/(n^T M^{-1} n)$;
$a := P_1(1)$;
$\alpha := \mu a/(\mu a - \mu b + \sqrt{c^2 + d^2})$;
$P := (1 - \alpha)P_1 + \alpha P$;
endif

$V_f := M^{-1} P + V_i$;

Chapter 7

Comparing/Evaluating Some Known Algebraic Collision Laws

In this chapter we examine the 2D restrictions of some 3D algebraic collision laws.

One possible way to compare and evaluate collision laws is to see how well their predictions match experimental data. Unfortunately, systematic and complete collision data is not readily available for many classes of objects other than uniform spheres and disks, where the local mass matrix is diagonal.

A second way to compare and evaluate collision laws is to look at the set of all possible predictions of each collision law, for various choices of the collision parameters. The larger the set of possible predictions, the more likely it is that the outcome of some real, given collision can be captured by some collision law for *some* choice of its parameters. We adopt this second approach, and geometrically characterize the set of all possible impulse predictions, for several collision configurations, of some currently known algebraic collision laws.

For 2D collisions, the accessible region in impulse space is two dimensional. In principle, this 2D region can be parameterized using two collision parameters (see also the discussion in Section 10.6). In the approach adopted in this thesis, the coefficient of friction μ is taken to be an independent parameter (or constraint), and the two parameters used to parameterize the accessible region in impulse space are understood to be in addition to the specified friction coefficient.

The rationale for not treating μ as one of the two collision parameters is as follows. Since the same mass matrix M, pre-collision velocity V_i and friction coefficient μ can occur for infinitely many pairs of bodies with equally varied collisional interactions, the role of μ in a general study of collision modeling is limited to laying down the friction inequality for impulses, $|P_T| \leq \mu P_N$. For general 2D collisions and general discussion of collision laws, even for a *given* coefficient of friction μ, the accessible region in impulse space is still two dimensional. In order to access all points in this region or even a finite fraction of them, a collision law would need at least two more collision parameters.

The collision laws of Kane and Levinson [32], Smith [55] and Routh [52, 33, 70] each have only one free collision parameter, called the coefficient of normal restitution e, in addition to the coefficient of friction. Therefore, for generic collisions with given μ, each of these collision laws can only access one-dimensional subsets (curves) of the accessible region, in both 2D and 3D collisions. The collision laws proposed in Chapter 6 each depend on two free collision parameters, in addition to the coefficient of friction. Therefore, for generic collisions with given μ, these three laws can access two-dimensional subsets of the accessible region for both 2D and 3D collisions. None of these three collision laws can access the *entire* accessible region, however, even for 2D collisions.

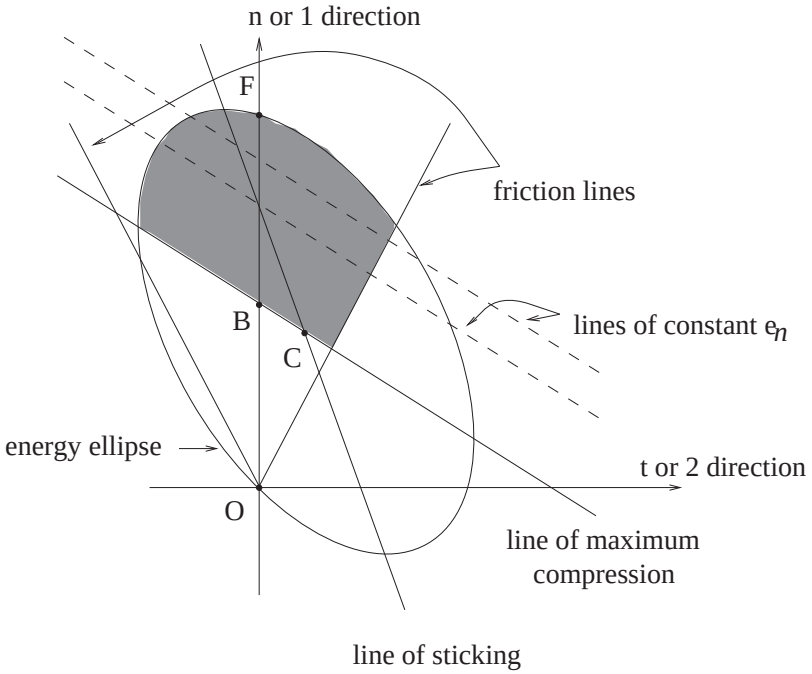

Figure 7.1: The accessible region in 2D impulse space

In the following, the regions accessible to three 2-parameter laws (Kane and Levinson, Smith, and Routh) and the three 3-parameter laws presented in Chapter 6 are shown geometrically. All but the last example considered in this chapter are presented not in terms of specific colliding objects, but instead in terms of an appropriate diagram in impulse space. We adopt this approach because each such diagram automatically determines the mass matrix for the collision, and all mass matrices are physically realizable (see Chapter 2).

7.1 A Generic Collision

Figure 7.1 shows the accessible region in impulse space for a generic collision. Lines parallel to the line of maximum compression mark impulses along which the post-collision normal component of relative velocity at the contact point, V_{fN}, is a constant. Along these lines, therefore, the kinematic restitution e_n is constant. Points B and F mark frictionless collisions with e_n equal to zero and one respectively. The line of sticking marks impulses for which the post-collision tangential component of relative velocity at the contact point, V_{fT}, is zero. At C, the center of the ellipse, both components of the post-collision relative velocity are zero.

The regions accessible to laws I and II proposed in Chapter 6 are shown shaded in Figs. 7.2 and 7.3, respectively. In Figs. 7.2 and 7.3, the line AD is the line of maximum compression. Lines OE and OH are the friction lines. C is the center of the ellipse. G is the intersection with the ellipse with the extension of line OC. It may be shown that line FG is parallel to line AB[1]. The region

[1]Lines of constant kinematic coefficient of restitution are parallel to the line of maximum compression, due to the linearity of the impulse-momentum relation $P = M\Delta V$. Point F corresponds to a frictionless, energy-preserving collision, or $e_n = 1$, while point G corresponds to an energy-preserving collision with perfect velocity reversal, or $e_n = 1$ also. Thus, line FG is parallel to the

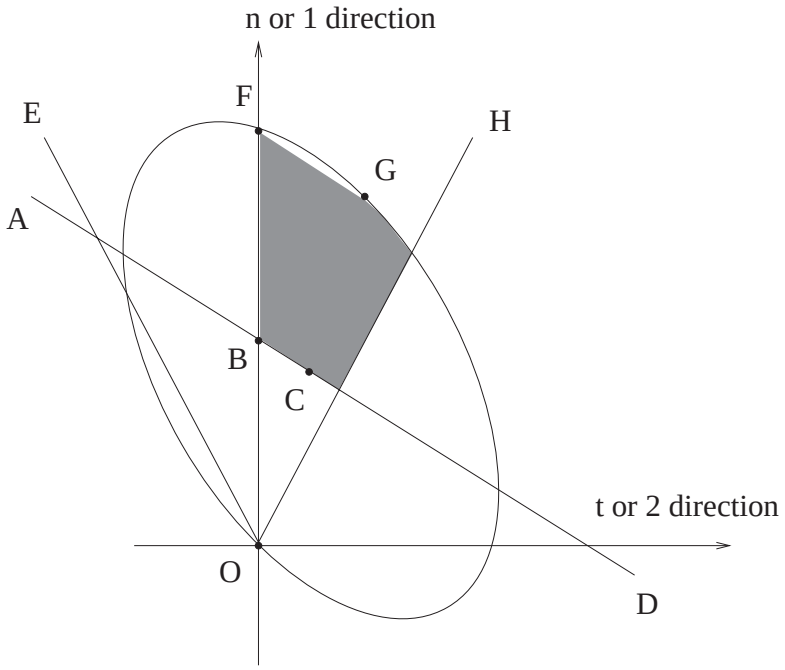

Figure 7.2: Region accessible in impulse space to law I

accessible to law II is included within that accessible to law I, in this case.

The region accessible to law III proposed in Chapter 6 is shown in Fig. 7.4. This region is the intersection of the region inside the energy ellipse, the region inside the friction lines, and a parallelogram, as shown in the figure.

For this same collision, the regions accessible to the laws of Kane and Levinson, of Routh, and of Smith, are shown in Fig. 7.5. It is seen that for some choices of collision parameters, Kane-Levinson can predict an increase in system kinetic energy.

7.2 A Collision with Diagonal M

Figure 7.6 shows the accessible regions for the various collision laws, when the local mass matrix M is diagonal. For this case, all three collision laws of Chapter 6 are identical; the region accessible to these laws is shown shaded in the figure. The laws of Routh and of Kane-Levinson are identical; the region accessible to these laws is shown by a thick solid line. The region accessible to Smith's law is shown by a thick dashed line.

Due to the decoupling of inertias in the normal and tangential directions, the kinematic (or Newtonian), kinetic (as in Routh's model) and energetic (as in Stronge's approach) coefficients of normal restitution are equivalent when the mass matrix is diagonal. All collision models based on one of the above three definitions of the coefficient of restitution e are confined, by the friction inequality and the condition $0 \leq e \leq 1$, to the shaded region of Fig. 7.6. For nearly grazing collisions, the region in impulse space that is accessible to any such collision law is then a small area just above the line of maximum compression, while the full accessible region is considerably larger, as shown in Fig. 7.7.

---

line of maximum compression.

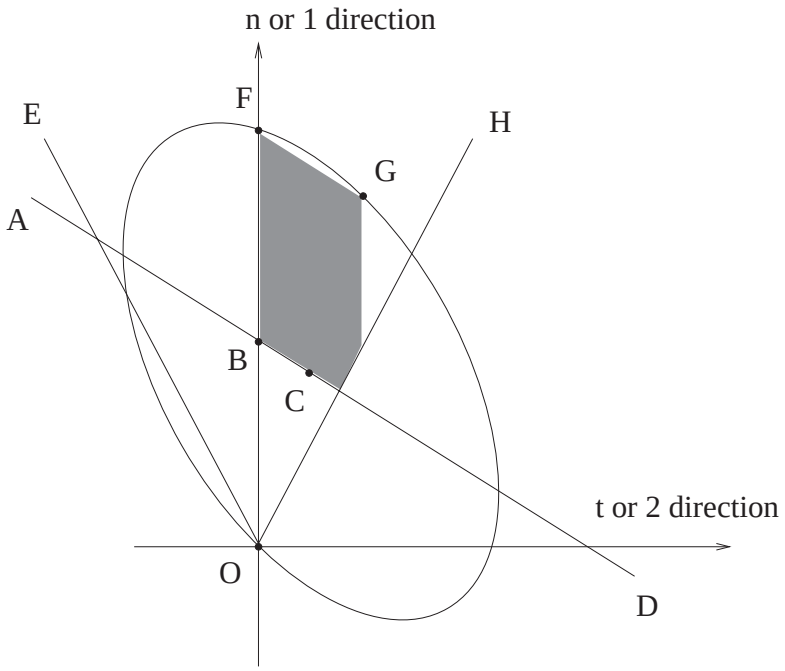

Figure 7.3: Region accessible in impulse space to law II

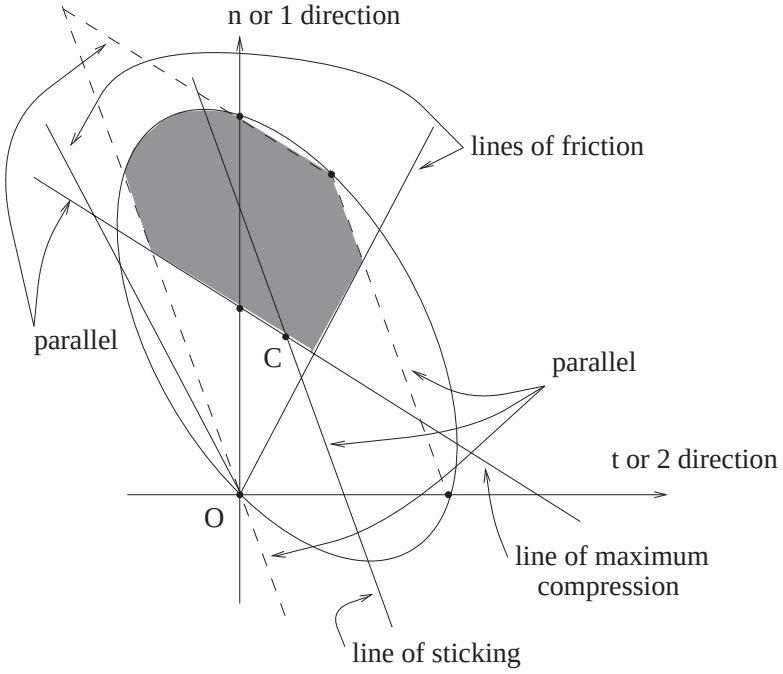

Figure 7.4: Region accessible in impulse space to law III

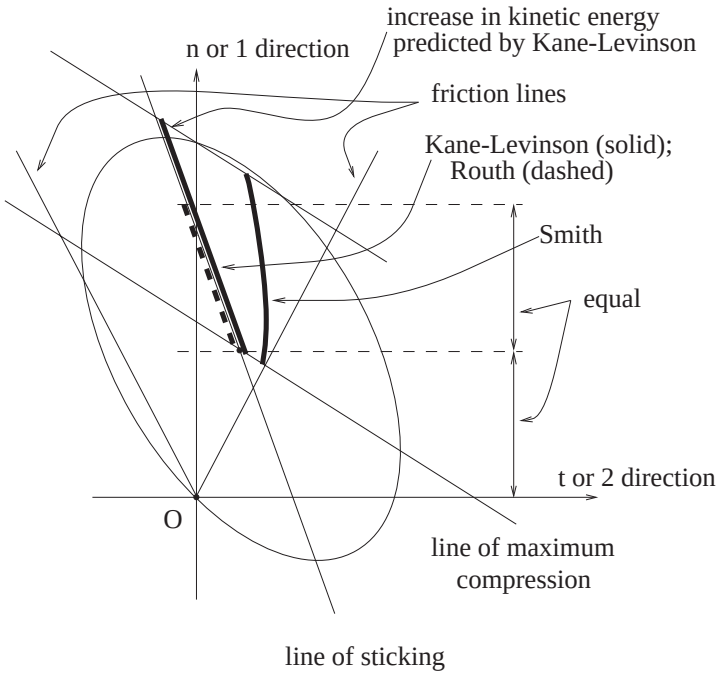

Figure 7.5: Region accessible in impulse space to laws of Routh; Kane and Levinson; Smith

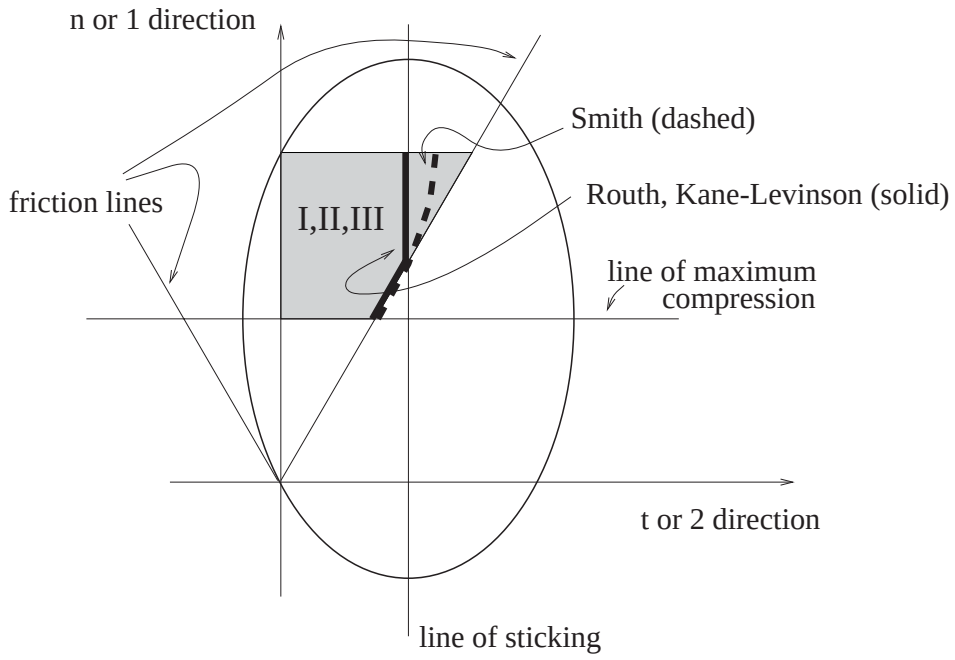

Figure 7.6: Region accessible in impulse space to various laws, for diagonal M

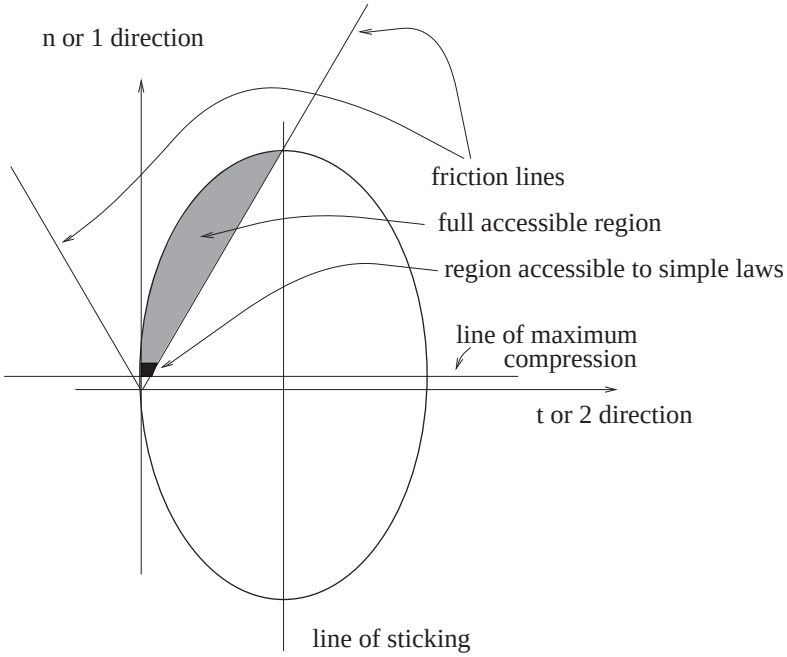

Figure 7.7: Nearly grazing collision for diagonal mass matrix; comparison between region accessible to simple collision laws and full accessible region

7.3 A Tangential Collision ($V_{iN} \rightarrow 0^-$)

Often one assumes that the pre-collision normal component of relative velocity at the contact point, V_{iN}, is strictly negative. However, sometimes collisions occur even for $V_{iN} = 0$, for certain orientations of the colliding bodies, and for large enough coefficients of friction. We consider tangential collisions as the limit $V_{iN} \rightarrow 0^-$. Tangential collisions have also been discussed, for example, by Wang and Mason [70].

Figure 7.8 shows the regions accessible to various collision laws for a typical tangential collision. Law I reduces to a point for all values of the normal restitution parameter $0 \leq r_n \leq 1$, and for values of the tangential restitution parameter $-1 < r_t \leq 1$. For $r_t = -1$, law I predicts zero impulse (no collision). Laws II and III can access all points on the line of maximum compression that are inside the energy ellipse (shown by a thick line in the figure). The regions accessible to Smith's law and to Kane and Levinson's law shrink to points (see figure). Routh's law can access points along the line of sticking, shown by the thick dashed line.

Laws II and III, as well as the Laws of Kane-Levinson and of Smith predict post-collision velocities with zero normal component, since they are based on a kinematic coefficient of restitution. Of these four laws, laws II and III do allow some variation in the tangential component of post-collision velocity, while Kane-Levinson and Smith allow none. Law I does predict a nonzero normal component of post-collision velocity, but that is due to an *ad hoc* "fix" in the collision law that is motivated more by the need to satisfy basic constraints than by any expectations of realism. Routh's law also allows a nonzero normal component of post-collision velocity, whose magnitude (within some range) changes with the specified value of e. On the other hand, Routh's law allows no variation in the tangential component of post-collision velocity, since all collisions corresponding to the energy ellipse shown in Fig. 7.8, for all values of e, are predicted to terminate on the line of

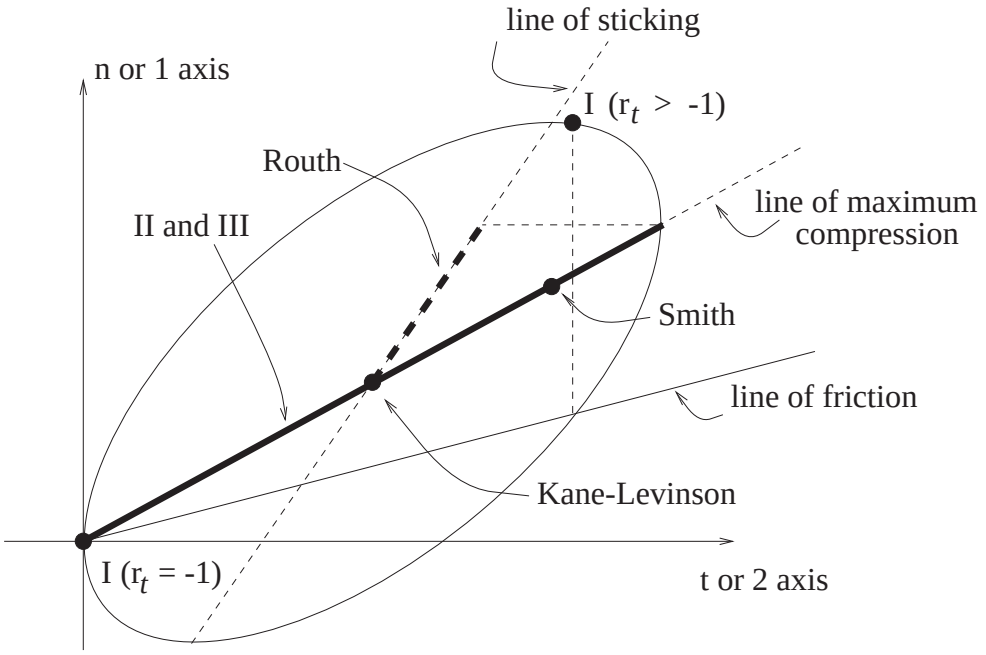

Figure 7.8: Region accessible in impulse space to various laws, for a tangential collision

sticking.

7.4 A Collision with Infinite Friction, $\mu \to \infty$

Figure 7.9 shows a collision where $\mu \to \infty$. The friction lines lie on the 2-axis. For the case shown, the center of the energy ellipse is below the 2-axis. As a result a perfectly plastic, sticking collision ($V_f = 0$) *cannot* occur in this case, since it would require a negative normal impulse. The region accessible to Routh's law is the line segment DJ (heavy, solid line in the figure). The region accessible to Kane and Levinson's law is the broken line segment DJH (heavy, with short dashes). The region accessible to Smith's law is the line segment DK (heavy, with long dashes). The regions accessible to laws I, II and III are given by the closed regions $BCGF$ (darkest shading), $BDKF$ (intermediate shading), and $ADKF$ (lightest shading), respectively. Here the curve FA coincides with the ellipse. Line CG makes an angle β with the 1-axis, given by $\beta := \tan^{-1}\left(\frac{2m_{22}V_{iT}}{m_{11}V_{iN}}\right)$, where m_{11} and m_{22} are the (1,1) and (2,2) elements respectively of the mass matrix, and V_{iT} and V_{iN} are the tangential and normal components respectively of the pre-collision relative velocity at the contact point (we assume that both V_{iT} and V_{iN} are negative).

It is interesting to note that for a special incidence angle the points D, E and J can merge for this collision. For that situation, a perfectly plastic, sticking collision can occur for a purely tangential collision. Line DJ shrinks to a point, and Routh's method can predict *only* a perfectly plastic, sticking collision, regardless of the choice of e.

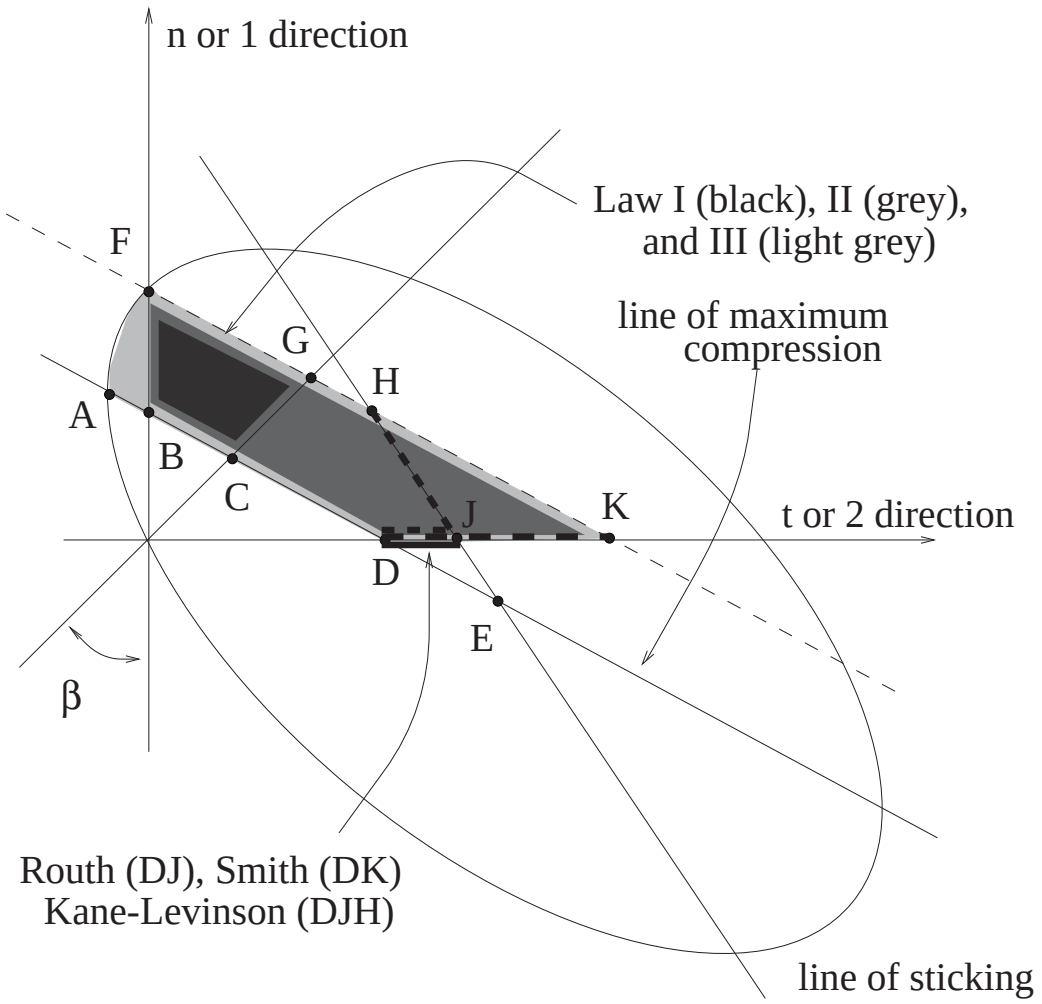

Figure 7.9: Region accessible in impulse space to various laws, for $\mu \to \infty$

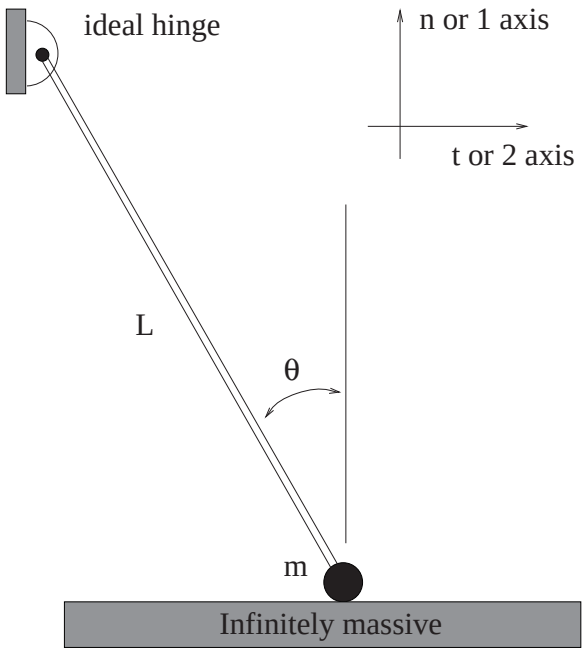

Figure 7.10: A 2D pendulum strikes a wall

7.5 A Collision with Unbounded M

Figure 7.10 shows a pendulum striking a rigid, immovable surface. A 3D version of this problem using Routh's incremental law has been considered, for example, by Stronge [64]. Here we consider this problem in 2D, for the various collision laws discussed in this chapter. The problem is interesting because the kinematic constraint makes the problem one dimensional, but the direction of relative motion at the contact point is not lined up with the normal direction as is usually the case in one dimensional collisions. We assume that the friction coefficient $\mu > \tan\theta$, for in this case very large contact impulses may act along the rod (see Fig. 7.10).

The mass matrix M has an eigenvector perpendicular to the rod, along the direction $\{\sin\theta, \cos\theta\}^T$, with corresponding eigenvalue m (recall that equal and opposite contact forces acting along an eigenvector, at the contact point, must produce a relative acceleration in the same direction). The other eigenvector is parallel to the rod, along $\{\cos\theta, -\sin\theta\}^T$, and the corresponding eigenvalue is infinite.

This problem may be treated as a constrained, effectively 1D problem, with suitable additional hypotheses. This would be in the same spirit as Stronge's treatment of the same problem in 3D as a constrained 2D problem[2].

An alternative approach might be to treat the second eigenvalue of the mass matrix as the limiting case of a very large number, say λ. The solutions obtained may then be checked to see if they are reasonable for the constrained problem. This is the approach adopted in the present study. For all values of λ, we kept V_i the same as in the constrained problem, i.e., perpendicular to the rod.

[2]Note that the solution to the lower dimensional constrained problem will be *no more* accurate than any of the *ad hoc* methods discussed here, since Routh's contact assumptions will be seriously violated due to flexibility in the slender rod as well as clearance/compliance effects at the hinge.

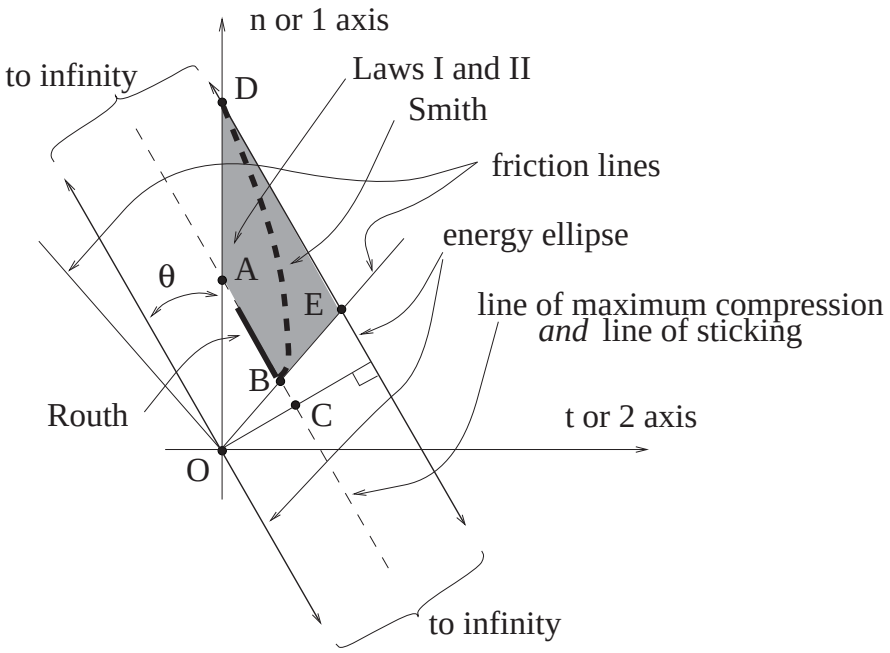

Figure 7.11: A finite portion of the energy ellipse in impulse space, for $\lambda \to \infty$

For $\lambda \to \infty$, Routh's collision law predicts $V_f \to 0$ all the kinetic energy being dissipated, for any e between 0 and 1. Smith's law predicts $V_f \to -eV_i$, with a fraction $1 - e^2$ of the total kinetic energy dissipated. Kane-Levinson predicts $V_{fN} = -eV_{iN}$ and $V_{fT} = 0$, with system kinetic energy *increasing* by an amount proportional to λ; for this law, too, there is an impulse along the rod proportional to λ, and the constraint at the hinge is violated because the contact point acquires a velocity component along the rod. For a numerical example, see Table 7.1 below.

7.5.1 The Energy Ellipse in Impulse Space, for $\lambda = \infty$

If we draw energy ellipses in impulse space for increasing λ, then the ellipses grow longer as λ becomes larger. In the limiting case, we can draw a *finite portion* of the energy ellipse, in a region near the origin (see Fig. 7.11). If we fix a region of finite size, and then draw the portion of the ellipse that lies inside this region for increasing values of λ, then in the limit we obtain two parallel lines as shown in the figure. Also, *inside* this finite region, the lines of maximum compression and of sticking merge. This line, as well as the edges of the ellipse, all make the same angle θ with the normal direction (like the rod in Fig. 7.10). Figure 7.11 shows the center of the energy ellipse (point C). The impulses predicted by Kane-Levinson are infinite, and thus lie outside the region shown in the figure. The region accessible to Routh's law, for various values of normal restitution e, is the heavy solid line along BA. The region accessible to Smith's law is the thick dashed curve from B to D. The regions accessible to laws I and II are identical for this example – the trapezoid $ABED$. The limiting behavior as $\lambda \to \infty$ for law III is more complicated. The accessible region for law III is the line segment BE, for cases when the tangential restitution parameter is greater than or equal to the normal restitution parameter, i.e., $r_t \geq r_n$ (Fig. 7.11). When $r_t < r_n$ there is an impulse proportional to $\lambda^{1/2}$ along the rod. Thus, two qualitative types of behavior exist. A numerical example is given in Table 7.2.

Table 7.1: Routh, Kane-Levinson, and Smith's Law

		$\lambda = 4$	$\lambda = 20$	$\lambda = 100$	$\lambda = 500$	$\lambda = \infty$
Routh	V_{fN}	0.247214	0.092121	0.021158	0.004357	0
	V_{fT}	-0.069222	0	0	0	0
	ΔKE	-0.368355	-0.422836	-0.479733	-0.495706	-0.5
Kane & Levinson	V_{fN}	0.247214	0.247214	0.247214	0.247214	0.247214
	V_{fT}	-0.069222	0	0	0	0
	ΔKE	-0.368355	+0.055704	+2.26685	+13.3226	$+\infty$
Smith	V_{fN}	0.247214	0.247214	0.247214	0.247214	0.247214
	V_{fT}	-0.069222	0.432100	0.657373	0.736339	0.760845
	ΔKE	-0.368355	-0.278047	-0.202765	-0.184037	-0.180000

In conclusion, the limiting case is handled well by Routh's law, Smith's law, and by laws I and II. Kane-Levinson and law III both encounter difficulties for this problem, including infinite impulses. Kane-Levinson, in the limit, predicts an infinite gain in kinetic energy along with a post-collision relative velocity that violates the kinematic constraint in the problem. Law III predicts an energy preserving collision with an impulse proportional to $\lambda^{1/2}$, and with V_f proportional to $\lambda^{-1/2}$. The limiting value of $V_f = 0$ is allowed by the kinematic constraint of the problem, but the accompanying prediction of law III that $\Delta K.E. = 0$ is not consistent with $V_f = 0$ for the constrained problem.

7.5.2 Numerical Example for Collision with Unbounded M

See Fig. 7.10. Here, we take $\theta = \pi/10$, $m = 1$, the second (large) eigenvalue of the mass matrix to be λ, friction coefficient $\mu = 1/2 > \tan\theta$, normal restitution $e = 0.8$ and the pre-collision relative velocity V_i to be $\{-\sin\theta, -\cos\theta\}^T$ in appropriate units. Note that the choice of V_i respects the constraint on the actual system. The predictions of the laws of Routh, Kane and Levinson, and Smith are given in Table 7.1 for increasing λ.

Results of similar calculations with law III are given in Table 7.2 (we use the same values of θ, μ and e). As seen in Table 7.2, for $r_t < r_n$ in law III, the impulse grows roughly as $\lambda^{1/2}$, and the direction gets aligned with the rod (note, $976/3008 \approx \tan(\pi/10)$). Zero energy dissipation is predicted. At the same time the post-collision relative velocity goes to zero as $\lambda^{-1/2}$. The limiting case is $V_f = 0$ *and* zero energy dissipation, which is not consistent with the constrained pendulum case. For $r_t \geq r_n$ in law III, the limit of $\lambda \to \infty$ is well behaved and consistent with the constrained pendulum case.

Table 7.2: Law III, for r_t less than, equal to, and greater than r_n

		$\lambda = 10$	$\lambda = 10^3$	$\lambda = 10^5$	$\lambda = 10^7$	$\lambda = \infty$
$r_t < r_n$, $r_t = 0.6$, $r_n = 0.8$	P_N	1.748086	28.94058	300.9031	3007.798	∞
	P_T	0.874043	-8.01963	-96.6829	-976.238	$-\infty$
	V_{fN}	0.247214	0.126185	0.0132927	0.0013300	0
	V_{fT}	0.310244	0.291269	0.0306830	.0030700	0
	ΔKE	-0.334068	0	0	0	0
$r_t = r_n$, $r_t = 0.8$, $r_n = 0.8$	P_N	1.748086	2.287176	2.294251	2.294322	2.294323
	P_T	0.874043	1.143588	1.147126	1.147161	1.147161
	V_{fN}	0.247214	0.247214	0.247214	0.247214	0.247214
	V_{fT}	0.310244	0.754950	0.760786	0.760845	0.760845
	ΔKE	-0.334068	-0.182810	-0.1800283	-0.1800003	-0.18
$r_t > r_n$, $r_t = 0.9$, $r_n = 0.8$	P_N	1.748086	2.257637	2.283677	2.293140	2.294323
	P_T	0.874043	1.128818	1.141839	1.146570	1.147161
	V_{fN}	0.247214	0.240030	0.244650	0.246927	0.247214
	V_{fT}	0.310244	0.732916	0.752896	0.759962	0.760845
	ΔKE	-0.334068	-0.200994	-0.186630	-0.180742	-0.18

Chapter 8

More on Some Incremental Collision Models

This chapter contains discussions of some specific incremental models for rigid body collision laws. All the incremental models are simple, and it is difficult to properly allocate credit for them to specific people. These incremental laws are discussed in the context of some ideas developed in this thesis, such as homogeneity in velocity and/or mass (see Chapter 3), as well as the behaviors of these laws in simple situations like one dimensional and/or frictionless collisions; to this extent, some of the ideas may be new, even for laws that are not new. I believe the split-mass collision model of Section 8.1 is essentially new, as is the second bilinear spring model of Section 8.4.

All incremental collision models based on passive physical contact mechanisms are automatically guaranteed to satisfy fundamental physical restrictions like nonnegative dissipation of kinetic energy. Such models are fairly popular in multibody dynamics simulation applications, both because of the guarantee that basic constraints will not be violated, and because this "soft contact" approach (see e.g., Goyal, Pinson and Sinden [21]) can model both simultaneous multiple impacts[1] as well as treat collisions and enduring contacts in a unified environment.

On the other hand, the soft contact approach of putting springs and dashpots at every contact location suffers from some practical difficulties, too. For general impulse-response rigid systems, these incremental approaches are bound to be as inaccurate as more simplitic approaches, since they are based on force-response rigidity assumptions. In general simulation settings, even for objects that are assumed to be force-response rigid, the selection of spring-dashpot combination will often be arbitrary and correspondingly inaccurate. The simulation procedure will be numerically troublesome because of stiff spring-dashpot contacts becoming active during collisions (and also during enduring contacts). For single impacts (generally more common than multiple impacts), simple qualitative ideas like coefficient of restitution may be difficult to retain, as also features like homogeneity in velocity and/or mass (see Chapter 3). For the simplest collision configurations such as spheres, ideas like tangential restitution for frictional collisions may not be retained, since the tangential component of post-collision velocity in frictional collisions will turn out to be a somewhat erratic function of the ratio of characteristic times of harmonic oscillations in the normal and tangential directions.

It is well recognized that the coefficient of restitution has no fundamental validity as a constant that characterizes a pair of colliding bodies. Any collision law that, given a normal restitution parameter $0 \leq e \leq 1$, always predicts a post-collision relative velocity with Newtonian restitution

[1] Although simultaneous impact models attempt to predict something that is essentially unpredictable in general cases. See discussion in Section 10.1.

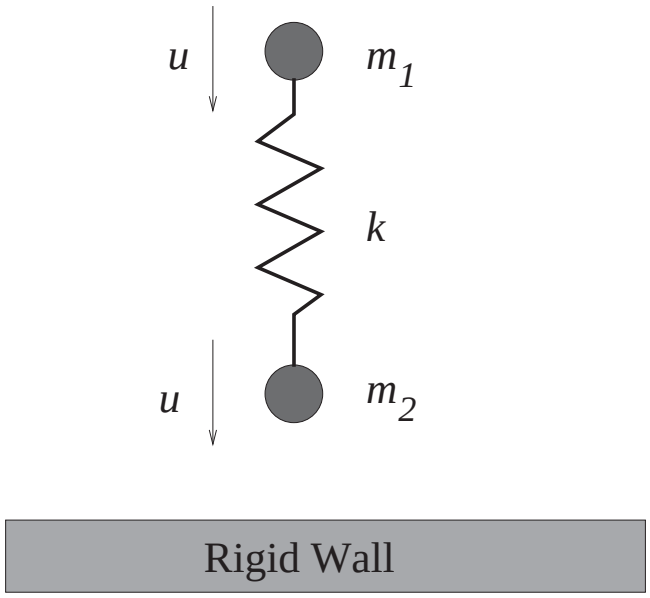

Figure 8.1: Split-mass collision model

e, must be considered an *ad hoc* modeling effort at best. On the other hand, incremental collision laws based on arbitrarily chosen physical contact mechanisms are also fundamentally incorrect for similar reasons. Since it is usually not clear which contact mechanism, if any, is best suited for general collision laws, a possible criterion for selecting a contact mechanism might be based on its predictions for the simplest collision configurations. One might, for example, examine the effective normal restitution predicted for 1D collisions by a given contact model (the restitution predicted will typically depend on the mass, the pre-collision relative velocity, as well as details of the contact mechanism). This is not to say that all models *should* reduce to Newtonian restitution, rather to suggest that the 1D and/or frictionless cases are worth looking at in detail.

The objective of this chapter is to examine in simple 1D situations some contact models that may be used in incremental 3D collision laws. The dependence of the observed coefficient of restitution in 1D collisions on various quantities including mass, pre-collision velocity as well as parameters of the contact mechanism, will give an indication of what might be expected in general 3D settings. It will be seen that a fairly common feature of simple collision laws, homogeneity of degree zero in mass and degree one in velocity, does not carry over to many incremental collision laws based on simple contact mechanisms.

8.1 A Split-Mass Collision Model

In a 1D example, consider two point masses m_1 and m_2, connected by a spring of stiffness k, colliding with a rigid wall as shown in Fig. 8.1. Here, the mass m_2 has an instantaneous, plastic collision with the wall[2]. Subsequently, the spring gets compressed and contact is maintained between the

[2]This 1D model of two masses connected by a spring, with the contacting mass having a perfectly plastic collision, is essentially the same physical model used by Mindlin [43] in his study of the impact behavior of packaged objects. However, Mindlin's model was restricted to 1D, and meant to be a somewhat realistic model for the specific system he was studying. The 3D version suggested

mass m_2 and the wall as long as the spring stays compressed. When the spring gets completely relaxed again, the collision ends (maintaining contact would require negative normal interaction force). At that instant, the velocity of mass m_2 is still zero, while that of mass m_1 is u upwards. The net momentum of the system is therefore $m_1 u$, which yields an average separation velocity of $\frac{m_1 u}{m_1 + m_2}$ for an approach velocity of u, and hence an effective coefficient of restitution

$$e = \frac{m_1}{m_1 + m_2}. \tag{8.1}$$

This idea can be used in a 3D collision model as follows. We consider a fictitious anisotropic point mass given by the mass matrix M, and split it into two parts, αM and $(1-\alpha)M$ for some $0 \leq \alpha \leq 1$, where the αM corresponds to m_1 and the $(1-\alpha)M$ to m_2. In order to match the restitution condition, we set $\alpha = e$, using Eq. 8.1. Then, in the spirit of Figs. 5.1 and 8.1, we construct a model with the "contact point" of Fig. 5.1 having anisotropic mass $(1-\alpha)M$ and the "anisotropic point mass" having the remaining αM. The $(1-\alpha)M$ is assumed to have a perfectly dead collision ($e = 0$) with the rigid wall, using (say) Routh's model [52] or the model discussed in Kane and Levinson[3] [32] (see Chapter 5). The mass αM interacts with the mass $(1-\alpha)M$ through spring/dashpot type contact elements, while the mass $(1-\alpha)M$ slides on the contact surface with Coulomb friction. Equations of motion for this system are numerically integrated until the natural termination condition of zero normal force is attained. Finally, the effective post-collision velocity is calculated as a weighted average of the velocities of the two point masses.

The spring stiffnesses in the normal and (two) tangential directions are arbitrary so far, and may be selected to possibly match experimental data in practical applications.

One might ask what advantages such an incremental model might have over simpler models, given that part of the calculation (the collision of the dead mass) is already carried out using some other collision model. A possible answer is that the plastic part of the collision model might be simple to implement, but might not have some desired features like tangential restitution. Another advantage of this particular incremental law is that the springs do not have any dissipation, making the equations of motion simpler. All non-frictional energy dissipation occurs in the initial plastic collision. Finally, except for the special case of $e = 1$, the contact point in this model is not massless. Hence, after the initial collision, its velocity is continuous, making numerical integration of the equations of motion simpler than for some models with massless contact points which can have discontinuous velocities.

Note that the split-mass model is homogeneous of degree zero in the mass, and of degree one in velocity (see discussion in Chapter 3).

8.2 A Model with Velocity-Dependent Restitution

Since the coefficient of restitution in head-on collisions usually decreases with increasing velocity (see e.g., Goldsmith [20]), one might want a collision model that incorporates velocity dependence. As discussed in Chapter 3, no such collision model can depend solely on dimensionless collision parameters. One possibility for such models, in the context of incremental collision models, is with some form of nonlinear damping.

---

here, as well as the its use in general rigid body collision modeling, is new to the best of my knowledge.

[3] Kane and Levinson's collision law never predicts an increase in kinetic energy for $e = 0$, so its use here would be safe.

As a particular example, consider a contact law with a linear spring and nonlinear dashpot, given by

$$F = -kx - cx\dot{x}.$$

This contact model is a special case of a more general nonlinear model of the form $F = -kx^m - cx^n\dot{x}$ discussed briefly by Walton [69]. The linear spring/nonlinear dashpot contact model, along with Coulomb friction, has also been used by Stoianovici and Hurmuzlu [58] in some 2D collision calculations; however, they considered bending effects in the colliding bodies, so their approach is outside the purview of rigid body collision modeling. An analysis of this contact model in 1D is presented below.

Consider the equation

$$m\ddot{x} + cx\dot{x} + kx = 0, \tag{8.2}$$

with initial conditions $x(0) = 0, \dot{x}(0) = \dot{x}_0 > 0$. We would like to know the value of $\dot{x} < 0$ when $x = 0$ again (actually the point of interest is when the force drops to zero, but it turns out to be when x becomes zero).

Changing the independent variable from time t to the nondimensional $\tau = \sqrt{k/m}\, t$, we obtain

$$x'' + \frac{c}{\sqrt{mk}}\, xx' + x = 0,$$

with initial conditions $x(0) = 0, x'(0) = \sqrt{m/k}\, \dot{x}_0$, where primes denote differentiation with respect to τ.

Changing the dependent variable from x to X, defined by $x = \sqrt{m/k}\, \dot{x}_0 X$, we obtain

$$X'' + \frac{c\dot{x}_0}{k} XX' + X = 0,$$

with initial conditions $X(0) = 0, X'(0) = 1$. The magnitude of X' at the next instant when $X = 0$ will be the effective coefficient of restitution for this "collision". It is seen that the dimensionless quantity $a := c\dot{x}_0/k$ determines the coefficient of restitution, which therefore depends on the velocity magnitude but, interestingly, is independent of the mass[4].

Given

$$X'' + aXX' + X = 0,$$

$X(0) = 0, X'(0) = 1$, we call $Y(X) := X'$ and obtain

$$Y\frac{dY}{dX} + (1 + aY)X = 0,$$

which gives

$$Y - \frac{1}{a}\ln(1 + aY) = 1 - \frac{1}{a}\ln(1 + a) - \frac{aX^2}{2}.$$

We are interested in the value of $Y = X'$ when X becomes zero again, or the negative root of

$$Y - \frac{1}{a}\ln(1 + aY) = 1 - \frac{1}{a}\ln(1 + a).$$

The magnitude of the negative root is equal to the coefficient of restitution. Thus, e may be found by solving

$$-e - \frac{1}{a}\ln(1 - ae) = 1 - \frac{1}{a}\ln(1 + a). \tag{8.3}$$

[4]Consequently, this contact law might be used to construct a collision law that is homogeneous in the mass but not in the velocity.

For a very small, we obtain by Taylor expansion from Eq. 8.3

$$e = 1 - 2a/3 + 4a^2/9 + \cdots.$$

For a very large, it is clear that the right hand side of Eq. 8.3 is approximately equal to one. It follows that $-\ln(1-ae)$ must be $O(a)$, or $1-ae$ must be $O(\exp(-a))$. Therefore, for large a, $e \approx 1/a$. Note that a is linear in the actual pre-collision velocity, so for large pre-collision velocities and fixed nonzero k and c in Eq. 8.2, the rebound velocity actually tends to the constant, k/c.

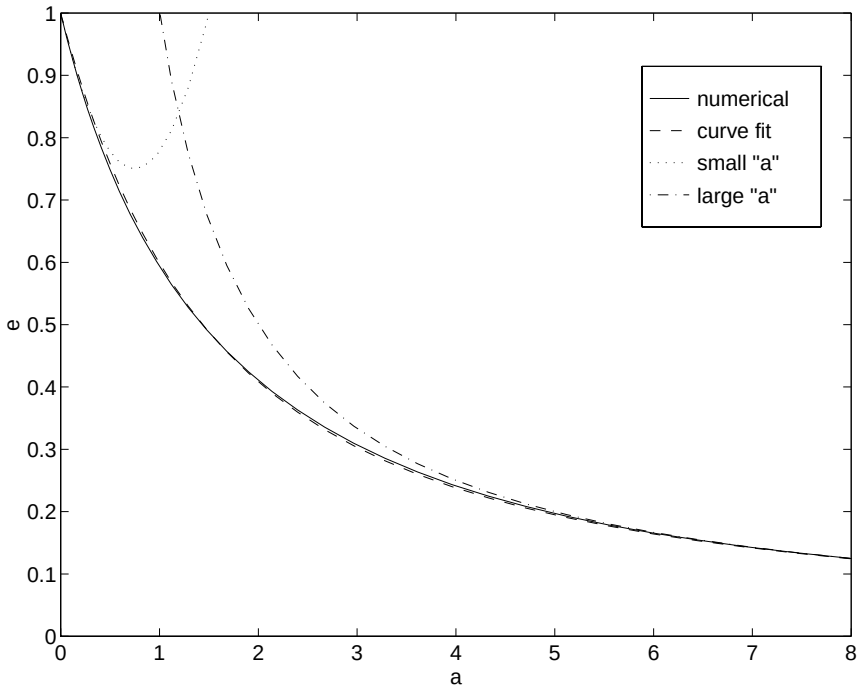

Figure 8.2: Restitution e vs. nondimensional damping a; linear spring/nonlinear dashpot

Other than the asymptotic approximations shown above, Eq. 8.3 can only be solved numerically. It turns out that solutions to Eq. 8.3 lie on a curve that satisfies the differential equation

$$\frac{de}{da} = \frac{(1+e)(1-e-ae)}{ae(1+a)},$$

with initial conditions $e(0) = 1$. Numerically obtained values of e against a are shown in Fig. 8.2, along with the graphs of the asymptotic solutions for small a and large a mentioned above. The function $e(a)$ is well-approximated (within 1.5 percent) by the expression

$$e \approx \frac{1}{\exp(-0.4a) + a},$$

which is also plotted in Fig. 8.2.

If the velocity-dependent restitution produced by a contact model of the form of Eq. 8.2 is found acceptable, then the interaction in the normal direction may be modeled by such a spring/nonlinear dashpot. Tangential interaction may be modeled with other springs or with infinite stiffness as in Routh's model, along with Coulomb friction. In such collision models, the ratio k/c might be used as a dimensional parameter. The approximation given above for e in terms of a may be used to pick the parameters k and c for a given or desired coefficient of normal restitution.

8.3 A Linear Spring/Dashpot Model

A linear spring-mass-dashpot collision model is possibly one of the simplest incremental collision models one might think of, and it has certainly been used in many applications (e.g., Goyal, Pinson and Sinden [21], [22] use linear springs and dashpots in a 3D, multiple contact setting). A brief analysis in 1D is presented below.

Consider the familiar spring-mass-dashpot model,

$$m\ddot{x} + c\dot{x} + kx = 0,$$

with $x(0) = 0$ and $\dot{x}(0) = \dot{x}_0 > 0$. We are interested in the (negative) value of $\dot{x}$ at the instant when the contact force $c\dot{x} + kx$ drops to zero.

Upon rescaling variables, we obtain the equation

$$x'' + 2\zeta x' + x = 0,$$

where the nondimensional $\zeta := \dfrac{c}{2\sqrt{km}}$, primes denote derivatives with respect to nondimensional time $\tau = \sqrt{k/m}\, t$, and we use initial conditions $x(0) = 0$ and $x'(0) = 1$ (x' may be scaled arbitrarily due to linearity). We are interested in the (negative) value of x' at the instant when $2\zeta x' + x = 0$. The magnitude of x' at that instant will be the effective coefficient of restitution e, which is seen to depend on m, c and k but not on the pre-collision velocity. Thus, such contact models may be used to construct collision laws that are homogeneous of degree one in velocity, but not homogeneous in the total mass.

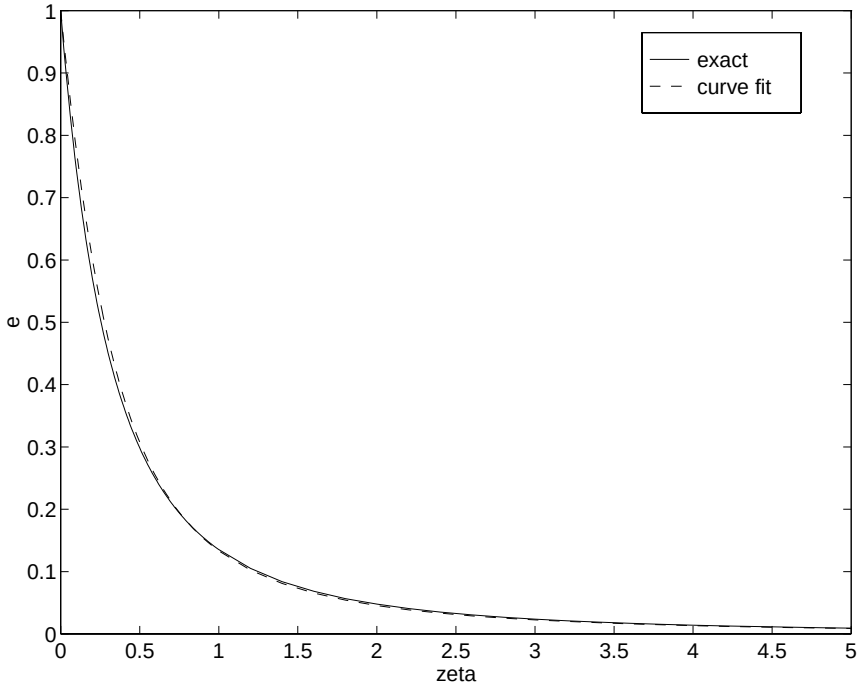

Figure 8.3: Restitution e vs. nondimensional damping ζ; linear spring/linear dashpot

It may be shown that e is given in terms of ζ by the relations

$$e = \exp\left(-\frac{\zeta}{\sqrt{1-\zeta^2}}\cos^{-1}(2\zeta^2 - 1)\right), \text{ for } \zeta < 1$$

$$e = \exp(-2) \approx 0.1353, \text{ for } \zeta = 1$$

$$e = \frac{1}{4\zeta\sqrt{\zeta^2-1}}\,\beta^{-\frac{\zeta}{\sqrt{\zeta^2-1}}}\left(\beta - \frac{1}{\beta}\right), \text{ for } \zeta > 1$$

$$\text{where } \beta := \sqrt{\frac{2\zeta^2 - 1 + 2\zeta\sqrt{\zeta^2-1}}{2\zeta^2 - 1 - 2\zeta\sqrt{\zeta^2-1}}}. \tag{8.4}$$

In Eq. 8.4 above, the limit $\zeta \to 1$ is well behaved. For large ζ (highly overdamped), $e \approx \frac{1}{4\zeta^2}$, and e can be fairly well approximated (within 6 percent) for all ζ by the expression

$$e \approx \frac{1}{1 + 2.5\zeta + 4\zeta^2},$$

as shown in Fig. 8.3. This approximation for e in terms of ζ may be used in 3D collision models, to appropriately pick c and k for a given mass matrix and a desired coefficient of normal restitution.

8.4 Bilinear Spring Models

Generally, nonlinear contact laws lead to collision laws with not all parameters dimensionless, and hence not homogeneous in both mass *and* velocity. However, some bilinear contact models *do* lead to a collision law homogeneous of degree zero in mass and degree one in velocity. In this contact model, there is no viscous damping. The contact force increases and decreases linearly with displacement, but at different rates. The collision ends when the contact force becomes zero.

There are two simple possibilities:

1. This model has been used by some researchers (see e.g., Drake and Walton [16] and Stronge [63]). We might require the contact force to be continuous, and the unloading line to be steeper than the loading line (in fact, the slope of the unloading line should be $1/e^2$ times the slope of the loading line, where e is the specified coefficient of restitution). In this case we have the situation depicted by the solid line OAB in Fig. 8.4. The collision terminates at some nonzero value of displacement, as in the linear spring/linear dashpot model. A possible difficulty of this model is that at the end of a collision it has a net accumulated relative displacement[5]. If the collision calculation is conducted in a unified environment with enduring contacts, then the colliding bodies may acquire a significant amount of overlap if several collisions occur.

2. Alternatively (new approach), we might require the contact force to drop to zero only at zero displacement. In this case, we allow a discontinuity in the contact force, at the point of maximum compression. The unloading line is less steep than the loading line in this case (in fact, the slope of the unloading line is e^2 times that of the loading line). In this case we have the situation depicted by the dashed line $OACO$ in Fig. 8.4.

A possible advantage of approach (2) over (1) is that for very small but nonzero e, the unloading curve becomes very steep and numerically troublesome for approach (1). Such problems are avoided in approach (2).

The load-displacement graphs given in Fig. 8.4 are unambiguous as long as monotonic loading is followed by monotonic unloading. If partial unloading is followed by reloading, then further

[5]Also noted by S. Goyal (personal communication).

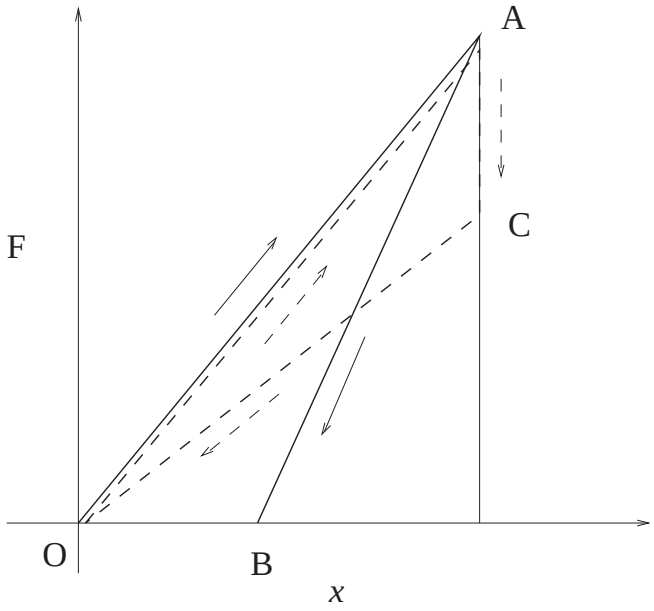

Figure 8.4: Bilinear spring contact model

hypotheses are needed about the reloading path. For some plausible reloading curves, if such bilinear laws are used in detailed modeling of slightly deformable bodies as in Chapter 9, small vibrations in the colliding bodies might lead to discontinuities in the contact force, particularly for approach (2).

For modeling collisions of force-response rigid bodies, both approaches (1) and (2) seem viable (for a discussion of force-response and impulse-response rigidity, see Chapter 2).

These bilinear contact models are possible physical realizations of a work-based definition of the coefficient of normal restitution, referred to as an *energetic* coefficient, discussed by Stronge (see e.g., [60]).

8.5 Contact Elements Aligned with Eigenvectors of M

As discussed briefly under general frictional point-contact models in Chapter 5, for collisions with *diagonal* mass matrices and high coefficients of friction, tangential restitution effects largely depend on the difference in time periods of the normal and tangential spring-mass systems. Hence, the observed coefficient of tangential restitution depends strongly on the ratios of the inertias and the spring stiffnesses in the normal and tangential directions. As also mentioned earlier, it is not known how best to think about tangential restitution for collisions where the mass matrix is *not* diagonal. A possible approach is to think of restitution in the directions along the eigenvectors of the mass matrix (the eigenvectors become aligned with the normal and tangential directions when the mass matrix is diagonal).

In simple spring-mass contact models, for an arbitrary mass matrix and high coefficient of friction, the resulting collisional interaction becomes roughly decoupled if the contact springs are aligned with the eigenvectors of the mass matrix. In this case, the collision model reduces to the system depicted schematically for 2D in Fig. 8.5. The point masses λ_1 and λ_2 (the eigenvalues of the mass matrix) move along the eigendirections only, and are connected to the contact point C by springs of stiffnesses k_1 and k_2. The contact point C may or may not have mass.

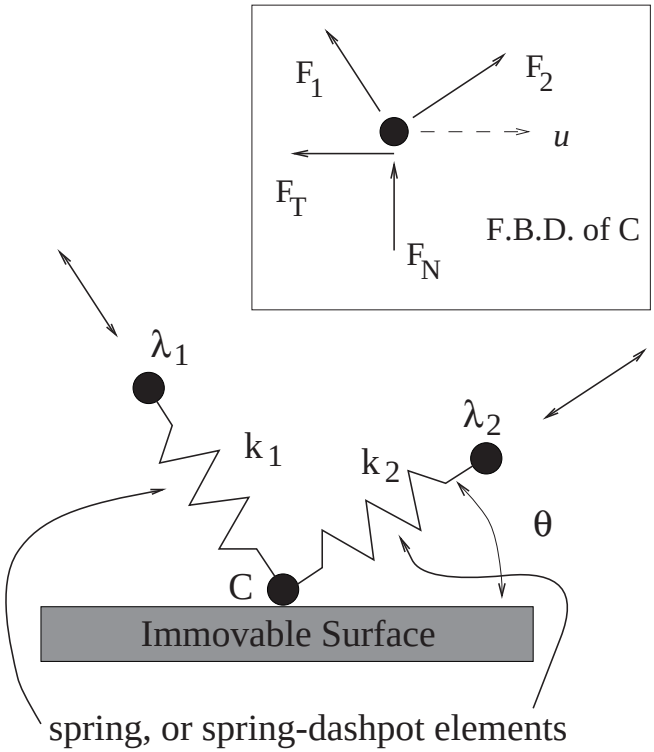

Figure 8.5: Contact model with springs aligned with eigenvectors

Such models with contact elements aligned along the eigenvectors will reduce to the familiar case of contact elements aligned with the normal and tangential directions, whenever the mass matrix is diagonal. Hence, if the springs (and their dissipation mechanisms, such as dashpots) are chosen based on simple 1D analyses such as those presented earlier in this chapter, the resulting collision law will reduce to the usual normal restitution for 1D collisions. However, the effective restitution observed for *frictionless* 3D collisions may not be the same as in the 1D case, i.e., simple rules for choosing the stiffness and damping parameters in the contact model may produce a pre-specified restitution in 1D collisions, but not in frictionless 3D collisions.

If the contact point C has nonzero mass, then it must first have a collision with the immovable surface at the start of the calculation, as discussed earlier in this chapter under split-mass models. While this requires an extra calculation, it also makes the equations of motion better behaved because the velocity of the contact point must then be continuous. On the other hand, if the contact point C is massless, then its velocity at each instant of time must be found by force balance. This is troublesome, both numerically (because the velocity can be discontinuous), as well due to possible non-uniqueness of solutions.

It is interesting to note that Goyal *et al.* [21, 22] discuss the use of linear spring and dashpot elements at general orientations in their dynamic simulation program; thus their model might allow, as a special case, the contact model considered in this section, with contact elements aligned with the eigenvectors of M. As shown below, when the eigenvectors are not aligned with the normal and tangential directions, it is possible to have nonuniqueness of solutions. However, Goyal *et al.* [21] mention that they have found it sufficient in their experience to just use contact elements lined up with the normal and tangential directions, not necessarily along the eigenvectors of M (in which case, nonuniqueness does not occur).

8.5.1 An Example of Nonuniqueness

As an example, consider the Free Body Diagram of contact point C shown in Fig. 8.5. The velocity u of C is along the tangential direction, and is shown by a dashed arrow. If C is massless, then we have

$$F_2 \cos\theta - F_1 \sin\theta - F_T = 0,$$

$$\text{and } F_2 \sin\theta + F_1 \cos\theta + F_n = 0.$$

Consider a contact model with linear springs and linear dashpots. Let the dashpot constants be c_1 and c_2, the extensions of the springs be x_1 and x_2, the velocities of masses λ_1 and λ_2 be v_1 and v_2 in directions pointing away from C, and the extension rates of the springs be $\dot{x}_1$ and $\dot{x}_2$. Under the assumption of displacements being small compared to the lengths of the springs, we ignore changes in the angle θ.

We have the following relations:

$$\dot{x}_1 = v_1 + u\sin\theta,$$

$$\dot{x}_2 = v_2 - u\cos\theta,$$

$$F_1 = k_1 x_1 + c_1 \dot{x}_1 = k_1 x_1 + c_1 v_1 + c_1 u \sin\theta,$$

$$F_2 = k_2 x_2 + c_2 \dot{x}_2 = k_2 x_2 + c_2 v_2 - c_2 u \cos\theta.$$

For Coulomb friction, we have the additional requirements that either $u = 0$ and $|F_T| \le F_N$, or $u \neq 0$ and $F_T = \text{sign}(u)\ \mu F_N$, where we assume $F_N > 0$. Thus, we have three possible cases, $u > 0$, $u = 0$, and $u < 0$. If more than one consistent solution can be found, then solutions are not unique.

Let $\theta = \pi/4$, $c_1 = 2$, $c_2 = 1$ and $\mu = 6$. Let $k_1 x_1 + c_1 v_1 = -3\sqrt{2}$, and $k_2 x_2 + c_2 v_2 = 2\sqrt{2}$ at some instant.

Solution 1: Setting $u = 0$, we obtain $F_1 = -3\sqrt{2}$, $F_2 = 2\sqrt{2}$, hence $F_N = 1 > 0$ and $F_T = 5 < \mu F_N = 6$.

Solution 2: Setting $u = 2/3$, we obtain $F_1 = -7\sqrt{2}\ /3$, $F_2 = 5\sqrt{2}\ /3$, hence $F_N = 2/3 > 0$ and $F_T = 4 = \mu F_N$.

8.5.2 Uniqueness for $\theta = 0$ or $\pi/2$

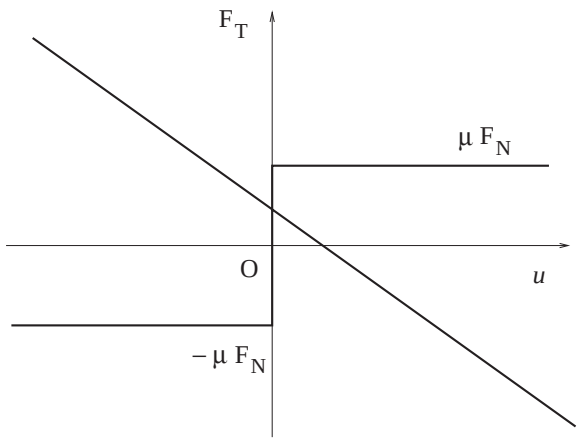

Figure 8.6: F_T vs. u for $\theta = 0$

By symmetry, $\theta = 0$ is equivalent to $\theta = \pi/2$, so we consider just $\theta = 0$. (This is the case where the eigenvectors of M are lined up with the contact surface normal and tangential directions.) We then have

$$F_N = -F_1 = -k_1 x_1 - c_1 v_1,$$
$$F_T = F_2 = k_2 x_2 + c_2 v_2 - c_2 u, \tag{8.5}$$

along with the friction condition that either $u = 0$ and $|F_T| \leq F_N$, or $u \neq 0$ and $F_T = \text{sign}(u)\, \mu F_N$, where we assume $F_N > 0$.

Note that for a massless contact point we permit discontinuous velocities, but still require continuity of displacement. Thus, x_i and v_i, $i = 1, 2$ are assumed known at any instant, and so is F_N. Given F_N and μ, the graph of F_T vs. u as given by the friction inequality is the broken line shown in Fig. 8.6, while Eq. 8.5 gives a line with *negative* slope whenever $c_2 > 0$. It follows that there must always be one and only one point of intersection. This proves uniqueness.

Chapter 9

Non-rigid Body Collisions with Linear Vibrations

The discussion of rigid body collisions can perhaps be put into perspective by considering a fairly simple kind of non-rigid body collision, where the internal dynamics of the colliding bodies is linear. By considering this example, it is possible to see the place and the validity of various aspects of rigid body collision modeling. The general treatment of this chapter appears to be new in the context of rigid body collisions, although specific dynamics problems of this type have of course been solved in other references (e.g., Goldsmith [20]). The connections made with ideas from rigid body collision modeling, such as local interaction or homogeneity in velocity and/or mass (see Chapter 3) appear to be new.

Figure 9.1 shows two colliding bodies. It is assumed that there is a small contact region where possibly nonlinear, but pseudostatic contact interaction occurs; and that over the duration of the collision, there are no large overall motions of the colliding bodies. It is also assumed that there exists an intermediate length scale (shown by a dashed line), much larger than the contact region but much smaller than typical dimensions of the colliding bodies. Under this assumption, the intermediate region on each body may be treated as a point with only translational degrees of freedom, in the equations of motion for the colliding bodies. At the same time, once the positions of the respective intermediate regions are known, the interference between these regions may be calculated and used with a nonlinear contact law to calculate the contact forces. In Fig. 9.1, $\mathbf{r}(t)$ represents the position vector from the intermediate region on one body to that on the other. By assumption, changes in $\mathbf{r}(t)$ may be calculated from the dynamic equations for the colliding bodies in response to contact forces, changes in the interference at the small contact region may be calculated from changes in $\mathbf{r}(t)$, and contact forces may be calculated from the interference. For all practical purposes, the interference at the contact region is equivalent to $\mathbf{r}(t)$.

9.1 Free Response

Picking a suitable coordinate system, we denote the 3×1 matrix of components of $\mathbf{r}$ as r. In the absence of contact forces, the general solution for $r(t)$ is expressible as (possibly after truncation)

$$r(t) = a_0 + a_1 t + \sum_{k=2}^{m} a_k \exp(\lambda_k t), \tag{9.1}$$

where the a's are arbitrary constant 3×1 matrices, with a_0 and a_1 representing rigid body motions, and where no λ_k has positive real part.

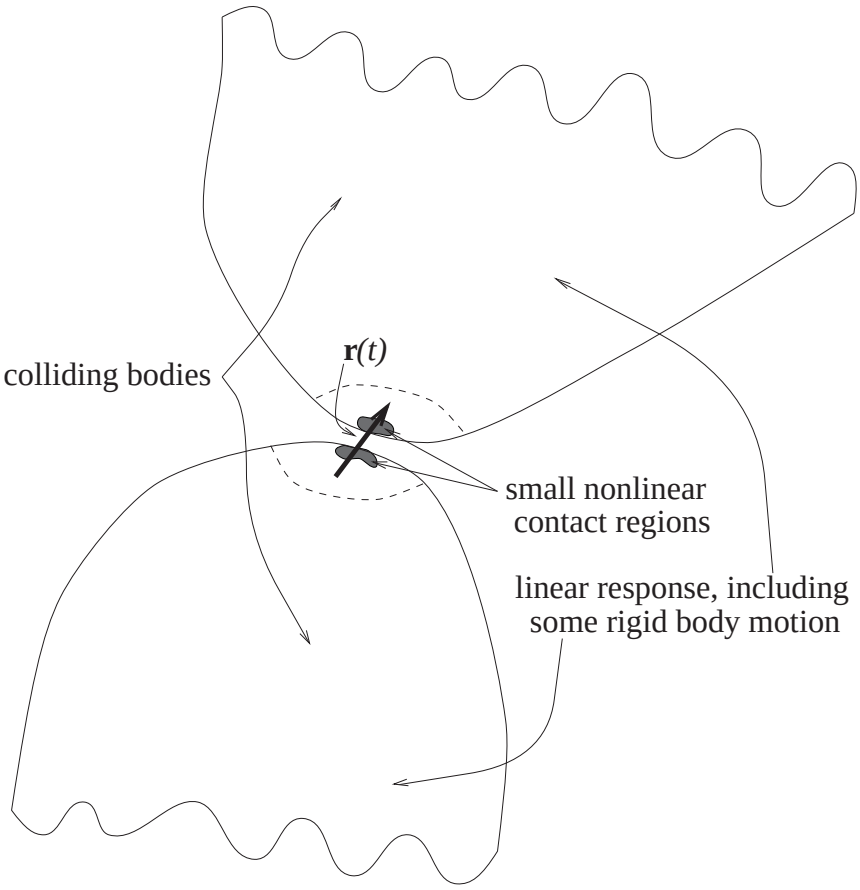

Figure 9.1: A Non-Rigid Body Collision

Observe that if $r(t) = a_0 + a_1 t + \sum_{k=2}^{m} a_k \exp(\lambda_k t)$, then it follows that

$$\dot{r}(t) = a_1 + \sum_{k=2}^{m} \lambda_k a_k \exp(\lambda_k t),$$

thus both r and $\dot{r}$ are known if the a's are known. In particular, $r(0) = a_0 + \sum_{k=2}^{m} a_k$, and $\dot{r}(0) = a_1 + \sum_{k=2}^{m} \lambda_k a_k$.

If we set $t = 0$ at the end of the collision, then we know the motions after the collision from Eq. 9.1. *During* the collision, at each instant there is a set of a's that would describe subsequent motions of the system were the collision to terminate at that instant. This evolving set of a's can be used as coordinates to describe the collisional interaction between the bodies.

In the absence of contact forces, from Eq. 9.1, note that $r(t + t_1) = (a_0 + a_1 t_1) + a_1 t + \sum_{k=2}^{m} \{a_k \exp(\lambda_k t_1)\} \exp(\lambda_k t)$. Thus, in the absence of forces, we have

$$\begin{aligned} \dot{a}_0 &= a_1 \\ \dot{a}_1 &= 0 \\ \dot{a}_k &= \lambda_k a_k, \text{ for } k = 2, \cdots, m. \end{aligned} \tag{9.2}$$

9.2 Impulse Response

Consider the response of the system to equal and opposite impulses acting at the contact point. Let initial conditions be zero, i.e., all the a's in Eq. 9.1 above be zero. Let a general impulse P act at time $t = 0$. Then the response of the system will be given by

$$r(t) = b_1 t + \sum_{k=2}^{m} b_k \exp(\lambda_k t),$$

for some constant b's that depend *linearly* on P. Thus, for a given system, there must be 3×3 matrices A_k such that $b_k = A_k P$ for each $k = 1, 2, \cdots, m$. Of these A's, A_1 will be the inverse of the by now familiar local mass matrix. Thus we may write the response to an impulse P as

$$r(t) = M^{-1} P t + \sum_{k=2}^{m} A_k P \exp(\lambda_k t), \tag{9.3}$$

where M and the A's are known constant matrices for any given pair of colliding bodies.

9.3 Collision Calculation

Using Eqs. 9.2 and 9.3, we may write equations describing the evolution of a collision, when there is a contact force F present. The force F will generally depend on the interference $r(t)$, its derivative $\dot{r}(t)$, and possibly on the time histories of these quantities as well. Since both r and $\dot{r}$ are known if the a's are known, we write $F = F(\mathbf{a},\ \text{history}\ )$, where $\mathbf{a}$ is shorthand for $a_0, a_1, \cdots, a_m$. Therefore, the equations describing the collisional interaction are

$$\begin{aligned} \dot{a}_0 &= a_1 \\ \dot{a}_1 &= M^{-1} F(\mathbf{a},\ \text{history}\ ) \\ \dot{a}_k &= A_k F(\mathbf{a},\ \text{history}\ ) + \lambda_k a_k, \text{ for } k = 2, \cdots, m. \end{aligned} \tag{9.4}$$

One expects that at the start of collision, $a_0 = 0$, $a_1 = V_i$, and $a_k = 0$ for $k = 2, \cdots, m$.

We can now examine several ideas from this thesis in the light of Eqs. 9.4.

9.3.1 Local Interaction

To the extent that Eq. 9.4 is an accurate representation of the dynamic interaction of the bodies, and given that the initial conditions for the collision are $a_k = 0$ for $k \neq 1$ and $a_1 = V_i$ as suggested above, the result of the collision is determined by the velocities of only the contact points on the bodies; hence a collision model based on these ideas is automatically a local interaction model (see discussion in Chapter 3). If the initial conditions are different, i.e., if there are significant vibrations in the colliding bodies at the start of the collision, then the model is not local in the sense of Chapter 3.

Note, also, that if the *contact model* is local, then the contact force only depends local quantities like $r(t)$, its derivatives, and possibly their time history. The dependence of the force on each a_k, as in $F(\mathbf{a},\ \text{history}\ )$, implies a possibly non-local contact model. Usually, contact models will be local though the overall interaction might not be. However, since no explicit calculations are carried out, the general form of $F(\mathbf{a},\ \text{history}\ )$ is retained for simplicity.

9.3.2 Force-response rigidity

If each λ_k has a large imaginary part and strictly negative real part, and if the force F varies slowly, then each a_k, for $k = 2, \cdots, m$, will closely match the static response

$$a_k \approx -\frac{1}{\lambda_k} A_k F,$$

which itself will be of $O(|\lambda_k|^{-1})$ in magnitude (hence, small and slowly varying). Under these circumstances, it is justifiable to ignore the dependence of F on a_k, for $k = 2, \cdots, m$, and to assume that

$$F = F(a_0, a_1,\ \text{history of}\ a_0\ \text{and}\ a_1).$$

This assumption is exactly equivalent to assuming that the colliding bodies are force-response rigid, i.e., that they behave like rigid bodies moving under the influence of contact forces even *during* the collision (see Chapter 2).

9.3.3 Homogeneity of Collision Laws in Velocity

The principal conclusions we may draw about when the collisional interaction will be homogeneous of degree one in the relative velocity, are as follows.

1. If the contact force F is itself homogeneous of degree one in the a's, or the relative displacement and velocity, then the net interaction will be homogeneous of degree one in velocity. Forces homogeneous in velocity include forces that are linear, as well as Coulomb friction forces as well as forces that switch off and on again as contact is broken and reestablished.

2. If the amplitude of internal vibrations is large and the contact interaction is stiff and well damped, then the contact may be approximated as a dead contact, and the interaction will be approximately homogeneous in velocity.

3. If the amplitude of internal vibrations is small, and the contact interaction is not homogeneous of degree one in the a's, then the interaction will *not* be homogeneous of degree one in the velocity.

The reasoning behind these ideas is given below.

In Eqs. 9.4, assume that the interaction force F is not history dependent, and switches on (or off) when some scalar quantity that is *linear* in the a's changes sign. This assumption is not too restrictive. For example, the force may switch on whenever the normal component of the interference $r(t)$ becomes positive, and switch off whenever the normal component of $r(t)$ becomes negative; as another example, the force F may be linear in r and $\dot{r}$, with positive normal component, and zero otherwise. Assume, further, that F is linear in the a's. In that case, the entire collisional interaction may be divided into two phases, with F switched on and F switched off. In each phase, the equations of motion are linear. It follows that given any solution, all scalar multiples of that solution are also solutions to the system equations, since the equations of each phase are linear and the switching between phases occurs at the same point in time as before. For such contact forces, then, the post-collision relative velocity at the contact point scales linearly with the pre-collision relative velocity magnitude, i.e., the collision law is homogeneous of degree one in the input velocity (see discussion in Chapter 3). As a matter of fact, if the force F is not linear in the a's but only homogeneous of degree one in the a's (such as Coulomb friction forces), the collision law will still be homogeneous of degree one.

The conclusions of the previous paragraph obviously hold even for collisions where contact is broken and reestablished several times in the course of one collision, with the contact force switching off and on each time. Such multiple-impact collisions are in fact fairly common for slender bodies with persistent, slow vibrations, such as the slender steel rods studied recently by Stoianovici and Hurmuzlu [58].

If the colliding bodies have persistent, slow vibrations, and if there are several short periods of contact with long periods without contact, one might approximate each period of contact by an instantaneous impulsive interaction, or an impact (one of several in the full collision). If the impulse transmitted at each impact is homogeneous of degree one in the a's, then the overall collision law must again be homogeneous of degree one in the velocity. In particular, a "dead" impact law, such as $n^T\dot{r} \rightarrow 0$ (normal component dies at each impact), is homogeneous of degree one in the a's. So also is a law where the normal component is reversed using some coefficient of restitution type interaction law for each impact within the big collision.

Finally, if the nonlinear contact mechanism is very stiff and well-damped, so the the normal component of the interference r is small compared to some of the vibrational coordinates (the a's), then the contact may be approximated as a dead contact, and hence homogeneous of degree one in the a's, *whether or not* the contact law is homogeneous in reality. For such cases, with most of the action occurring on the slow vibrational time scale of the colliding bodies, the net collision is expected to be homogeneous of degree one in velocity. The ideas in this paragraph are supported by the data of Stoianovici and Hurmuzlu [58], who observed that the net coefficient of restitution observed for slender rods dropped onto a massive anvil was strongly dependent on collision configuration but effectively independent of velocity magnitude in the range studied.

In contrast, consider a force-response rigid body as described in the previous subsection, where the internal vibrations of the colliding bodies are negligible. In this case all the action is in the nonlinear contact mechanism, and the collision will typically not be homogeneous in the velocity if the contact force F is not homogeneous in the a's.

9.3.4 Homogeneity of Collision Laws in Mass

The idea of homogeneity in mass is not well defined in the context of this chapter. Given a pair of colliding bodies, for example, the mass matrix may be scaled by a constant either by "changing" the densities, or the sizes, or both. So it is not clear which pairs of colliding bodies are to be

compared. At the same time, as bodies of different sizes or densities are compared, it is not clear whether the contact interaction laws should be changed or not.

In the special case of lightly damped bodies, "changing" the densities or the sizes by scaling factors comparable to unity changes the time scale of the collision without changing the damping characteristics much. In such cases the collisional interaction can be homogeneous of degree zero in the mass. However, homogeneity in the mass will be lost if there are significant slow vibrations leading to *multiple impacts* within the collision. This is because the times of the multiple impacts depend in a complicated way on the natural frequencies of vibration, as well as the relative amplitudes of the different modes of vibration. If the density of the material is "changed", then the matrices A_k and the natural frequencies scale in different ways[1], and the sequence of multiple collisions will be altered. As demonstrated by Stoianovici and Hurmuzlu [58], multiple collisions are the dominant mechanism for qualitative changes in the collisional behavior of different rods of the same material and different slenderness ratios.

[1] The natural frequencies are proportional to $\sqrt{1/\rho}$, while the A_k are proportional to $1/\rho$, where ρ is the density.

Chapter 10

Some Miscellaneous Topics

This chapter presents some miscellaneous topics that, though relevant to rigid body collisions, do not fit naturally into the development of the preceding chapters. Included are a discussion of the ill-posedness of simultaneous multiple impacts, some general theoretical conclusions about the collisional behavior of nearly spherical objects, a proof of existence of solutions for Smith's law (discussed in Chapter 5), a proof that arbitrary local mass matrices are in fact physically realizable using unconstrained bodies of finite mass (recall that in Chapter 3 it was only demonstrated that arbitrary mass matrices were realizable using *mechanisms*, which may be thought of as unconstrained objects with infinite inertia in some directions), a discussion of a somewhat little-known, alternative definition of the coefficient of restitution due to Ivanov [24], and finally a brief discussion of some of the issues involved in constructing an algebraic collision law that can access the entire region in impulse space that is reasonably available in a general collision (i.e., a law that, for suitably chosen values of collision parameters, can capture *any* observed outcome, and that can predict impossible behaviors for *no* permissible values of collision parameters).

10.1 Simultaneous Multiple Impact Problems

The rigid body collisions considered in this thesis are restricted to collisions with single contact points, i.e., single impacts. In the discussion of basic assumptions in Section 2.2, it was mentioned briefly that simultaneous multiple impact problems are even more ill-posed than single contact problems and require additional hypotheses before a solution can be found. This section presents an overview of the basic issues involved. For an excellent discussion of the difficulties involved in multiple impact problems, see Ivanov [25].

In general motions of generic rigid body systems, single impacts are far more common than simultaneous multiple impact problems. Simultaneous multiple impacts in many systems will break up into sequences of closely spaced single impacts under slight perturbations in initial conditions. For such systems, simultaneous impacts are zero probability events. In fact, under the rigid body idealization, *infinitesimal* perturbations can break up simultaneous impacts into sequences of single impacts, as shown by a simple example of three spheres[1] in Fig. 10.1.

Nevertheless, simultaneous multiple impacts can frequently occur in systems with special geometries, particularly systems with already existing sustained contacts that transmit impulses during collisions. An example of such a system is a ladder resting on a frictional floor, and falling towards a wall (see Fig. 10.2).

[1] This particular example is a classical problem – see Ivanov [25].

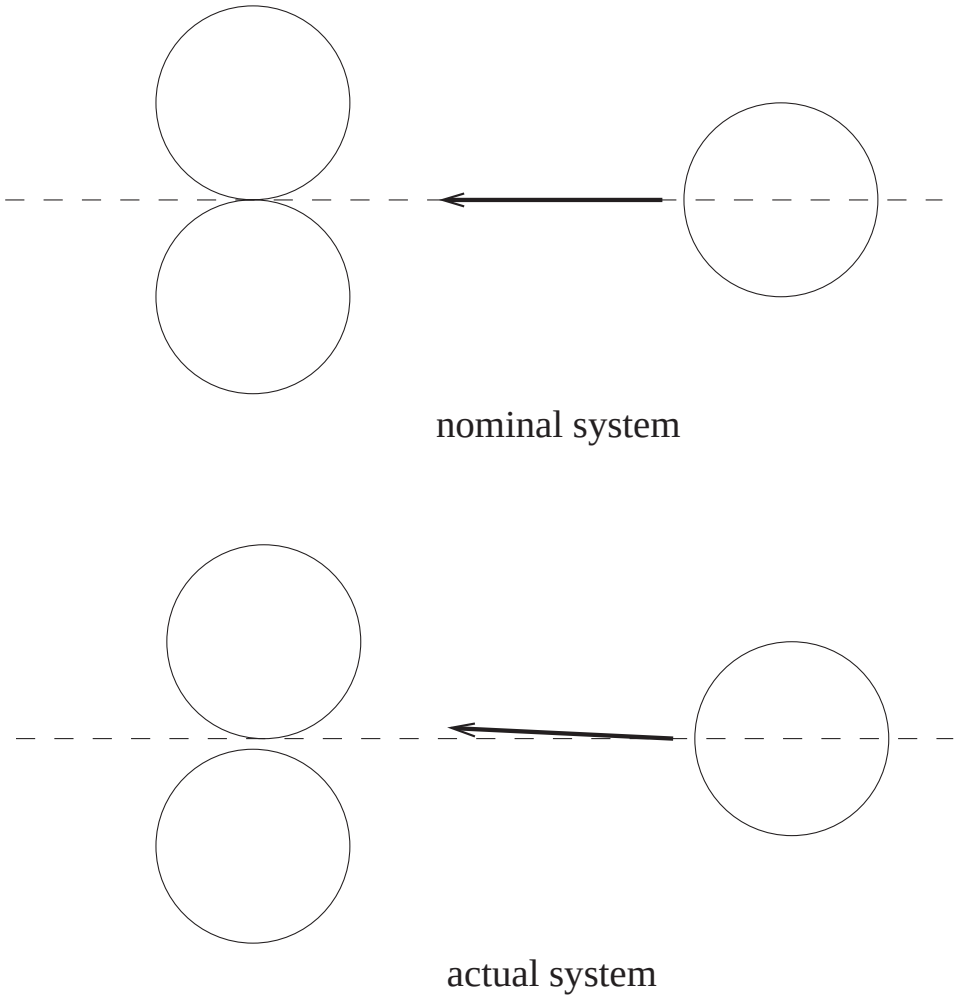

Figure 10.1: Infinitesimal perturbations can break up simultaneous impacts into sequences of single impacts

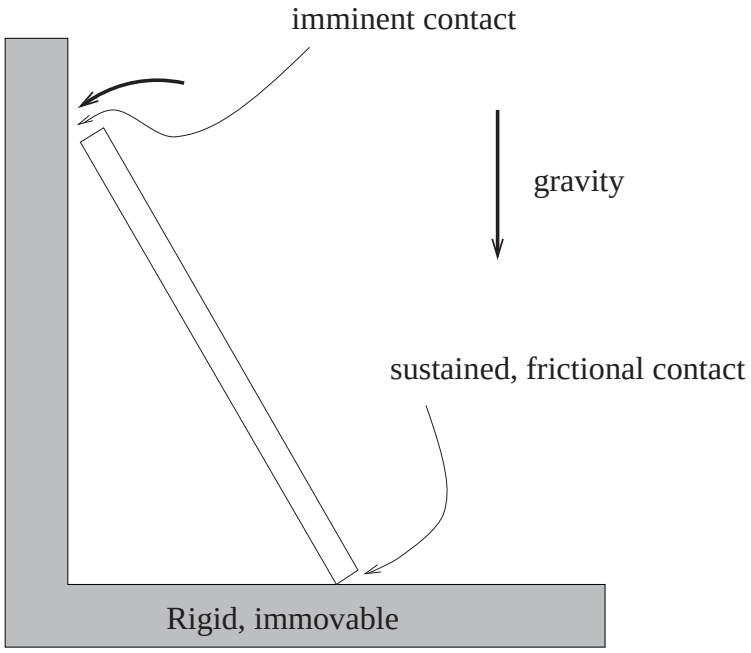

Figure 10.2: A simultaneous impact occurs when collisional contact at one point causes impulsive constraint forces at a pre-existing sustained contact

In a simultaneous multiple impact problem that *can* reasonably be broken up into a sequence of single impact problems by a slight perturbation in initial conditions, the actual sequence of impacts obtained depends on the perturbation used. Perturbations smaller than the accuracy of physical measurements can dramatically change the outcomes of "simultaneous" collisions in such systems. In such cases, Ivanov [25] suggests that the outcome of the collision be treated as a random variable which can take a discrete (possibly large) number of values. An example of such a problem is an even break of the rack in a game of pool (see e.g., the cover of *Scientific American,* January 1994).

In a model of real objects involved in multiple collisions, one might specify different local, pseudostatic contact laws at every contact location and then integrate the resulting equations of motion (this is the approach adopted by Goyal, Pinson and Sinden [21]). However, the outcome depends strongly on the details of the different contact models used, especially the ratios of stiffnesses of the different contacts. Moreover, as indicated through an example by Ivanov [25], this approach has the following features. For a given magnitude of error, uncertainty or perturbation in initial conditions, the uncertainty in the computed solution decreases as the local contact mechanisms used become softer. At the same time, the displacements during the collision increase in magnitude and the rigid body approximation becomes weaker. Conversely, for a given magnitude of error, the uncertainty in the computed solution increases as the contacts become stiffer. As a result, the problem of simultaneous impacts in a system with extremely stiff contacts is essentially indeterminate unless the initial conditions are known to correspondingly extreme accuracy. In the limiting case of "rigid" bodies, the precision required is infinite.

In a system of real bodies which have displacements on the order of, say, hundreds of microns during collisions, a simultaneous impact problem might be[2] indeterminate unless the initial conditions are known to an accuracy of, say, a few microns or better. If these "initial" conditions are

[2]Ivanov [25] identifies certain special multiple impact problems that are *not* ill-posed, but concludes that ill-posed simultaneous rigid body collisions are far more common than well-posed ones.

themselves the calculated/predicted outcomes of earlier collisions, then accuracy of a few microns cannot reasonably be expected. In such cases, the final outcome (as suggested by Ivanov [25]) is might probably best be treated as a random variable.

In practical dynamic simulations of general multibody systems with simultaneous impacts, one might want a deterministic solution procedure. In such cases, *while aware of the pitfalls of such a procedure*, one might base a modeling approach on special extra assumptions about the collision. As an example, consider Pfeiffer and Glocker's text [47], where it is assumed that *all contact locations participating in the collisional interaction reach maximum compression at the same instant of time.* Since the point of maximum compression is an ill-defined idea even for general *single* impacts (see footnote on page 60), Pfeiffer and Glocker's assumption is a very strong one! Their statement in the preface of their text, "The level of confidence in the theory is very high," is true in that their treatment of the *assumed collision model*, from a computationally oriented viewpoint, is thorough, clear and consistent. However, the confidence in the collision model itself, as in any other model for simultaneous rigid body collisions, cannot realistically be called high.

10.2 Collision Laws for Nearly Spherical Bodies

In applications like granular flow, one is sometimes interested in large collections of "nearly spherical" bodies. For example, one might be interested in collections of ellipsoids whose ratios of smallest to largest principal radii r_{min}/r_{max} are nearly equal to one. For $r_{min}/r_{max} = 1$, we have spheres. In what follows, we assume some such definition of near-sphericity. Under such circumstances, one might be interested in finding reasonable collision laws for these ellipsoids in the form of slight perturbations to collision laws for spheres.

Assume that we are interested in collision laws of the form

$$V_f = f(M, V_i, \text{ dimensionless parameters }).$$

The coordinate system is still the same as in Chapter 3, with the 1-axis along the normal to the contact surface, the 2-axis opposing the tangential component of the pre-collision relative velocity, and the 3-axis normal to the 1- and 2-axes. For dimensionless parameters, we have homogeneity of degree zero in the mass and degree one in the velocity. Therefore, we may scale the pre-collision velocity to unit magnitude, and write

$$V_f = f(M, \theta, \text{ parameters }), \tag{10.1}$$

where $0 \leq \theta \leq \pi/2$ is the angle made by the pre-collision velocity with the negative 1-axis, and the "parameters" are dimensionless quantities. We further assume that the collision parameters *do not* depend on the mass matrix for a given collision, and that the same values of these parameters characterize all possible collisions between all possible pairs of the slightly aspherical ellipsoids under consideration.

For slightly aspherical objects, we may write

$$M = M_0 + \Delta M,$$

where M_0 is the mass matrix for collisions between spheres, and ΔM is the perturbation to the mass matrix for a given collision due to asphericity of the bodies. Generally, given any pair of aspherical bodies, ΔM will depend on the contact configuration.

We write

$$V_f = V_{f0} + \Delta V_f = f(M_0 + \Delta M, \theta, \text{ parameters }),$$

or, formally,

$$V_{f0} + \Delta V_f = f(M_0, \theta, \text{ parameters }) + \frac{\partial f}{\partial M}(M_0, \theta, \text{ parameters }) \cdot \Delta M + o(\|\Delta M\|).$$

Since $V_{f0} = f(M_0, \theta, \text{ parameters })$ by assumption, we obtain

$$\Delta V_f \approx \frac{\partial f}{\partial M}(M_0, \theta, \text{ parameters }) \cdot \Delta M. \tag{10.2}$$

While the quantity $\dfrac{\partial f}{\partial M}$ is unknown, some things can be said about it.

Define the third order tensor $\mathbf{D}$ by its coordinates in the given coordinate system, $D_{ijk} := \frac{\partial f_i}{\partial M_{jk}}$. Recall that the coordinate system chosen has the 1-direction determined by the surface normal, the 2-direction determined by the pre-collision velocity, and the third direction determined up to a change in sign. Under a change of coordinates from (x_1, x_2, x_3) to $(x_1, x_2, -x_3)$, the components D_{ijk} transform to $(-1)^{\delta_{i3}+\delta_{j3}+\delta_{k3}} D_{ijk}$, where δ is the Kronecker delta. That is, D_{ijk} remains unchanged whenever none or two of (i, j, k) have the value 3, and D_{ijk} transforms to $-D_{ijk}$ whenever one or three of (i, j, k) have the value 3. However, the functional dependence of D_{ijk} is on $(M_0, \theta, \text{ parameters })$, each of which is unchanged by the change of coordinates, since the mass matrix for spheres, M_0, is diagonal. It follows that the value of D_{ijk} for *any* (i, j, k) is unchanged under the change of coordinates from (x_1, x_2, x_3) to $(x_1, x_2, -x_3)$. This demonstrates that $D_{ijk} = 0$ whenever one or three of (i, j, k) have the value 3.

Other restrictions on D_{ijk} may be proved in this same general setting. However, the symmetry $M_{ij} = M_{ji}$ makes it convenient to use a simpler matrix form. Define $m_1 := M_{11}$, $m_2 := M_{22}$, $m_3 := M_{33}$, $m_4 := M_{12}$, $m_5 := M_{13}$, and $m_6 := M_{23}$. Then, in Eq. 10.2, we interpret ΔM to mean the column matrix $\{\Delta m_1, \Delta m_2, \Delta m_3, \Delta m_4, \Delta m_5, \Delta m_6\}^T$, and the Jacobian $\dfrac{\partial f}{\partial M}$ to mean the 3×6 matrix

$$J := \begin{bmatrix} \frac{\partial f_1}{\partial m_1} & \frac{\partial f_1}{\partial m_2} & \cdots & \frac{\partial f_1}{\partial m_6} \\ \frac{\partial f_2}{\partial m_1} & \frac{\partial f_2}{\partial m_2} & \cdots & \frac{\partial f_2}{\partial m_6} \\ \frac{\partial f_3}{\partial m_1} & \frac{\partial f_3}{\partial m_2} & \cdots & \frac{\partial f_3}{\partial m_6} \end{bmatrix}.$$

By the 3-direction symmetry argument of the previous paragraph, we have

$$J_{31} = J_{32} = J_{33} = J_{34} = J_{15} = J_{16} = J_{25} = J_{26} = 0.$$

This leaves ten possibly nonzero elements in J,

$$J = \begin{bmatrix} J_{11} & J_{12} & J_{13} & J_{14} & 0 & 0 \\ J_{21} & J_{22} & J_{23} & J_{24} & 0 & 0 \\ 0 & 0 & 0 & 0 & J_{35} & J_{36} \end{bmatrix}.$$

Next, recall that the dimensionless collision parameters imply that the collision law is homogeneous of degree zero in the mass matrix. Therefore, the mass matrix may be multiplied by an arbitrary scalar without affecting the outcome in Eq. 10.1. We might assume without loss of generality that the mass matrix M in Eq. 10.1 is always scaled so that its trace is unity. In this case there would be five instead of six possible independent perturbations of the mass matrix. In the analysis presented here, we allow six independent perturbations, and enforce the condition of homogeneity of degree zero in mass as an extra condition, as follows. Since the mass matrix for spheres, M_0, is diagonal with elements in the ratio 7:2:2 (see Subsection 2.3.1), homogeneity in the

mass implies that a perturbation ΔM consisting of $\Delta m_1 : \Delta m_2 : \Delta m_3$ in the ratio 7:2:2 has *no effect* on the outcome of the collision. Therefore, $J \cdot \{7, 2, 2, 0, 0, 0\}^T = 0$, or

$$J_{11} = -\frac{2}{7}(J_{12} + J_{13}),$$

$$J_{21} = -\frac{2}{7}(J_{22} + J_{23}).$$

We are now left with eight independent nonzero elements of J.

The number of independent elements of J may be reasonably reduced under some further assumptions. Many collision models, when specialized to collisions with diagonal mass matrices, have the following feature: since the pre-collision velocity, by choice of coordinate system, has no 3-component, the post-collision velocity is totally unaffected by the (3,3) component of M. This property is found, for example, in the collision models of Kane and Levinson [32], Smith [55], Routh [52, 70], Stronge [64], the bilinear law of Section 6.4, the three new laws presented in Chapter 6, as well as *all* incremental rigid body collision laws based on local contact mechanisms with symmetry in the 3-direction whose parameters do not depend on the (3,3) element of M. It is, therefore, a reasonable hypothesis that the outcome of the collision should be unaffected by a change in only the (3,3) element of M. This hypothesis implies that $J_{13} = J_{23} = 0$, giving

$$J = \begin{bmatrix} J_{11} & -\frac{7}{2}J_{11} & 0 & J_{14} & 0 & 0 \\ J_{21} & -\frac{7}{2}J_{21} & 0 & J_{24} & 0 & 0 \\ 0 & 0 & 0 & 0 & J_{35} & J_{36} \end{bmatrix}.$$

Thus there remain only six independent nonzero elements of J (each a function of M_0, θ and the collision parameters).

Here the mass matrix for spheres, M_0, is known and constant. Moreover, in a collection of nearly spherical ellipsoids, one might reasonably assume that the same values of collision parameters describe the collisional behavior of all the objects under consideration. Hence, the nonzero elements of J may be treated as functions of θ only, for a *given* collection of nearly spherical objects.

Consider $J_{11}(\theta)$, the sensitivity of the normal component of post-collision relative velocity to changes in the (1,1) element of the mass matrix. We may conclude that $J_{11}(\theta)$ must be an *even* function of θ. This is due to the fact that, having picked a coordinate system, we might imagine both negative and positive values of θ. Due to the symmetry in the $\pm$ 2 direction of diagonal mass matrices, the 1-component of post-collision velocity must be an even function of θ. Moreover, at $\theta = 0$, $J_{11}(0)$ is equivalent to the sensitivity of the coefficient of restitution in head-on collisions to small changes in the total mass. Under some circumstances, this sensitivity may be significant (see, for example, the results of the preliminary experiments described in Chapter 11). However, if the same values of various collision parameters are assumed to represent all the nearly spherical bodies under consideration, and if the coefficient of normal restitution is assumed to be a valid collision parameter, then $J_{11}(0)$ *must* be set to zero in our approach. This is not necessarily bad, since slight changes in shape of bodies with uniform material properties may not affect the normal restitution much. See, for example, **(a)** the results of experiments in Chapter 11 with more carefully made pucks, with masses attached or removed more carefully (the coefficient of restitution did not vary to any noticeable degree in these cases), and **(b)** the results reported by Stoianovici and Hurmuzlu [58], where rods with an aspect ratio as high as about 5 had a variation in the normal restitution of under 5 percent (making it plausible that aspect ratios slightly over or under 1 would not show any change in normal restitution at all). Therefore, it is reasonable to assume that $J_{11}(\theta)$ is an even function of θ, *and* $J_{11}(0) = 0$. Finally, for collision models where the kinematic resitution in the

normal direction is independent of θ for diagonal mass matrices (this includes the models of Kane and Levinson [32], Smith [55], Routh [52, 70], Stronge [64], the bilinear law of Section 6.4, the three new laws presented in Chapter 6, as well as many other incremental local contact laws without coupling in the normal and tangential directions), we have $J_{11}(\theta) \equiv 0$. Under this assumption, J reduces to

$$J = \begin{bmatrix} 0 & 0 & 0 & J_{14} & 0 & 0 \\ J_{21} & -\frac{7}{2}J_{21} & 0 & J_{24} & 0 & 0 \\ 0 & 0 & 0 & 0 & J_{35} & J_{36} \end{bmatrix},$$

with only five independent nonzero elements.

10.3 Existence of Solutions for Smith's Collision Law

The equations describing Smith's collision law are nonlinear (see Chapter 5), and therefore it is not clear that unique solutions always exist. In Smith's paper [55], the questions of existence and uniqueness are not addressed. Mac Sithigh [37] mentions that Smith's collision law might have zero or multiple solutions. In numerical experiments, I have always been able to find a solution by continuation from the $\mu = 0$ solution. Based on my numerical studies, I suspect that solutions to Smith's collision law do always possess unique solutions. I have not been able to prove uniqueness of solutions, but existence of solutions may be proved.

Roughly, the idea is as follows. A unique solution exists for $\mu = 0$, the frictionless case. Continuously increasing μ from 0, one can obtain a solution branch parameterized by μ. The starting point is within the accessible region in impulse space, and all solutions obtained by this continuation procedure must also lie inside the accessible region. This is because Smith's law satisfies a kinematic restitution condition, always predicts nonnegative energy dissipation for positive normal impulse, and always satisfies the friction inequality (see Smith [55]), and also because no solution can have zero normal impulse. Since we start with one solution, and since new solution branches (if any) must be born or die in pairs, we are assured of at least one solution at any specified positive μ.

A proof of existence follows.

10.3.1 Existence and Uniqueness for $\mu = 0$

For $\mu = 0$, the equations describing the collision reduce to

$$P_N \begin{Bmatrix} 1 \\ 0 \\ 0 \end{Bmatrix} = M \begin{Bmatrix} -(1+e)V_{iN} \\ V_{fT} - V_{iT} \end{Bmatrix}.$$

These are linear equations in the unknowns P_N and V_{iT}, with the coefficient matrix

$$J := \begin{bmatrix} 1 & -m_{12} & -m_{13} \\ 0 & -m_{22} & -m_{23} \\ 0 & -m_{23} & -m_{33} \end{bmatrix}, \tag{10.3}$$

where the m_{ij} are the corresponding elements of the mass matrix M. Since M is positive definite, its trailing 2×2 block is invertible. Hence, J is invertible, and there is a unique solution.

10.3.2 Existence and Uniqueness Near $\mu = 0$

Recall (Eq. 5.1) that Smith's law is given by

$$P_N \left\{ \begin{array}{c} 1 \\ -\mu \frac{\|V_{iT}\| V_{iT} + \|V_{fT}\| V_{fT}}{\|V_{iT}\|^2 + \|V_{fT}\|^2} \end{array} \right\} - M \left\{ \begin{array}{c} -(1+e) V_{iN} \\ V_{fT} - V_{iT} \end{array} \right\} = 0. \tag{10.4}$$

In Eq. 10.4, the left hand side may be looked upon as a map from $\mathbf{R}^3 \times \mathbf{R}$ to $\mathbf{R}^3$, where $\{P_N, V_{iT}^T\} \in \mathbf{R}^3$, and $\mu \in \mathbf{R}$. The Jacobian of the left hand side with respect to $\{P_N, V_{iT}^T\}$, evaluated at $\mu = 0$, is simply the matrix J given in Eq. 10.3 above, which is invertible. By the implicit function theorem (see Rudin [53]), unique solutions of Eq. 10.4 for P_N and V_{iT} as functions of μ exist in some neighborhood of $\mu = 0$.

10.3.3 The Special Case of $V_{iT} = 0$

Note that if $V_{iT} = 0$ (i.e., the pre-collision velocity is along the normal), then Eq. 10.4 reduces to

$$P_N \left\{ \begin{array}{c} 1 \\ -\mu \frac{V_{fT}}{\|V_{fT}\|} \end{array} \right\} = M \left\{ \begin{array}{c} -(1+e) V_{iN} \\ V_{fT} - V_{iT} \end{array} \right\}. \tag{10.5}$$

The left hand side of this equation is discontinuous at $V_{fT} = 0$. A logical way to interpret Eq. 10.5 in this special case is (like Kane and Levinson's law, see [32]) to say that either **(a)** $V_{fT} \neq 0$ and Eq. 10.5 holds, or **(b)** $V_{fT} = 0$, P is given by $M(V_f - V_i)$, i.e., the right hand side of Eq. 10.5 with $V_{fT} = 0$, P obeys the friction inequality, $\|P_T\| \leq \mu P_N$ *and* $P_N > 0$.

If P is given by $M(V_f - V_i)$, i.e., the right hand side of Eq. 10.5 with $V_{fT} = 0$, and if the P_N so calculated satisfies $P_N > 0$, then we may compute

$$\mu^* := \frac{\|P_T\|}{P_N}.$$

If the specified friction $\mu \geq \mu^*$, then sticking occurs and a solution exists. If $0 \leq \mu < \mu^*$, then sticking cannot occur, and we may assume $V_{fT} \neq 0$.

10.3.4 Existence of Solutions in the General Case

In the following, we look upon Eq. 10.4 as a map from $\mathbf{R}^4$ to $\mathbf{R}^4$. The map from $\mathbf{u} := \{P_N, V_{iT}^T, x\}^T \in \mathbf{R}^4$ to $\mathbf{R}^4$ (recall, $V_{iT} \in \mathbf{R}^2$) is defined as

$$f(\mathbf{u}) := \left\{ \begin{array}{c} P_N \left(\begin{array}{c} 1 \\ -x \frac{\|V_{iT}\| V_{iT} + \|V_{fT}\| V_{fT}}{\|V_{iT}\|^2 + \|V_{fT}\|^2} \end{array} \right) - M \left(\begin{array}{c} -(1+e) V_{iN} \\ V_{fT} - V_{iT} \end{array} \right) \\ x \end{array} \right\} \tag{10.6}$$

Solutions of the equation $f(\mathbf{u}) = \{0, 0, 0, \mu\}^T$ give solutions to Eq. 10.4.

Some ideas from degree theory are now required. For details and proofs of theorems, see e.g., Rothe [51] and Milnor [42]. We consider a bounded open subset E of $\mathbf{R}^n$ and differentiable maps from $\bar{E}$ to $\mathbf{R}^n$, i.e., $f : \bar{E} \to \mathbf{R}^n$. Let the boundary of E be denoted by ∂E.

1. A point $y \notin f(\partial E)$ is called a *regular value* for f if the Jacobians evaluated at each point $x \in f^{-1}(y)$ are nonsingular. For a regular value y, there can at most be a finite number of such x. At a regular value y, each $x \in f^{-1}(y)$ is assigned the index $+1$ if the Jacobian of f at x has positive determinant, and the index -1 if the Jacobian of f at x has negative determinant; and the *degree* $d(f, E, y)$ is defined to be the sum of the indices of each $x \in f^{-1}(y)$.

2. Fact: $d(f, E, y)$ is continuous at a regular value y; it is also an integer. Therefore, $d(f, E, y_0) = d(f, E, y_1)$ for any two regular values y_0 and y_1 that are sufficiently close to each other.

3. Fact: For $y_0 \notin f(\partial E)$, any neighborhood of y_0 contains a point that is a regular value for f. Using this fact, the degree of all points $y \notin f(\partial E)$ may be defined (the degree of a points that is not a regular value of f is defined to be equal to the degree of a sufficiently nearby regular value).

4. Fact: If , is a connected open subset of $\mathbf{R}^n$ with , $\cap f(\partial E) = \phi$, then $d(f, E, y)$ is constant for all $y \in$, .

In order to use the results given above, we need to identify a suitable bounded open set E. The variables we use are $\mathbf{u} := \{P_N, V_{fT}^T, x\} \in \mathbf{R}^4$. Now, the map from $P \in \mathbf{R}^3$ to $\{P_N, V_{fT}^T\} \in \mathbf{R}^3$ is invertible. To see this, note first that P obviously determines V_f and hence V_{fT}. Next, given P_N and V_{fT}, we have the equations

$$\left\{ \begin{array}{c} P_N \\ P_T \end{array} \right\} = M \left\{ \begin{array}{c} \Delta V_N \\ V_{fT} - V_{iT} \end{array} \right\}.$$

This matrix equation is equivalent to three scalar equations. The first one determines ΔV_N uniquely, since positive definiteness of M guarantees that $m_{11} > 0$. Knowing ΔV_N, the next two equations determine P_T uniquely. Thus, open sets in P space are mapped invertibly to corresponding open sets in $\{P_N, V_{fT}^T\}$ space.

We can now define the bounded, open set E of interest. In impulse space, we consider the region accessible to an arbitrary collision. Given that *any* solution to Eq. 10.4 with $P_N > 0$ must satisfy energy conservation as well as the friction inequality (see Smith [55]), all solutions must be inside the accessible region, for a collision with friction coefficient μ. The accessible region is a closed, bounded set. However, we can construct a bounded, open set E_1 that is only slightly larger than the accessible region and contains the accessbile region. This set E_1 is mapped to another bounded open set E_2 in $\{P_N, V_{fT}^T\}$ space. For our set E, we take the Cartesian product of E_2 and the interval $(0, \mu+\epsilon)$, where ϵ is a small positive number. (In the special case discussed above where $V_{iT} = 0$, we assume $\mu < \mu^*$ and pick a small ϵ such that $\mu + \epsilon < \mu^*$.) Thus, $E := E_2 \times (0, \mu + \epsilon)$. The set E is open and bounded, and a differentiable map f from $\bar{E}$ to $\mathbf{R}^4$ is given by Eq. 10.6.

From subsection 10.3.2 it is known that for some $\delta > 0$, and $y = \{0, 0, 0, \delta\}$, Eq. 10.6 has a unique solution. Consider the line segment in $\mathbf{R}^4$ joining the points $y_1 := \{0, 0, 0, \delta\}$ and $y_2 := \{0, 0, 0, \mu\}$. For any point y on the line segment $y_1 y_2$, $f^{-1}(y)$ has no points on ∂E. This is because (i) all points in the accessible region satisfy $P_N > 0$; (ii) the set E_1 of impulses is only slightly larger than the accessible region, and hence any points on the boundary ∂E_1 also satisfy $P_N > 0$; (iii) any solution of Eq. 10.4 that satisfies $P_N > 0$ must lie inside or on the boundary of the accessible region, and hence strictly inside E_1. Due to continuity of the map f, it is possible to construct an open set , that contains the line segment $y_1 y_2$, such that $f^{-1}(,)$ has no points on ∂E.

Based on the results from degree theory and the construction above, all points $y \in$, must have the same degree. Since the determinant of matrix J given in Eq. 10.3 is positive, the degree of $y_1 := \{0, 0, 0, \delta\} \in$, is 1. It follows that the degree of $y_2 := \{0, 0, 0, \mu\} \in$, is 1 also, which proves that there is at least one solution for Smith's law for any given symmetric positive definite mass matrix M, pre-collision relative velocity V_i with $V_{iN} < 0$, $0 \leq e \leq 1$, and $\mu \geq 0$.

10.3.5 Uniqueness of Solutions

As noted in Chapter 5, I have been unable to prove uniqueness of physically admissible solutions for Smith's law. At the same time, I have been unable to find an example with two physically

admissible solutions.

10.4 Physical Realization of Arbitrary Mass Matrices Using Finite Masses

It is demonstrated in Chapter 2 with two colliding mechanisms that all symmetric positive definite matrices are physically realizable (see Fig. 2.9). It is clear that the constraints on these mechanisms are equivalent to appropriately placed infinite point masses. It is, therefore, clearly possible to come arbitrarily close to any given mass matrix with large but finite masses. In this section it is demonstrated that all symmetric positive definite matrices are, in fact, exactly realizable using objects of finite mass.

Consider the system shown in Fig. 10.3. This system is based on the one shown in Fig. 2.9, with the constraint of a ball-and-socket joint replaced by a large point mass M_c, and the constraint of the hinge replaced by two large point masses, each also equal to M_c, attached to a rod lined up with the axis of the hinge. All the lengths of all the rods, for simplicity, are set equal to unity in appropriate units. In the limit as $M_c \to \infty$, we obtain the constrained system in Fig. 2.9.

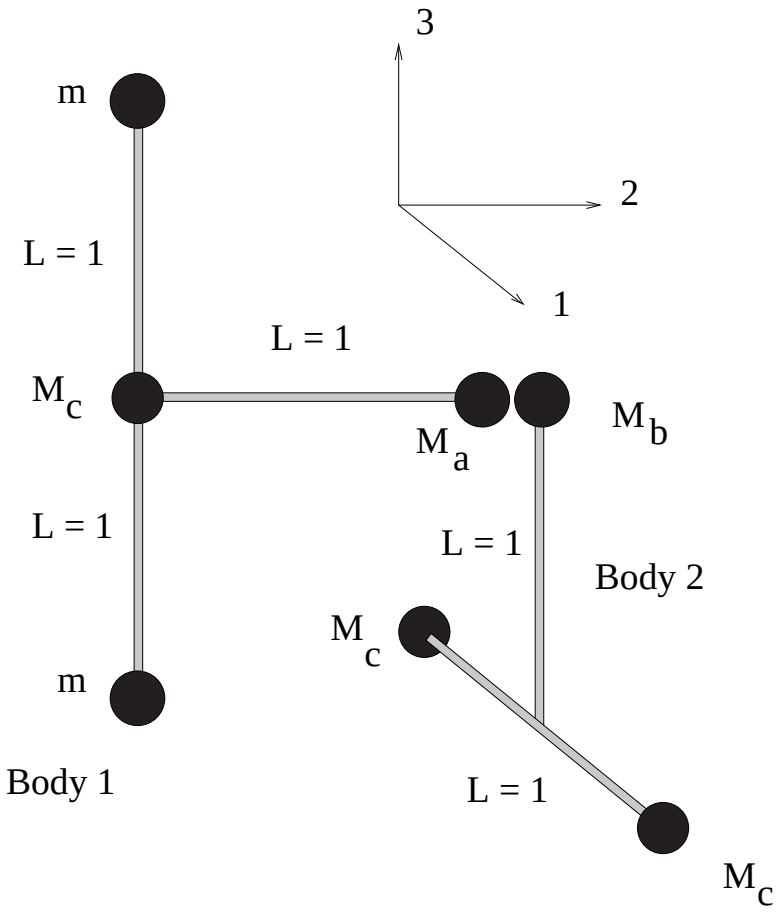

Figure 10.3: Physical realization of arbitrary mass matrices

As discussed earlier in Chapter 2, the normal and tangential directions may be oriented as we please by small changes in the positions of the colliding bodies, or by suitably selecting the shapes of the masses M_a and/or M_b. It is only necessary to be able to select combinations of the masses

M_a, M_b, M_c, and m to obtain any specified eigenvalues, $\lambda_1 \leq \lambda_2 \leq \lambda_3$. In the special case of $M_c = \infty$, we obtain the constrained case with $\lambda_1 = M_a$, $\lambda_2 = M_b$, and $\lambda_3 = M_a + 2m$.

For finite values of M_c, the mass matrix in the coordinate system shown in Fig. 10.3 may be shown to be[3] the diagonal matrix

$$\begin{bmatrix} \frac{M_a(3M_b+2M_c)}{3M_b+3M_a+2M_c} & 0 & 0 \\ 0 & \frac{M_b(M_a+2m+M_c)}{M_b+M_a+2m+M_c} & 0 \\ 0 & 0 & \frac{(M_b+2M_c)(4mM_a+M_cM_a+4m^2+2mM_c)}{4mM_b+M_cM_b+4mM_a+M_cM_a+4m^2+10mM_c+2M_c^2} \end{bmatrix}.$$

Setting $\epsilon := 1/M_c$, we obtain for the diagonal elements,

$$\begin{Bmatrix} M_{11} \\ M_{22} \\ M_{33} \end{Bmatrix} = \begin{Bmatrix} \frac{2M_a+3M_aM_b\epsilon}{2+3(M_a+M_b)\epsilon} \\ \frac{M_b+M_b(M_a+2m)\epsilon}{1+(M_a+M_b+2m)\epsilon} \\ \frac{2M_a+4m+(M_aM_b+2mM_b+8mM_a+8m^2)\epsilon+4mM_b(M_a+m)\epsilon^2}{2+(M_a+M_b+10m)\epsilon+4m(M_a+M_b+m)\epsilon^2} \end{Bmatrix}. \tag{10.7}$$

Setting $\epsilon = 0$ gives $M_{11} = M_a$, $M_{22} = M_b$, and $M_{33} = M_a + 2m$, as expected. By the implicit function theorem (see e.g., Rudin [53]), if the Jacobian of the right hand side of Eq. 10.7 with respect to $\{M_a, M_b, m\}$, evaluated at $\epsilon = 0$, is invertible, then there is a neighborhood of $\epsilon = 0$ for which there exist unique functions $\{M_a(\epsilon), M_b(\epsilon), m(\epsilon)\}$ that satisfy Eq. 10.7 for given constants $\{M_{11}, M_{22}, M_{33}\}$.

The Jacobian in question is the matrix

$$\begin{bmatrix} 1 & 0 & 0 \\ 0 & 1 & 0 \\ 1 & 0 & 2 \end{bmatrix},$$

which is clearly invertible.

Thus, there is some *nonzero* ϵ (therefore, some *finite* M_c) for which we can find $\{M_a(\epsilon), M_b(\epsilon), m(\epsilon)\}$ that satisfy Eq. 10.7 for given constants $\{M_{11}, M_{22}, M_{33}\}$. This proves that arbitrary mass matrices are in fact realizable for collisions of two unconstrained bodies of finite mass.

By expanding in powers of ϵ and collecting terms, it may be shown that in fact

$$M_a(\epsilon) = M_{11} + \frac{3M_{11}^2}{2}\epsilon + O(\epsilon^2),$$

$$M_b(\epsilon) = M_{22} + M_{22}^2\epsilon + O(\epsilon^2),$$

$$m(\epsilon) = \frac{M_{33} - M_{11}}{2} + \frac{3M_{33}^2 - 4M_{11}M_{33} - M_{11}^2}{4}\epsilon + O(\epsilon^2).$$

This demonstrates that, in principle, we cannot depend on M being anything less general than an arbitrary symmetric potitive definite matrix, even for collisions of two unconstrained, finite bodies.

10.5 More on Ivanov's Definition of the Coefficient of Restitution

Ivanov's definition of restitution [24] for a known impulse direction $\hat{P}$ (see Section 3.3) is given by

$$\eta^2 := \frac{E_f - E_{min}}{E_i - E_{min}}, \tag{10.8}$$

[3]Using the symbolic computation program MACSYMA

where E_f and E_i are the post- and pre-collision local kinetic energies, and E_{min} is the local kinetic energy at that impulse magnitude $\|P\|$ along $\hat{P}$ at which maximum energy dissipation occurs (see Section 3.3).

To simplify the presentation, let us define P^* to be the impulse at which E_{min} occurs, and V^* to be given by $P^* = M(V^* - V_i)$. Note, $P^* = \|P^*\| \hat{P}$. By the normality principle of Section 3.3, at the point of maximum energy dissipation we have the condition ${P^*}^T V^* = 0$, which may be combined with $P^* = M(V^* - V_i)$ to yield

$$\begin{bmatrix} \hat{P} & M \\ 0 & \hat{P}^T \end{bmatrix} \begin{Bmatrix} \|P^*\| \\ V^* \end{Bmatrix} + \begin{Bmatrix} MV_i \\ 0 \end{Bmatrix} = 0. \tag{10.9}$$

Equation 10.9 may be used to solve for $\|P^*\|$ and the corresponding V^*, which may be directly used to calculate $E_{min} := {V^*}^T M V^*/2$. Knowing V_i and hence E_i, and given η, we may calculate E_f from Eq. 10.8. Knowing E_f and the impulse direction $\hat{P}$, we may use Eq. 3.1 to obtain a quadratic equation in $\|P\|$,

$$(\|P\| \hat{P} + MV_i)^T M^{-1} (\|P\| \hat{P} + MV_i) = E_f,$$

which will generally have two real, positive roots of which the larger one corresponds to a positive value of η, while the smaller root corresponds to a negative value of η. Once $\|P\|$ is known, V_f may be calculated.

10.5.1 Ivanov's Restitution for Frictionless Collisions

For frictionless collisions, $\hat{P} = n$, the unit normal. The condition ${P^*}^T V^* = 0$, therefore, means that the normal component of V^* is zero when the local kinetic energy is E_{min}. Using the expression for energy dissipation in a collision (see e.g., Smith [55])

$$E_f - E_f = P^T (V_i + V_f)/2,$$

we may write

$$\begin{aligned} \eta^2 &= \frac{E_f - E_i + E_i - E_{min}}{E_i - E_{min}}, \\ &= \frac{-P^T(V_i + V_f) + {P^*}^T(V_i + V^*)}{{P^*}^T(V_i + V^*)}, \\ &= \frac{-(1+e)n^T(V_i + V_f) + n^T V_i}{n^T V_i}, \end{aligned} \tag{10.10}$$

where in Eq. 10.10 e is the Newtonian coefficient of normal restitution, and use has been made of the facts that, for a frictionless collision, $\hat{P} = n$ and the definition of e implies that $\|P\|/\|P^*\| = 1 + e$. Finally, noting that $n^T V_f = -e n^T V_i$, we obtain after simplification of Eq. 10.10, $\eta^2 = e^2$, or $\eta = e$ for a *frictionless* collision.

10.5.2 Knowing P Uniquely Determines η

For any given impulse vector P that points inside the energy ellipse (see Chapter 3), there is a unique number $-1 \leq \eta \leq 1$. This is because, given P, we may compute $\hat{P}$, the unit vector in the direction of P, and then P^* and η^2 as indicated above. Thus, η is determined up to a sign. Then we take η to be positive whenever $\|P\| > \|P^*\|$, zero if $\|P\| = \|P^*\|$, and negative whenever $\|P\| < \|P^*\|$. If $P = 0$, then $\hat{P}$ is not defined. However, we then let $\eta = -1$.

10.5.3 The Region in Impulse Space Covered by $0 \leq \eta \leq 1$

Consider all impulse on the energy ellipsoid in impulse space, i.e., those that satisfy the equation $(P + MV_i)^T M^{-1}(P + MV_i) = V_i^T MV_i$, or

$$P^T M^{-1} P + 2P^T V_i = 0. \tag{10.11}$$

For each such $P \neq 0$, there is an impulse P^* in the same direction, but with smaller magnitude, such that P^* produces the largest possible dissipation of kinetic energy among all impulses in the direction of P. Let $V^* := M^{-1}P^* + V_i$. Then, by the discussion in Section 3.3, we must have $P^T V^* = 0$ (the impulse vector P from the origin must be tangent to the ellipsoid of constant dissipation passing through the point of maximum kinetic energy dissipation; by the normality principle, V^* must be normal to the surface of the ellipsoid at that point). Note that the surface defined by the P^* corresponding to different P will be the surface on which $\eta = 0$, while the energy ellipsoid itself will correspond to $\eta = 1$. If we set $P^* = \alpha P$, we obtain $V^* = \alpha M^{-1}P + V_i$, or $2P^T V^* = 2\alpha P^T M^{-1} P + P^T V_i$. Subtracting from Eq. 10.11, we obtain

$$(1 - 2\alpha)P^T M^{-1} P = 0,$$

or $\alpha = 1/2$ since $P \neq 0$ and M is positive definite.

Therefore, we have $P^* = P/2$, which defines an ellipsoid of exactly half the size of the energy ellipsoid, as shown for a 2D case in Fig. 10.4. It is clear that some points of the region covered by

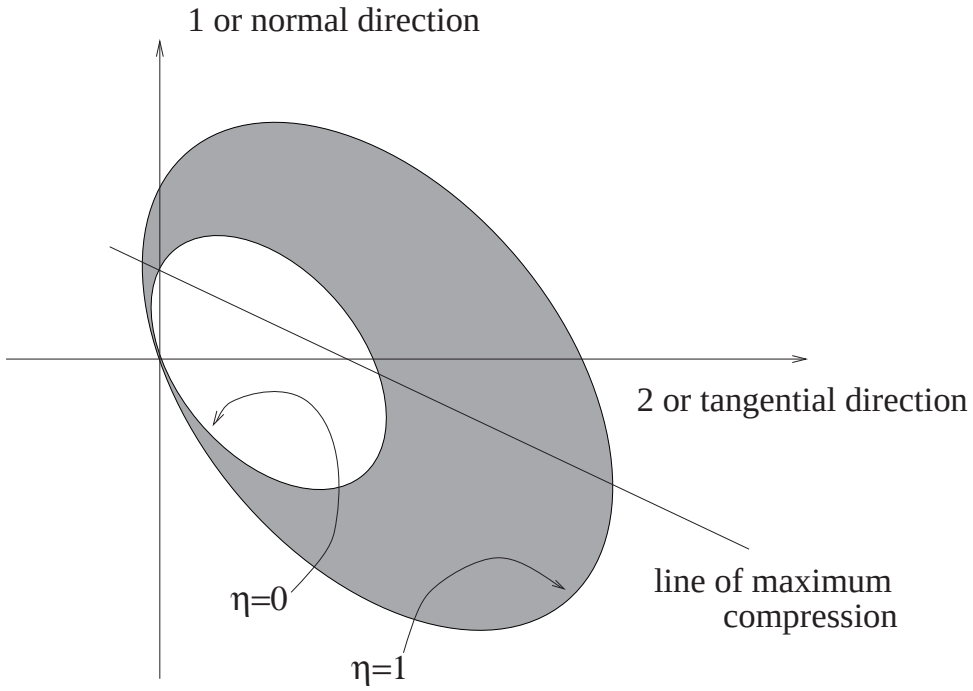

Figure 10.4: Region in impulse space covered by Ivanov's restitution parameter, for values between 0 and 1

$0 \leq \eta \leq 1$ are below the plane of maximum compression and thus violate the non-interpenetration condition (assumption 11 of Section 2.2). This means that Ivanov's restitution has configuration-dependent bounds, which makes it somewhat awkward to implement in simple collision laws. It is also clear that some points above the plane of maximum compression are not inside the region

covered by $0 \leq \eta \leq 1$. This is a feature common to other definitions of restitution, such as kinematic or Newtonian restitution, kinetic or Poisson restitution [52], as well as the energetic restitution discussed by Stronge [59, 61, 60].

10.6 Algebraic Collision Laws That Cover the Accessible Region in Impulse Space

None of the collision laws discussed in this thesis can cover the entire accessible region in impulse space, except possibly Brach's laws. However, Brach's laws can access points in impulse space that are outside the physically permissible region, as well as all points inside the region.

A possible modeling approach might be to try and construct an algebraic collision law that depends on *four* parameters including the friction coefficient[4], with clearly defined bounds and nice physical interpretations, such that the entire accessible region can be covered, *and* no points outside the region are accessible. Ideally, these parameters should be measurable in independent experiments and have some chance of being roughly constant over some range of collisions for at least some special bodies.

No such models are currently available. Specifically, there is no known collision model, algebraic or incremental, with the following features:

1. It depends on four parameters, including a coefficient of friction $\mu > 0$, and three collision parameters.

2. The three collision parameters have simple bounds, clear physical interpretations, and are roughly constant for some range of collisions of some pair of bodies (above and the extremely simple, 2D case of spheres).

3. For arbitrary frictionless collisions, the collision law reduces to the usual Newtonian restitution.

4. Every accessible point in impulse space corresponds to some choice of collision parameters, and vice versa, i.e., the collision law can cover the entire accessible region, and it cannot violate fundamental constraints.

Note that the accessible region is closed, bounded and convex. As such, in principle, it can easily be parameterized using three parameters that take values between, say, zero and one. As one family of examples, note that we can pick any point inside the accessible region as a reference point, and then parameterize the region using two angles to specify a direction in 3D (normalized to unity) along with a distance parameter that takes the value 0 at the reference point and 1 on the boundary. However, given such a parameterization of the accessible region, there is no reason to believe that these parameters will be constant over any interesting range of collisions of any real or imagined bodies.

[4]Four is the minimum number required to cover the entire accessible region for an arbitrary 3D frictional collision with given coefficient of friction.

Chapter 11

Experimental Data

In practical applications of collision modeling, one might often be dealing with complicated, composite objects under somewhat uncontrolled conditions. The collisional behavior of composite objects made up of several pieces that are glued, screwed, or snap-fitted together, or connected to each other with bearings, will probably be more complicated than the behavior of simpler objects with more uniform properties. Controlled experiments with simple objects might give a better understanding of some basic aspects of the collisional behavior of solid bodies in two or three dimensions.

There is much data available for 1D collisions (see e.g., Goldsmith [20]) and for 2D collisions of particles from studies related to the wear of surfaces (see e.g., Brach [11] for some discussion and further references). However, there have been few 2D or 3D experimental studies where complete kinematic data was collected from many collisions of the same simple objects under controlled conditions in which the basic assumptions of rigid body collision theory are valid[1].

Data of interest in rigid body collision modeling is almost exclusively restricted to experiments with disks (see e.g., Maw *et al.* [40]) and with spheres (see e.g., Foerster *et al.* [17]), both being simple objects to study, as discussed in Chapter 4. Lewis and Rogers [36] have studied oblique collisions of a sphere attached to a long beam.

Recently, Stoianovici and Hurmuzlu's experiments with slender steel rods [58] in 2D have provided a partial look at some 2D collisions with non-diagonal mass matrices. However, in their study the pre-collision velocity was always along the normal to the contact surface. Moreover, the friction coefficient at the contact point was only about 0.1, and so the complications that sometimes arise in frictional collisions with non-diagonal mass matrices were missing. An interesting aspect of their study is that the objects examined had significant bending vibrations on a time scale comparable to that of the collision and so *were not* well modeled as force-response rigid, but *were* well modeled as impulse-response rigid.

As discussed in Chapter 4, collisions of spheres in space as well as of disks in the plane are two dimensional. Moreover, the assumption of homogeneity of the collision law in velocity[2], and the fact that all points on the circumferences of spheres and disks are equivalent, reduce the problem to essentially one of characterizing the post-collision velocity through two scalar functions of one variable, the incidence angle θ (the angle between the pre-collision relative velocity and the common normal at the contact point). Stoianovici and Hurmuzlu's experiments with rods are similar in the

[1] For example, 3D studies of the "impact response" test dummies in car crashes [46] are not relevant to this thesis since they involve large interaction times, large motions, and only "plastic" impacts in the sense that the dummy stays attached to the car seat with seat belts.

[2] A fairly good assumption, if the range of velocities is not very large – say, within one order of magnitude

sense that, given homogeneity in velocity *and* the fact that the pre-collision velocity was always in the same direction, the problem once again was reduced to characterizing the post-collision velocity through two scalar functions of one variable, namely the angle of orientation of the rod.

There seem to have been no studies, to date, where the collisional behavior of some simple body has been investigated under conditions where the experimental data could not reasonably be reduced to one dimension.

This chapter presents the results of some 2D collision experiments conducted at Cornell University under my supervision by REU[3] students John Calsamiglia and Scott Kennedy, in the summers of 1995 and 1996 respectively. Calsamiglia's experiments were with axisymmetric flat pucks colliding with a heavy steel plate on an air table, and Kennedy's experiments were with a non-axisymmetric (semicircular) puck colliding with a heavy steel plate. A principal conclusion reached from the experiments is that the coefficient of normal restitution of a composite object can depend strongly on the details of how the component parts are put together, and is consequently somewhat unpredictable, while the coefficient of restitution of an object with more uniform properties is largely dependent on material properties and overall shape, and is consequently more predictable (at least in principle). Other conclusions are that *for the collisions investigated* **(a)** the coefficient of normal restitution is approximately constant, with only a slight dependence on the incidence angle and on the location of the contact point on the puck (even for the asymmetric puck case), and **(b)** the tangential component of impulse is *not* equal to μ times the normal impulse even for collisions where the tangential component of contact point relative velocity *does not* change direction, i.e., collisions which would be considered to be "sliding" collisions in most collision models. Conclusion (b) above is particularly interesting because it is in direct contradiction to the predictions of practically all algebraic rigid body collision models, in addition to some incremental models including Routh's model. A discussion is presented of the anomalous frictional behavior observed in these collisions, in the context of lack of force-response rigidity in the disks.

The basic feature of previous experimental studies, that each collision could be characterized by a single variable, is also present in most of the data presented in this chapter. For collisions of the non-axisymmetric puck, it was found that some interesting conclusions could be drawn from studying the variation of relevant quantities against one of the independent variables at a time, while experimental scatter in the data made it difficult to fruitfully examine the variation of relevant quantities against both independent variables at the same time.

11.1 Study of Axisymmetric Pucks, with John Calsamiglia

This section contains a brief description of, and fairly detailed results from, experiments conducted in the Theoretical and Applied Mechanics Department at Cornell University in the summer of 1995, under my supervision, by undergraduate REU student John Calsamiglia.

2D collisions of flat pucks on an effectively frictionless air table, with a massive steel plate clamped to the table, were studied using strobe[4] photographs taken with a digital camera[5]. The entire experimental procedure is described in detail in Calsamiglia's report [13], and presented here in a more concise manner.

[3]Research Experience for Undergraduates

[4]General Radio, Strobotac Type 1538-A

[5]Nikon F3 with Tamron (90mm) or Nikon (Nikkor AF 35-70mm) with attached Kodak Professional DCS (Digital Camera System).

11.1.1 Preliminary Experiments

In a preliminary study, the pucks originally supplied with the air table were used in binary collisions (collisions between two pucks). The principal results are mentioned below; detailed results from this preliminary study are not given here. The primary purpose of the study was to identify possible sources of difficulty, which were removed in a more careful set of experiments.

In this preliminary study, the speeds at which the pucks collided were kept fairly low, in the range 0.25-0.75 m/s, but not controlled accurately. The strobe frequency was set to a suitable value, typically in the range 4-8 Hz., so as to obtain four to six pictures of each colliding puck in each frame. The exact strobe frequencies were not recorded for individual pictures, due to the prior assumption that the collisional interaction was homogeneous of degree one in the velocity. To obtain kinematic data, the pucks were marked with little dots whose coordinates were later picked manually off the computer screen using the software *NIH Image*[6].

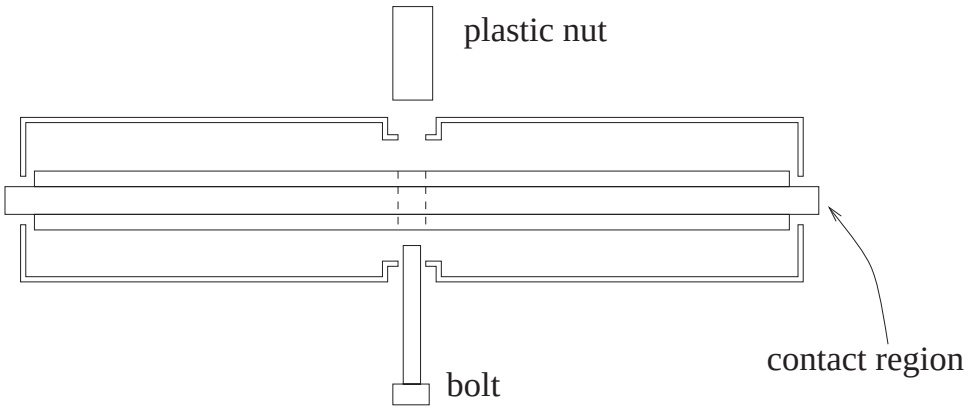

Figure 11.1: Composite axisymmetric puck

The pucks used in the preliminary study (see Fig. 11.1) were actually composite objects made of three pieces held together by a bolt (they were the standard pucks that were originally supplied with the air table). In an effort to reduce "rattle" in their dynamic behavior, the three pieces were first glued together, in addition to being bolted together. However, it was found that various collision "parameters" showed considerable scatter (for example, the coefficient of restitution showed a variation of about $\pm$ 5 percent about a mean of roughly 0.85). The following were thought to be possible reasons for the scatter.

1. The pucks were composite bodies which, though glued and bolted together, became "rattly" and effectively loose under large collision forces.

2. The intermediate disks in the pucks were where contact was made. The circumference, or the contacting surface (see Fig. 11.1), possibly had non-uniform surface finish. Also, since it wasn't rounded, the contact "point" is indeterminate since the contact is nominally along a line.

3. The precision of kinematic measurements was fairly low. Each dot could be located on the digitized picture to an accuracy of roughly one pixel; for these pictures the resolution was roughly 1.7 pixel/mm.

[6]Available via anonymous ftp at zippy.nimh.nih.gov

4. For collisions of two pucks, the direction of the normal at the point of contact was not known in advance, and was calculated from the kinematic data. Subsequent calculations rested on the accuracy of the normal direction calculation, which was sensitive to error in measurements except in nearly head-on collisions.

Some more experiments were conducted with the same pucks, but now with a small mass attached to the nut on each colliding puck. A substantial difference in the coefficient of normal restitution was observed for these pucks with added masses (down from about 0.85 to about 0.7). A possible explanation for this phenomenon is that adding the mass to the flexible plastic nut effectively made the puck lose its force-response rigidity. That is, it is possible that the dynamics of internal vibrations in the puck became a significant factor in determining the outcome of the collision for the puck with the attached mass, while for the original puck the collisional interaction may have been more localized and closer to pseudo-static. In a simplistic model of the system (in the spirit of Mindlin's basic model in his study [43] of the impact response of packaged objects), we might model the puck as a single rigid body of mass m_1 and given coefficient of restitution e, with the added mass m_2 attached to the puck through a soft spring, as shown in Fig. 11.2. In this

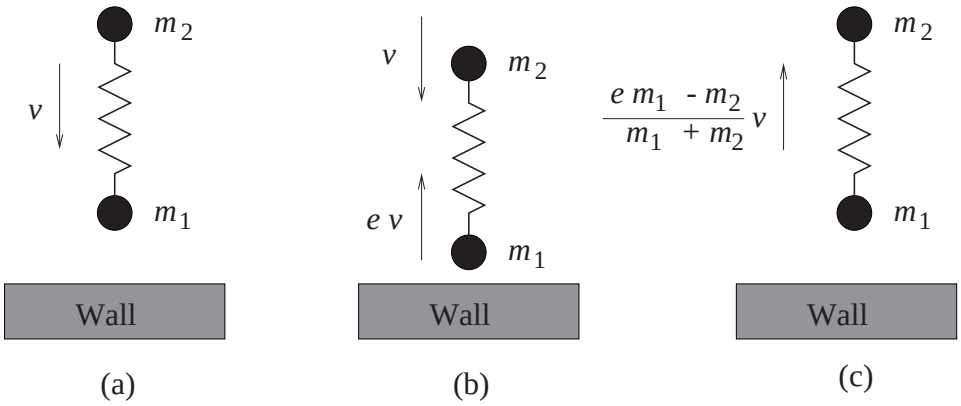

Figure 11.2: Two-stage collision of simplified puck model

case, the collision is assumed to occur in two decoupled stages. First, one body collides with the wall, with a given coefficient of restitution e. Next, transient vibrations occur in the composite body. When the transients die out, the composite body moves away with an effective coefficient of restitution given by $\frac{em_1 - m_2}{m_1 + m_2}$. By this calculation, given that the mass of the puck was 52.6 gm while the added mass was 9.85 gm, and using $e = 0.85$, we obtain an effective restitution of 0.56. Therefore, this simple model overestimates the reduction in the coefficient of restitution. If the spring is stiff enough so that internal, transient dynamics occur on a time scale comparable to that of the collisional interaction between the mass m_1 and the wall, then the collisional interaction will be more complicated and it is likely that the reduction in the effective restitution will be smaller.

11.1.2 Subsequent Experiments

Guided by the conclusions of the first study, a second set of experiments was conducted. In these experiments, collisions of various single pucks with a heavy steel plate were studied.

The steel plate (dimensions 40.6 cm × 20.3 cm × 1.9 cm) was about 130 times more massive than the most massive pucks, and its mass was treated as infinite. The plate was clamped to the air table; as a result, the direction of the normal at the contact point was known in advance and did

not have to be calculated from kinematic data. The contacting surface on the plate was polished with a surface grinder, to make its properties uniform.

The pucks themselves were made out of Delrin[7] (a material similar to Teflon). They were machined out of a long rod, and the surface properties were made uniform by turning each puck on a lathe. Finally, the circumference was rounded so as to produce "point contact" between the pucks and the plate. The radius imparted to the end was about 5 mm; it was ignored in calculations of rigid body collision quantities, but used in the Hertz-contact based discussion of the compression of thin, elastic disks at the end of this chapter.

It was initially assumed that the mass distribution in the pucks was uniform. However, later measurements of a portion of one puck indicated that the mass distribution was actually nonuniform, though perhaps (approximately) radially symmetric. In analyzing experimental data, the pucks were assumed to be radially symmetric, in that all contact points were treated as equivalent, and the mass matrix was taken to be diagonal. To account for radial variation in mass distribution, the diagonal elements of the mass matrix were not calculated based on a uniform mass distribution assumption, but rather calculated from measured values of both the total mass as well as the moment of inertia about the center of mass[8] (see Eq. 11.1 below).

The speed of the pucks was kept approximately constant by using a simple rubber-band powered launcher. The launcher also released the pucks approximately without initial spin. The strobe rate was held constant for these experiments at 530 cycles per minute, or 8.8 Hz.

Half as many pictures (of pucks) as in the preliminary study were required for each collision, since there was only one puck to watch. Moreover, the use of the launcher made the collision location more controlled. Due to these two reasons, the field of view required became much smaller for these experiments, and the precision of kinematic measurements increased to about 4.35 pixels/mm compared to the earlier 1.7 pixel/mm.

Three basic types of Delrin pucks were studied: uniform disks, disks with holes in their centers, and disks with smaller aluminum disks glued to them (see Fig. 11.3). The objective was to study the collisional behavior of axisymmetric objects with different mass distributions. During the experiments, it was found that the pucks with holes through them would not float on the air table unless a circular backing piece of paper was glued to the lower surface. The paper used was thin and light; its effect on the dynamics was ignored in all calculations. The properties of the pucks used are summarized in Table 11.1. The quantity λ_2/λ_1 in the table is the dimensionless ratio of the smaller to the larger eigenvalue of the local mass matrix, given by (see Chapter 2)

$$\frac{\lambda_2}{\lambda_1} = \frac{I}{I + mr^2}, \tag{11.1}$$

where r is the radius of the disk, m its mass, and I its moment of inertia about its center of mass. Note that, as a check for consistency of data, pucks 1 & 2, pucks 4 & 5, and pucks 6 & 7 were made identical[9].

[7]McMaster-Carr Supply Company, (908) 329 3200. 1 foot Delrin rod, 4" diameter. Item: 8572k36. Price: $68.63 per foot. General properties: low moisture absorption, abrasion resistance, dimensional stability and toughness; easy to machine.

[8]The moment of inertia for pucks 2 through 9 was found from measuring the time period of free oscillations of the pucks under gravity, when suspended on a knife edge inserted into a small hole made near the outer edge. The moment of inertia of puck 1 could not be found in this manner because it had unfortunately already been cut in half for the experiments described in the next section. However, since pucks 1 and 2 were almost identical to start with, the same ratio of λ_2/λ_1 was used for both of them.

[9]Actually, *almost* identical, due to imperfect workmanship.

Table 11.1: Properties of axisymmetric pucks used

	Puck No.	radius (mm)	radius (mm) of disk/hole	thickness (mm)	mass (gm)	λ_2/λ_1
Regular	1	49.1	0	6.4	67.8	0.336
	2	49.1	0	6.4	67.2	0.336
With hole	3	49.7	19.7	6.9	59.2	0.362
	4	49.6	29.4	6.9	45.4	0.400
	5	49.5	29.4	6.9	46.2	0.402
With disk	6	49.1	30.5	6.5	92.0	0.289
	7	49.2	30.5	6.4	91.5	0.289
	8	49.2	25.4	6.3	82.8	0.295
	9	49.1	20.3	6.2	74.6	0.308

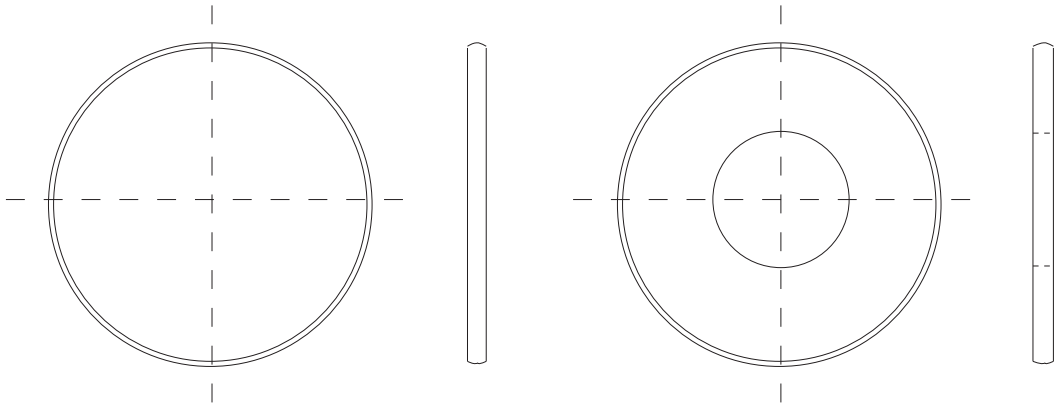

(a) regular puck

(b) puck with hole

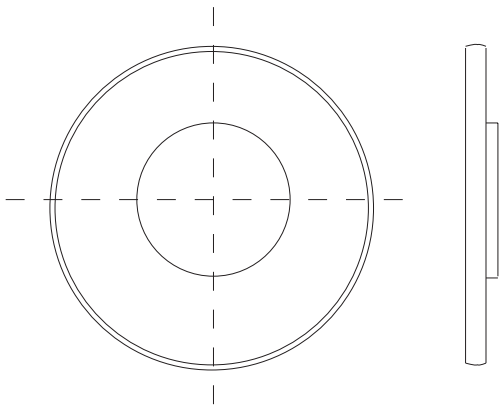

(c) puck with disk attached

Figure 11.3: Axisymmetric delrin pucks

Based on an assumption of homogeneity in velocity in the range studied (see Chapter 3), the pre-collision relative velocity at the contact point, for each collision, may be characterized by just the incidence angle θ (made with the common normal). The normal and tangential components of the observed post-collision relative velocities were normalized by the pre-collision relative velocity magnitude.

Note on Error Bars

The error bars shown in the figures in this chapter indicate *estimated upper bounds* on the errors in the various quantities being plotted. The procedure used to estimate these bounds is described below.

For each collision, the measured quantities were the x and y coordinates of eight points, i.e., sixteen scalar quantities. Each calculated quantity, such as the coefficient of restitution or the angle of incidence, is thus a scalar function of these sixteen variables.

Now for a function $f(q_1, q_2, \cdots, q_n)$, if the measured quantities $q_1, q_2, \cdots, q_n$ have errors Δq_1, $\Delta q_2, \cdots, \Delta q_n$, then the error in the calculated value of f is given to first order by the expression

$$\Delta f \approx \frac{\partial f}{\partial q_1}\Delta q_1 + \cdots + \frac{\partial f}{\partial q_n}\Delta q_n = \nabla f \cdot \Delta \mathbf{q}.$$

Now each of the Δq_i would typically be about one pixel or less (the precision of the digital imaging system). However, it is possible that for some data points the error was two pixels. From this, we obtain the error bound

$$|\Delta f| \leq \sum \left| \frac{\partial f}{\partial q_i}\Delta q_i \right| \leq h \sum \left| \frac{\partial f}{\partial q_i} \right|,$$

where h, in this case, is *twice* the data acquisition precision (length/pixel).

Results for Axisymmetric Pucks

The observed coefficient of restitution e is plotted for the different pucks as a function of incidence angle θ in Figs. 11.4 through 11.9, along with error bars for both e and θ. It is observed that

1. The data sets for puck pairs (1,2), (4,5) and (6,7) are fairly consistent for each pair.

2. The amount of scatter in the measurements is fairly small on the whole, and generally greater for values of θ closer to $\pi/2$ (glancing collisions). There are two possible reasons for this: (a) the normal velocity measurements have the same absolute precision but less relative precision at near-glancing incidence angles, as indicated by the error bars, and (b) small surface irregularities can have larger effects at near-grazing angles of incidence. In fact, some measured values of restitution are slightly more than unity (e.g., Figs. 11.4, 11.5 and 11.7), by amounts that are perhaps not convincingly larger than the estimated upper bounds on measurement errors. Note that there is *no* fundamental reason why the coefficient of normal restitution *cannot* be greater than one for general frictional collisions (see e.g., discussion of near-grazing collisions of objects with diagonal mass matrices, in Chapter 7, of Fig. 7.7).

3. There is a slightly increasing trend in the measured normal restitution, with increasing incidence angle. This may be due to one or both of (a) the variation in the normal component of pre-collision velocity, and (b) actual dependence of e on incidence angle, due to effects like possible coupling between the local deformations occurring in the normal and tangential directions. However, the data collected was over a small range of velocities and so it cannot be said which effect, if any, is the dominant one.

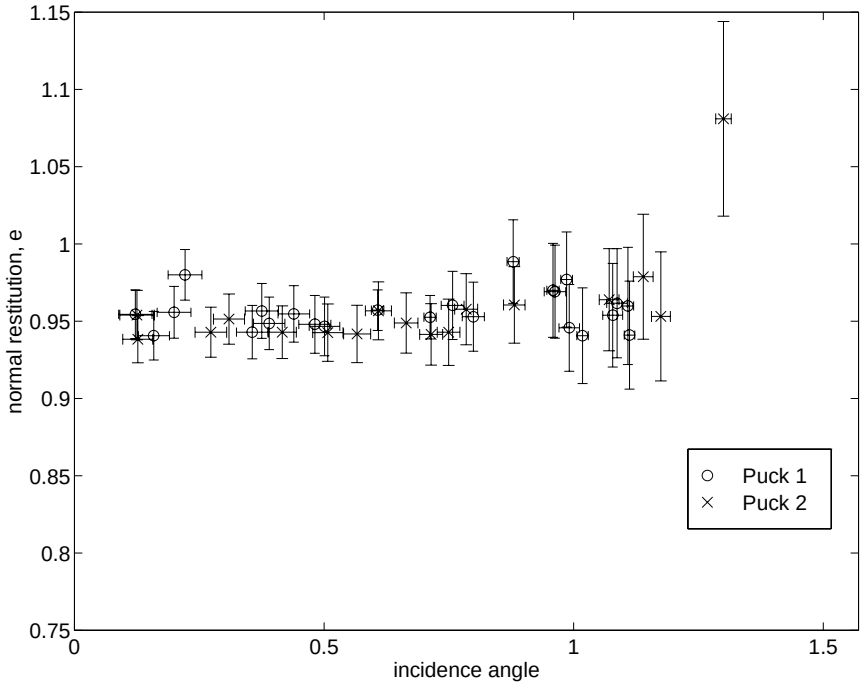

Figure 11.4: Normal restitution for pucks 1 and 2; identical, regular circular pucks

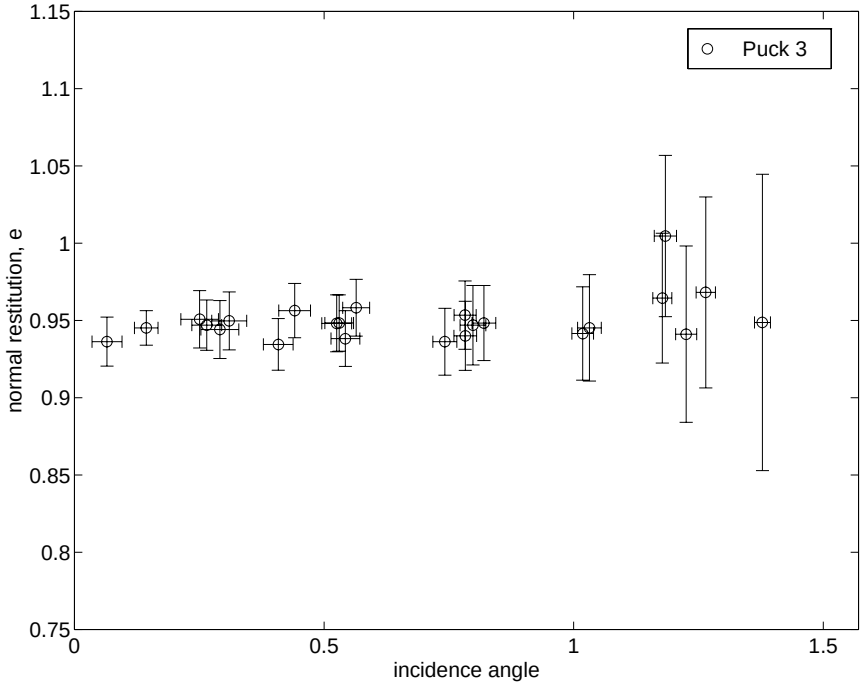

Figure 11.5: Normal restitution for puck 3; circular puck with hole

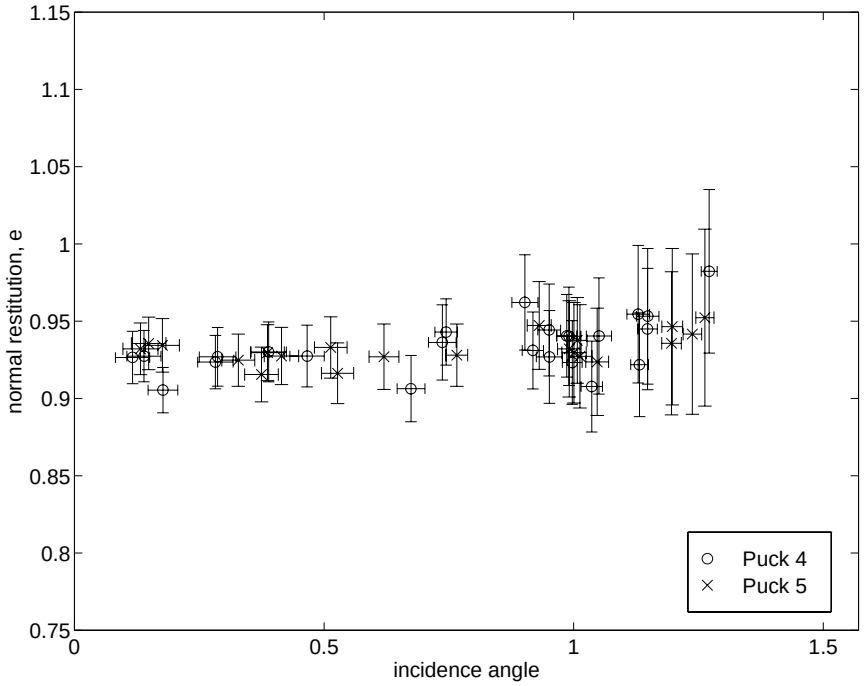

Figure 11.6: Normal restitution for pucks 4 and 5; identical circular pucks with holes

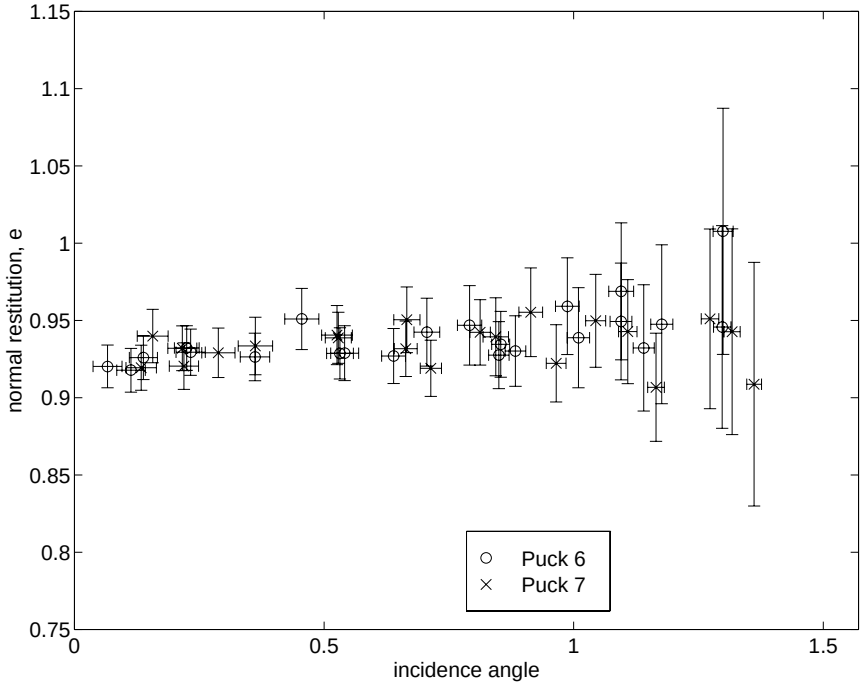

Figure 11.7: Normal restitution for pucks 6 and 7; identical circular pucks with attached disks

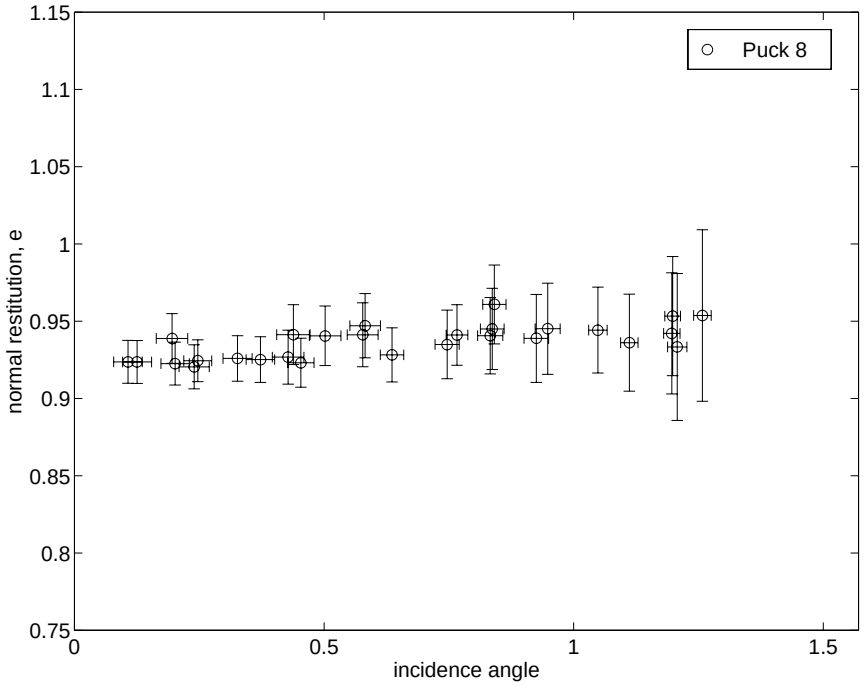

Figure 11.8: Normal restitution for puck 8; circular puck with attached disk

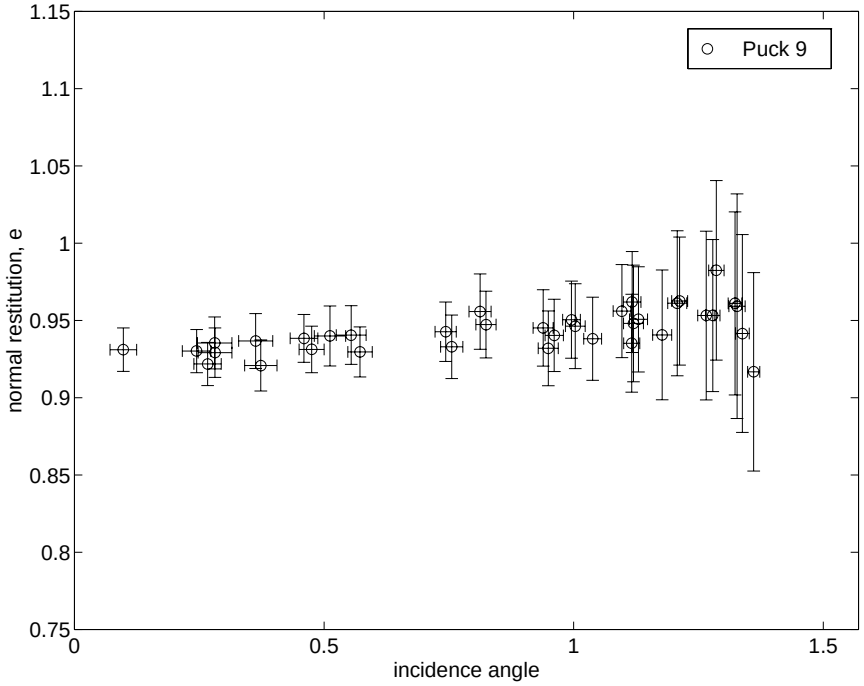

Figure 11.9: Normal restitution for puck 9; circular puck with attached disk

4. Although the added mass (disks) or removed mass (holes) changed the total mass of the pucks considerably, the measured coefficient of restitution did not show any dramatic changes from puck to puck, in contrast to the preliminary experiments with composite pucks described earlier in this section.

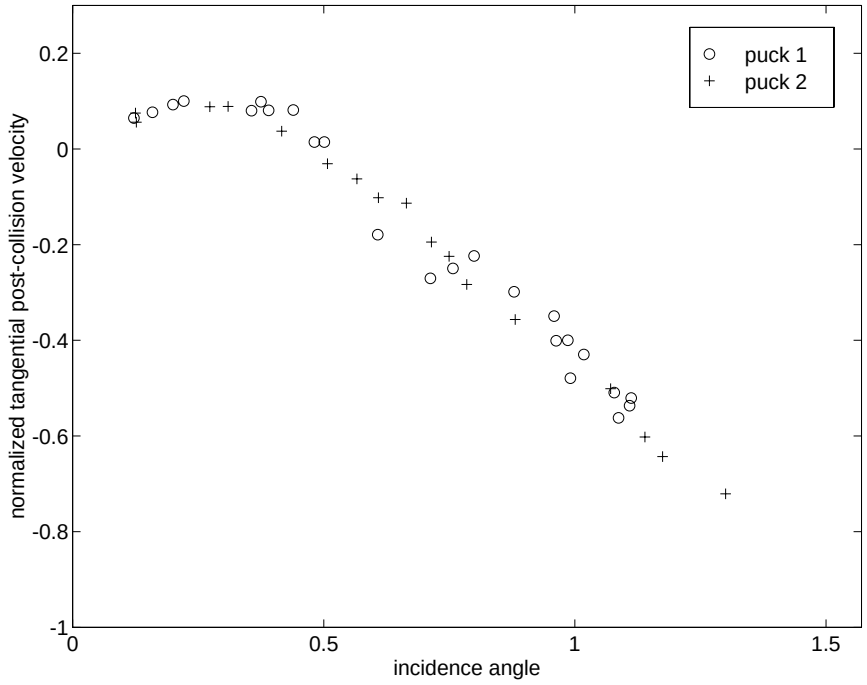

Figure 11.10: Post-collision tangential velocity V_{fT} for pucks 1 and 2; identical, regular circular pucks

The observed tangential components of the post-collision velocity, V_{fT}, which is a scalar in the 2D case, were normalized with respect to the magnitude of V_i. Normalized tangential post-collision velocity as a function of incidence angle θ is plotted[10] for the different pucks in Figs. 11.10 through 11.15. Once again, the data sets for puck pairs (1,2), (4,5) and (6,7) are fairly consistent.

One representation of the data that is sometimes used (see e.g., Maw *et al.* [40] or Foerster *et al.* [17]) is a graph of the tangent of the angle ϕ made by the post-collision velocity V_f with the normal direction, against the tangent of θ, the incidence angle, made by the pre–collision velocity V_i with the normal direction[11] (see Fig. 11.16).

Plots of $\tan\phi$ vs. $\tan\theta$ are shown in Figs. 11.17 through 11.22 (with error bars).

It is seen in these plots that $\tan\phi$ is roughly linearly related to $\tan\theta$, for larger values of $\tan\theta$. A common interpretation of this is as follows. One usually assumes that for collisions with diagonal mass matrices, where the tangential component of relative velocity does not change direction in the collision, the tangential impulse may be given by μ times the normal impulse. For a pre-collision velocity given by $V_{iN} = -\cos\theta$ and $V_{iT} = -\sin\theta$, and a coefficient of normal restitution e, we

[10] Without error bars, for simplicity – the error in the measurements of tangential motions *is* displayed in the plots of $\tan\phi$ vs. $\tan\theta$ shown later in this chapter (Figs. 11.17 through 11.22).

[11] Actually, Maw *et al.* and Foerster *et al.* plot the tangents of these angles scaled by quantities involving the elastic constants of the colliding objects. Unscaled plots are presented here.

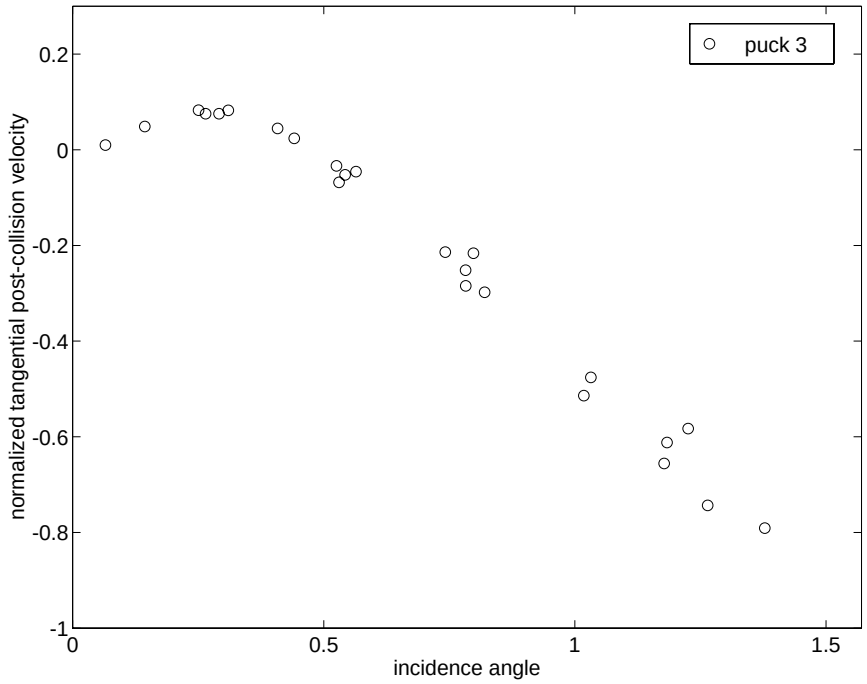

Figure 11.11: Post-collision tangential velocity V_{fT} for puck 3; circular puck with hole

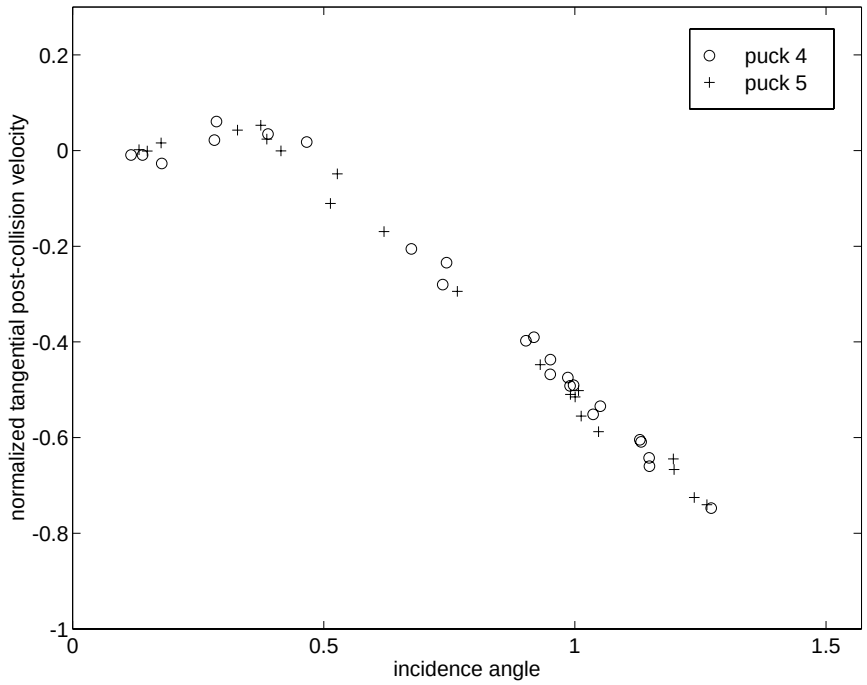

Figure 11.12: Post-collision tangential velocity V_{fT} for pucks 4 and 5; identical circular pucks with holes

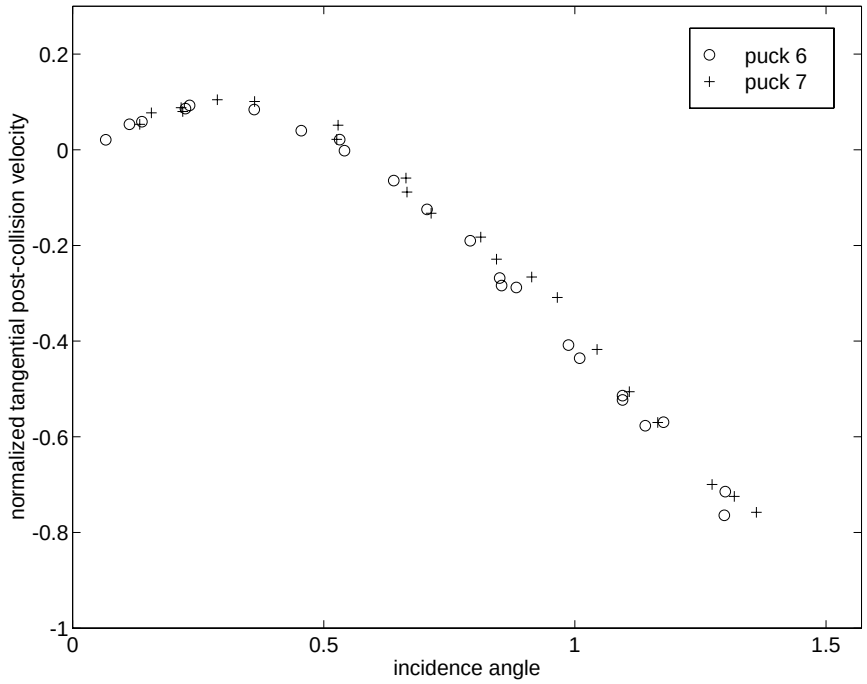

Figure 11.13: Post-collision tangential velocity V_{fT} for pucks 6 and 7; identical circular pucks with attached disks

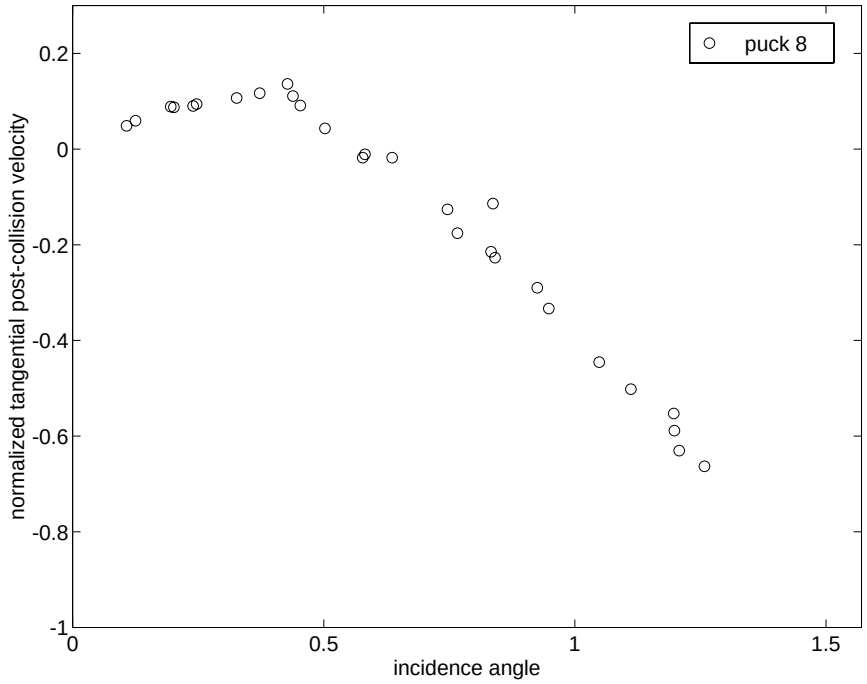

Figure 11.14: Post-collision tangential velocity V_{fT} for puck 8; circular puck with attached disk

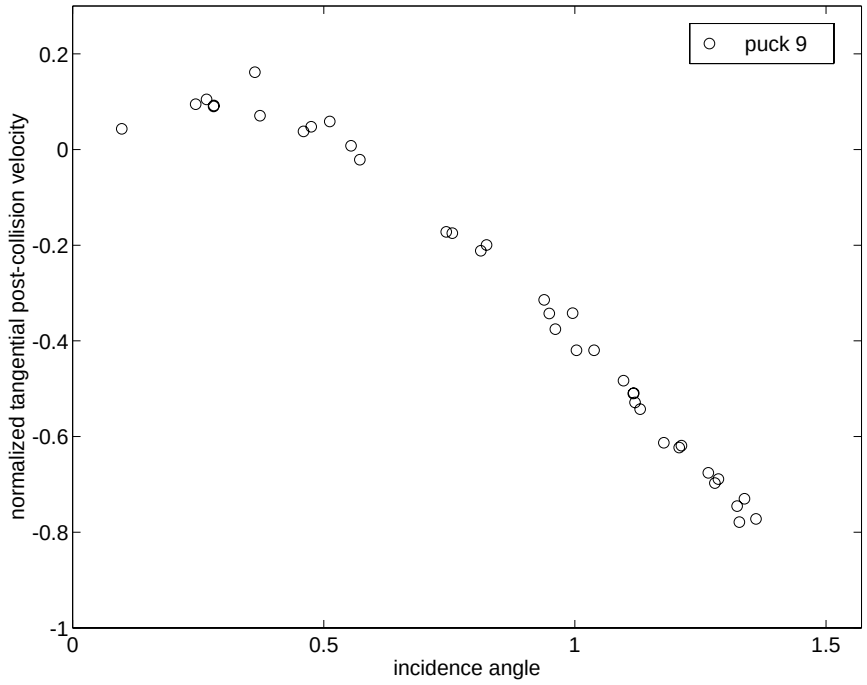

Figure 11.15: Post-collision tangential velocity V_{fT} for puck 9; circular puck with attached disk

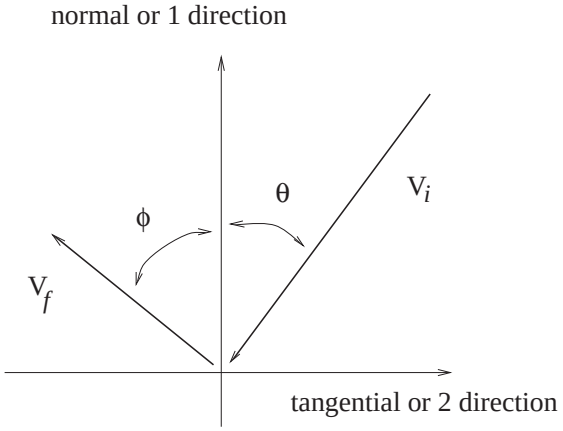

Figure 11.16: Angles θ and ϕ

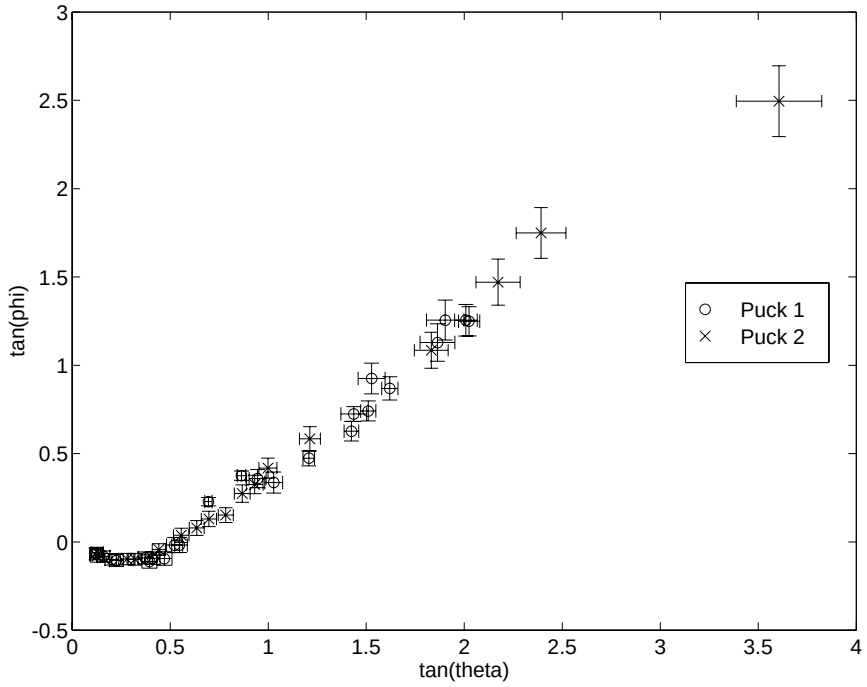

Figure 11.17: $\tan\phi$ vs. $\tan\theta$ for pucks 1 and 2; identical, regular circular pucks

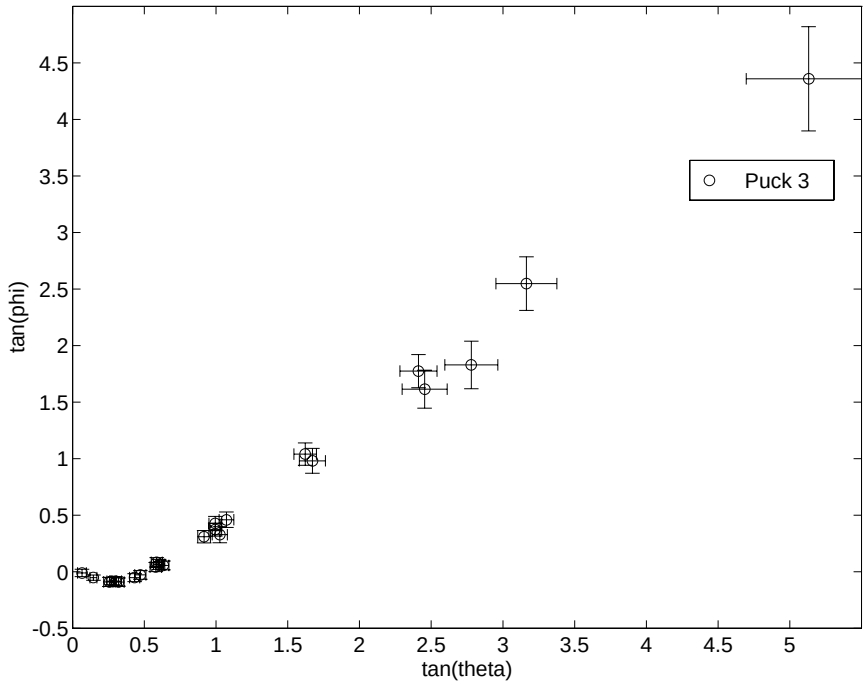

Figure 11.18: $\tan\phi$ vs. $\tan\theta$ for puck 3; circular puck with hole

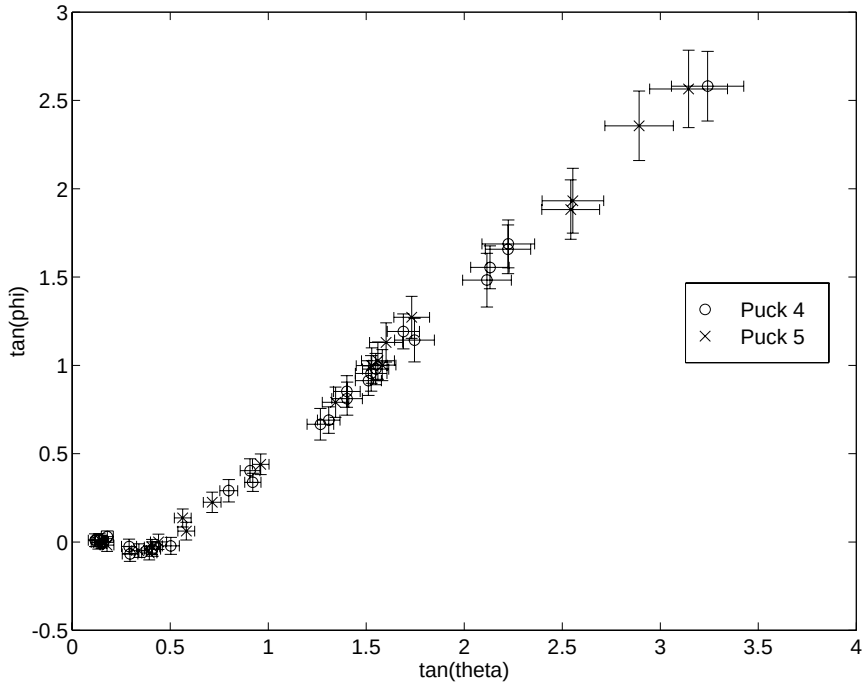

Figure 11.19: $\tan\phi$ vs. $\tan\theta$ for pucks 4 and 5; identical circular pucks with holes

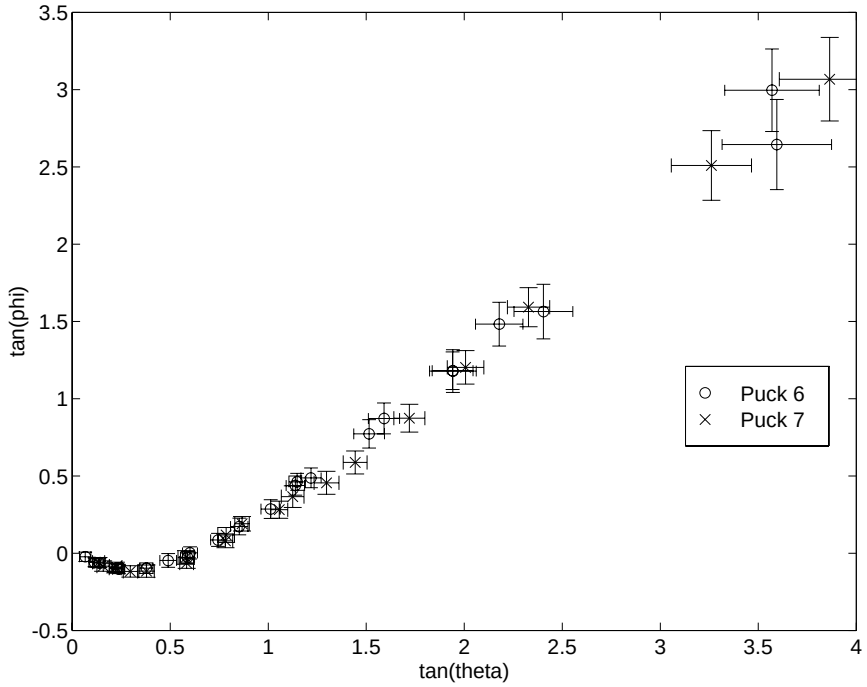

Figure 11.20: $\tan\phi$ vs. $\tan\theta$ for pucks 6 and 7; identical circular pucks with attached disks

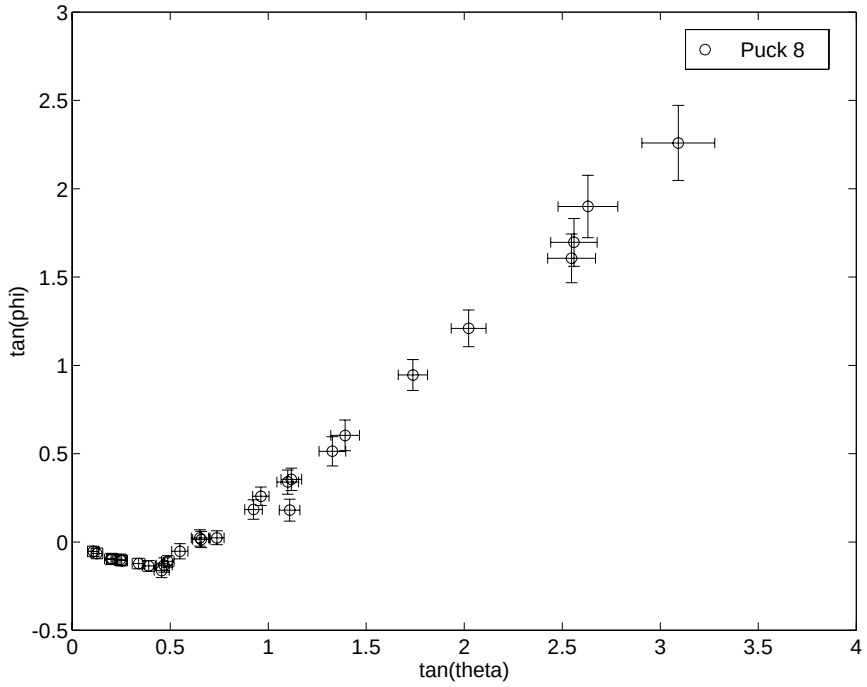

Figure 11.21: $\tan\phi$ vs. $\tan\theta$ for puck 8; circular puck with attached disk

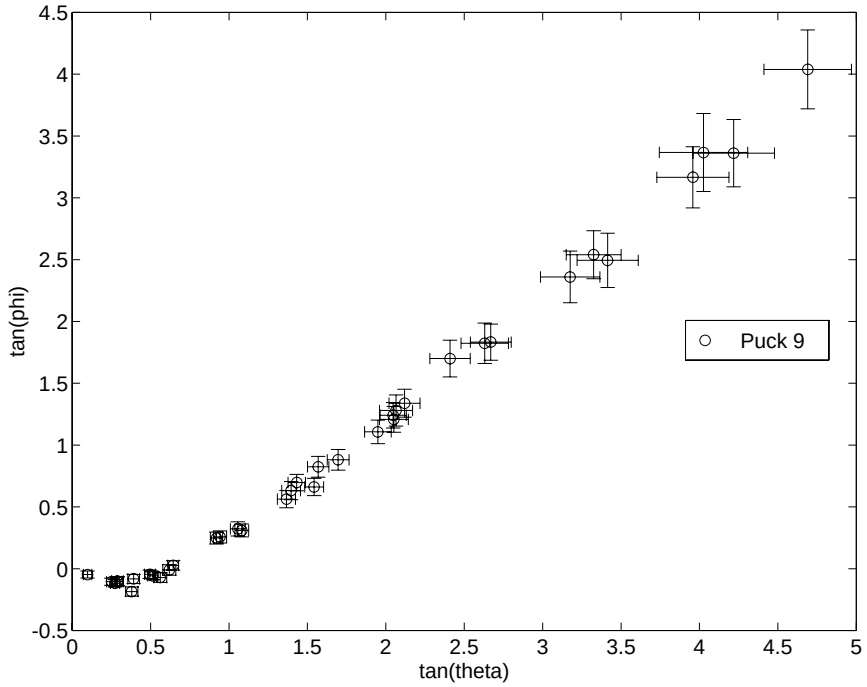

Figure 11.22: $\tan\phi$ vs. $\tan\theta$ for puck 9; circular puck with attached disk

obtain

$$\tan\phi = \tan\theta + \mu(1+e)\frac{\lambda_1}{\lambda_2},$$

where λ_1 and λ_2 are the inertias in the normal and tangential directions, respectively. However, as per this simple model, the slope of the linear portions of the data in Figs. 11.17 through 11.22 should be exactly unity. It may be seen in the figures that the slope is actually noticeably less than unity. This mismatch in the slope indicates that the simple model of friction used above does not apply to the collisions studied here. This anomalous frictional interaction is discussed next.

Practically *all* simple rigid-body collision models, when specialized to the case of diagonal mass matrices and the "sliding regime", assume that the tangential impulse is μ times the normal impulse, as discussed above. Such models include Kane and Levinson's model, Smith's model, Routh's model and the Mindlin-Deresiewicz model (see Chapter 5), as well as the bilinear law and the new algebraic collision laws discussed in Chapter 6. Some studies of collisions of spheres against flat plates at relatively higher speeds have shown that the effective coefficient of friction, defined as the impulse ratio in the sliding regime, can actually *decrease* for higher incidence angles (see e.g., Vinogradov *et al.* [68]). However, in the experiments reported here, it was found that the impulse ratio in the sliding regime actually *increased significantly* with increasing incidence angle, as shown next.

Plots of the ratio of tangential to normal impulses in the collisions against the incidence angle θ, calculated from the kinematic data and the ratio λ_2/λ_1 from Table 11.1, for the different pucks, are shown in Figs. 11.23 through 11.28, with error bars. Note that the error bars are based on estimates of the maximum possible error, and it is likely that most of the errors are about half or less of what the error bars indicate.

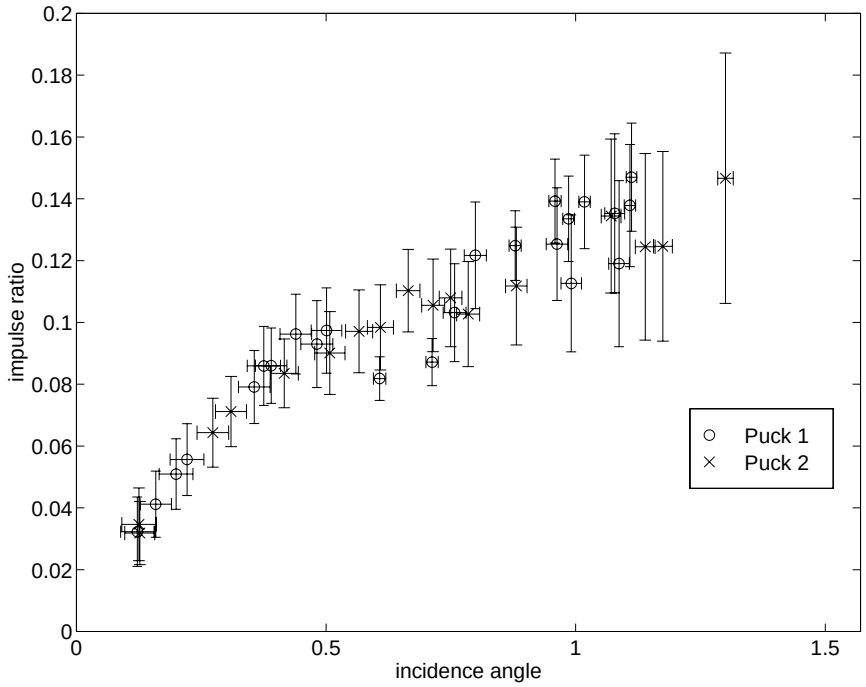

Figure 11.23: Impulse ratio for pucks 1 and 2; identical, regular circular pucks

For each case, in the sliding regime, the impulse ratio is seen to be increasing from roughly 0.1 to an extrapolated value of roughly 0.16 at $\theta = \pi/2$. A likely explanation for this is that even in

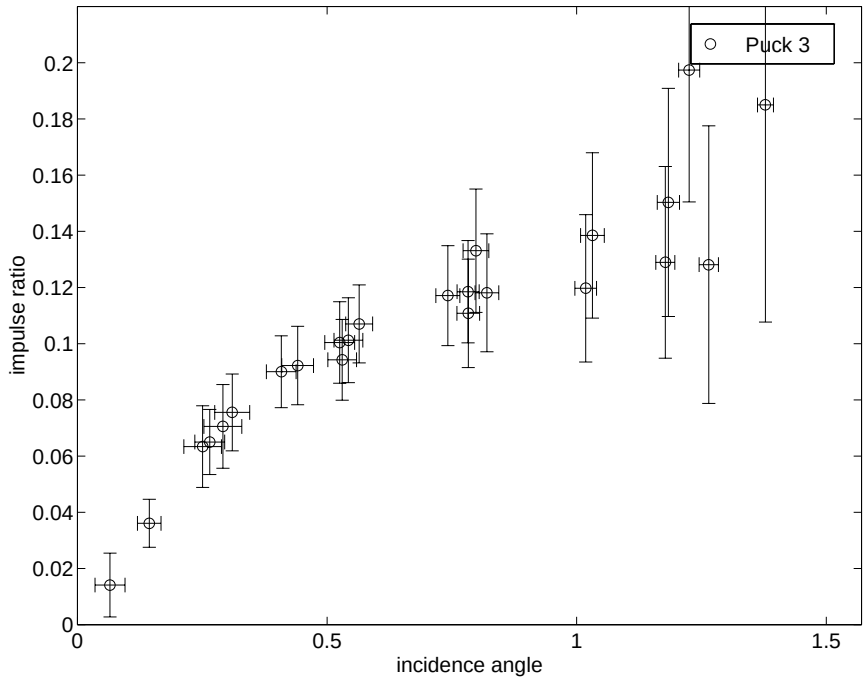

Figure 11.24: Impulse ratio for puck 3; circular puck with hole

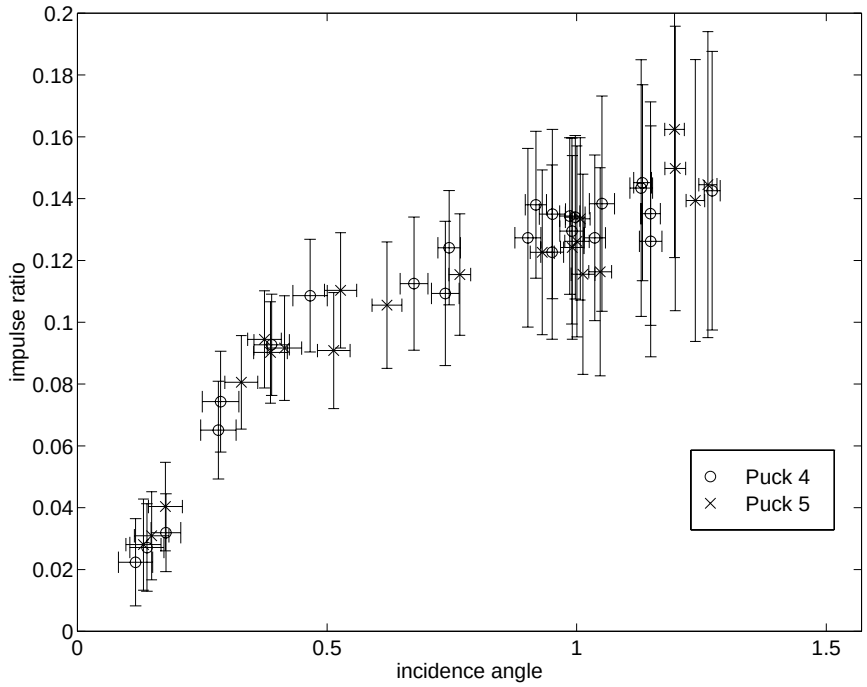

Figure 11.25: Impulse ratio for pucks 4 and 5; identical circular pucks with holes

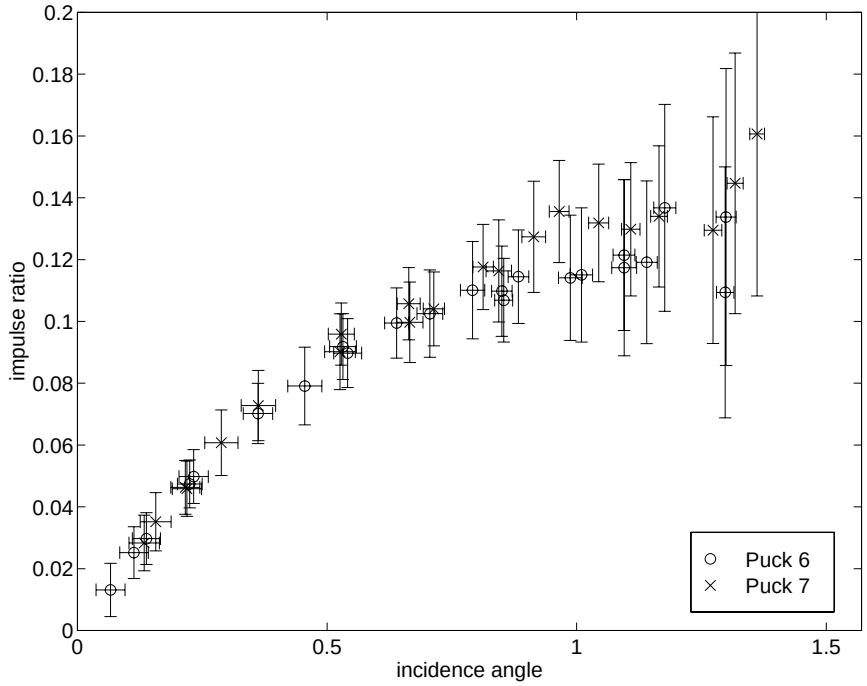

Figure 11.26: Impulse ratio for pucks 6 and 7; identical circular pucks with attached disks

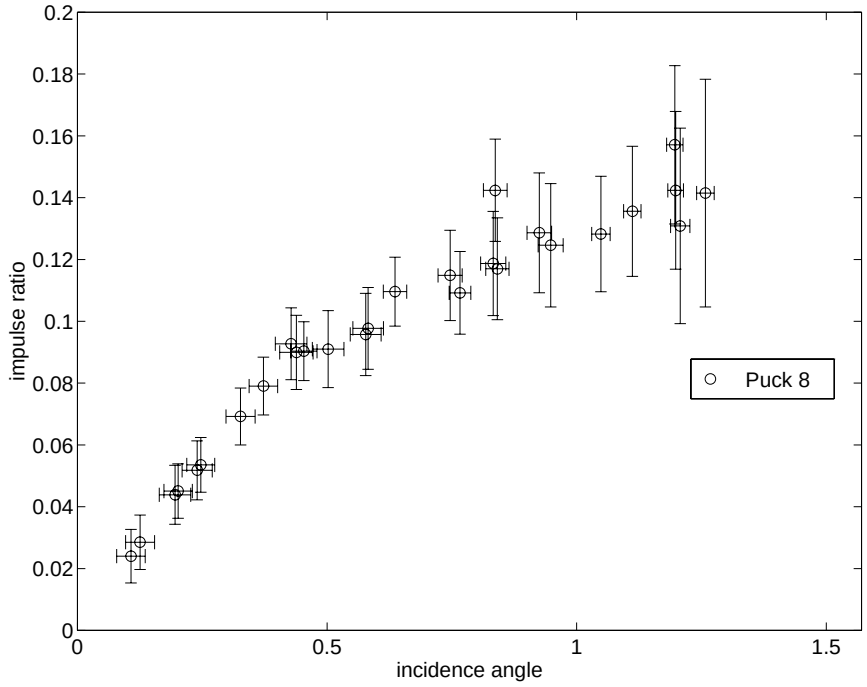

Figure 11.27: Impulse ratio for puck 8; circular puck with attached disk

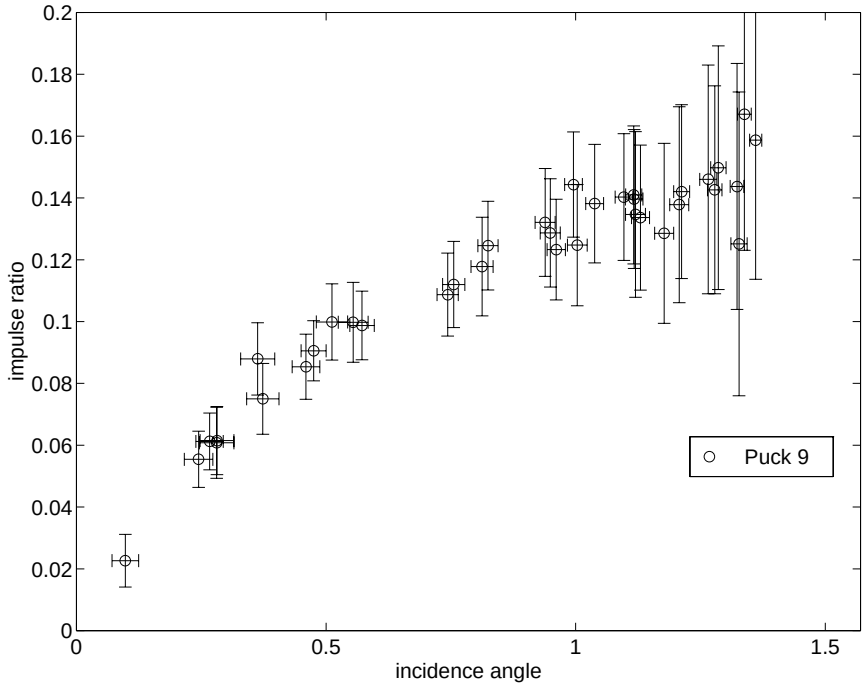

Figure 11.28: Impulse ratio for puck 9; circular puck with attached disk

collisions where the contact point has the same velocity direction before and after collision, some parts of the contact region stick for some of the time during the collision. It is expected that the extrapolated graph should give the "true" coefficient of friction at $\theta = \pi/2$. In an independent and somewhat crude experiment, the coefficient of kinetic friction between one of the pucks and a smooth steel surface[12] was estimated to be a little under 0.2, which is consistent with the rest of the data.

Figure 11.29 shows the impulse ratio calculated for every single collision of every puck (1 through 9) in a single graph. Considering that the ratio λ_2/λ_1 varied by a factor of about 1.4, and that the mass of the pucks varied by a factor of 2, the agreement observed is remarkable. Particularly interesting is that the frictional behavior common to all 9 pucks is in direct contradiction to the predictions of many collision laws (including the bilinear law and the three new laws presented in Chapter 6, as well as the following laws discussed in Chapter 5: Kane and Levinson's law, Smith's law, Routh's law, the Mindlin-Deresiewicz model and all general point contact incremental laws where pure frictional sliding occurs beyond some critical incidence angle).

For comparison, the predicted impulse ratios for the cases of Routh's law, Kane and Levinson's law, and Smith's law, using $e = 0.92$ and $\lambda_2/\lambda_1 = 1/3$ (uniform disk), are plotted against incidence angle, in Fig. 11.30. The experimental data is represented by a simple bilinear curve. The significant mismatch in the sliding regime is readily seen.

[12]The friction experiment was conducted by Scott Kennedy in 1996, a year after the original collision experiments were conducted by John Calsamiglia. Unfortunately, during the intervening year, the original plate used by Calsamiglia had been misplaced and a different steel plate was used for the experiment. It will be seen that the friction coefficient observed between Delrin and steel, in the experiments conducted in 1996, were somewhat higher than that observed in the experiments of 1995. This may be due to either the difference in the steel surface finish, or different ambient conditions, or both.

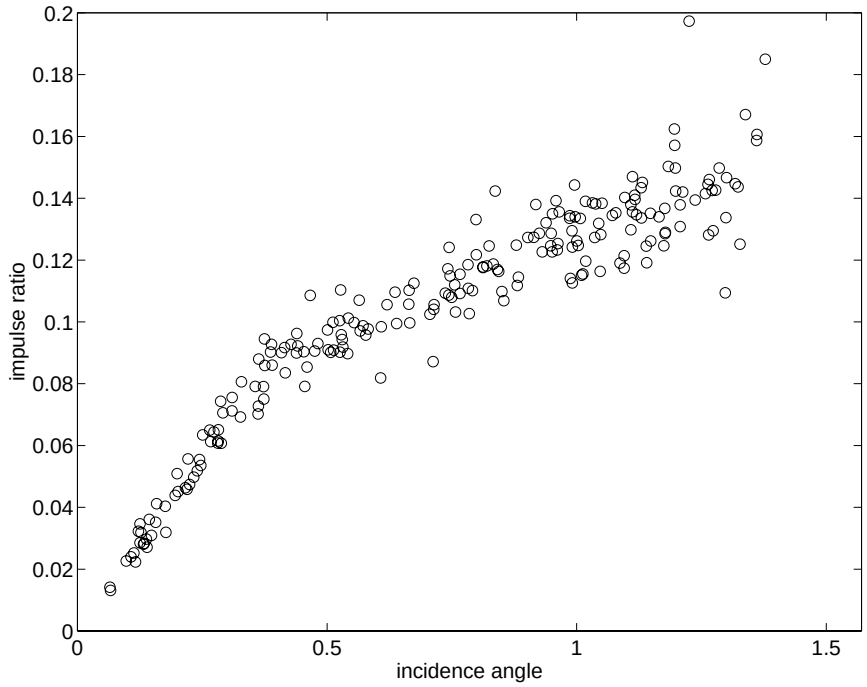

Figure 11.29: Impulse ratio for *all* pucks

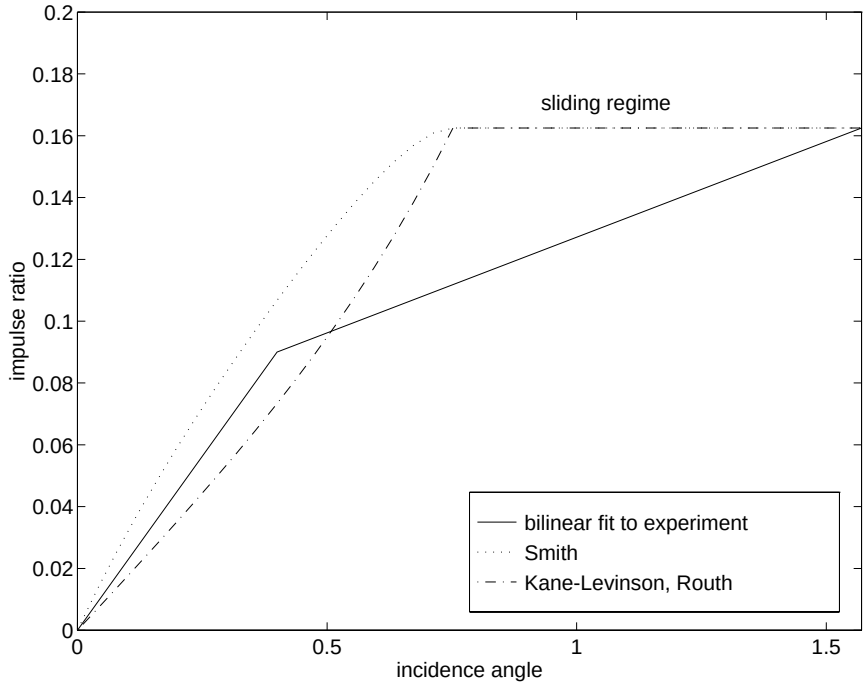

Figure 11.30: Impulse ratio predicted by some collision laws

11.2 Study of Non-axisymmetric Pucks, with Scott Kennedy

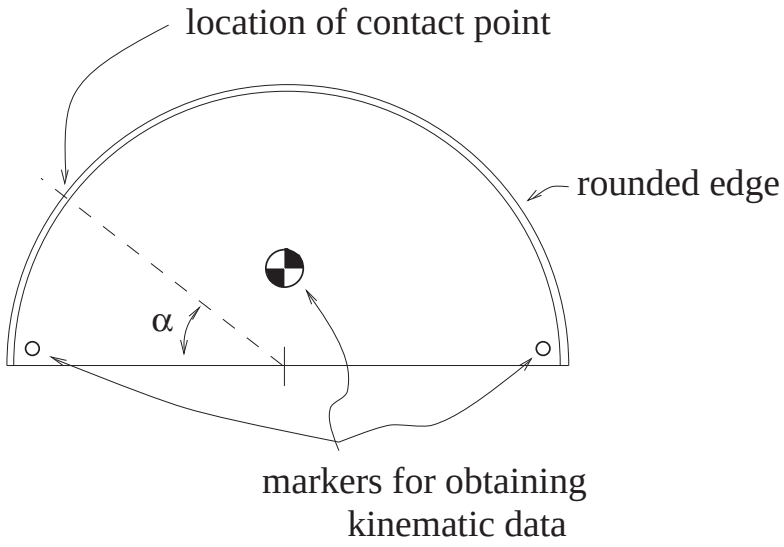

Figure 11.31: Non-axisymmetric Delrin puck

This section contains a brief description of, and fairly detailed results from, experiments in 2D collisions of a non-axisymmetric (semicircular) puck with a massive steel plate clamped to an air table. The experiments were conducted in the Theoretical and Applied Mechanics Department at Cornell University in the summer of 1996, under my supervision, by undergraduate REU student Scott Kennedy.

The semicircular puck studied in the experiments described in this section is shown in Fig. 11.31. The center of mass (shown in the figure) was found by balancing the puck on a knife edge. It was found that the center of mass was *not* located at the centroid of the disk; however, it *was* located approximately on the axis of symmetry of the semicircle. Based on these observations and the fact that the puck was machined out of a piece of cylindrical stock (which might reasonably be expected to be axisymmetric), it was assumed that the mass distribution was approximately radially symmetric. The mass of the puck was measured to be 33.4 gm, and the moment of inertia about the center of mass to be 265 gm cm^2.

The center of mass was marked on the blackened puck with a white dot. Two other white marks were also made on the puck (see Fig. 11.31). In the pictures taken during the experiments, the position of the center of mass along with any one of the other markers was sufficient to determine the position of the puck. The reason for having two markers was that one of the markers might be outside the field of view of the camera, for some positions of the puck in some pictures. In such cases, the other marker would be available and the picture could still be used. The net result of having two markers was that the field of view of the camera could be kept small, leading to higher resolution (in pixel/mm).

For each collision, four positions of the puck were used – two before and two after the collision. For each position of the puck, the coordinates of the center of mass and of one of the markers was obtained manually using *NIH Image*, as in Calsamiglia's experiments (described earlier in this chapter).

Unlike collisions of axisymmetric objects, the location of the contact point on the puck needs to be found for each collision. The location of the contact point on the puck, calculated from the raw

kinematic data, is designated by the angular coordinate α (see Figs. 11.31 and 11.32), which takes values between 0 and π. Details of the experimental procedure and of the calculations performed may be found in Scott Kennedy's report [34].

The steel plate used in the experiments was more than 200 times more massive than the puck, and its mass was treated as infinite in all calculations.

Under the assumption of homogeneity of degree one in the input velocity, the magnitude of the pre-collision velocity for each collision was be scaled to one. Each collision of the puck is thus characterized by two parameters – the direction of the precollision velocity (incidence angle θ), and the location of the contact point on the puck (angle α from Fig. 11.31). The incidence angle θ can take values between $-\pi/2$ and $\pi/2$, while α takes values between 0 and π. However, due to symmetry in the puck, we restrict θ between 0 and $\pi/2$ and change α to $\pi - \alpha$ if necessary, as indicated in Fig. 11.32.

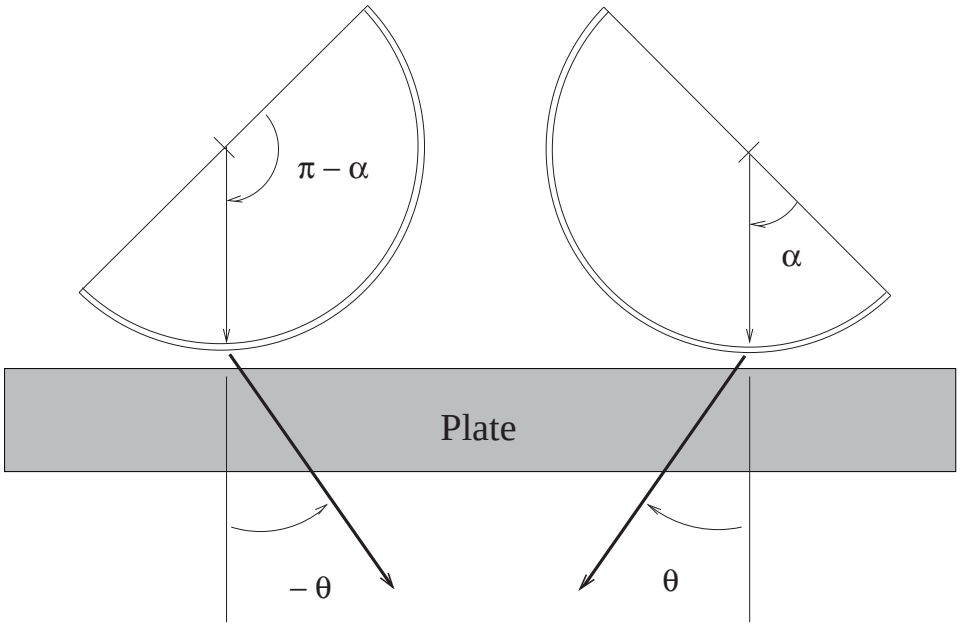

Figure 11.32: Due to symmetry in the puck, θ may be assumed to be nonnegative (between 0 and $\pi/2$)

Note on error bars: Error bars for the results presented in this section were computed in the same manner as indicated in the previous section. The precision of measurements of kinematic data for the semicircular puck was about 4.9 pixel/mm.

The two independent variables make the results of the experiments somewhat difficult to present graphically. For example, a 3D plot of the observed ratio of tangential to normal impulse transmitted in each collision, plotted vs. θ and α, is shown in Fig. 11.33. It is not difficult to discern the basic rising trend in the data, but the scatter in the experimental data makes it hard to detect small variations in the basic trend (trends within trends), if any.

One might initially expect that the results might be plotted as a surface. Unfortunately, there were not enough data points to sufficiently "fill" the plane. The sample of data points obtained is shown in a plot of incidence angle θ vs. contact point location α for the different collisions, in Fig. 11.34.

Though the scatter in the data itself makes it difficult to fit a suitable surface to it, it was found that plotting quantities of interest (like the coefficient of restitution) against only one of θ or α in

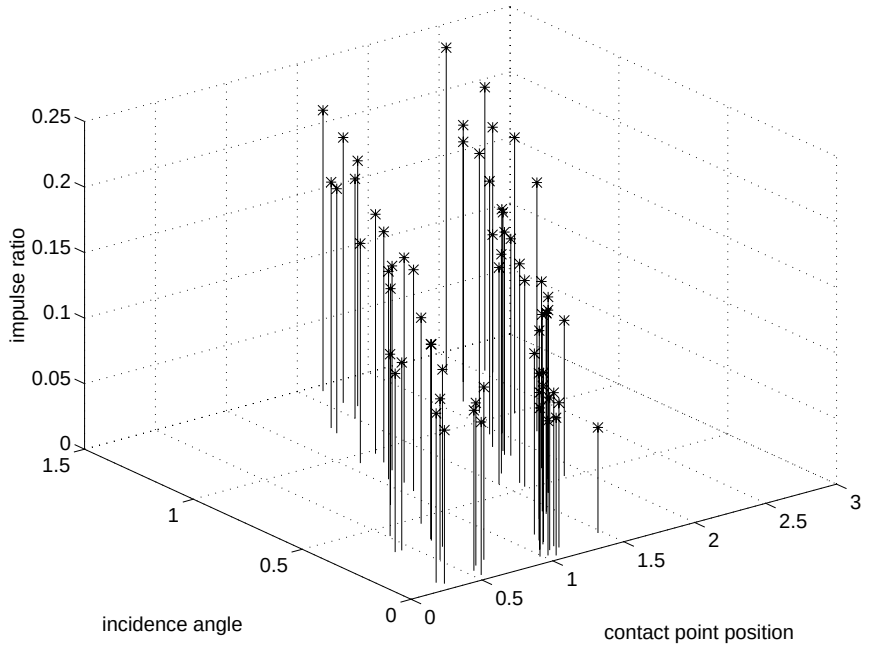

Figure 11.33: Ratio of tangential to normal impulse vs. contact point location α and incidence angle θ

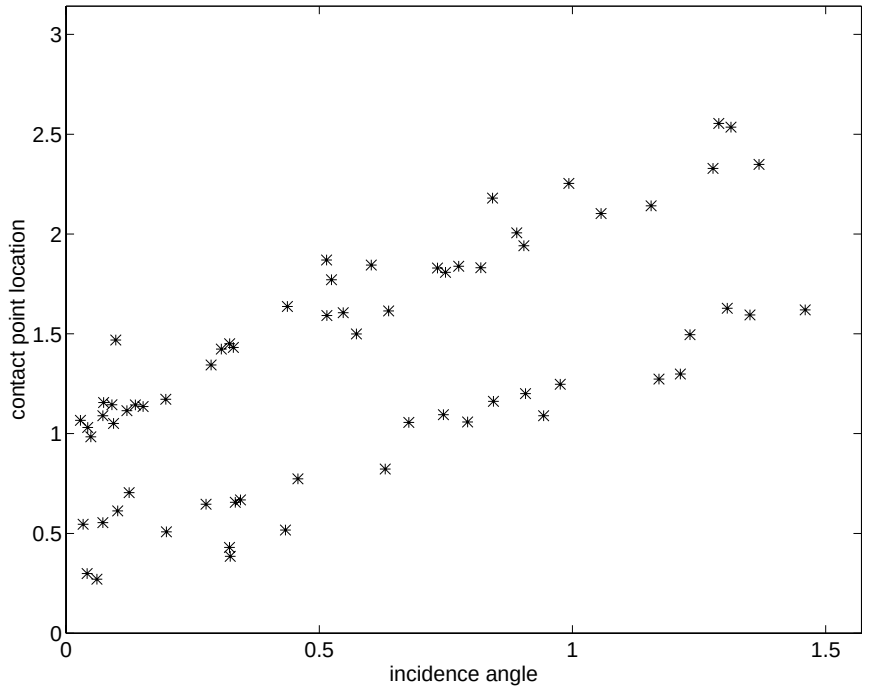

Figure 11.34: Sample of data points: θ vs. α

2D graphs was instructive.

Of the collision quantities studied, two are particularly interesting; these are the coefficient of normal restitution, and the ratio of tangential to normal impulses transmitted in the collision. They are presented in separate subsections below.

11.2.1 The Coefficient of Normal Restitution

As mentioned earlier in this thesis, the coefficient of normal restitution e_n has no fundamental validity as a constant parameter that the characterizes the general collisional behavior of a given body. The results of experiments with axisymmetric disks, from the previous section, indicate that e_n is roughly constant for those objects (for collisions with a massive steel plate), with perhaps a weak dependence on the incidence angle. On the other hand, the data of Stoianovici and Hurmuzlu [58] clearly demonstrates that the coefficient of normal restitution of slender steel rods (for collisions with a massive anvil) strongly depends on the configuration of the rod.

In the experiments with the non-axisymmetric puck, it was found that the coefficient of restitution *was* approximately constant, with a mild dependence on the incidence angle and on the location of the contact point on the puck. The variation of e_n with the contact point location α, *ignoring* the dependence on the incidence angle θ, is shown in Fig. 11.35 (with error bars).

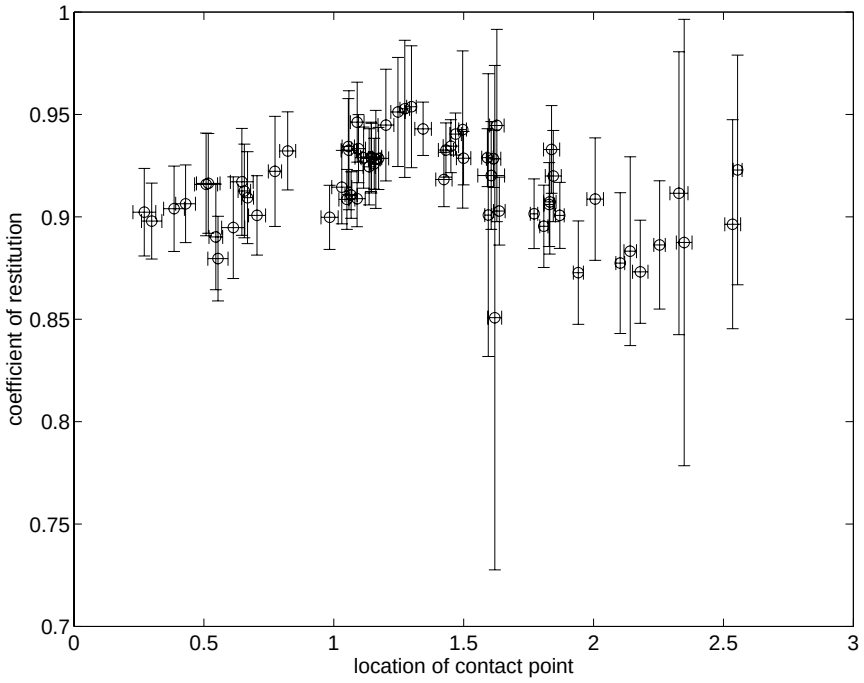

Figure 11.35: Coefficient of normal restitution vs. contact point location α

An interesting feature of the data is that the values of e_n appear to reach a maximum at some value of α that is slightly less than $\pi/2$. Note that $\alpha = \pi/2$ corresponds to a symmetric configuration (see Fig. 11.31) but not necessarily a head-on collision, because the incidence angle θ, which is not indicated in the figure, might be nonzero. Kennedy [34] has observed that the values of e_n appear to reach a maximum for those collisions where the impulse transmitted at the contact point is directed roughly towards the center of mass of the puck. Let ψ denote the angle between the impulse vector and the position vector from the contact point to the center of mass (see Fig. 11.36). The coefficient of restitution e_n is plotted against ψ in Fig. 11.37. It is seen that the graph

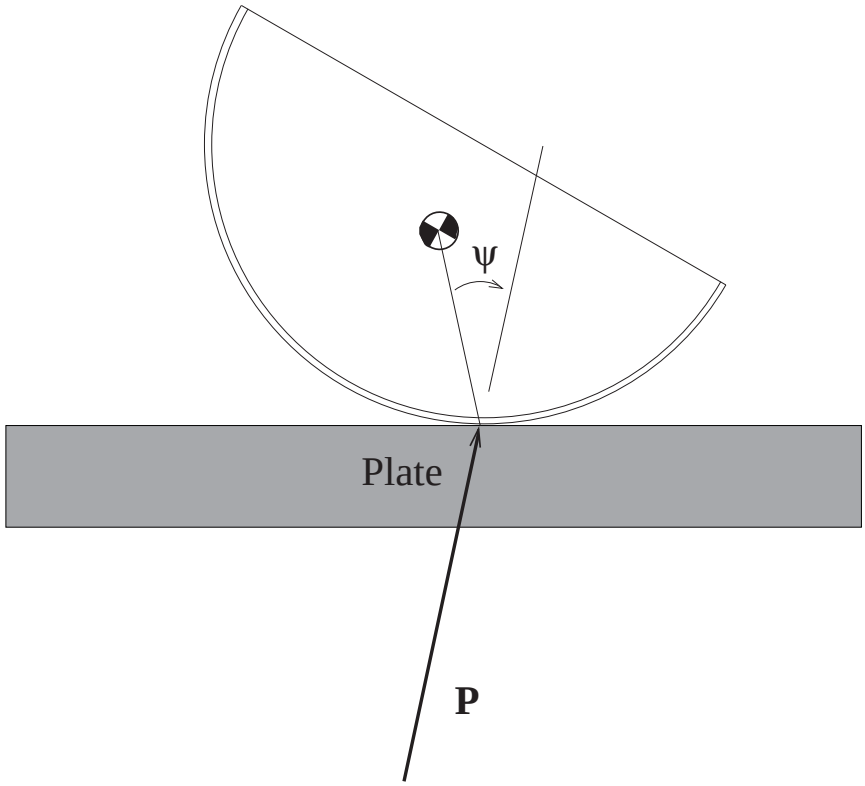

Figure 11.36: The angle ψ between the transmitted impulse vector and the position vector from the contact point to the center of mass

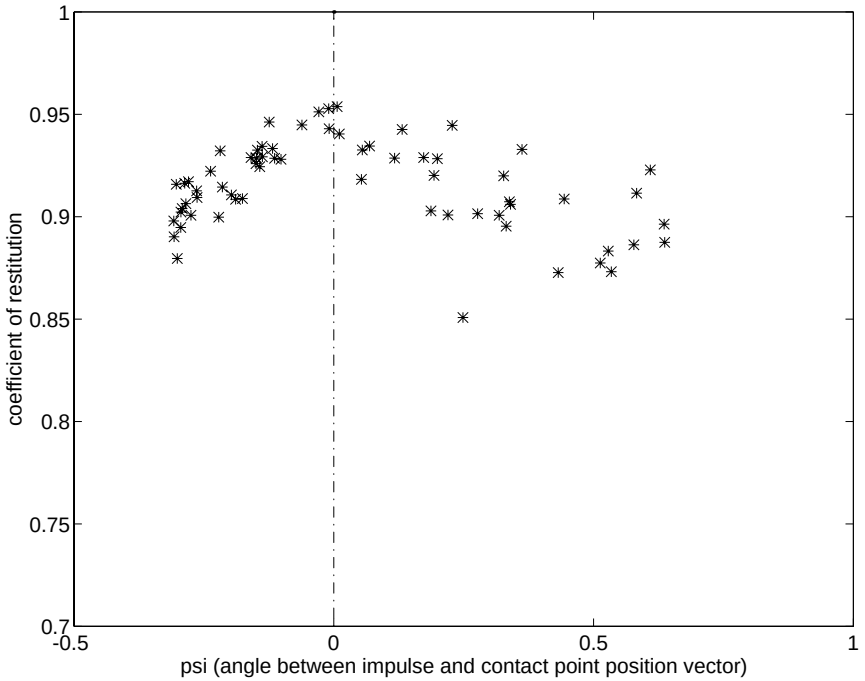

Figure 11.37: Coefficient of normal restitution vs. angle ψ (between impulse vector and position vector from contact point to center of mass)

reaches a maximum around $\psi = 0$.

The principal conclusions regarding the coefficient of restitution for collisions between the semi-circular puck a the steel plate are:

1. As a *rough* approximation, the coefficient of restitution may be treated as a constant, with a value of around 0.92 in this case.

2. There appears to be a mild dependence of the coefficient of restitution on the location of the contact point on the body. This dependence is likely to be stronger for many bodies (such as slender rods), but may be mild for some roundish and "chunky" homogeneous objects.

11.2.2 The Frictional Impulse

The frictional interaction observed in the collisions of the non-axisymmetric puck was qualitatively similar to that observed for the axisymmetric pucks. It was found, as for the axisymmetric pucks, that even for collisions where slip was *not* reversed, the ratio of tangential to normal impulses was not constant. The impulse ratio was significantly lower than the coefficient of friction for impacts that were not close to grazing incidence. As discussed earlier, these collisions would typically be considered to be sliding collisions in many collision models (such as practically all algebraic collision models as well as some incremental models such as Routh's model).

Figure 11.38 shows the impulse ratio plotted (with error bars) against the incidence angle θ, ignoring the dependence on the contact point angle α. It is seen that the impulse ratio *increases* on average as the incidence angle θ goes from 0 to $\pi/2$. The impulse ratio varies roughly by a factor of two, which is similar to the behavior observed with the axisymmetric disks. An interesting feature of the data is that Fig. 11.38 shows *all* the data points, including both collisions where the direction of tangential velocity of the contact point is reversed ("sticking" collisions) as well as ones where the velocity is *not* reversed ("sliding" collisions). Figure 11.39 shows the impulse ratio, plotted against θ, with separate symbols for the sticking and sliding collisions. It is interesting to note that the impulse ratio does *not* appear to depend much on whether the tangential velocity at the contact point was reversed or not.

On the whole, the frictional behaviors of the axisymmetric and non-axisymmetric pucks are consistent with each other. They might both be considered anomalous in the context of commonly used rigid body collision models.

At the grazing limit ($\theta = \pi/2$) the ratio of tangential to normal impulse is about 0.22. That this value of 0.22 is slightly higher than the limiting value of about 0.18 observed for the axisymmetric pucks is not too surprising considering that **(a)** the steel plate used was different, with a different surface finish, and **(b)** the coefficient of friction between two given surfaces varies with ambient conditions, which were quite likely different for the two sets of experiments (they were conducted roughly a year apart). The impulse ratio is plotted against contact point location α in Fig. 11.40, which may be compared with Fig. 11.38. There appears to be a discernible upward trend in the impulse ratio with increasing α, but the scatter is higher in this figure than Fig. 11.38. It is likely that the trend observed in Fig. 11.40 is due to the somewhat correlated nature of θ and α themselves, as shown in Fig. 11.34.

11.3 Discussion of Anomalous Frictional Interaction

As mentioned in the previous two sections, the frictional behavior observed in the 2D collisions of the axisymmetric and non-axisymmetric pucks may be said to be anomalous in the context of most rigid body collision models. This section explores some possible reasons for such behavior.

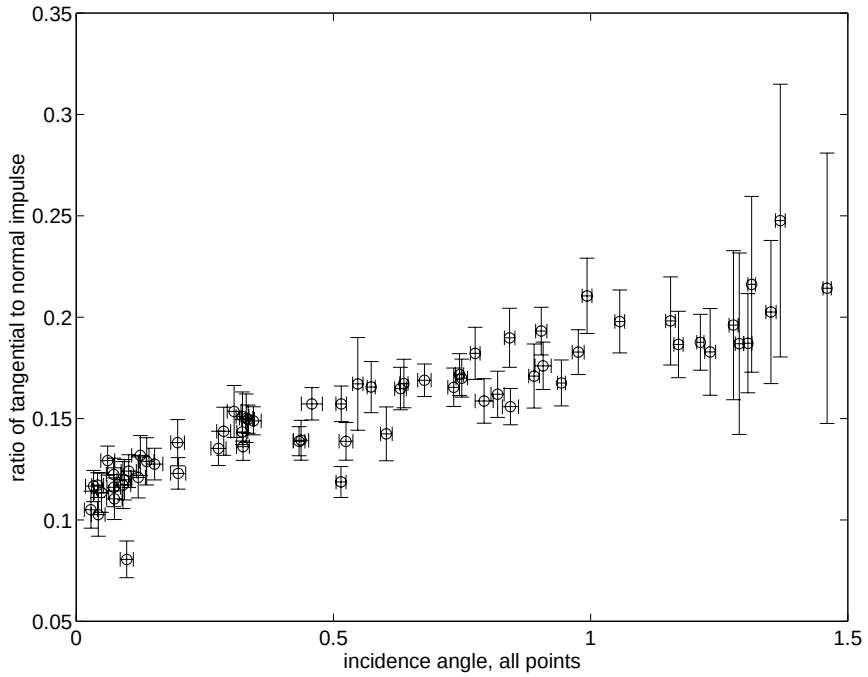

Figure 11.38: Ratio of tangential to normal impulses observed for both sticking and sliding collisions, vs. incidence angle θ

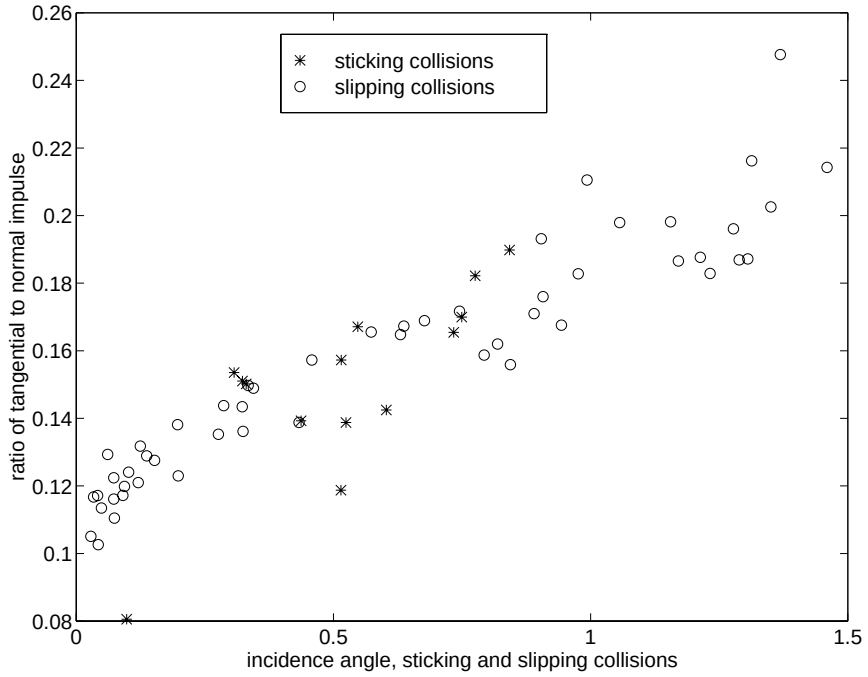

Figure 11.39: Impulse ratio vs. incidence angle θ, showing sticking and sliding points separately

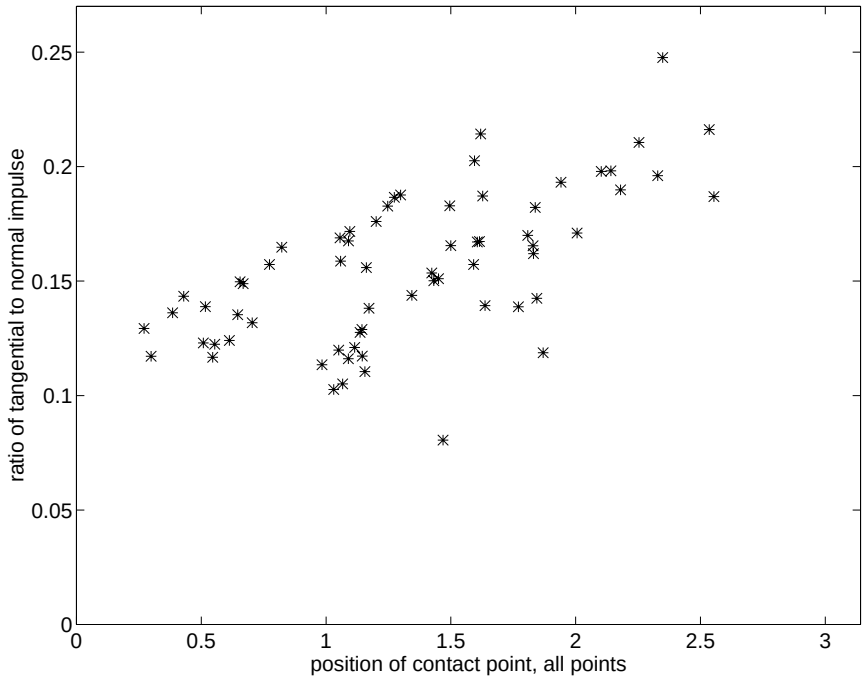

Figure 11.40: Ratio of tangential to normal impulses observed for both sticking and sliding collisions, vs. contact point angle α

11.3.1 Dependence of Impulse Ratio on Velocity Magnitude

Although unusual, it is possible that the friction coefficient for truly sliding collisions might itself depend on the magnitude of the normal component of force, impulse, or velocity (for a given body, the three are related).

Considering the collisions of the axisymmetric pucks, it is clear that if the magnitude of the pre-collision velocity is held roughly constant, then the magnitude of the normal impulse transmitted goes to zero roughly as $\cos\theta$, as the incidence angle θ approaches $\pi/2$. Dependence of the impulse ratio, for a given incidence angle, on the magnitude of the normal impulse (or velocity) can be verified by experiments where the incidence angle θ is held roughly constant, while the velocity magnitude is varied.

A set of new experiments was conducted with puck no. 2 of the axisymmetric pucks from Table 11.1. The steel plate used was the same one as that used for the experiments with the non-axisymmetric puck (note that the contacting surface on this plate appears to have a slightly higher coefficient of friction with the Delrin pucks than the plate used in 1995 by John Calsamiglia). In the new experiments, it was attempted to keep the incidence angle constant for several collisions at each of two velocities – 0.5 m/s and 0.9 m/s. The results, shown in Fig. 11.41 superimposed on the previous results from Calsamiglia's experiments, support the common assumption that the coefficient of friction is *not* significantly dependent on the magnitude of velocity, force or impulse.

In another experiment, the coefficient of sliding friction between the pucks and a steel plate was measured for different magnitudes of normal force. The coefficient of friction was found to be essentially constant as the normal force was varied over two orders of magnitude. (Details may be found in Kennedy's report [34].)

From these experiments we may conclude that the observed increase in the impulse ratio as the incidence angle increases, even for nominally "sliding" collisions, is due to some portion of the

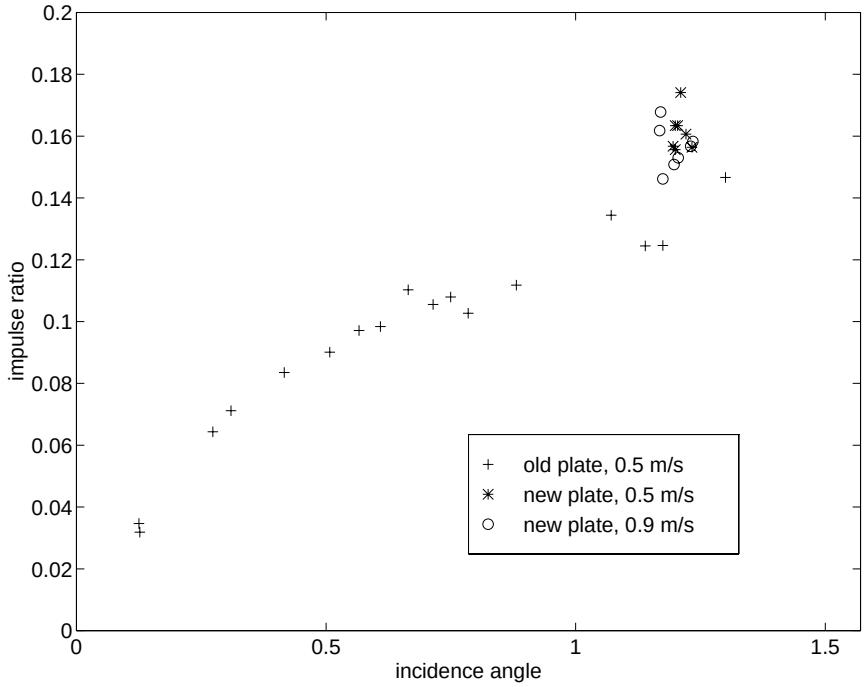

Figure 11.41: Impulse ratio for puck no. 2, for two velocities

contact region sticking for some part of the collision duration. This result is interesting at two levels.

At one level, if one compares previous studies of the collisions of spheres [17] or of disks that were slices of spheres [40], the experimental data was found to roughly match the predictions of a model that used the Mindlin-Deresiewicz solution [44] to describe the contact interaction in the collision. In modeling a collision using the Mindlin-Deresiewicz solution the crucial assumptions are that the interaction is pseudostatic, with much of the colliding bodies moving like rigid bodies and the small contact region acting essentially as a massless nonlinear spring-like device. In the Mindlin-Deresiewicz solution, beyond some intermediate incidence angle that depends on the friction coefficient, *all* collisions are sliding collisions. Thus, the Mindlin-Deresiewicz solution *cannot* predict a steady increase in the impulse ratio all the way up to $\theta = \pi/2$.

At another level, one might think of various simpler pseudostatic point-contact interaction models with linear or nonlinear springs in the normal and tangential directions (see Fig. 5.1). If the stiffnesses in the normal and tangential directions have a fixed ratio (as they will for linear springs, as well as for nonlinear springs where the nature of the nonlinearity, such as the power in a power law, is the same for both normal and tangential directions), then again the impulse ratio should be a constant for all incidence angles higher than some critical value.

Note that for both the Mindlin-Deresiewicz type as well as the simpler point-contact with springs type collision law, there is an implicit assumption of *force-response rigidity* – the interaction force developed by the local contact mechanism is essentially assumed to be given by the relative displacement between the contact "point" and the corresponding point on an ideal rigid body. This basic feature of such contact models rests on the assumption that deformations during the collision are strongly localized. However, for collisions of a thin disk, the deformations during the collision will be less localized than for collisions of spheres, since the stress field decays more slowly with increasing distance from the contact region.

A discussion of the non-localized deformations in thin, elastic disks in compression along a diameter is presented below.

11.3.2 Compression of Thin, Elastic Disks

Some insight into the anomalous frictional behavior of the Delrin pucks might be gained from first considering head-on (central), frictionless collisions of thin disks with rounded edges.

The classical treatment of frictionless collisions between elastic *spheres* (see e.g., Goldsmith [20] or Johnson [31]) has the following features:

1. The spheres are treated as force-response rigid objects, with the bulk of the spheres moving as rigid objects under the action of contact forces which arise from an essentially pseudostatic interaction in a small contact region.

2. The pseudostatic interaction in the contact region is assumed to be given by the Hertz contact solution for spheres.

The pseudostatic nature of the interaction is usually justified at one of two possible levels. At one level, one assumes that the duration of the collision is long enough so that elastic waves have time to traverse the colliding bodies many times during the collision. Under this assumption, it is safe to assume that internal vibrations damp out to zero and may be neglected on the time scale of the collision. For the Hertz contact solution for the impact of elastic spheres, this assumption is equivalent to requiring that $(V/c)^{1/5} \ll 1$, where V is the normal component of the relative velocity at the contact point, and c is the speed of a longitudinal wave in the colliding body. At a second, less restrictive level, one assumes that although the elastic waves might not have the time to traverse the colliding bodies many times during the collision, the energy associated with these waves is still small, though not negligible. This less restrictive assumption is equivalent to requiring, again for elastic spheres, that $0.3(V/c)^{1/3} \ll 1$, where V and c are defined as above.

Note that for elastic spheres, assuming that the pseudostatic solution is valid, strains at points far from the contact region decay as $1/r^2$, where r is the distance from the contact "point" of a point inside the sphere. Displacements of points far from the contact region are of the form $a + b/r$, for suitable a and b. Thus, distant points have essentially the displacement a, and most of the sphere may be considered to be moving as a rigid body.

The Hertz contact solution for spheres has been successfully used by Maw, Barber and Fawcett to model the collisions of disks that were (presumably thick) slices of spheres. However, on trying to extend the pseudostatic, Hertz contact approach to the collisions of *thin* disks, one encounters difficulties. In fact, there is no Hertz contact type solution for the impact of thin disks. This is essentially due to the fact that for *thin* disks, the deformations are not as strongly localized as in the 3D (sphere or thick slice thereof) case. If a half-plane in 2D is loaded in compression on a finite portion of its boundary, the strains at points far (compared to the width of the contact region) from the contact region decay as $1/r$. Consequently, displacements grow as $\ln r$, which is unbounded at infinity. What this means for finite-sized disks is that the Hertz-contact solution can only determine the local stresses, but cannot determine the overall deformations. The nature of the remaining forces on the disk (including inertial forces, in a collision calculation) determine the overall deformations of the disk. This basic difficulty due to the slow decay of deformations with distance from the contact region, makes a Hertz-contact type solution to the impact problem impossible even if the interaction is pseudostatic.

The pucks used in the experiments reported in this chapter had a thickness of about 13 percent of the radius. Also, the edge was rounded. As a result, for some (very small) range of contact forces,

the contact interaction might well be described by the 3D Hertz contact solution. However, for somewhat larger contact forces, the 2D nature of the disk might begin to have a significant effect. While the solution for a collision of a disk is unavailable, the problem of a cylinder compressed along a diameter by rigid flat plates has been solved (see Johnson [31]). For a crude, order of magnitude comparison, we calculated the displacement of the contact point relative to the center of mass as given by the 2D solution for compression of cylinders, the 3D solution for the known principal radii, and the sum of the 2D and 3D solutions[13], as a function of net compressive force P. These calculated results were compared with the results of a simple static load test where the disk was compressed along a diameter between two parallel steel plates. In the calculations, E (Young's modulus) was taken to be 2700 MPa (see Harper [23]), Poisson's ratio was taken to be 0.3 (typical for many materials, including polymers), the principal radii of the contact surface were taken to be 4.95 cm and 0.50 cm, and the steel plate was treated as perfectly rigid (because it is almost 80 times stiffer than Delrin).

The results are shown in Fig. 11.42, which shows the compression predicted by the 2D solution, the 3D solution, the sum of the 2D and 3D solutions, as well as the experimentally measured points for a range of loading forces. There is a roughly constant offset between the sum of the 2D and 3D compressions and the experimental data. This may be due to error in identifying the point of zero deflection at the start of the compression test. It is seen that shifting the experimental data

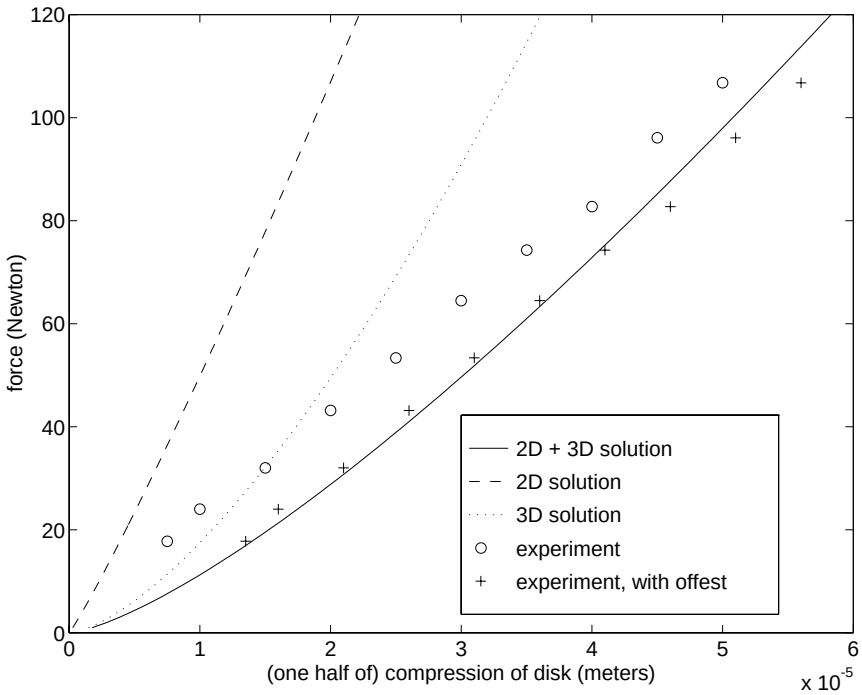

Figure 11.42: Load-displacement graph of Delrin puck loaded along diameter between flat steel plates

points a suitable constant amount to the right makes them agree fairly well with the "theoretical" curve, i.e., the sum of the 2D and 3D compressions. In the range considered, the data points

[13]The rationale for directly summing the two compliances is that the two effects (2D and 3D) accumulate over disparate length scales. The 3D strain field is more strongly localized than the 2D strain field.

may be reasonably fitted with a straight line of slope approximately 2×10^6 N/m. Assuming that the pseudostatic approach may be used, it is clear that the initial soft contact ($F = K\delta^{3/2}$) characteristic of the Hertz contact solution in 3D should be used for small forces (say, around 10 N), but becomes more or less insignificant for larger forces (say, around 100 N). For larger forces, a linear fit can be used for the crude analysis presented here.

11.3.3 Approximate Analysis Using Linear Spring

If the mass of the puck ($m \approx 67$ gm) is assumed to interact, during the collision, with a rigid surface through a linear spring of spring constant $k = 2 \times 10^6$ N/m, then in the course of the collision the mass describes half a cycle of simple harmonic motion. The time of the collision is independent of the collision velocity under the linear-spring assumption, and is about 0.5 millisecond for the values of k and m mentioned above. Also under the linear-spring approximation, the maximum compression as well as the maximum force are directly proportional to the pre-collision velocity. For a pre-collision velocity of 0.5 m/s the maximum force is about 185 N and the corresponding compression is just over 9×10^{-5} m.

11.3.4 The Experiments of Maw, Barber and Fawcett

It is interesting to note that the compliance of the disk from the "2D portion" of the displacement field is *inversely proportional* to the thickness of the disk, while the compliance from the "3D portion" is assumed to be independent of the thickness. Thus, for a thicker disk, the 3D portion will be more dominant. On the other hand, if the disk is so thin that the 3D portion of the compression is comparable to the thickness of the disk, then the 3D solution is not valid. For a given force, the thicker the disk, the more accurate and dominant the 3D portion and the smaller the 2D portion of the compliance is.

Moreover, for the linear-spring approximation, the maximum compression for a fixed pre-collision velocity is proportional to $\sqrt{m/k}$. For a *steel* disk of the same dimensions, colliding against a steel plate, we might expect the maximum compression to be smaller – the ratio of densities of steel to Delrin is about 6, and the ratio of effective effective elastic moduli (since the plate is made of steel also) is about 40. Using these values, we conclude that the maximum compression, using the linear-spring approximation, is about $\sqrt{6/40}$ or 40 percent as that for Delrin. For the smaller compression, the "3D portion" of the compliance dominates to a greater extent, and the linear approximation is poorer.

In conclusion, collisions of a thicker, steel disk might be expected to be described fairly well by the 3D solution alone, and the contribution of the 2D portion of the compliance might reasonably be neglected, as in the study of Maw, Barber and Fawcett [40].

11.3.5 The Pseudostatic Interaction Assumption

Let us examine the approximate solution for the collision of the Delrin puck using the linear spring. In the time duration of the collision (about 0.5 millisecond), a compression wave can travel a distance of only about 7 diameters of the puck, i.e., the time scale of the internal dynamics of the disk is not much faster than the time scale of the collision. It is likely that the collision duration is too brief for the transient vibrations to die out. The pseudostatic approximation may still, however, be a reasonable one (as in the case of the weaker requirement for spheres, discussed above).

It is interesting to note that for collisions of any disk of the same shape and size as the Delrin disk, but of some other material, under the linear-spring approximation, the time of collision is inversely proportional to $\sqrt{k/m}$, and hence $\sqrt{E/\rho}$, while the wave speed is directly proportional to

$\sqrt{E/\rho}$. Therefore the pseudostatic assumption is about equally valid (or invalid) for steel and Delrin disks, under the linear-spring approximation. However, as discussed above, for thick steel disks colliding at the same speeds as Delrin disks, the contact interaction of the steel disks will be closer to the 3D Hertz contact solution. Consequently, the time duration of the collision *will* be longer for lighter impacts, and thus the pseudostatic interaction model might be a fair approximation for light impacts.

11.3.6 Comments on the Frictional Interaction

In conclusion, we can make the following comments about the anomalous frictional interaction observed in the collisions of the Delrin disks.

1. If the bulk of the disk is thought to move more or less as a rigid body, then due to the *non-localized* nature of the deformations the contact region can stick while the corresponding "contact point" on the idealized rigid body is slipping. Thus, the collision might start and end with the contact point tangential velocity in the same direction, yet the contact region might stick for a while during the collision. In contrast, for collisions of spheres or thick slices of disks, the deformation field *is* strongly localized. Consequently, it is more difficult for the contact region to stick for any appreciable length of time while the corresponding "contact point" on the idealized rigid body is slipping. This may be a reason, based on a pseudostatic interaction assumption, why the impulse ratio is less than the coefficient of friction for apparently sliding collisions.

2. It appears that the contact compliance is initially higher for spheres and thick disks, and hence the time duration of light impacts is longer. Under these assumptions, the pseudostatic approximation is a better one. On the other hand, for thin disks, the contact interaction is closer to linear, and so the pseudostatic approximation may not be a good one. It may be that due to complicated dynamic effects absent in the collisions of thicker disks, the contact region sticks for a period of time during the collision. This idea might possibly be investigated further in terms of compression and shear wave propagation characteristics of the material.

3. It appears that the anomalous frictional effects observed might be more pronounced if the disk was thinner. This might be verified experimentally in future work, using a set of disks of different thicknesses.

Bibliography

[1] D. Baraff. *Dynamic Simulation of Non-Penetrating Rigid Bodies*. PhD thesis, Cornell University, 1992.

[2] D. Baraff and A. Witkin. Dynamic simulation of non-penetrating flexible bodies. *Computer Graphics*, 26(2):303–308, 1992.

[3] J. A. Batlle. On Newton's and Poisson's rules of percussive dynamics. *ASME Journal of Applied Mechanics*, 60:376–381, 1993.

[4] J. A. Batlle. Rough balanced collisions. *ASME Journal of Applied Mechanics*, 63:168–172, 1996.

[5] V. Bhatt and J. Koechling. Classifying dynamic behavior during three dimensional frictional rigid body impact. In *Proceedings, 1994 IEEE International Conference on Robotics and Automation*, pages 2342–2348. IEEE Robotics and Automation Society, May 1994.

[6] V. Bhatt and J. Koechling. Partitioning the parameter space according to different behaviors during three-dimensional impacts. *ASME Journal of Applied Mechanics*, 62:740–746, 1995.

[7] V. Bhatt and J. Koechling. Three-dimensional frictional rigid-body impact. *ASME Journal of Applied Mechanics*, 62:893–898, 1995.

[8] V. Bhatt and J. C. Koechling. Incorporating frictional impacts in dynamic simulations of planar multi link chains. In M. H. Hamza, editor, *Proceedings of the IASTED International Conference on Modelling and Simulation, Pittsburgh*, pages 454–457, 1993.

[9] V. Bhatt and J. C. Koechling. Modeling 3-d frictional rigid body impact: Dealing with degenerate singularities. In M. H. Hamza, editor, *Proceedings of the IASTED International Conference on Modelling and Simulation, Pittsburgh*, pages 5–8, 1993.

[10] R. M. Brach. Rigid body collisions. *ASME Journal of Applied Mechanics*, 56:133–138, 1989.

[11] R. M. Brach. *Mechanical Impact Dynamics: Rigid Body Collisions*. John Wiley and Sons, New York, 1991.

[12] R. M. Brach. Predicting rebounds using rigid-body dynamics – Discussion. *ASME Journal of Applied Mechanics*, 59:700, 1992.

[13] J. Calsamiglia. 2D collisions in uniform and nearly uniform disks. Report submitted to T&AM, Cornell University, describing experiments in 2D collisions conducted as part of the REU program, August 1995.

[14] H. Cohen and G. P. Mac Sithigh. Impulsive motions of elastic pseudo-rigid bodies. *ASME Journal of Applied Mechanics*, 58:1042–1048, 1991.

[15] F. S. Crawford. A theorem on elastic collisions between ideal rigid bodies. *American Journal of Physics*, 57(2):121–125, 1989.

[16] T. G. Drake and O. R. Walton. Comparison of experimental and simulated grain flows. *ASME Journal of Applied Mechanics*, 62:131–135, 1995.

[17] S. F. Foerster, M. Y. Louge, H. Chang, and K. Allia. Measurement of the collision properties of small spheres. *Physics of Fluids*, 6(3):1108–1115, 1994.

[18] R. L. Garwin. Kinematics of an ultraelastic rough ball. *American Journal of Physics*, 37(1):88–92, 1969.

[19] C. Glocker and F. Pfeiffer. Multiple impacts with friction in rigid multibody systems. *Nonlinear Dynamics*, 7:471–497, 1995.

[20] W. Goldsmith. *Impact: The theory and physical behavior of colliding solids.* Edward Arnold, Ltd., London, 1960.

[21] S. Goyal, E. N. Pinson, and F. W. Sinden. Simulation of dynamics of interacting rigid bodies including friction I: General problem and contact model. *Engineering with Computers*, 10:162–174, 1994.

[22] S. Goyal, E. N. Pinson, and F. W. Sinden. Simulation of dynamics of interacting rigid bodies including friction II: Software system design and implementation. *Engineering with Computers*, 10:175–195, 1994.

[23] C. A. Harper. *Handbook of Plastics, Elastomers and Composites.* McGraw-Hill, New York, second edition, 1992.

[24] A. P. Ivanov. Energetics of a collision with friction. *Journal of Applied Mathematics and Mechanics*, 56(4):527–534, 1992.

[25] A. P. Ivanov. On multiple impact. *Journal of Applied Mathematics and Mechanics*, 59(6):887–902, 1995.

[26] A. P. Ivanov. Visco-elastic approach to impact with friction. In R. C. Batra, A. K. Mal, and G. P. Mac Sithigh, editors, *Impact, Waves and Fracture*, pages 115–127. ASME, AMD-Vol. 205, 1995.

[27] J. Jaeger. Oblique impact of similar bodies with circular contact. *Acta Mechanica*, 107:101–115, 1994.

[28] J. Jaeger. Contact with friction of elastically similar bodies. In R. C. Batra, A. K. Mal, and G. P. Mac Sithigh, editors, *Impact, Waves and Fracture*, pages 129–152. ASME, AMD-Vol. 205, 1995.

[29] J. T. Jenkins. Rapid flows of granular materials. In R. J. Knops and A. A. Lacey, editors, *Non-Classical Continuum Mechanics: Proceedings of the London Mathematical Society Symposium, Durham*, pages 213–225. London Mathematical Society Lecture Note Series. 122, 1986.

[30] J. T. Jenkins. Boundary conditions for rapid granular flow: Flat, frictional walls. *ASME Journal of Applied Mechanics*, 59:120–127, 1992.

[31] K. L. Johnson. *Contact Mechanics*. Cambridge University Press, Cambridge, 1985.

[32] T. R. Kane and D. A. Levinson. *Dynamics: Theory and Applications*. McGraw-Hill, New York, 1985.

[33] J. B. Keller. Impact with friction. *ASME Journal of Applied Mechanics*, 53:1–4, 1986.

[34] S. Kennedy. Collisions: for axisymmetric and non-axisymmetric disks. Report submitted to T&AM, Cornell University, describing experiments in 2D collisions conducted as part of the REU program, August 1996.

[35] H. M. Lankarani and P. E. Nikravesh. A contact force model with hysteresis damping for impact analysis of multibody systems. *Journal of Mechanical Design*, 112:369–376, 1990.

[36] A. D. Lewis and R. J. Rogers. Experimental and numerical study of forces during oblique impact. *Journal of Sound and Vibration*, 125(3):403–412, 1988.

[37] G. P. Mac Sithigh. Rigid-body impact with friction - various approaches compared. In R. C. Batra, A. K. Mal, and G. P. Mac Sithigh, editors, *Impact, Waves and Fracture*, pages 307–317. ASME, AMD-Vol. 205, 1995.

[38] D. B. Marghitu and Y. Hurmuzlu. Three-dimensional rigid-body collisions with multiple contact points. *ASME Journal of Applied Mechanics*, 62:725–732, 1995.

[39] N. Maw, J. R. Barber, and J. N. Fawcett. The oblique impact of elastic spheres. *Wear*, 38(1):101–114, 1976.

[40] N. Maw, J. R. Barber, and J. N. Fawcett. The role of elastic tangential compliance in oblique impact. *Journal of Lubrication Technology*, 103:74–80, 1981.

[41] A. Mayer. Über den zusammenstoßzweier körper unter berücksichtigung der gleitenden reibung. *Berichte über die Verhandlungen der königlich sächsischen Gesellschaft der Wissenschaften zu Leipzig*, 54:208–243, 1902. (On the Collision of Two Bodies with Consideration of Sliding Friction).

[42] J. W. Milnor. *Topology from the Differentiable Viewpoint*. The University Press of Virginia, Charlottesville, 1981. Based on notes by David W. Weaver.

[43] R. D. Mindlin. Dynamics of package cushioning. *The Bell System Technical Journal*, 24:353–461, 1945.

[44] R. D. Mindlin and H. Deresiewicz. Elastic spheres in contact under varying oblique forces. *ASME Journal of Applied Mechanics*, 75:327–344, 1953.

[45] B. Mirtich and J. Canny. Impulse-based dynamic simulation. In *Proceedings of the Workshop on Algorithmic Foundations of Robotics*, San Francisco, CA, February 1995.

[46] G. S. Nusholtz. Geometric methods in determining rigid-body dynamics. *Experimental Mechanics*, pages 153–158, June 1993.

[47] F. Pfeiffer and C. Glocker. *Dynamics of rigid body systems with unilateral constraints.* Wiley series in nonlinear science. John Wiley and Sons, New York, 1996. Series editors: Ali H. Nayfeh and Arun V. Holden.

[48] V. Y. Plyavniyeks. Three-dimensional collision of two bodies. *Vopr. Dinamiki i Prochnosti*, 20:75–88, 1970.

[49] S. D. Poisson. *Traité de Mécanique.* Bachelier, Paris, second edition, 1833.

[50] M. H. Raibert. *Legged Robots that Balance.* MIT Press, Cambridge, MA, 1986.

[51] E. H. Rothe. *Introduction to Various Aspects of Degree Theory in Banach Spaces*, volume 23 of *Mathematical Surveys and Monographs.* American Mathematical Society, Providence, RI, 1986.

[52] E. J. Routh. *Dynamics of a System of Rigid Bodies.* Macmillan and Co., London, sixth edition, 1897.

[53] W. Rudin. *Principles of Mathematical Analysis.* McGraw-Hill, New York, third edition, 1976.

[54] M. Seabra Pereira and P. Nikravesh. Impact dynamics of multibody systems with frictional contact using joint coordinates and canonical equations of motion. *Nonlinear Dynamics*, 9:53–71, 1996.

[55] C. E. Smith. Predicting rebounds using rigid-body dynamics. *ASME Journal of Applied Mechanics*, 58:754–758, 1991.

[56] C. E. Smith. Predicting rebounds using rigid-body dynamics – Author's Closure. *ASME Journal of Applied Mechanics*, 59:700, 1992.

[57] C. E. Smith and P.-P. Liu. Coefficients of restitution. *ASME Journal of Applied Mechanics*, 59:963–969, 1992.

[58] D. Stoianovici and Y. Hurmuzlu. A critical study of the applicability of rigid-body collision theory. *ASME Journal of Applied Mechanics*, 63:307–316, June 1996.

[59] W. J. Stronge. Rigid body collisions with friction. *Proceedings of the Royal Society of London* A, 431:169–181, 1990.

[60] W. J. Stronge. Friction in collisions: Resolution of a paradox. *Journal of Applied Physics*, 69:610–612, 1991.

[61] W. J. Stronge. Unraveling paradoxical theories for rigid body collisions. *ASME Journal of Applied Mechanics*, 58:1049–1055, 1991.

[62] W. J. Stronge. Two-dimensional rigid-body collisions with friction – Discussion. *ASME Journal of Applied Mechanics*, 60:564–566, 1993.

[63] W. J. Stronge. Planar impact of rough compliant bodies. *International Journal of Impact Engineering*, 15(4):435–450, 1994.

[64] W. J. Stronge. Swerve during three-dimensional impact of rough bodies. *ASME Journal of Applied Mechanics*, 61:605–611, 1994.

[65] W. J. Stronge. Theoretical coefficient of restitution for planar impact of rough elasto-plastic bodies. In R. C. Batra, A. K. Mal, and G. P. Mac Sithigh, editors, *Impact, Waves and Fracture*, pages 351–362. ASME, AMD-Vol. 205, 1995.

[66] C. Thornton and C. W. Randall. Applications of theoretical contact mechanics to solid particle system simulation. In M. Satake and J. T. Jenkins, editors, *Micromechanics of Granular Materials*. Elsevier Science Publishers B. V., Amsterdam, 1988.

[67] P. Villagio. The rebound of an elastic sphere against a rigid wall. *ASME Journal of Applied Mechanics*, 63:259–263, 1996.

[68] V. N. Vinogradov, V. I. Biryukov, S. I. Nazarov, and I. B. Chervyakov. Experimental investigation of the coefficient of friction in the collision of a sphere with the flat surface of a material. *Trenie i Iznos*, 2:896–899, 1981.

[69] O. Walton. *Particulate Two-Phase Flow*, chapter 25. Butterworth-Heinemann, Boston, 1992. Edited by M. C. Roco.

[70] Y. Wang and M. T. Mason. Two-dimensional rigid-body collisions with friction. *ASME Journal of Applied Mechanics*, 59:635–642, 1992.

[71] E. T. Whittaker. *A Treatise on the Analytical Dynamics of Particles and Rigid Bodies*. Dover, New York, fourth edition, 1944.